THE ROLE OF OXIDATIVE STRESS AND CD154-MEDIATED REACTIVE OXYGEN SPECIES IN REGULATING HEPATOCYTE CELL DEATH DURING HYPOXIA AND HYPOXIA-REOXYGENATION

by

RICKY HARMINDER BHOGAL

UNIVERSITY OF BIRMINGHAM

A Thesis submitted to
The University of Birmingham
For the degree of
DOCTOR OF PHILOSOPHY

Centre for Liver Research
School of Infection and Immunity
College of Medical Sciences
The University of Birmingham
December, 2012

ABSTRACT

Hypoxia and hypoxia-reoxygenation (H-R) are pathogenic factors in many liver diseases and lead to hepatocyte death as a result of reactive oxygen species (ROS) accumulation. Activation of the Tumour Necrosis Factor-α (TNFα) super-family member CD40 by its cognate ligand CD154 can induce hepatocyte apoptosis via induction of autocrine/paracrine Fas Ligand/CD178 expression but the relationship between CD40 activation, ROS generation and hepatocyte cell death is poorly understood. Therefore, human hepatocytes were isolated from liver tissue and exposed to an *in vitro* model of hypoxia and H-R in the presence or absence of CD154 and/or various inhibitors. Hepatocyte ROS production, apoptosis, necrosis and autophagy were determined by a four-colour reporter flow cytometry assay. The *in vivo* regulation of liver injury by CD40 and CD154 was determined using a murine model of partial liver ischaemia. Exposure of human hepatocytes to recombinant CD154 or platelet-derived soluble CD154 augmented ROS accumulation during H-R resulting in NADPH oxidase-dependent apoptosis and necrosis. The cyto-protective mechanism of autophagy limited apoptotic cell death during hypoxia and H-R. CD40 and CD154 knockout mice but not wild type mice were protected from ischaemic liver injury. Hence, CD40:CD154 mediate hepatocytes cell death *in vitro* and *in vivo* during hypoxia and H-R.

DEDICATION

I dedicate my thesis to the most important entity in my life, my family, Dad, Mum, Rav, Jit, Gogs and my wonderful son, Arjun.

ACKOWLEDGMENTS

I would first like to thank Mr Simon R. Bramhall for providing me with the opportunity to carry out my research project at the University of Birmingham. I would also like to thank my supervisors, Dr Simon C. Afford and Professor David H. Adams, for all their advice, support and encouragement during my studies. I am very grateful to The Wellcome Trust and St John's Ambulance Service for funding my research studies. I am also very grateful to many of my colleagues past and present within the Centre for Liver Research for their help and assistance with many aspects of my PhD. In particular, I would like to extend my gratitude to Dr Christopher J. Weston and Dr Stuart M. Curbishley. Both have provided me with clear scientific advice and expertise and have always been available for advice throughout my studies. Mrs Gillian Muirhead, Mrs Jean Shaw and Mrs Janine Youster have provided me excellent technical support that has been indispensable for the success of my project. Finally, I would like to thank Dr Matthew Armstrong, Mr Rupesh Sutaria and Mr Barnaby Stephenson for their helpful discussions and support during the long evening hours within the laboratory.

The animal work within my PhD would not have been possible without the endeavours of Professor Henri Leuvenink, University of Groningen, Netherlands. I am indebted to him for organising the murine experiments for my study and organising my stay in Groningen.

I would also like to extend my thanks to the organ retrieval team at the Queen Elizabeth Hospital, Birmingham for the procurement of liver tissue and Dr Gary Reynolds for processing donor livers for my usage.

Table of Contents

List of Figures

List of Tables

List of Abbreviations

3-MA	3-methyladenine
7-AAD	7-Amino-Actinomycin D
ALD	Alcohol liver disease
ALT	Alanine Aminotransferase
AST	Aspartate Aminotransferase
Atg	Autophagy related proteins
BSA	Bovine Serum Albumin
CK18	Cytokeratin 18
CK19	Cytokeratin 19
DCF	2',7'-dichlorofluorescin
DMEM	Dulbecco's Modified Eagles Medium
DMSO	Dimethyl sulfoxide
DPI	Diphenyliodonium
EDTA	Ethylenediaminetetraacetic acid
EGTA	Ethylene Glycol Tetraacetic Acid
ELISA	Enzyme-linked Immunosorbent Assay
FACs	Fluorescent Activated Cell sorting
FasL	Fas Ligand
FITC	Fluorescein Isothiocyanate
FS	Forward Scatter
H&E	Haematoxylin & Eosin
HBSS	Hank's Balanced Salt Solution
HEPES	4-(2-hydroxylethyl)-1-piperazineethanesulfonic acid

H-R	Hypoxia-reoxygenation
HSEC	Hepatic Sinusoidal Endothelial Cells
IL	Interleukin
IRI	Ischaemia-reperfusion injury
JAK	Janus Kinase
JNK	c-Jun *N*-terminal kinase
JC-1	5,5',6,6'-tetrachloro-1,1',3,3'-tetraethylbenzimidazolylcarbocyanine iodide
KC	Kupffer cells
MAP3K/MEKK	Mitogen-activated protein kinase kinase kinase
MAP2K/MEK	Mitogen-activated kinase kinase
MAPK	Mitogen-activating protein kinase
MCP-1	Monocyte Chemoattractant Protein-1
MDC	Monodansylcadaverine
MFI	Mean Fluorescence Intensity
NAC	N-acetylcysteine
NADPH oxidase	Nicotinamide adenine dinucleotide phosphate hydrogenase oxidase
NFκB	Nuclear Factor kappa B
OLT	Orthotopic Liver Transplantation
PBC	Primary Biliary Cirrhosis
PBS	Phosphate Buffered Saline
PCM	Platelet Conditioned Media
PE/RPE	R-phycoerythrin

PI-3K	Phosphatidylinositol 3-kinase
PP	Peri-portal
PSC	Primary Sclerosing Cholangitis
PMN	Polymorphonuclear Cells
PV	Peri-venular
ROS	Reactive oxygen species
SS	Side Scatter
STAT	Signal transducer and activator of transcription
TNFα	Tumour Necrosis Factor-α
TRAF	Tumour Necrosis Factor-α Associated Factor
TBS	Tris Buffered saline
XO	Xanthine oxidase

CHAPTER 1 - GENERAL INTRODUCTION

1.1 Overview

1.1.1 Liver Transplantation & Hepatic Ischaemia-Reperfusion Injury

The first orthotopic liver transplant (OLT) was performed in 1963 by Dr Thomas Starzl in Denver, Colorado on a three year-old child with biliary atresia. Unfortunately, the child died during the operation from overwhelming haemorrhage and it took over four years from the initial attempts at OLT for the first patient to survive one year. Much of these early problems encountered by the nascent field of liver transplantation were technical in nature. The surgical and anaesthetic techniques required for successful liver transplantation were in development and immunosuppression following transplantation was not to become common clinical practice until the 1980's. Yet despite the above advancements liver allografts still sustained significant injury following transplantation and many allografts failed to function adequately in the post-operative period. These latter observations were in large part due to the as yet unknown entity of ischaemia-reperfusion injury (IRI). Furthermore despite nearly 50 years of experience with OLT worldwide, IRI is the primary cause of initial poor allograft function and primary non-function of the liver allograft.

The phenomenon of IRI was first suggested by experimental studies conducted in the 1970's. IRI is now understood to be a common and important mechanism of injury in many different organ systems and in many different clinical scenarios. For instance, IRI is seen during and after myocardial infarctions [1], strokes [2], acute kidney injury [3], haemodynamic shock [4] and systemic shock [5]. IRI is a common feature in all deceased donor solid organ transplantation. Both clinical and experimental data demonstrates that IRI has deleterious short- and long-term effects upon allografts after transplantation [6, 7]. Following OLT, IRI can manifest as increased episodes of acute rejection and chronic allograft dysfunction [8].

As emphasised above, IRI is of particular relevance to the field of liver transplantation. There is a well publicised shortage of donor liver organs available for transplantation and the number of patients requiring a liver transplant continues to rise year on year across the United Kingdom and Europe [9]. Current estimates show that 4% of liver transplants are subject to organ dysfunction after transplantation and 2% sustain primary graft non-function as a result of IRI [10]. Moreover, IRI is responsible for 81% of all liver re-transplantations, demonstrating the extent of the clinical impact of liver IRI [11, 12]. This clinical impact of IRI has become more pronounced during the last decade due to the increase in the utilisation of extended criteria donor livers [13]. This particular group of organs includes livers retrieved from elderly patients, steatotic livers and non-heart beating donor livers. These allografts are more susceptible to IRI and hence to organ dysfunction after OLT when compared to standard criteria donors [14]. Importantly it is well known that IRI hinders liver regeneration [15] and therefore limiting allograft injury after OLT would have dual benefits upon patient outcome following transplantation. Minimising the adverse effects of hepatic IRI could potentially increase the number of suitable allografts for transplantation and also enhance the number of patients who successfully recover from OLT. Amelioration of IRI would also potentially reduce the need for re-transplantation and improve patient morbidity and mortality after OLT. Therefore investigating the fundamental biological aspects of hepatic IRI represents an important area of research within the field of transplantation.

Paramount to achieving the goal of improved understanding of the IRI process is gaining a complete understanding of the molecular mechanisms involved in hepatic IRI. In order to obtain the understanding of the effects of IRI upon human liver physiology after OLT it is essential that the effects of IRI are studied upon human livers and human liver cells. This information would better serve in developing strategies to limit IRI in the clinical scenario of

OLT. However this approach has obvious practical and ethical barriers. Although limited studies have investigated the effects of IRI upon the human liver [16] these studies have largely looked at the effects of IRI upon hepatic architecture [17] and limited physiological responses [16]. As a result, studies have utilised murine [18-20] and rodent models [21, 22] of IRI to investigate the deleterious effects of IRI upon liver physiology. Whilst these studies have obvious merit there is likely to exist differences between these models and the clinical events following OLT.

In vivo models of IRI have the obvious advantage of studying the liver within the whole organism and can be akin to the clinical setting encountered after organ transplantation. However, it is well appreciated that the hepatocyte is the main cellular target of hepatic IRI [23]. Therefore *in vivo* models of IRI by their very nature do not allow the delineation of specific hepatocyte responses during IRI. However, the *in vitro* modelling of IRI also has the obvious disadvantage of studying the cell type of interest outside its normal physiological and anatomical parameters. Indeed, the *in vitro* modelling of IRI is unlikely to reflect the *in vivo* microenvironment during and after IRI. Nonetheless understanding the specific response of individual cell types to IRI would allow the delineation of cellular and molecular mechanisms that contribute to IRI.

As discussed above all cell types within the liver are affected by IRI but the main cell type targeted by the injurious process during IRI is the hepatocyte. The response of hepatocytes, and particular human hepatocytes, to IRI is surprisingly not well studied or well known. Early studies and more recent studies have investigated the effects of IRI upon hepatocytes using human hepatoma cell lines such as HepG2 cells in experimental models [24, 25]. These hepatoma cells were found to be relatively resistant to *in vitro* IRI [26, 27] and thus have led to the widely accepted notion that hepatocytes are relatively resistant to IRI.

However, more recent studies utilising a variety of primary animal hepatocytes have shown that hepatocytes may be more susceptible to IRI than first thought [28-32]. These latter studies using different animal hepatocyte have however led to much confusion and discrepancies within the literature regarding hepatocyte responses to IRI. This is in large part due to the different models of IRI used in these studies. For instance these studies have used differing times of ischemia, differing times of reperfusion and differing oxygen tensions and concentrations. Taken together these experiments have not assisted in clarifying the role and response of hepatocytes to IRI.

Despite this large body of literature there have been no studies to date that have investigated the effects of IRI upon isolated primary human hepatocytes. This has left a large void within the literature regarding the role of human hepatocytes in IRI and in the general understanding of hepatic IRI. The reasons for the paucity of this data are in part due to the complexities and technical demands of routine human hepatocyte isolation [33], the establishment of an efficient and effective *in vitro* IRI model for human hepatocytes and the development of reliable assays for measuring meaningful outputs for IRI. There are also other added difficulties in using human hepatocytes to investigate the mechanisms of IRI. Human hepatocytes can be isolated from both diseased and normal liver tissue [34]. Indeed, normal liver can encompass both donor livers and/or normal resected liver tissue. The latter describes livers that have been resected from patients with neoplastic disease following which liver tissue has been obtained from macroscopically normal liver well away from the primary liver lesion. As stated above authors have used hepatoma cells as a surrogate for primary hepatocytes assuming that these cells would have very similar physiological responses to extracellular cues such as ischaemia/hypoxia because both these cell types express similar intracellular enzymes [35]. Importantly, this latter hypothesis has not been

objectively tested in any studies to date and recent studies do reveal fundamental differences between these two cell types [36]. The study of human hepatocyte responses to IRI would be of undoubted benefit to understanding the fundamental responses of human hepatocytes to hypoxic stress as well as providing potential therapeutic targets to manipulate with drug therapy that will ultimately improve patient outcome after OLT. Without an understanding of the response of primary human hepatocytes during IRI the precise mechanisms involved in the whole process of IRI will remain elusive and poorly understood.

1.1.2 Mechanisms Regulating Hepatic Ischaemia-Reperfusion Injury

Cerra *et al* were among the first groups to describe the phenomenon of IRI in 1975 using experimental canine models [37]. In these studies the authors examined the myocardial pedicles of canine hearts after myocardial IRI and found that increased ischaemic times were associated with increased sub-endothelial haemorrhagic necrosis within the heart. In the same year the first study documenting IRI within the liver was reported by Toledo-Pereyra *et al* [38]. This landmark study established the detrimental effects of IRI within the liver. In a series of elegant experiments the authors reported that intravenous pre-treatment of dogs with isoproterenol, allopurinol and heparin significantly reduced liver injury prior to auxiliary liver transplantation. However, it was not apparent from these early experiments as to the mechanism of protection of the aforementioned drugs. Since these early experimental studies the understanding of IRI [39] and in particular hepatic IRI [40] has increased substantially. Many studies have investigated the effects of hepatic IRI both *in vitro* and *in vivo* and a large body of literature is now established on the subject. Hepatic IRI is now recognised as a highly complex cascade of events that includes interactions between vascular endothelium, interstitial compartments, circulating cells and numerous biochemical entities

[41]. The aetiology of IRI is a multi-factorial process and many of the mechanisms involved have been extensively discussed in many recent reviews [7, 41-43].

As discussed above, IRI is well known to be an obligatory part of all solid organ transplantation. In general, ischaemia or hypoxia is a state of tissue oxygen deprivation accompanied by a reduced clearance of the resulting toxic metabolites. During liver ischaemia, liver parenchymal damage occurs from both direct micro-vascular dysfunction and the subsequent inflammatory response [44]. Acute ischaemia leads to oxygen deprivation and adenosine triphosphate (ATP) depletion resulting in direct parenchymal damage through tissue apoptosis and necrosis [23]. During hepatic IRI all parenchymal and non-parenchymal cells resident within the liver are exposed to ischaemia. In general, previous studies have shown that parenchymal cells and in particular hepatic sinusoidal endothelial cells (HSEC) are more susceptible to cell death during the ischaemic portion of IRI than hepatocytes [45]. The responses of other parenchymal cells such as cholangiocytes have not yet been fully investigated and remain the subject of ongoing research. Moreover, as stated above the effects of IRI upon human hepatocytes has not been objectively studied and thus it remains to be determined whether these particular cells are also relatively resistant to cell death during ischaemia/hypoxia. Acute ischaemia also triggers a vigorous immune response and causes the activation of the endothelium resulting in increased permeability and increased expression of adhesion molecules such as Intracellular Adhesion Molecule-1 (ICAM-1), p-selectin and E-selectin [46]. Hence during ischaemia as well as parenchymal cell death the endothelial cells acquire an adhesive, thrombogenic surface that latter amplifies liver injury through the recruitment of effector cells [46].

Following the ischaemic portion of IRI, reperfusion restores blood flow to the ischemic tissue. Despite the unequivocal benefit of reperfusion of blood to the ischaemic tissue,

reperfusion itself can and does elicit a cascade of adverse reactions that paradoxically injure tissue [41]. Upon restoration of blood flow to the ischaemic tissue, a 'no-flow' phenomenon occurs. Capillaries and microcapillaries are not perfused, potentiating further tissue damage. Reperfusion is a much more complex process than ischaemia in that it has diverse effects upon parenchymal and non-parenchymal cells. The sequelae of events described above leads to direct microvascular dysfunction and further parenchymal injury. The primed endothelial cells are more adhesive, and upon, reperfusion, inflammatory cells attach to the endothelium [46]. In addition, shear stress, the tangential component of haemodynamic forces, can also activate cellular signalling pathways within liver endothelial cells during IRI [47]. Moreover shear stress can induce the expression various molecules upon liver endothelial cells such as Vascular Adhesion Protein-1 (VAP-1), ICAM-1 and VCAM-1 [48]. These adhesion molecules can then regulate the adhesion and transmigration of effector cells during IRI that then perpetuates liver injury. However, shear stress may also be beneficial during liver IRI thorough the release of Nitric Oxide (NO) that induces vasodilatation counteracting microvascular dysfunction [49] and also by promoting liver regeneration [47].

Reactive oxygen species (ROS), cytokines, chemokines and adhesion molecules are also generated, secreted and released augmenting the pro-inflammatory reaction [40]. The combination of vascular permeability and increased cellular signalling augments the recruitment and infiltration of circulating leukocytes into the post-ischaemic liver tissue [46]. Reperfusion also causes the swelling of non-parenchymal cells resident within the liver such as Kupffer cells (KC) and liver resident macrophages, which then upon activation release a plethora of pro-inflammatory mediators such as ROS and cytokines [50]. Although the effects of infiltrating and resident inflammatory cells during reperfusion has been well studied the effects of reperfusion upon parenchymal cells is less well defined. In general,

work in rodent and murine hepatocytes has shown that during reperfusion hepatocytes undergo cell death primarily in the form of necrosis due to the depletion of ATP and the lack of oxygen [51]. When ATP is present, cells preferentially die via apoptosis [23, 51]. Some authors have argued that both forms of cell death occur within the liver during IRI and have termed this overall process as necro-apoptosis [52, 53]. *In vivo* this appears histopathologically as hepatocyte blebbing and causes the detachment of hepatocytes from the sinusoidal plate and may lead to the obstruction of sinusoidal flow and the phenomenon of secondary necrosis [54]. HSEC undergo necrosis and can cause disruption to the hepatic microcirculation once again leading to secondary necrosis [40]. The pro-inflammatory response seen during IRI has been shown in both experimental models of hepatic IRI and the limited human studies performed in livers after ischaemia [16, 39]. The overall process results in tissue destruction, organ dysfunction and in the case of organ transplantation possible allograft failure.

The relationships between the signalling pathways involved in hepatic IRI are highly complex and are yet to be fully ascertained. Figure 1.1 shows the current paradigm for the processes thought to be involved in and regulate hepatic IRI. Among the important regulators of hepatic IRI are Nitric Oxide (NO), Tumour Necrosis Factor-α (TNFα), Nuclear Factor kappa B (NFκB) and both the innate and adaptive immune system. A brief description of the key regulators and mediators of hepatic IRI is discussed below. This section is not exhaustive and recent reviews give a much more comprehensive review of all the potential mechanisms involved in hepatic IRI [39, 40, 43].

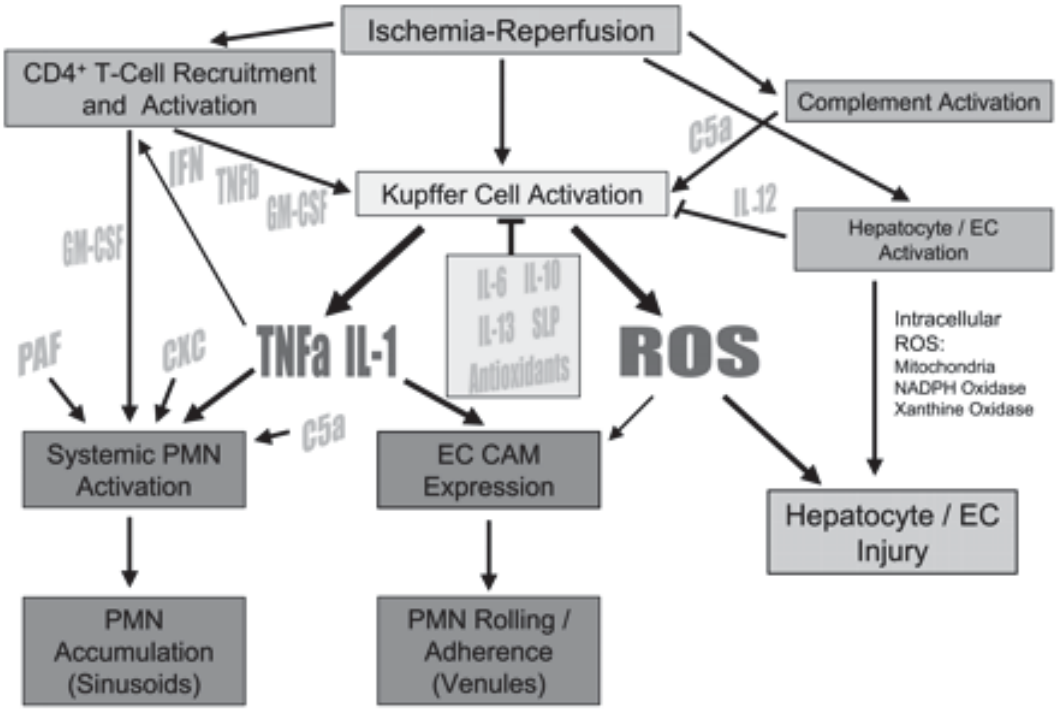

Figure 1.1 The Major Regulators of Hepatic IRI
The overall mechanisms involved during the process of hepatic IRI. In general IRI is a pro-inflammatory process and during the ischaemic portion of IRI the hepatic endothelium is primed and has a thrombotic adhesive surface due to effects of pro-inflammatory cytokines such as TNFα and Interleukin-1 (IL-1). Upon reperfusion of the liver the classical model of IRI describes the activation of KCs. These liver resident macrophages release a plethora of pro-inflammatory cytokines such as TNFα and ROS. These soluble mediators induce the expression of adhesion molecules and induce the influx of leukocytes and polymorphonuclear cells into the liver that perpetuate liver parenchymal injury. Extracellular ROS released by KCs also induce parenchymal injury, as does the generation of intracellular ROS. IRI also causes the activation of innate and later the adaptive immune system that also induces liver injury. EC, endothelial cells; CAM, cellular adhesion molecules; PMN, polymorphonuclear leukocyte neutrophil; ROS, reactive oxygen species, TNF, Tumour Necrosis Factor; GM-CSF, granulocyte macrophage colony stimulating factor; PAF, platelet activating factor; CXC, CXC chemokines; C5a, activated complement factor; SLP, secretory leukocyte protease inhibitor. (Taken from Jaeschke H, American Journal Physiology. 2003 284; G15-G26).

1.1.2.1 The Immune System

Inflammation is known to be a key mediator of IRI and considerable data exists demonstrating the key role of the innate and adaptive immune system in the process [39, 55]. The inflammatory response to acute ischaemia in the classic model of IRI is predominantly an innate immune response [56, 57]. In liver IRI there is no microbial infection present and the innate immune response is triggered by non-infectious stimuli [40]. These non-infectious stimuli contribute to the initiation of an inflammatory response in part by signalling via Toll-like receptor (TLR) mediated signalling pathways [56]. TLRs are a family of pattern recognition receptors that are activated by specific components of microbes and certain other molecules. TLRs form the first line of immune defence and are expressed on antigen-presenting cells (APCs), macrophages, dendritic cells and B-cells [58]. Specifically, TLR4 is involved in innate immunity primarily by recognising lipopolysaccharides (LPS). Activation of TLR4 is linked to NFκB activation and secretion of pro-inflammatory cytokines (TNFα, IL-β) as well as inducible NO synthase and ICAM-1 [59]. TLR4 activation is likely to play an important role in KCs activation during liver IRI [60]. Indeed, TLR4 deficient mice are less prone to liver IRI [61]. These findings suggest that endogenous TLR ligands are the primary stimuli initiating liver IRI through the innate immune system. As well as TLRs, complement and DCs have a profound effect upon the development of liver IRI [40]. DCs in particular are likely to be one of the key regulators for the development of an adaptive immune response during IRI [62]. In addition to TLR4 and DCs, the damage-associated molecular pattern (DAMPs) molecules may also key initiators of the immune response seen during IRI. These molecules regulate immune responses in non-infectious inflammatory scenarios. Specifically, the DAMP molecules, high-mobility group box 1 (HMGB1) and interferon regulatory factor 1 (IRF-1) have been shown mediate the progression liver IRI

[63]. In addition, recently histones have been identified as a new class of DAMP molecules that link initial damage and the subsequent activation of innate immunity during sterile inflammation [64]. These observations collectively demonstrates that many mediators are involved in triggering the innate immune response seen during liver IRI.

T-lymphocytes constitute one of the primary arms of the adaptive immune response during IRI. According to classical immunological dogma, these cells were not suspected to play a role in IRI [46]. However recent studies have shown that mice lacking CD4/CD8 T-lymphocytes are protected from IRI and adoptive transfer of T-lymphocytes into T-lymphocyte knockout mice restores ischaemic injury [65]. More recent studies have refined these observations and have shown that CD4-positive T-lymphocytes are the mediators of late liver injury during IRI [66].

1.1.2.2 Reactive Oxygen Species

Of undoubted importance in the development of parenchymal injury during IRI is the generation of ROS [43]. ROS are a family of oxygen intermediates that can cause cellular damage. In the classical model of hepatic IRI it is thought to be extracellular ROS released by KCs and PMN that is responsible for parenchymal injury [40]. Some studies have evaluated the role of intracellular ROS production by hepatocytes during IRI [67, 68]. These early experiments proposed xanthine oxidase (XO) was the main generator of ROS in hepatocytes [69]. However, more recent data has shown that the mitochondria are likely to be the main ROS generators in hepatocytes [70, 71]. Controversy still exists as to whether it is intracellular or extracellular ROS that is of primary importance with regard to parenchymal injury during IRI. ROS is likely to have multiple effects during IRI [43]. These include direct oxidation of cellular components and lipids (lipid peroxidation), activation of

inflammatory gene transcription and possible activation of the innate immune response. ROS can also generate other potentially harmful compounds such as peroxynitrites [42]. The specific role of ROS in hepatic IRI is discussed in more detail in section 1.1.3.

1.1.2.3 NO & Haem Oxygenase (HO)

The role of NO during hepatic IRI remains controversial [72]. Some studies have stated that NO exerts a beneficial effect during IRI by limiting liver injury [73] whilst others report detrimental effects [74]. The discrepancy is likely to arise from the fact that endothelial NO synthase (eNOS)-derived NO production is protective in IRI whereas inducible NO synthase (iNOS)-derived NO may contribute to IRI. This may be a function of the NO generation kinetics from the two isoforms in IRI. eNOS may help abrogate microcirculatory stress but iNOS-derived NO takes several hours to be generated because of the requirement of transcriptional activation [75]. Excessive levels of iNOS-derived NO maybe detrimental through the generation of peroxynitrites [42] (see section 1.1.3). NO can also promote apoptosis through inducing cytochrome c release and caspase activation [76].

HO, a rate-limiting enzyme, catalyses the degradation of heme into free iron, carbon monoxide (CO) and biliverdin. HO overexpression is protective in IRI and has anti-inflammatory and anti-apoptotic effects [77]. These effects are likely to be mediated by the by-products of HO-1 activity namely biliverdin, bilirubin, ferritin, and CO.

1.1.2.4 TNFα & NFκB

Similar to NO, TNFα, have been reported to be both protective and injurious during IRI [78]. For example the deleterious effects of TNFα in local and systemic damage associated with hepatic IRI is well established [79]. However TNFα is also an important mediator of hepatic

regeneration [80]. Indeed pre-treatment with low-dose TNFα is known to be highly protective against hepatic IRI [81]. The differential effects observed for TNFα can be attributed to the differential activation of transcription factors. For further discussion on the wider role of the TNFα family members in regulating hepatic IRI see section 1.1.4.

It is well known that NFκB can regulate various downstream pathways and thus has the potential to be both pro- and anti-apoptotic [82, 83]. It is likely that NFκB has a myriad of effects on cellular processes such as anti-apoptosis and reducing pro-inflammatory cytokine activation. Indeed NFκB inhibition decreases neutrophil accumulation after partial liver IRI and protects against liver injury [84].

1.1.2.5 Neutrophils/Polymorphonuclear (PMN) cells

PMN cells have been shown to be the major leukocytes found in necrotic liver tissue following ischaemic injury [85]. Neutrophils are thought to be the early cellular mediators of local microvascular changes and parenchymal damage [86]. Monocytes and macrophages infiltrate the liver later in IRI and likely extend and amplify the early injury phase [87]. Activation of neutrophils has been implicated in hepatic microvascular dysfunction and parenchymal damage associated with IRI [46]. It is thought that the expression of ICAM-1 and p-selectin may facilitate neutrophil accumulation in the liver after ischaemia [88]. However, mechanical factors such as vasoconstriction, oedema, and reduced membrane flexibility may also trap these leukocytes in liver sinusoids. Due to the HSEC damage that is seen during reperfusion, neutrophils have direct access to hepatocytes and may perpetuate parenchymal injury [40].

1.1.2.6 Hypoxia Inducible Factor-1α (HIF-1α) and ischaemic pre-conditioning (IPC) in IRI

The transcription factor HIF-1α is involved in regulating a wide variety of cellular signalling pathways during hypoxia. Specifically, the role of HIF-1α in mediating liver ischaemic injury was initially reported in the late 1990's [89]. These studies showed that HIF-1α protein levels were up-regulated and that HIF-1α was activated during ischaemia. Moreover the upregulation of HIF-1α was associated with cytoprotection.

These experimental observations lead several groups worldwide to assess whether IPC could ameliorate liver injury after OLT. IPC involves short periods of liver ischaemia induced by total hepatic vascular occlusion. IPC has been comprehensively reviewed recently [90-92]. Studies indicated that 10 minutes of occlusion increased HIF-1α levels as well as other hepatoprotective factors within the liver and reduced liver injury although this did not reach statistical significance when compared to the control group [93]. In addition, IPC increases levels of NO and attenuates the overproduction of ROS and IRI induced inflammation [94]. Hence, IPC may protect the liver from IRI via an Akt-eNOS-NO-HIF-1α dependent pathway [94]. Moreover studies suggest that HIF-1α is the main factor involved in the protective effects of IPC and may protect hepatocytes in particular from the detrimental effects of hypoxia [90, 95].

The use of IPC clinically is determined by personal surgeon preference but allied strategies to IPC such as post-conditioning may further enhance the protective effects of IPC and increase its use during liver surgery [96, 97]. In general, IPC appears to be hepato-protective by in part up-regulating HIF-1α levels but further clinical trials are required before it can be widely adopted.

1.1.3 ROS & Hepatic IRI

Pro-oxidants or oxidative agents are molecules that abstract electrons from other molecules. Oxidative stress occurs when pro-oxidants overwhelm cellular anti-oxidants defence mechanisms. In hepatocytes the antioxidant defences are primarily in the form of intracellular glutathione [42, 98-100]. Therefore oxidant stress can result from either excessive generation of oxidizing agents or a relative deficiency of anti-oxidants. The oxidizing species most implicated in oxidative stress include the superoxide anion, hydrogen peroxide, the hydroxyl radical, hypochlorous acid, chloramines, singlet oxygen, and peroxyradicals [6]. In most systems superoxide anions are often the initial toxic oxygen species generated during oxidative stress. Superoxides, within hepatocytes, are generally generated during physiological activities in mitochondria, microsomes and peroxisomes [101, 102]. Indeed, 1%-2% of oxygen consumed by mitochondria undergoes reduction to form superoxide anions by the coenzyme Q and the reduced nicotinamide adenine dinucleotide (NADH)-coenzyme Q reductase complex (see Figure 1.2). Disruption of the mitochondrial electron transport chain can lead to increased production of superoxide anions [103]. In mammalian cells, enzymatic dismutation of superoxide anions to hydrogen peroxide occurs rapidly by the enzyme superoxide dismutase. Subsequently, hydrogen peroxide can be converted to the highly reactive hydroxyl radical by transition metal-catalysed reactions [103]. In the liver, hepatic microsomes through the activity of the cytochrome P450 can also generate superoxide anions and hydrogen peroxide [104].

Reoxygenation injury is defined as cellular injury caused by reintroduction of physiological concentrations of oxygen to viable cells that have been exposed to injurious but non-lethal hypoxic conditions. Reoxygenation injury results from the generation of toxic oxygen species generated after reintroduction of oxygen to ischaemic tissues. Upon the

reintroduction of oxygen to ischaemic hepatocytes reduced mitochondrial electron carriers generate a burst of superoxide anions as a result of increased auto-oxidation rates of complexes III and I in pre-mitochondrial respiratory chain [26, 27]. The lack of oxygen as a terminal electron carrier for the mitochondrial respiratory chain immediately interrupts electron flow, causing the respiratory chain to become reduced as opposed to its usual aerobic oxidised state. The mitochondria no longer accept electron from substrates and hence a reduction of pyridine nucleotides occurs resulting in an increase in the intracellular NADH/oxidized NAD+ ratio [103]. The cessation of oxidative phosphorylation rapidly leads to cellular ATP depletion once glycolytic substrates have been used. If the hypoxic insult is reversed in the early stages then mitochondrial function can recover and cell death prevented [105].

Cytosolic oxidases can also generate ROS [106-108]. The most widely studied cytosolic system within hepatocytes is the XO-xanthine dehydrogenase enzyme system [109]. As a result of oxidative stress xanthine dehydrogenase activity is converted to XO function. ATP hydrolysis as is seen during IRI results in the production of xanthine, the substrate for XO, and results in the production of superoxide anion. Other cytosolic enzymes such as cyclooxygenase and lipoxygenase activity can also generate ROS but their function within hepatocytes remains to be established [106, 107]. The role of cytosolic enzymes production of ROS during reoxygenation remains controversial. Indeed, no studies have evaluated the role of these cytosolic enzymes in the production of ROS in human hepatocytes.

Extracellular ROS also plays an important role in hepatic IRI [40]. Neutrophils form superoxide anions and hypochlous anion through a membrane-associated reduced nicotinamide adenine dinucleotide phosphate (NADPH) oxidase and myleoperoxidase, respectively, which plays a key role in neutrophil-mediated cytotoxicity [110]. Activated KC

generate superoxide anions by NADPH oxidase activity [111]. Macrophages, KC and endothelium can also generate NO, by the conversion of L-arginine to L-citrulline by NO synthase [72]. Recent studies suggest that NO reacts with superoxide anions to form peroxynitrate ions [42, 112]. This anion can oxidise sulfhydryl groups and when protonated may decompose to form nitrogen and superoxide anion-like species.

In many models of cell injury superoxide anions are thought to be the cytotoxic bullet generated during oxidative injury [76]. Toxic oxygen species are thought to cause cell necrosis via oxidation of critical cellular proteins, DNA and lipids [113]. In general oxidation of critical thiols leads to loss of protein function, oxidation of cytoskeletal proteins may lead to bleb formation, whereas oxidative damage to mitochondria causes a loss of oxidative phosphorylation and ATP depletion [113]. In addition oxidative stress can cause permeability transition of the inner mitochondrial membrane which contributes to cell death in the form of apoptosis [43]. Most early changes in hypoxic cell injury occur in the mitochondria.

Despite this large body of literature the precise role of ROS in human hepatocytes during IRI is not known. Moreover, the precise role of the mitochondrion and cytosolic enzymes in generating ROS within human hepatocytes remains to be established.

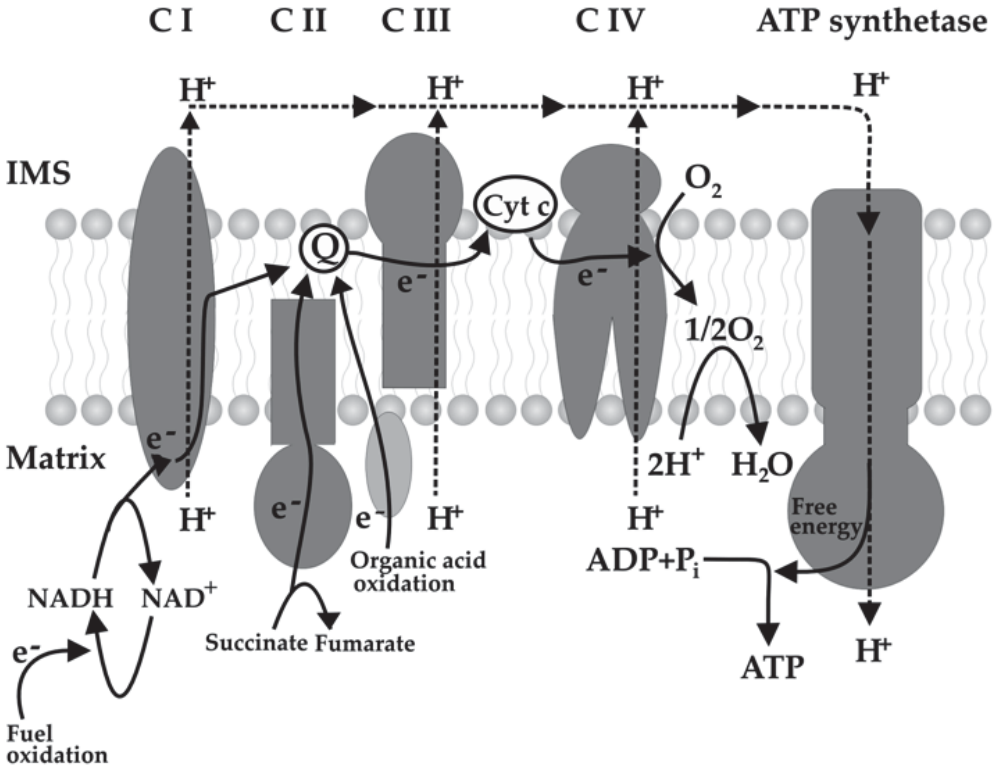

Figure 1.2 The Mitochondrial Electron Transport Chain and the Generation of ROS
The main mechanisms for mitochondrial ROS generation are illustrated above. Reduced substrates synthesized in metabolic pathways supply electrons (e^-) to complex I (CI) and complex II (CII) of the electron transport chain. The main centres for superoxide formation are complex I and complex III (CIII), although small amounts can be formed at complex II and complex IV (CIV). The electron carrier of complex III ubiquinone (Q) is reduced to ubiquinol that transfers an electron to cytochrome c (Cyt c) through an iron protein. The resulting semiubiquinone is oxidized back to ubiquinone by cytochrome b and can also transfer electrons to oxygen to form superoxide anions. Rotenone, a complex I inhibitor, inhibits electron flow proximal to superoxide generation.

1.1.4 The Role of TNFα Family Members in Hepatic IRI

1.1.4.1 Introduction

The TNFα superfamiliy of ligands and receptors consist of approximately 50 membrane and soluble proteins that can modulate a wide range of cellular function including cellular differentiation, survival and production of inflammatory cytokines and chemokines [114]. The most widely studied molecule within the superfamily is TNFα itself. Most of the TNFα superfamily ligands and receptors are expressed by or primarily target cells of the immune system. However, epithelial cells, endothelial cells and stromal cells also express molecules of the TNFα superfamily. In addition, the superfamily is an important regulator of inflammatory, neoplastic and autoimmune disease processes. Hence the TNFα superfamily in an important regulator of the pro-inflammatory hepatic IRI process. Selected members of the TNFα superfamily involved in regulating hepatic IRI are discussed below.

1.1.4.2 TNFα

TNFα is a pro-inflammatory cytokine that as discussed in section 1.1.2.4 regulates diverse functions such as cell proliferation, apoptosis and survival [78]. It represents the most widely studied TNFα superfamily member. TNFα has two cognate receptors, TNFR1 and TNFR2. TNFR1 is efficiently activated by soluble TNFα whereas TNFR2 is activated by membrane bound TNFα. Binding of TNFα to its type I receptor (TNFR1) results in the sequential formation of two signalling complexes. The rapidly formed complex I is assembled on the receptor's cytoplasmic tail and consists of the adaptor TNF-α receptor death domain-associated protein (TRADD), the protein kinase Receptor Interacting Protein-1 (RIP1) and the signal transducer TNF-α Receptor Associated Factor-2 (TRAF2). This complex signals inflammation and survival through IκB kinase (IKK)-dependent activation of NFκB [79].

Subsequently, complex I dissociate from the receptor and TRADD together with RIP1 associate with the adaptor protein Fas-associated Death Domain (FADD) and procaspase 8 to form complex II. Activation of caspase 8 can lead to the proteolytic activation of the executioner caspase 3 and subsequent apoptosis. TNFR2 has no death domain and interacts directly with TRAF2. TNFα induced death signals usually require mitochondrial signals whereas Fas-dependent death signalling pathways are mitochondrial independent. TNFR2 exclusively activates pro-inflammatory pathways but not apoptosis [79].

The role of TNFα in pro-inflammatory liver disease has been recently reviewed [78]. In general the inhibition of TNFα function has improved liver IRI [115]. The mechanism of action of TNFα is likely to be multifactorial including generation of ROS, modulation of immune cell function and pro-inflammatory cytokine secretion.

1.1.4.3 CD40:CD154

The main function of CD40:CD154 was thought to be in providing the essential second signal in the initiation and maintenance of T-lymphocyte dependent immune responses [116]. However, a large body of research has investigated the role of the TNFα family members, CD40 and CD154, within the context of liver physiology and patho-physiology [19, 117-122]. CD40 is a type I trans-membrane receptor that is expressed upon a wide range of cells within the liver including hepatocytes, HSEC, cholangiocytes, immune cells and macrophages [123]. For further details of the role of CD40:CD154 in liver physiology see Chapter 4. The function of CD40 within cholangiocytes [118] and HSEC [120] has been well studied but its role in hepatocytes and particularly human hepatocytes remains to be fully determined. Specifically, the signalling pathways employed by CD40 following activation remain elusive. The delineation of these pathways is important as CD40 itself has

no intrinsic kinase activity [123]. Furthermore, the effect of hypoxia and H-R upon CD40 activated signalling pathways is unknown. CD154 is the cognate receptor for CD40 and has a much more limited expression repertoire being expressed upon immune cells and released by activated platelets [124]. The activation of CD40 by CD154 is likely to play an important role in IRI and in parenchymal injury [19]. However the effects upon human hepatocyte physiology and susceptibility to cell death remain to be determined. In particular whether CD40 activation can couple to ROS generation within human hepatocytes and regulate cell death is not known.

A number of studies investigating hepatic IRI have examined the role of CD40 and CD154 *in vivo* [19, 117]. These studies have uniformly shown that genetic deletion of either the receptor or ligand protects the liver against IRI. However, the studies have not investigated whether the protection is afforded by reduction in ROS generation or tissue hypoxia within parenchymal cells. Indeed the efficacy of CD154-targetted therapy to prevent rejection and to induce tolerance in some transplant models has been established [125]. Much less is known about the role of CD154 signalling in antigen-independent inflammatory responses triggered by IRI. It is known that disruption of CD154 co-stimulation or treatment with CD154 monoclonal antibody prevents hepatic IRI in mice whereas gene transfer of CD40 immunoglobulin protects rat livers from IRI [19]. However, the effects of CD40 activation upon hepatocytes during hypoxia and H-R are not known. Although it is known that CD40 activation upon human hepatocytes during normoxic conditions can induce apoptosis [122]. Therefore the investigation of the effects of hypoxia and H-R upon human hepatocyte function in the presence and absence of CD154 and its effect upon ROS generation will allow fundamental underpinning of the responses of cells to important pro-inflammatory ligands.

1.1.4.4 Fas: Fas Ligand (FasL)

The Fas receptor is a death receptor that is expressed upon numerous cells within the liver and leads to apoptosis following activation by its cognate ligand, FasL [126]. Previous studies have shown that following CD40 activation in human hepatocytes these cells can express FasL and can then induce autocrine/paracrine apoptosis [122]. This latter observation illustrates the complex role of TNFα family members in liver physiology. The role of Fas:FasL has been well studied with respect to hepatic IRI. The silencing of Fas ameliorates hepatic IRI within rodent models of liver transplantation [127] and in patients undergoing OLT the levels of soluble Fas and soluble FasL are found to be significantly higher during reperfusion implying their role in mediating liver injury [128, 129]. Following Fas activation, intracellular signalling pathways lead to the activation of caspases and in particular caspase 3 that ultimately lead to apoptosis. Certainly blockade of Fas:FasL may offer therapeutic options for IRI [130], inflammatory liver disease and liver cancer [131].

1.1.4.5 TNFα-related Apoptosis-inducing Ligand (TRAIL)

TNFα-related apoptosis-inducing ligand (TRAIL) also known as Apo2L is also a member of the TNFα family. It induces apoptotic death in a variety of cell types [132]. TRAIL binds to five membrane-bound death receptors: TRAIL-R1/DR4, TRAIL-R2/DR5, TRAIL-R3/DcR1, TRAIL-R4/DcR2 and the soluble osteoprotegerin receptor [132]. Among these, only DR4 and DR5 possess cytoplasmic tails containing a death domain that can induce apoptosis [133]. Studies in human hepatoma cell line have shown that TRAIL can induce apoptosis [133]. Whether the same is observed in primary human hepatocytes is not known. Early studies did question whether TRAIL could induce hepatocyte apoptosis during H-R [134] but more recent studies have shown TRAIL is hepatotoxic [23]. Much of the research

focusing upon TRAIL effects upon liver physiology have been centred upon its role in Hepatitis C Virus [135, 136] and the role of TRAIL in IRI remains to be firmly established.

1.1.4.6 TNF-α-related Apoptosis-inducing Ligand (TWEAK):Fibroblast Growth Factor-inducible 14 (Fn14)

TWEAK is also a member of the TNFα superfamily. TWEAK functions as a type II transmembrane protein and is the ligand for the receptor Fn14 [137]. TWEAK treatment of freshly isolated monocytes can induce apoptosis [138] but also promotes proliferation of vascular endothelial cells [139]. TWEAK may also have a role in cell migration and secretion of pro-inflammatory cytokines and adhesion molecules [137]. With regard to IRI no studies have evaluated the role of TWEAK:Fn14 in hepatic IRI but studies in models of renal IRI have shown that TWEAK:Fn14 promotes cell death and fibrosis after IRI [140].

1.1.4.7 Other TNFα Super-family Members

TNFα-related ligands usually share a number of common features. With the exception of nerve growth factor (NGF) and TNF-β, all ligands are synthesized as type II transmembrane proteins that contain a short cytoplasmic segment and a relatively long extracellular region [141]. In general, TNFα superfamily members form trimeric structures, and their monomers are composed of β-strands that orient themselves into a two sheet structure [141]. As a consequence of the trimeric structure of these molecules, it is suggested that the ligands and receptors of the TNSF and TNFRSF superfamily undergo "clustering" during signal transduction. A complete review of all TNFα family members and their individual role in hepatic IRI is beyond the scope of this thesis. Indeed no studies have evaluated the role of other TNFα superfamily members during liver IRI. Limited studies have assessed the role of

CD27 during renal IRI showing it to be pro-apoptotic and having deleterious effects upon renal physiology [142].

1.1.5 Aims of the Thesis

The broad aim of the thesis was to establish a standardised protocol for human hepatocyte isolation, establish an *in vitro* model of human hepatocyte IRI, investigate the response of human hepatocyte to hypoxia and H-R and investigate the effects of CD40 and CD154 upon liver physiology *in vivo*. More precisely the specific aims were:

I. To establish a stringent protocol for the isolation and successful culture of primary human hepatocytes.

II. To assess the effects of hypoxia and H-R upon human hepatocytes *in vitro* in terms of ROS production and susceptibility to cell death.

III. To assess the effects of CD40 activation upon human hepatocytes with CD154 during hypoxia and H-R in terms of ROS generation and susceptibility to cell death

IV. To ascertain the role of CD40 and CD154 in regulating hepatic IRI *in vivo*.

CHAPTER 2 - HUMAN HEPATOCYTE ISOLATION

2.1 Introduction

To enable the study of the effects of hypoxia and H-R upon human hepatocyte physiology and susceptibility to cell death the isolation and regular culture of primary cells needs to be standardised. This would ensure that reproducible and high quality data is obtained from *in vitro* experimental models. Furthermore, high quality primary human hepatocytes represent a valuable resource for biomedical research, commercial and, potentially, therapeutic purposes. For instance, isolated human hepatocytes infusions are used clinically in the treatment of children with in-born errors of metabolism [143]. Furthermore, to assess the effects that IRI has upon human livers and in particular how parenchymal/hepatocyte injury is induced, the regular isolation and culture of human hepatocytes is indispensible. It is becoming widely accepted that the majority of hepatocyte and hepatoma cell lines, such as HepG2 cells, may not be representative of primary hepatocyte function and are unlikely to be used therapeutically in the clinical scenarios discussed above [144-146]. Indeed, studies carried out by several groups have consistently shown that hepatoma cell lines do not accurately reflect the responses of primary hepatocytes [36]. Therefore, for research focusing upon hepatocytes the use of primary cells is not only desirable but should be considered mandatory. Primary hepatocytes are also becoming increasingly used in drug development as an experimental model for the evaluation of key human-specific drug properties such as metabolic fate, drug-drug interactions, and drug toxicity. However, anecdotal evidence from many research groups worldwide suggests the quality and metabolic/functional activity of the cells may be highly variable. Meaningful human hepatocyte research requires the regular availability of cells isolated from human liver tissue ethically provided by hepatobiliary and transplant programs.

Previously authors have suggested protocols for successful human hepatocyte isolation but these have applied exclusively to donor liver tissue [147, 148] or normal resected liver tissue [34]. Human hepatocytes have been used for commercial and experimental research for over two decades. Research has encompassed the fields of toxicology, cell transplantation and phenotypic studies. This research without exception has focused on the use of normal resected livers and donor liver tissue as the source of human hepatocytes [34, 149-154]. Thus for research involving human hepatocytes to be reflective and applicable to hepatic patho-physiology, comparative studies need to be carried out in cells isolated from different hepatic diseases. To date no systematic studies evaluating the success of human hepatocytes from all types of livers have been conducted. Clearly for research involving human hepatocytes to be undertaken the latter point is of paramount importance.

The isolation of human hepatocytes has been difficult from steatotic livers [150]. Although some groups have detailed protocols that may lead to successful routine isolation, most groups show that overall results of human hepatocyte isolation can be unacceptably variable in terms of yield and quality of cells to the point where it can impact on the economic considerations and time constraints of laboratory investigations [34, 150]. Therefore in general, previous studies have reported outcomes of human hepatocyte isolation from normal resected and donor liver tissue [34, 148].

For large-scale research utilising human hepatocytes a protocol that establishes methodology, success rate and the types of livers to use is urgently demanded. To investigate the responses of human hepatocyte to a variety of stimuli or environments the establishment of the above protocol would be an essential first step.

2.2 Methods & Materials

2.2.1 Ethics Statement

Human liver tissue was obtained from surgical procedures carried out at the Queen Elizabeth Hospital, Birmingham, United Kingdom. These livers included donor livers that were surplus to requirement for liver transplantation, liver tissue obtained from hepatic resections carried out for colorectal metastatic disease and benign hepatic diseases and explanted livers after transplantation. The Local Research Ethics Committee (LREC) (reference number 06/Q702/61) granted ethical approval for the study. Informed written consent was obtained from all participants involved in the study.

2.2.2 Human Hepatocyte Isolation

All liver tissue was obtained from fully consenting patients undergoing liver transplantation for a variety of end-stage liver diseases. Human hepatocytes were isolated from explanted diseased livers from patients with alcoholic liver disease (ALD), biliary cirrhosis (primary biliary cirrhosis (PBC) and primary sclerosing cholangitis (PSC) and a variety of other end-stage liver diseases (Cystic Fibrosis, Cryptogenic Fibrosis, Alpha-1-antitypsin Deficiency, Autoimmune Hepatitis and Non-alcoholic Steatohepatitis). Human hepatocytes were also isolated from tissue taken from patients who had undergone hepatic resections for liver metastasis arising from colorectal carcinoma, hepatic resections carried out for benign disease (recurrent cholangitis, focal nodular hyperplasia and haemangiomas), cut-down specimens and normal donor tissue surplus to surgical requirements. For the purposes of analysis, liver tissue obtained from resections for benign lesions was included in the normal liver group whereas liver tissue obtained from hepatic resections carried out for metastatic disease was classified as normal resected tissue as is referred to as this hereafter. All the

patients included in this latter group had received pre-operative chemotherapy to reduce tumour mass prior to surgery.

For all liver tissue specimens a stringent and rigorous procurement and isolation protocol was adopted and adhered too for the entire duration of the study. Following explantation or resection, specimens were immediately placed on ice in a sterile sealed drawstring bag and processed within 1 hour if logistically possible. There were however exceptions to this, in cases were hepatic resections or liver transplants were carried out at in the late evening or at night, liver tissue was kept sterile on ice overnight in sterile conditions. The significant exception to this protocol was in the use of donor liver tissue. In all cases the donor liver was assessed for transplantation by the clinical liver transplantation team at the Queen Elizabeth Hospital, Birmingham and if deemed unsuitable for liver transplantation it was then used for hepatocyte isolation. Precise time delays between explantation or resection of the liver and commencement of the isolation procedure were recorded in each case and isolation.

In isolation procedures where donor liver or liver explants were used, liver wedges were obtained from either the segments II/III or segments V/VI. The reason for this being that these segments of the liver offered suitably shaped liver wedges conducive to cannulation. In procedures where normal resected tissue was used for isolating human hepatocytes, only patients who had undergone right hemi-hepatectomies were deemed suitable by the trained pathologist to obtain normal resected liver tissue from. Again tissue was only possible from these latter specimens if adequate clearance from the tumour could be obtained. This was obtained in all cases from segments V/VI. Liver wedges were cut and weighed by a trained pathologist. To eliminate interperson variability, the subsequent hepatocyte isolation procedures were carried out by a single individual (Ricky Harminder Bhogal) using a standardised protocol that is described below.

Hepatocyte isolations were carried out using a modified 'two-stage' collagenase procedure originally developed by Berry and Friend [155]**.** This method was originally described for the isolation of rodent hepatocytes but has been adapted by several laboratories worldwide to isolate human hepatocytes. After the liver wedge was cut from the appropriate segment of the liver it was weighed and was then placed into ice-cold Dulbecco's Modified Eagles Medium (DMEM) (Gibco, Paisley, UK). The liver was then transferred to sterile CAT2 laboratory hood were it was then washed through the exposed, cut, vessels with Phosphate-buffered Saline (PBS), pH 7.2. This was to remove any remaining blood from within the liver wedge and to identify two suitable vessels that could be used for cannulation and subsequent perfusion of buffers. The vessels for cannulation were chosen using two criteria. Firstly, when washing the liver through with PBS, it is apparent which parts of the wedge were being 'perfused' by that particular vessel, hence the greater the liver area 'perfused' the more favourable the vessel was thought to be and secondly the two vessels should be in different parts of the liver wedge to ensure optimum perfusion of the whole wedge. These criteria were used in all cases of liver perfusion. Subsequently two 20-gauge cannulae (Becton-Dickinson, Oxford, UK) were sutured into the chosen vessels using a 3/0 prolene (Covidien, Hampshire, UK) purse string suture (Figure 2.1). The cannulae were then primed with PBS to ensure that subsequent buffers used for perfusion would run correctly. The final stage of preparing the liver wedge involved oversewing any major vessels that were present on the cut surface of the liver wedge, to ensure minimal loss of perfusion fluids. This also helped maintain pressure within the liver wedge throughout the hepatocyte isolation procedure.

The perfusion circuit was set up according to the widely established routine protocol detailed by previous groups (Figure 2.2). One end of the perfusion tube was fed into the perfusion

buffer, the central segment of the tubing was within the peristaltic pump (Model IP 505Du, Watson-Marlow Ltd, Falmouth, UK), and the two outlets of the tubing were connected to the sutured cannulae. The liver wedge was held over a container during the procedure. This container also contained the waste tubing that connected the container to the waste reservoir. At the commencement of the procedure, all rubber tubing remained 'open' allowing the free flow of perfusion and waste fluids. All buffers used in the isolation procedure were pre-warmed to 42^0C in a water bath. At this stage, liver wedges were first perfused with 'non-recirculating' wash buffer (10 mM 4-(2-hydroxylethyl)-1-piperazineethanesulfonic acid (HEPES) pH 7.2) (Sigma, Dorset, UK) at room temperature using a flow rate of 75 ml/min, ensuring flushing out of any remaining blood from within the liver vasculature. After this, the wedge was perfused with chelating solution (non-recirculating) (10 mM HEPES, 0.5 mM Ethylene Glycol Tetraacetic Acid (EGTA), pH 7.2) (Sigma) in order to disrupt cell adhesion to the underlying matrix. This was followed by further perfusion with (non-recirculating) wash buffer to remove any remaining EGTA from the liver vasculature, as the enzymes used to dissociate the liver are dependent upon calcium and magnesium for activation. At this point the waste tubing was clamped to allow recirculation of the enzymatic buffer. Enzyme buffer perfusion solution was made up as follows: Fresh aliquots of enzymes were removed from -20^0C storage and dissolved in Hank's Balanced Salt Solution (HBSS) (Gibco, Paisley, UK) that had been supplemented with calcium chloride (5 mM) and magnesium chloride (5 mM). Following enzyme dissolution the solution was filtered through a 0.5 μm sterile filter (Miltenyi Biotec Ltd, Surrey, UK) back into the HBSS solution. Specifically, 0.5% w/v Collagenase A (from Clostridium Histolyticum, Roche, Hertford, UK, Lot number 70273822), 0.25% w/v Protease (Type XIV from Streptomyces Griseus, Sigma, Lot number 076K1177, 4.5 units/mg), 0.125% w/v Hyaluronidase (from bovine testes, Sigma, Lot

number 025K7015, 451 units/mg) and 0.05% w/v Deoxyribonuclease (from bovine pancreas, Sigma, Lot number 107K7013, 552 units/mg) were the enzymes used. The liver wedge was perfused with the recirculating enzyme solution at 37^0C using a flow rate 75ml/min for between 1-19 min, this time was designated to be the perfusion time. The decision to stop perfusion was made when the cut surface of the liver allowed the admission of a digit into the substance of the liver. At this point the perfusion tubing and cannulae were removed and the liver was then transferred to a sterile glass dish and dissociated using manual force whilst in DMEM supplemented with 10% v/v heat inactivated foetal calf serum (Gibco), 2mM glutamine (Gibco), 20,000 units/l Penicillin, and 20mg/ml Streptomycin (Gibco) and 2.5 μg/ml Gentamycin (Gibco). Following manual dissociation of the liver wedge the suspension was passed through a sterile nylon mesh of 250 μm (John Staniar Ltd, Manchester, UK) followed by a sterile nylon mesh of 60 μm (John Staniar Ltd). Suspensions were then washed three times at 50 x g for 10 min at 4^0C in supplemented media.

Immediately after washing, cell viability was determined by trypan blue dye exclusion and deemed acceptable if greater than >50% at this stage. Hepatocytes were then plated out in supplemented media. If viability was lower than 50% but total cell yield was high (> 2 million viable cells/ cell), Percoll density gradient centrifugation of cell suspensions was carried out to improve yield of viable cells. Percoll (Sigma**)** was made by adding to PBS pH 7.2 to density of 4.5 g/ml. Percoll was added to cell suspensions and washed at 300x*g* for 30 min at room temperature. Cell viability was again determined by trypan blue dye exclusion and if improved to >50% cells were plated out at 5 x 10^5 per well in supplemented media for 2 hours onto type 1 rat collagen coated plates to allow adherence of cells. After this period, the media was changed to Arginine-free Williams E media (Sigma) containing Hydrocortisone (2 ug/ml), Insulin (0.124 U/ml), Glutamine (2 mM), Penicillin (20,000

units/l), Streptomycin (20 mg/l) and Ornithine (0.4 mmol/l). The media was exchanged every 24 hours and for subsequent functional studies, cells were used within 2 days of isolation. Liver samples from the normal liver category were histopathologically evaluated on formalin fixed paraffin-embedded sections. Steatosis was reported by the percentage of steatotic hepatocytes present and grouped accordingly: minimal/none=0-5%, mild=5-33%, moderate=33-66% and severe=>66%.

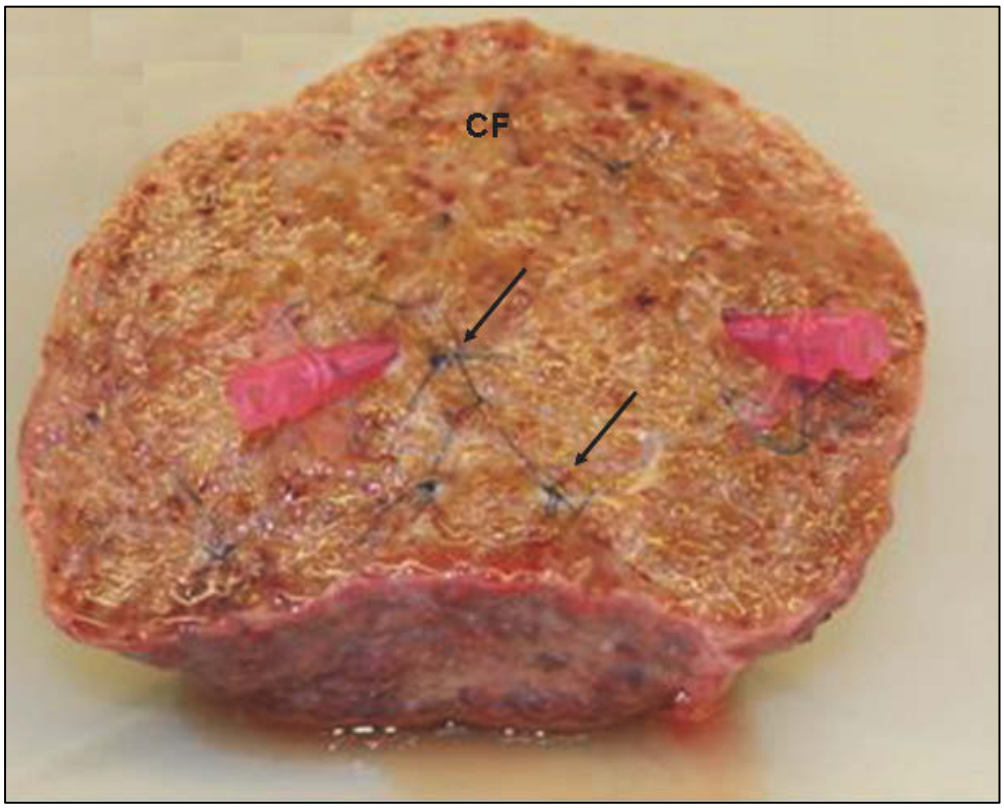

Figure 2.1 The Preparation of Liver Wedges Prior to Collagenase Perfusion
Isolation of human hepatocytes was performed from liver wedges that had been cut from either donor liver tissue, normal resected liver tissue or explanted livers (50–413 g). Liver wedges had one cut face (CF) with the remainder of the hepatic capsule being left intact. This was important to retain all perfusion fluids within the liver and prevent leakage. After washing the liver through exposed vessels with PBS, 20 G cannulae were sutured into suitable vessels with 3/0 prolene purse string sutures. The remaining vessels were oversewn using continuous 3/0 prolene sutures (arrowed). The liver wedge was then ready to be used for the perfusion isolation protocol. This processing of liver tissue was used in all cases of liver perfusions.

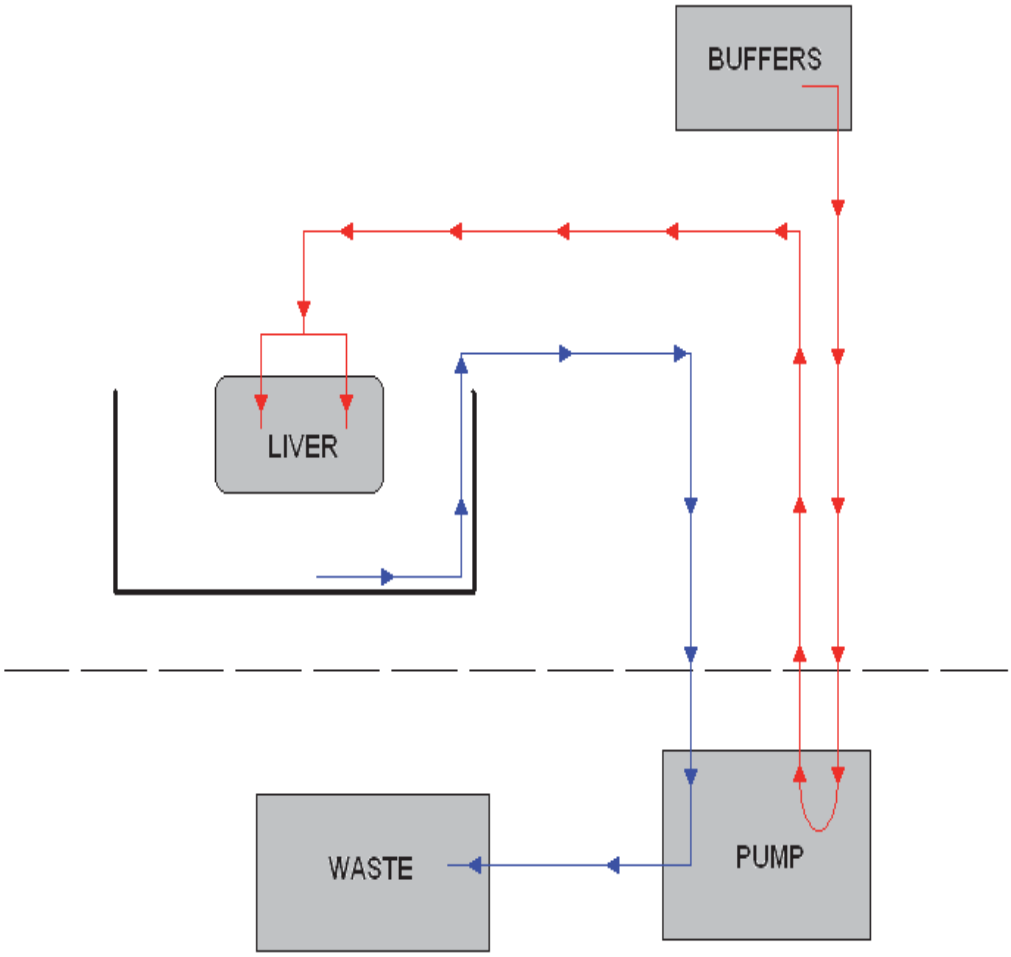

Figure 2.2 Schematic Diagram Illustrating the Set-up of Apparatus for Liver Wedge Perfusion

Illustrating the typical set-up of apparatus prior to the commencement of perfusion of liver wedges. Inlet piping (red) is connected to the relevant perfusion buffer (see Methods & Materials section) and then passed through a peristaltic pump and connected to the liver wedge via cannulae (Figure 2.1). The liver wedge and buffer are kept sterile in a CAT2 laboratory hood (dashed line). The liver is placed in a glass container that contains waste tubing (blue) that is finally connected to a waste pot. This apparatus set-up was used for all liver perfusion without exception. Following perfusion of buffers the waste tubing was clapped to allow non-recirculating perfusion of the enzymatic buffer. Once the liver was adequately perfused with the enzymatic buffer the liver was disconnected from all tubing and cannulae and broken up with mechanical disruption in a sterile bowl in the CAT2 laboratory hood.

2.2.3 Urea Synthesis Assay

Confirmation of urea synthesis by isolated human hepatocytes was performed using quantitative colorimetric urea determination (QuantiChrom™ urea assay kit-DIUR-500) (Bioassay Systems, Hayward, CA, USA). Urea is primarily produced in the liver and secreted by the kidneys. Urea is the major end product of protein catabolism in animals. It is the primary vehicle for removal of toxic ammonia from the body. The QuantiChrom assay kit measures urea directly in biological samples without any pretreatment. The adapted Jung method [156] utilises a chromogenic reagent that forms a coloured complex specifically with urea. The intensity of the colour, measured at 520 nm, is directly proportional to the urea concentration in the relevant sample. The optimised formulation substantially reduces interference by substances in the raw samples. Biological samples were assayed in triplicate and sample concentration of urea was determined by reference to standard curve and using the formula below:

[Urea] = OD sample – OD Blank/OD standard – OD blank x *n* x [STD] (mg/dL)

OD sample, OD blank and OD standard are OD values of sample, standard and water, respectively. *n* is the dilution factor. [STD] = 50

2.2.4 Albumin Synthesis Assay

Albumin is the most abundant plasma protein in humans. It accounts for about 60% of the total serum protein. Importantly albumin is synthesised by hepatocytes and is a reliable marker of hepatocyte function. Albumin synthesis by isolated human hepatocytes was confirmed using a colometric assay kit (Abnova, USA, Catalogue number KA1612). The

albumin kit quantified albumin using a colometric assay that utilizes the ability of bromcresol green to form a coloured complex specifically with albumin. The intensity of the colour was measured at 620 nm and the intensity was directly proportional to the albumin concentration in the sample. Albumin standard solutions were used to generate a standard curve.

To ascertain the precise concentration of albumin in a sample the reading for blank OD was subtracted from the standard OD values and these OD were plotted against the standard concentrations. This then generated a standard curve that was used to determine the sample albumin concentration (0.1 g/dL albumin equals 15 μM, 0.1% or 1000 ppm).

2.2.5 Immunostaining Human Hepatocytes for Cytokeratin 18, EpCAM, Cytokeratin 19

Following successful isolations, cytospins of hepatocytes were made on Poly-L-lysine coated glass slides and fixed for 5 min in acetone. Cells were then incubated with 20% normal rabbit serum (Dako, Cambridge, UK) in 2-Amino-2-(hydroxymethyl)-1,3-propanediol (Tris)-buffered saline pH 7.4 (TBS) for 30 min. Monoclonal antibody to Cytokeratin 18 diluted 1:100 (clone DC10, Dako) or monoclonal antibody to Cytokeratin 19 diluted 1:100 (clone RCK108, Dako) or monoclonal antibody to CD326 (Epithelial Cell Adhesion Molecule (EpCAM) diluted 1:100 (clone HEA125, Progen, Heidelberg, Germany) was applied for 60 min, followed by polyclonal rabbit-anti mouse IgG antibody (1:25 dilution, Dako) for 30 min and finally anti-alkaline phosphatase (APAAP) complex (1:50 dilution in TBS) for 30 min. After each incubation step cytospins were washed x3 in TBS. Antibody binding was visualised with 0.2 mg/ml naphthol-AS-MX-phosphate dissolved in Dimethylforamide, (Sigma), 1mg/ml Fast Red (Sigma) in 0.1 M Tris buffer (pH 8.2) and

0.25 mg/ml Levamisole (Sigma) for 15 min followed by counterstaining with Mayer's haematoxylin (Dako). Control cytospins were included where primary antibody was substituted with isotype-matched immunoglobulin. Slides were then mounted with Immunoblot mounting medium (Dako) and assessed for positivity using light microscopy.

2.2.6 Enzyme-linked Immunosorbent Assay (ELISA) of Human Hepatocytes and HSEC for Cytokeratin 18, Cytokeratin 19 and CD31

Cells (hepatocytes or HSEC) were plated on rat type 1 collagen-coated 96-well flat-bottom plates for 24 hours after successful isolation. Cells were then fixed in ice cold methanol for 5 min. Non-specific binding of monoclonal antibodies was inhibited by pre-incubation of cells for 1 hour at 37°C with 4% goat serum (Sigma) before the addition of mouse anti-human monoclonal antibody (IgG Isotype-matched control (Invitrogen) CD31 (Dako), cytokeratin 19 (Dako), cytokeratin 18 (Invitrogen) for 1 hour at 37°C. The cells were then washed thoroughly before incubation with peroxidase-conjugated goat anti-mouse secondary antibody (Dako). The ELISA was developed using *O*-phenylenediamine substrate (OPD, Dako) according to the manufacturer's instructions and the enzymatic reaction was stopped using 0.5 mol/L H_2SO_4 (Fisher Scientific, Leicestershire, UK). Colorimetric analysis was performed by measuring absorbance values at 490 nm using a Dynatech Laboratories MRX plate reader. All treatments were performed in triplicate for each experiment.

2.2.7 Statistical Analysis

For human hepatocyte isolations, univariable analysis was performed to test the effect of specific factors upon outcome measures, human hepatocyte cell viability following a preparation, total cell count after preparation and success. Success was defined as

maintenance of cell adherence and morphological integrity 48 hours after plating onto type I rat collagen and their subsequent use in functional studies. The specific factors analysed were hepatic disease type, time delay between hepatectomy and beginning of the liver perfusion, weight of liver wedge, perfusion time, the level of steatosis in the normal liver cohort, and the use of Percoll enrichment. In univariable analysis, Mann-Whitney tests were used for the time and weight variables, as these variables did not to follow a normal distribution, with Fisher's Exact test being used for the categorical variables. Multivariable analysis was performed by considering all specific factors simultaneously and assessing the effect upon the said outcome measures. For this analysis logistic regression models were used.

Repeated-measures ANOVA was utilised to analyse the synthesis of albumin and urea by human hepatocytes isolated from normal, PBC/PSC, ALD and normal resected liver tissue.

All data are expressed as mean ± S.E. Statistical comparisons between groups were analysed by Student's *t* test. All differences were considered statistically significant at a value of $p<0.05$. All data are expressed as mean ± S.E. Statistical comparisons between groups were analysed by using the Mann-Whitney test. All differences were considered statistically significant at a value of $p<0.05$.

2.3 Results

2.3.1 Morphology of Isolated Primary Human Hepatocytes

Liver wedges were prepared as shown in Figure 2.1 and processed as detailed in the Methods & Materials section above. Figure 2.3 shows representative images of primary human hepatocytes, isolated from PBC livers, in culture for the first week after isolation. Similar morphological changes were observed during the first week after successful cell isolation from normal, PSC, ALD and normal resected liver tissue. Indeed, Figure 2.4 demonstrates the morphological features of primary human hepatocytes isolated from these various livers 3 days after successful isolation. The morphology of primary human hepatocytes after 3 days in culture was maintained for at least one week after successful isolation.

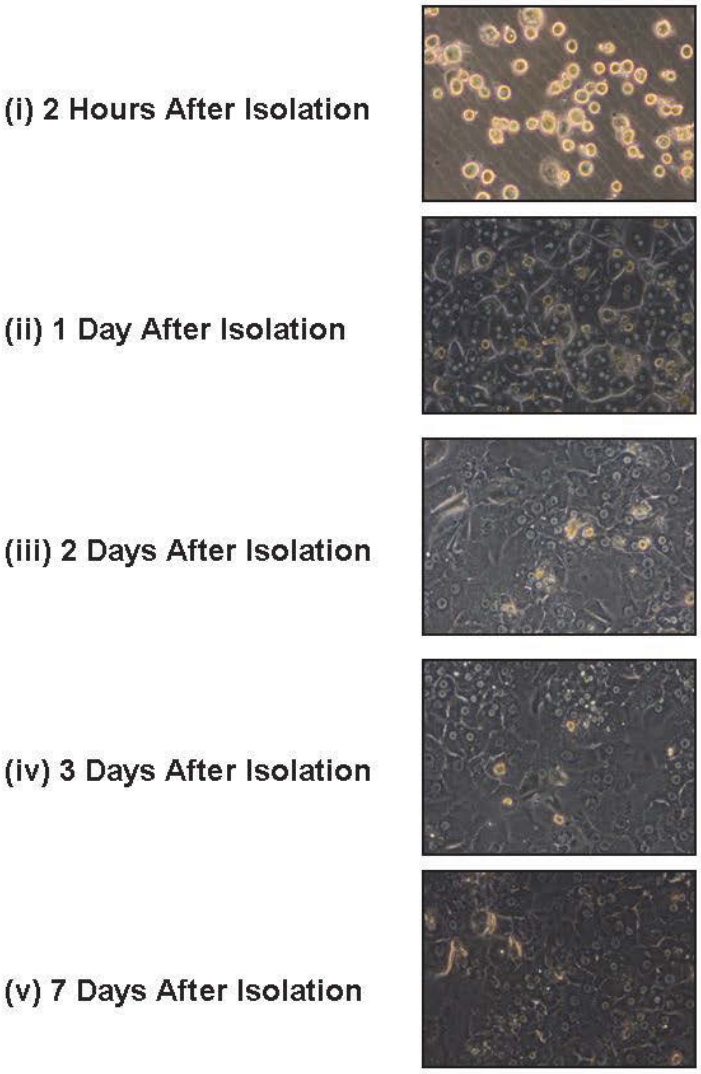

Figure 2.3 Morphology of Primary Human Hepatocytes after Isolation in Culture
Comparison of the morphological appearance of primary human hepatocytes isolated from PBC attached to collagen-coated plates at (i) 2 hours after isolation (magnification 20x), (ii) 1 day after isolation, (iii) 2 days after isolation, (iv) 3 days after isolation and (v) 1-week after isolation using light microscopy. The representative images show the change in morphology of primary human hepatocytes isolated from PBC livers during 1-week in culture. Immediately after isolation, cells appear ovoid and phase bright. Following 1 day in culture the cells appear binucleate and have formed a confluent monolayer. Primary human hepatocytes maintain this morphology throughout the one-week culture period. Similar morphological changes were observed for human hepatocytes isolated from normal, ALD and normal resected liver tissue.

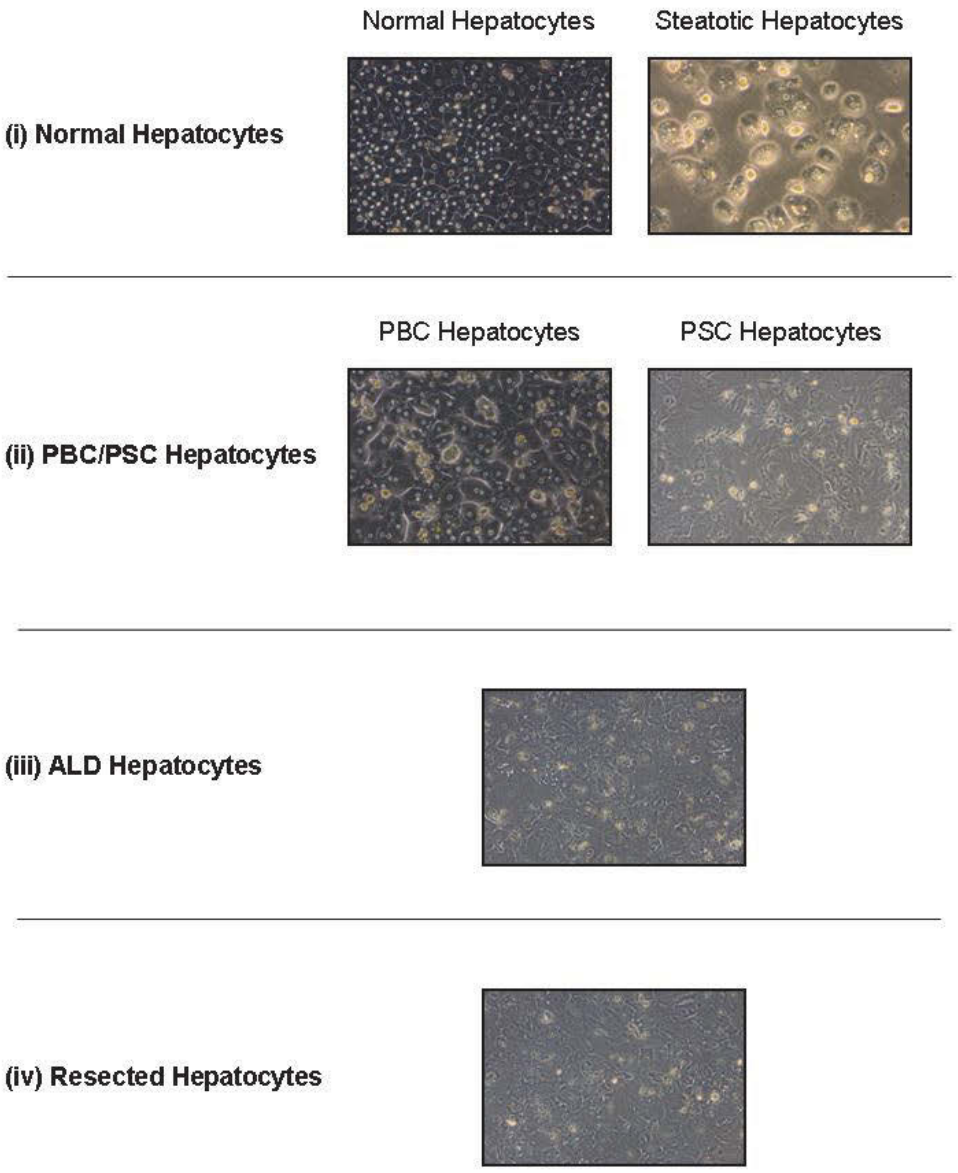

Figure 2.4 Morphology of Primary Human Hepatocytes in Culture at 3 Days
Representative images of the morphology of human hepatocytes isolated from normal, PBC/PSC, ALD and normal resected liver tissue are shown in culture 3 days after successful cell isolation. Human hepatocytes demonstrated and maintained this morphology for at least one week following successful isolation. (i) Demonstrates the morphology of human hepatocytes isolated from normal liver tissue and macro-steatotic liver tissue (magnification 20x). Primary human hepatocytes isolated from normal liver tissue display the typical cubic binucleate cell morphology. In contrast, primary human hepatocytes isolated from overtly macro-steatotic livers demonstrate obvious micro-vesicular steatosis. (ii) Human hepatocytes isolated from end stage biliary cirrhosis (PBC/PSC) again show the typical features of cells in culture with a cubic and binucleate morphology. (iii-iv) Cells isolated from ALD and normal resected liver show similar morphological features to human hepatocytes isolated from normal non-steatotic livers and biliary cirrhosis but also exhibit micro-vesicular steatosis.

2.3.2. Types of Liver Used and Success of Primary Human Hepatocytes Isolations

The type of livers used and the main results of all human hepatocyte isolations are shown in Table 2.1. In total 149 livers were processed and used for the isolation of primary human hepatocytes. A variety of liver diseases were used including ALD, biliary cirrhosis (PBC and PSC), normal resected liver and normal liver tissue (donor liver tissue, resections for benign liver disease, in-situ splits and cut-down specimens). A large proportion of livers used were from cirrhotic, end stage liver diseases (49%). Normal resected liver tissue was defined as liver tissue from patients with colorectal metastasis accounted for 18% of livers used. All these latter patients had received pre-operative chemotherapy for reduction of tumour mass prior to surgery.

Overall, for all human hepatocyte isolations a median cell viability of 37% was observed. Human hepatocytes isolated from biliary cirrhosis (PBC and PSC) had the highest median cell viability (57%). Univariable and multivariable analysis showed the only factor, which had an effect upon improving cell viability, was the time delay between hepatectomy and beginning of the perfusion procedure ($p<0.05$, Mann-Whitney test). Complete processing within 3 hours resulted in a significantly higher cell viability (> 50%), compared to time delays greater than 5 hours ($p<0.05$, Odds Ratio = 3.594). Whether the delay is 3-5 hours or more than 5 hours did not have a significant effect on the likelihood of the cell viability being greater than 50% ($p=0.375$, Odds Ratio = 1.725). These data are summarised in Table 2.2. Percoll density gradient centrifugation was used to enrich hepatocytes purity where cell viability was low but absolute cell count high (n=11). These data are summarised in Table 2.3. Percoll enhanced purity of human hepatocyte isolates but at the expense of cell count, hence the need for a relatively high absolute cell count after the initial liver preparation.

All donor liver tissue, resections performed for benign liver disease (recurrent cholangitis, focal nodular hyperplasia and haemangiomas), in-situ splits and cut down specimens were classified arbitrarily as 'normal' liver tissue. These livers had no macroscopic signs of intrinsic liver disease. This group was analysed as a whole and as a sub-group, where donor liver tissue was compared to normal liver tissue (resections from benign liver disease, in-situ splits and cut down specimens). Sub-group analysis was carried out to determine whether the level of steatosis had an effect upon absolute cell count, cell viability and success rate of subsequent human hepatocyte culture. The level of steatosis in the two groups is shown in Table 2.4. No differences in absolute cell count and cell viability between the donor liver and normal liver groups. The success of isolating human hepatocytes from this group as a whole was good (43%) but normal liver tissue obtained from hepatic resections carried out for benign disease, in-situ splits and cut-down specimens had a statistically higher success rate (50%) when compared to donor liver tissue (20%).

The reported data is the largest series within the literature of human hepatocyte isolations from cirrhotic end-stage liver disease (n=73). A median success rate of 42% was observed when isolating hepatocytes from cirrhotic livers. Indeed, as Table 2.1 shows liver wedges from biliary cirrhosis (PBC and PSC) had the highest success rate of all livers used in the study (71%). For all liver isolations, univariate analysis showed a significant difference in time delay between hepatectomy and beginning of liver perfusion ($p<0.001$, Mann-Whitney test), perfusion time ($p<0.05$, Mann-Whitney test) and disease type ($p<0.05$, Fisher's Exact test) between the groups of successful and unsuccessful isolations. Multivariable analysis revealed disease type ($p<0.05$) and time delay between hepatectomy and beginning of perfusion ($p<0.05$) were significant factors affecting successful human hepatocyte isolation. As described above for cell viability, success is significantly dependent upon time delay

($p<0.01$), with a delay of less than 3 hours resulting in improved success rates compared to those of more than 5 hours ($p<0.05$, Odds Ratio = 3.735).

Absolute cell count after isolation was an important parameter on which to assess efficacy of the procedure. Univariable analysis revealed that disease type ($p<0.001$, Fisher's Exact test) was the only factor to have a significant bearing upon total cell count after primary isolation. Multivariable analysis showed that ALD livers have a significantly lower cell yield when compared to other liver categories ($p<0.15$ – Table 2.1).

Table 2.1 The Type of Livers used and the Main Results of All Human Hepatocyte

Liver Type	Time Delay (hrs)	Weight (g)	Perfusion Time (min)	Absolute Cell Count After Perfusion $x10^3$	Viability (%)	Success Rate (%)
Normal (n=49)	2.5 (1-14)	110 (66-413)	1.5 (1-11)	75 (57-200,000)	46 (0-100)	43
Donor Liver (n=17)	6.5 (2-14)	117 (101-150)	2 (1-11)	1500 (25-200,000)	16 (0-60)	20
Normal Liver (n=32)	2 (1-4)	121 (66-413)	2.5 (1-7)	420 (75-32,000)	51 (10-100)	50
Resected (n=27)	2.5 (1-16)	90 (50-180)	1.5 (1-5)	220 (50-6,000)	50 (0-100)	53
Biliary Cirrhosis (n=31)	1.5 (1-11)	98 (78-200)	1.5 (1-8.5)	980 (200-7,000)	57 (0-100)	71*
ALD (n=30)	2.5 (1-13)	110 (64-220)	4 (1-19)	90** (20-3,000)	35 (0-100)	26
Others (n=12)	4.5 (1-12)	102 (56-115)	5.5 (3-17)	180 (40-3,000)	6 (0-70)	8
TOTAL (149)	2 (1-16)	115 (50-413)	2.5 (1-19)	370 (20-200,000)	37 (0-100)	45

The time delay, weight of liver wedges, perfusion time, absolute cell count after perfusion, cell viability and success rate are shown for various liver categories; Normal (donor liver tissue, normal benign tissue, in-situ splits and cut-down specimens), normal resected liver tissue, biliary tissue (PBC and PSC), ALD and others (cystic fibrosis 2, cryptogenic fibrosis 3, alpha-1-antitypsin deficiency 1, autoimmune hepatitis 1, primary graft non-function 1 and non-alcoholic Steatohepatitis 4). All values are represented as medians and the values in parentheses represent the range. n, number of cases.

** $p<0.05$, multivariable analysis showing ALD livers yield significantly lower cell yields when compared to other liver diseases.

* $p<0.05$, multivariable analysis showing biliary cirrhosis yielded a higher success rate of human hepatocyte isolation when compared to other liver diseases.

Table 2.2 Effect of Time Delay Between Hepatectomy and Beginning of the Perfusion Procedure Upon Human Hepatocyte Cell Viability Following Isolation

Time Delay (hrs)	Median Cell Viability (%)
<3	57
3-5	22
>5	20

Table 2.3 Effect of Percoll upon Cell Viability and Absolute Cell Count

Absolute Cell Count after Preparation $x10^3$	**Viability** (%)	**Absolute Cell Count after Percoll** $x10^3$	**Viability after Percoll** (%)
490 (200-200,000)	32 (10-50)	195 (100-400)	87 (55-90)

The effects of Percoll upon human hepatocyte isolation procedures. Percoll was used after eleven human hepatocyte isolation procedures (normal resected liver tissue 1, biliary cirrhosis 7, donor liver tissue 1, cryptogenic cirrhosis 1 and normal benign liver tissue 1). All values are represented as medians and the values in parentheses represent the range.

Table 2.4 The Level of Steatosis in Liver Wedges Taken from Donor Liver Tissue and Normal Liver Tissue

	Minimal/None	Mild	Moderate	Severe
Donor liver tissue (n=17)	1	5	7	4
Normal liver tissue (n=32)	16	8	4	-

The level of steatosis in liver wedges taken from normal liver tissue. The level of steatosis was classified as minimal/none=0-5%, mild=5-33%, moderate=33-66% and severe=≥66% after histological analysis of paraffin embedded sections. Classification of the level of steatosis was not possible in three liver wedges (1 donor liver and 4 normal livers) as the tissue from those particular livers was not available. n, number of livers.

2.3.3 Phenotype of Isolated Primary Human Hepatocytes

Isolated cells from human liver tissue showed 100% positivity for the hepatocyte cell marker, Cytokeratin 18 (CK 18) upon Immunostaining (Figure 2.5). Isolated human hepatocytes also show strong colometric absorbance with Cytokeratin 18 upon ELISA (Figure 2.6). Moreover, isolated hepatocytes showed no staining with the biliary epithelial cell marker, Cytokeratin 19 (CK 19), or the hepatic progenitor cell marker, CD326 (EpCAM) (Figure 2.5). Isolated human hepatocytes demonstrated no staining with the biliary epithelial cell marker CK19 and hepatic sinusoidal endothelial cell (HSEC) marker CD31 upon ELISA. In contrast, HSEC, which were isolated using a well-established isolation technique [157] demonstrate strong positivity for CD31 and no staining with CK 18. These findings show that the isolation technique isolates human hepatocytes of a high purity with little or no contamination from other liver cells.

Furthermore, all hepatocytes isolated from normal and diseased liver tissue demonstrated albumin and urea synthesis in the first week after isolation (Figure 2.7). Human hepatocytes isolated from normal, normal resected and biliary cirrhosis demonstrated significantly greater albumin synthesis after two days in culture. Interestingly, human hepatocytes isolated from ALD livers demonstrated significantly reduced levels of albumin production when compared to other hepatocytes. Urea synthesis by human hepatocytes demonstrated similar characteristics, with production of urea being significantly higher on day 2 when compared to other days in culture. Of note biliary cirrhosis and normal resected human hepatocytes produce significant greater amounts of urea in culture when compared to other human hepatocytes.

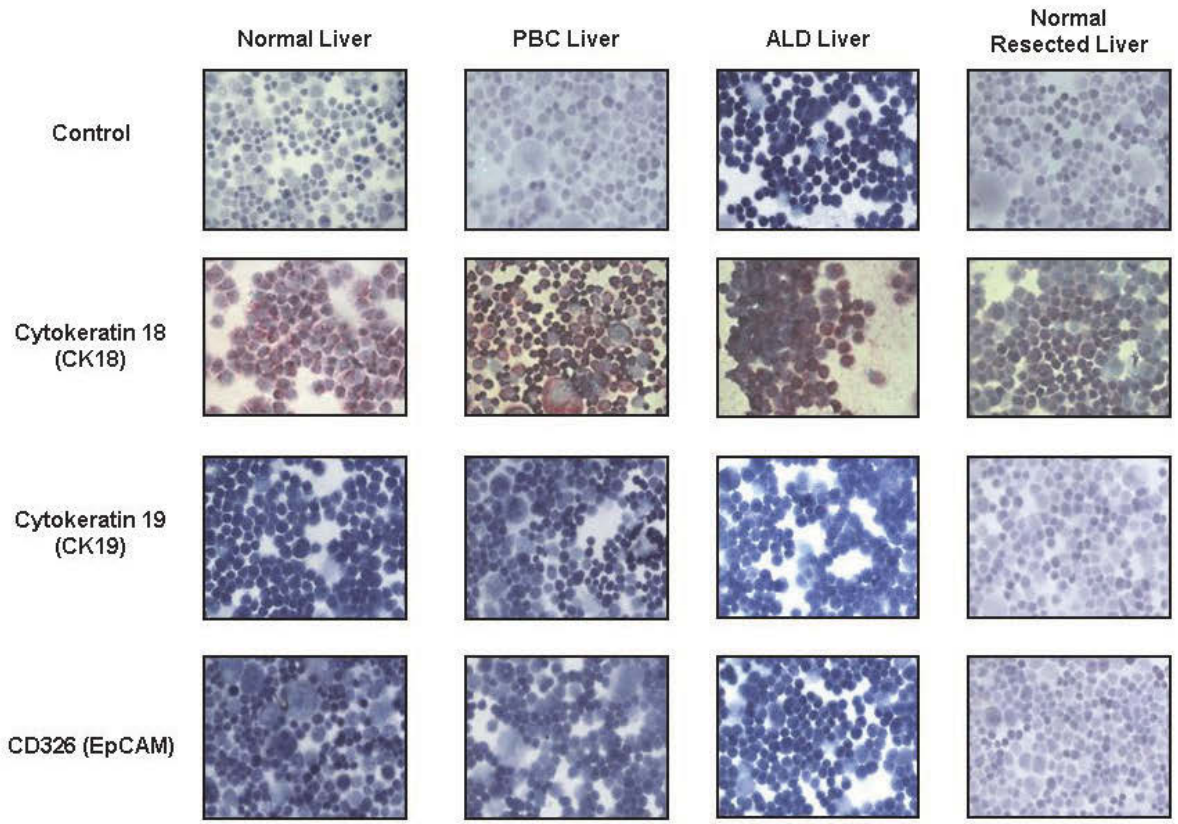

Figure 2.5 Immunostaining of CK18, CK19 and CD326 in Primary Human Hepatocytes Isolated from Normal and Diseased Liver Tissue

(a) Human hepatocytes isolated from normal, PBC, ALD and normal resected liver tissue show strong staining for the intracellular hepatocyte marker Cytokeratin 18 (CK18). In contrast, isotype matched controls immunoglobulin showed no positivity. Furthermore, isolated human hepatocytes showed no staining with the biliary epithelial cell marker Cytokeratin 19 (CK19) or hepatic progenitor cell marker CD326 (EpCAM). Cytospins of human hepatocytes were made immediately after successful cell isolation, fixed in acetone for 5 min and stored at -20^{o}C until immuno-staining was performed. (n=3).

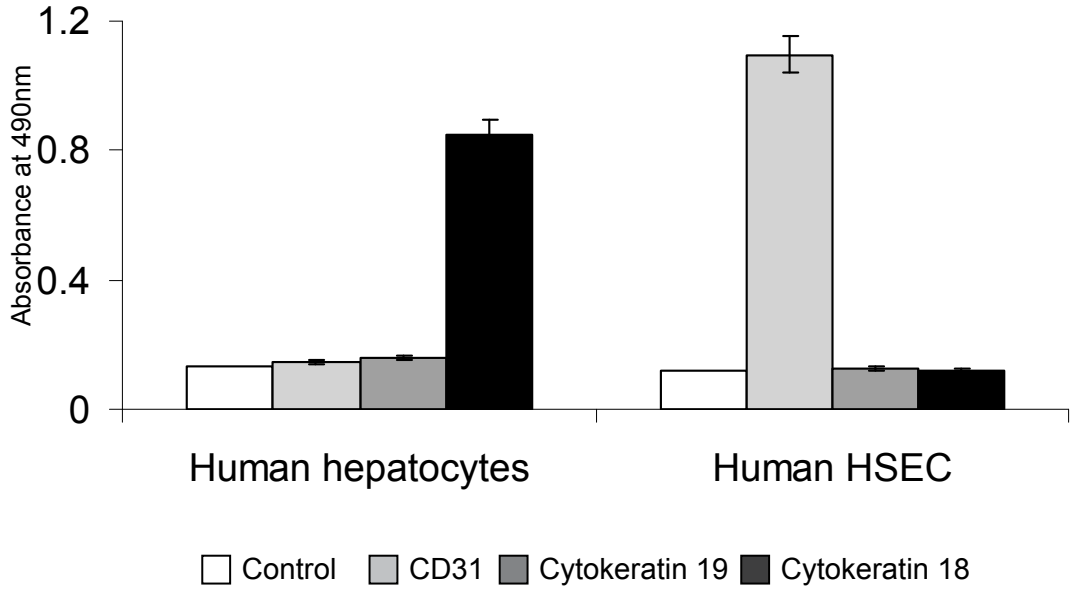

Figure 2.6 Primary Human Hepatocytes Express CK18 but not CD31 or CK19
The cell specific markers, Cytokeratin 18, Cytokeratin 19 and CD31 were determined using cell based ELISA as described in the Methods and Materials section. Primary human hepatocytes isolated using the protocol detailed above demonstrate strong staining for the hepatocyte specific marker, Cytokeratin 18. These cells show no staining for the biliary epithelial marker, Cytokeratin 19 or endothelial cell marker, CD31. In contrast, hepatic sinusoidal endothelial cells show strong positivity for the marker CD31 and no positivity for either Cytokeratin 18 or Cytokeratin 19. Data are expressed as mean ± S.E. (n= 5-7).

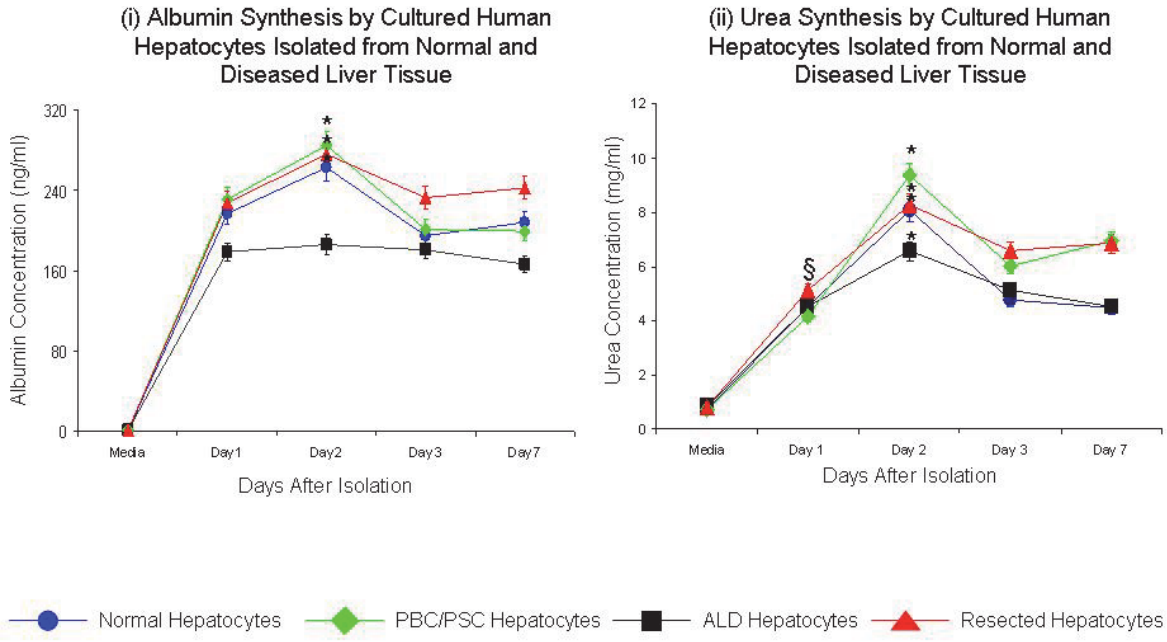

Figure 2.7 Albumin Synthesis and Urea Secretion by Primary Human Hepatocytes in Culture after Isolation
Following successful isolation, human hepatocytes isolated from normal, PBC/PSC, ALD or normal resected liver tissue were able to synthesise albumin (i) for at least one week demonstrating active metabolic activity in culture. Human hepatocytes isolated from normal, PBC/PSC and normal resected liver tissue show significantly greater albumin synthesis after two days in culture (*$p<0.05$). Moreover, human hepatocytes isolated from ALD livers synthesised significantly less albumin than other types of human hepatocytes ($p<0.05$). In addition, human hepatocytes isolated from normal resected liver tissue synthesised significantly greater amounts of albumin than normal hepatocytes ($p<0.037$). (n=3-4 separate samples). Human hepatocytes isolated from normal, PBC/PSC, ALD and normal resected liver tissue were also able to synthesise urea (ii) for at least one week following successful cell isolation. Human hepatocytes isolated from both normal and diseased liver tissue synthesised significantly lower levels of urea one day after isolation (§$p<0.001$) compared to the remainder of the culture period, but all human hepatocytes produced significantly more urea on day 2 when compared to other days (*$p<0.001$). Finally, PBC/PSC and normal resected human hepatocyte synthesis significantly greater amounts of urea when compared to the other human hepatocytes ($p<0.05$) but there was no significant difference between PBC/PSC and normal resected human hepatocytes. Data are expressed as mean ± S.E. (n=3-4 separate samples).

2.4 Discussion

There are numerous studies assessing the isolation of human hepatocytes from normal resected or donor liver tissue [34, 150, 151]. The preparation of primary human hepatocytes is a time consuming, logistically demanding, and expensive process. The demand for high quality human hepatocytes for cell transplantation and pharmo-toxicological studies continues to rise [143]. However, the availability of human liver tissue for laboratory investigation remains limited. Therefore, cirrhotic end-stage livers, which are more readily available to researchers, represent another potential source of human hepatocytes. No previous studies have systematically evaluated the isolation of human hepatocytes from all available livers, including end-stage liver disease, using one standardised isolation protocol and cohorts of specimens large enough to permit meaningful statistical analysis. The experience outlined above highlights some fundamental issues that are required for making isolation of primary human hepatocytes from normal or diseased livers a viable proposition.

The data suggests that isolating human hepatocytes from ALD livers is technically challenging even in experienced hands. With a success rate of 26%, the lowest success rate aside from the group containing 'other' liver types. The use of ALD livers for hepatocyte isolation is a questionable proposition. This may in part be explained by the variable disease stage of the ALD cohort that would have included in the analysis. These livers would have been from advanced stages of cirrhosis and would have sustained toxicological cell damage resulting from the effects of excessive alcohol. Excluding the 'other' disease categories, ALD livers had the longest median perfusion time again presumably reflecting that these livers were from patients with more advanced liver cirrhosis. Moreover, human hepatocytes isolated from ALD demonstrate significantly less albumin production when compared to the other human hepatocytes cohorts. This latter point would certainly support hypothesis of

alcohol having a directly toxic effect upon these hepatocytes. The presented data further highlights that patients in whom the primary cause of cirrhosis is biliary (PBC or PSC) human hepatocyte isolation can be very efficacious (success rate 71%). Furthermore, human hepatocytes isolated from biliary cirrhosis demonstrate the highest levels of albumin and urea production. As discussed below, this success rate is at least equivalent to normal benign resections and cut-down specimens despite having advanced end stage liver disease. In biliary cirrhosis cytoprotective agents such as ursodeoxycholic acid (UDCA) are routinely used therapeutically. Certainly, UDCA is known to inhibit the accumulation of ROS [158] and has anti-apoptotic effects upon hepatocytes [159]. These agents may therefore aid human hepatocytes isolation in an analogous way to that suggested in recent reports which show that the antioxidant, N-acetylcysteine (NAC), aids human hepatocyte isolation from donor liver disease [148]. Conversely, alcohol consumption increases ROS production and is known to be of the instigators of hepatocyte injury during ALD [160]. Furthermore, alcohol induces a plethora of toxic metabolites and cytokines that perpetuate hepatocyte injury. Hence the contact between end-stage ALD hepatocytes and enzymes used in the digestion process may create additional cellular stresses that precipitate human hepatocyte cell death and hence lower cell viability and cell yields. Human hepatocyte isolation from end-stage cirrhotic livers other than ALD and biliary cirrhosis had very poor results (success rate 8%) and hence the use of these particular livers would not be recommended for cell isolation.

A success rate of 53% for human hepatocyte isolation from normal resected livers was observed, which is lower than that reported by other authors [151, 161]. There are several potential explanations for this. Other studies have used different enzyme cocktails and may have been more selective initially when deciding which livers to process [34]. Recent studies have used the enzyme Liberase to isolate human hepatocytes from normal resected liver

tissue and have reported higher cell viabilities and cell yields [34]. The presented data does concur with previous studies that suggest normal resected tissue is a good source of human hepatocytes. Whether human hepatocytes isolated from normal resected liver tissue differ functionally in their response to physiological stimuli when compared to other human hepatocytes is not known (see Chapter 3). Most authors accept that there was no objective evidence that the function of human hepatocytes isolated from normal resected liver tissue was altered although this has not been objectively tested [161].

The reported successful isolation from normal liver tissue, both donor liver tissue and benign resection and cut down specimens is also lower than that reported by previous authors [151]. However, when this group was further analysed the isolations performed upon liver wedges from benign resections and cut down specimens gave good success rates (53%) compared to donor liver tissue (20%). Previous authors have also noted that the best results of human hepatocyte isolations, in terms of high cell viability and cell yield, were achieved with tissue removed from patients with benign liver diseases [34, 161]. The donor livers used in the data presented above had been turned down for transplantation as a result of macrosteatosis and as Table 2.4 demonstrates human hepatocytes from these steatotic livers also exhibit micro-vesicular steatosis. The rate of successful human hepatocyte isolation in livers with a low level of steatosis was greater than in those with a high level of steatosis (64% vs. 20%), although this was not statistically significant ($p=0.118$). The reason for the non-significance is likely to be down to the small sample size. Previous authors have also noted that high degrees of steatosis generally did not favour successful cell isolation [150, 151]. Certainly, steatotic hepatocytes have higher intracellular ROS levels and more susceptible to damage [148]. The recent work of Sagias *et al* suggests that the addition of NAC to perfusion fluids may improve hepatocyte yields from steatotic livers [148]. Another, contributory factor for

the lower cell viability and cell yield of human hepatocytes from donor liver is the longer cold ischaemic time that donor livers have been exposed to when compared to normal livers (Table 2.1).

Previous authors have suggested that the optimal liver wedge weight for human hepatocyte isolation is approximately 100 g [34]. The majority of liver wedges used in the data presented above were between 80-120 g. Therefore a relatively consistent liver wedge weight was used thus the effect of this parameter upon human hepatocyte isolation could not be evaluated.

A median perfusion time of 2.5 min was required to digest livers, as judged by the admission of a digit into the liver substance. Other studies report digestion times ranging from 20-47 min [34, 162]. This could simply be a reflection of different enzyme types, different enzyme concentrations and different enzyme lots. In the reported data series all enzyme lots and batches were kept constant. Certainly, this enzyme cocktail allowed isolation of cells from end-stage cirrhotic livers and it remains possible that this enzyme concentration may be excessive for normal resected and donor liver tissue thereby explaining the lower yield and viability compared with other reports.

Perfusion time, whilst being significant in the univariable analysis, was not found to be significant in the multivariable analysis. The reason for this is likely to be the fact that the variable is significantly correlated with the time delay between hepatectomy and beginning of liver perfusion (Spearman's Rho = 0.377, $p<0.01$). In the logistic regression model, time delay between hepatectomy and beginning of liver perfusion, remained significant even after adjusting for perfusion time.

Therefore, the presented data shows that for successful human hepatocyte isolation time delay between hepatectomy and beginning of liver perfusion should be kept to less than 3

hours. Perfusion time ($p<0.01$) and type of hepatic disease ($p<0.01$) both have significant effects upon successful human hepatocyte isolation. However, the fact that neither was significant in the multivariate analysis shows that the majority of this effect can be explained by other variables. The crucial factors for isolating human hepatocytes from all livers and especially cirrhotic livers appears to be that after an initial learning curve, operators become skilled at recognising when a cirrhotic have become adequately digested allowing the termination of the liver perfusion and avoiding overdigestion of tissue leading to reduced cell viability.

In conclusion, the time delay between hepatectomy and beginning of liver perfusion is the most important factor in determining good cell viability and likelihood of success of the procedure. Furthermore, the shortest possible digestion time is desirable. In terms of cirrhotic livers, biliary cirrhosis appears to have a better success rate when compared to ALD. In addition a unified protocol can be used to successfully isolate human hepatocytes from all liver types.

In the experience outlined above it is clear that a challenging operator learning curve has to be overcome before routine isolation of human hepatocytes from cirrhotic livers can yield acceptable success rates. Each study, detailing the procedure of human hepatocyte isolation brings us closer to improving the existing technologies and therefore aiding future research.

CHAPTER 3 - THE RESPONSE OF PRIMARY HUMAN HEPATOCYTES ISOLATED FROM NORMAL AND DISEASED LIVER TISSUE TO HYPOXIA AND HYPOXIA-REOXYGENATION

3.1 Introduction

3.1.1 Hepatocyte Responses to Hypoxia and H-R

Most studies that have investigated the mechanisms of liver damage that occur as a result of IRI have focused upon the broad setting of liver transplantation [16, 163, 164]. It is equally possible that relatively hypoxic conditions can occur during other episodes of hepatic inflammation and/or established chronic disease. Hepatocytes exposed to a hypoxic microenvironment would therefore be potentially sensitised to cell death, although no studies have yet explored this process in primary human hepatocytes. Previous studies have explored the responses of rodent and murine hepatocytes to hypoxia but these studies in general have failed to explore the effects that subsequent H-R has upon the same hepatocytes following hypoxia/ischaemia [21, 22, 117]. Moreover, it is well appreciated that there is considerable inter-species variability of hepatocytes to the same microenvironment and/or extracellular cues [165, 166]. Therefore, generalisation cannot be made about the physiological responses of hepatocytes based upon experimental findings from one species.

As discussed earlier, despite considerable advances in surgical practice and more judicious use of immunosuppression, hepatic IRI continues to adversely affect allograft function and patient survival following OLT. The work of Toledo-Pereyra *et al* established the detrimental effects of IRI during experimental liver transplantation [38]. Indeed as a result of this work and more recent studies hepatic IRI is now understood to be a pro-inflammatory, antigen-independent process that culminates in parenchymal injury [40]. The primary cellular target during hepatic IRI is the hepatocyte. Hepatocyte cell death seen during the hypoxic and reperfusion phases of IRI occurs within a relatively hypoxic environment and occurs during both phases of hepatic IRI. The early phase of IRI is thought to involve activation of KCs and other liver resident macrophages, which release pro-inflammatory

cytokines and ROS [6, 7]. The late phase is characterised by increased expression of chemokines and adhesion molecules and hepatic recruitment of effector cells that amplify the tissue damage (see Section 1.1.2). The latter phenomenon is a feature common to many other hepatic diseases such as cirrhosis. There is evidence to suggest that hepatocyte injury occurs during the relatively hypoxic early phase of IRI [163]. ROS, primarily in the form of hydrogen peroxide, is released and is one of the earliest and most important components of tissue injury after reperfusion of ischemic organs and a major contributor to hepatocyte death during reperfusion [167]. Moreover, diseases such as ALD are characterised by the chronic accumulation of ROS [160]. The source of hepatic ROS during liver injury remains controversial. Numerous studies suggest that KC derived extracellular ROS is the key trigger for hepatocyte damage [168, 169] whereas other studies have shown that absence/elimination of KCs does not prevent tissue damage in IRI [170]. This latter observation suggests that other cells within the liver, including hepatocytes, may be involved in the pathophysiological production of ROS during IRI and chronic hepatic inflammation.

Early work using rat hepatocytes suggested that XO was the main generator of ROS [69]. However the XO inhibitors used in these early studies such as allopurinol are now known to inhibit mitochondrial function too. Indeed, more recent studies have shown that the mitochondria are the main source of ROS within hepatocytes [71]. Furthermore, inhibition of mitochondrial complex I and III can ameliorate ROS production in human hepatoma cell lines [27] and rat hepatocytes [171]. Other enzymes such as the flavoenzyme NADPH oxidase can also produce ROS in rat hepatocytes [172]. Despite these observations the precise mechanisms involved in the generation of ROS within human hepatocytes remains elusive and no studies thus far have investigated this.

The accumulation of excess intracellular ROS induces cell death and during hepatic IRI and hepatocytes undergo cell death in the form of both apoptosis and necrosis [173]. Some studies support apoptosis and others necrosis as the primary mode of cell death [174]. In reality it is uncertain whether apoptosis and necrosis observed in liver tissue are separate processes since the terms primarily represent a morphological description, and it has been suggested that apoptotic cells not effectively cleared from inflammatory sites may eventually assume a necrotic appearance (so called secondary necrosis). This led Lemasters to propose the term necro-apoptosis, and it may be that both forms of cell death are in part related sharing some common intracellular pathways [175]. The key regulators of molecular switching between these different forms of cell death remain to be identified.

Despite the above observations, little is known about the relative contribution of endogenous hepatocyte ROS production and its potential impact upon hepatocyte cell death following hypoxia and H-R. Much of the understanding of hepatic IRI comes from studies of rodent hepatocytes and rodent experimental models. The response of human hepatocytes to hypoxia and H-R is unknown. In addition, the research that has been performed using human hepatocytes has used cells isolated from normal resected liver tissue from patients with neoplastic disease. As discussed in Chapter 2, whether cells from such sources can be considered to truly reflect normal hepatocytes has never been objectively studied.

3.1.2 Response of Peri-portal and Peri-venous Hepatocytes to Hypoxia and H-R

The functional unit of the liver is the acinus, which extends from the portal venule along the sinusoids to the terminal hepatic venule (Figure 3.1). The liver acinus in rodents extends for approximately 20 hepatocytes [176]. Peri-portal (PP) hepatocytes (zone 1) which are near the portal venule tend to be of a smaller in size than peri-venous (PV) hepatocytes (zone 3)

which are located near the terminal hepatic vein [177]. Indeed, some studies define and isolate large/PV and small/PP hepatocyte populations upon the basis of size [178]. Furthermore, these studies have utilised the technique of fluorescent-activated cell sorting (FACs) to consistently differentiate between large/PV and small/PP hepatocytes and study their respective metabolic functions [179-181]. Moreover, these studies have demonstrated that these hepatocytes have distinct and separate cellular functions. Whether large/PV and small/PP hepatocytes exhibit differential responses to hypoxia and H-R is not known.

There is a large body of evidence to support the concept of morphological, biochemical and metabolic heterogeneity of large/PV and small/PP hepatocytes [42, 169, 182, 183]. Indeed, various functions have been ascribed to specific zones of the liver acinus. Specifically, oxidative metabolism, gluconeogenesis, urea synthesis and bile formation are predominantly small/PP hepatocyte activities whereas glutamine synthesis, xenobiotic metabolism and ketogenesis are particularly prevalent in the large/PV hepatocytes [184, 185]. Moreover, studies have shown these differences in hepatocyte function are attributable to differences in enzyme expression [182, 183].

These differences in hepatocyte function are also likely to be important determinants in the evolution of liver injury. For instance, in rodent models, it is well documented that following ischemic liver injury, hepatocyte cell death is seen predominantly observed around the peri-venular region were the large/PV hepatocytes are located [186]. As discussed above ROS is thought to be one of the key regulators of IRI. However, whether small/PP and large/PV hepatocytes have differential ROS accumulation during hypoxia and H-R is not known. In particular, whether small/PP or large/PV human hepatocytes exhibit differential responses to hypoxia and H-R remains to be ascertained.

Previous studies have utilized various techniques to investigate the different functions of small/PP and large/PV hepatocytes. These include retrograde digitonin perfusion of livers [169] and elutriation [182]. However, as stated above FACs allows the differentiation between different sized hepatocytes on the basis of size and offers a method to study small/PP and large/PV human hepatocyte cell function using the isolation protocol detailed in Chapter 2.

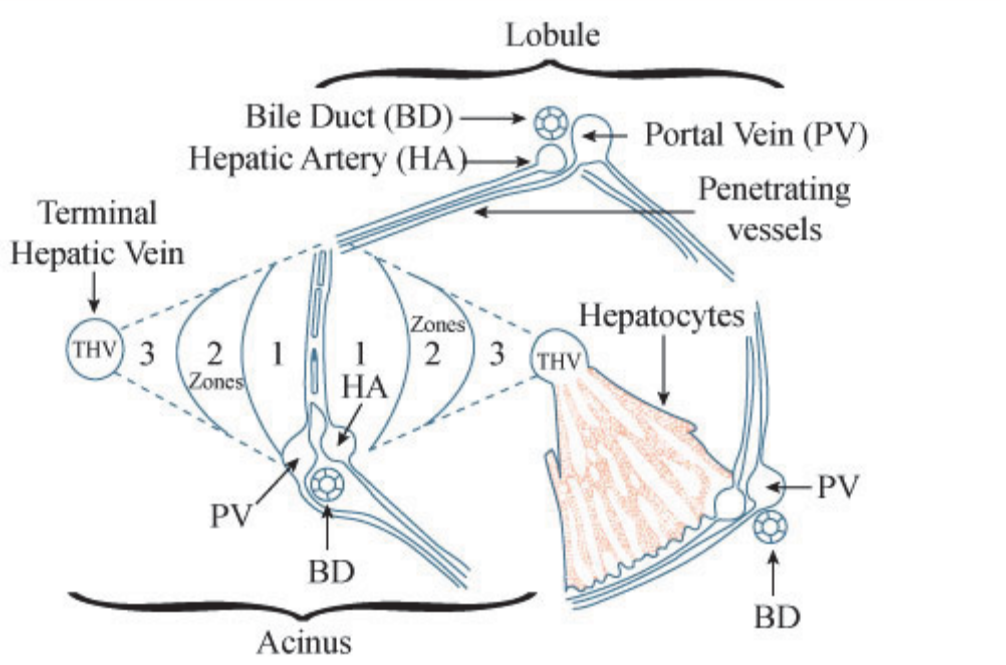

Figure 3.1 The Liver Acinus
Schematic of the liver operational unit the classic lobule and the acinus. The lobule is centered on the terminal hepatic vein (Central vein), where the blood drains out of the lobule. The acinus has its base the penetrating vessels where blood supplied by the portal vein and hepatic artery flows down the acinus past the cords of hepatocytes. Zone 1, 2 and 3 of the acinus represent metabolic regions that are increasingly distant from the blood supply. BD, bile duct, PV, Portal vein, HA, hepatic vein, THV, terminal hepatic vein.

3.1.3 Hepatic IRI and Autophagy

Whilst hepatocyte apoptosis and necrosis have been shown to occur during hypoxia, the role of hepatocyte autophagy during IRI remains controversial [187]. It is now widely recognised that autophagy is required for protein and organelle turnover and is typically a homeostatic cellular response to starvation [188]. Furthermore, autophagy degrades both long-lived cytoplasmic proteins and surplus or dysfunctional organelles by lysosome-dependent mechanisms [188]. Nearly all hepatocyte derived proteins are long-lived and autophagy is thought to be the primary process for hepatic protein catabolism [189]. Recent studies suggest that autophagy is another distinct and separate form of cell death that hepatocytes sustain when exposed to oxidative stress [190] but it has not been conclusively shown that cells undergoing autophagy are not committed irreversibly to death. The role of autophagy in liver disease has been comprehensively presented in recent reviews [187, 189, 191]. Autophagy is being shown to play an increasingly important role in many liver diseases [187, 189]. Indeed, Hepatitis B and C viruses may exploit the autophagy pathway to escape the innate immune response and to promote their own replication [192, 193]. Autophagy is decreased in response to chronic alcohol consumption [194]. In ALD autophagy is decreased and promotes cell death. Finally defective autophagy may promote the development of hepatocellular carcinoma [187].

Autophagy is an active process that involves sequestration of parts of the cytoplasm in double membrane vesicles that then fuse with lysosomes forming the autophagosome. The cytoplasmic material engulfed is then hydrolysed permitting recycling of amino acids and other macromolecular precursors. In contrast to classical apoptosis, the cellular machinery that regulates autophagy is known to be lysosomal proteinase-dependent and caspase-independent. In particular the Autophagy-related protein (Atg) proteins and

phosphatidylinositol 3-kinase (PI3-K) are crucial for autophagosome assembly. The initial step of autophagosome formation requires class III PI3-K and Beclin 1/Atg6 protein [195]. The assembly of the autophagosome can be inhibited pharmacologically by the specific class III PI3-K inhibitor 3-methyladenine (3-MA) [196, 197]. The formation and expansion of the autophagosome requires two further protein conjugation systems that involve several of members of the Atg protein superfamily [198], namely the Atg8/LC3-PE and Atg5-Atg12 conjugation systems (Figure 3.2). These conjugation events are regulated and involve Atg3, Atg4 and Atg10 [199]. In particular Atg8 serves as a substrate for the Atg4 family of cysteine proteases. Many Atg proteins can be regulated by ROS [198] and may mean that the increases in ROS observed during IRI may also regulate hepatocyte autophagy. Once activated Atg8 is able to associate with autophagosomes and remain there until fusion with lysosomes [189, 200].

Under starvation, cellular generation of ROS is essential for autophagosome formation and autophagic degradation. As stated above ROS is a common feature to many liver diseases. Therefore defining the relationship of ROS and autophagy would provide important mechanistic links between these two entities and provide important insights into the potential role of autophagy during hepatic IRI.

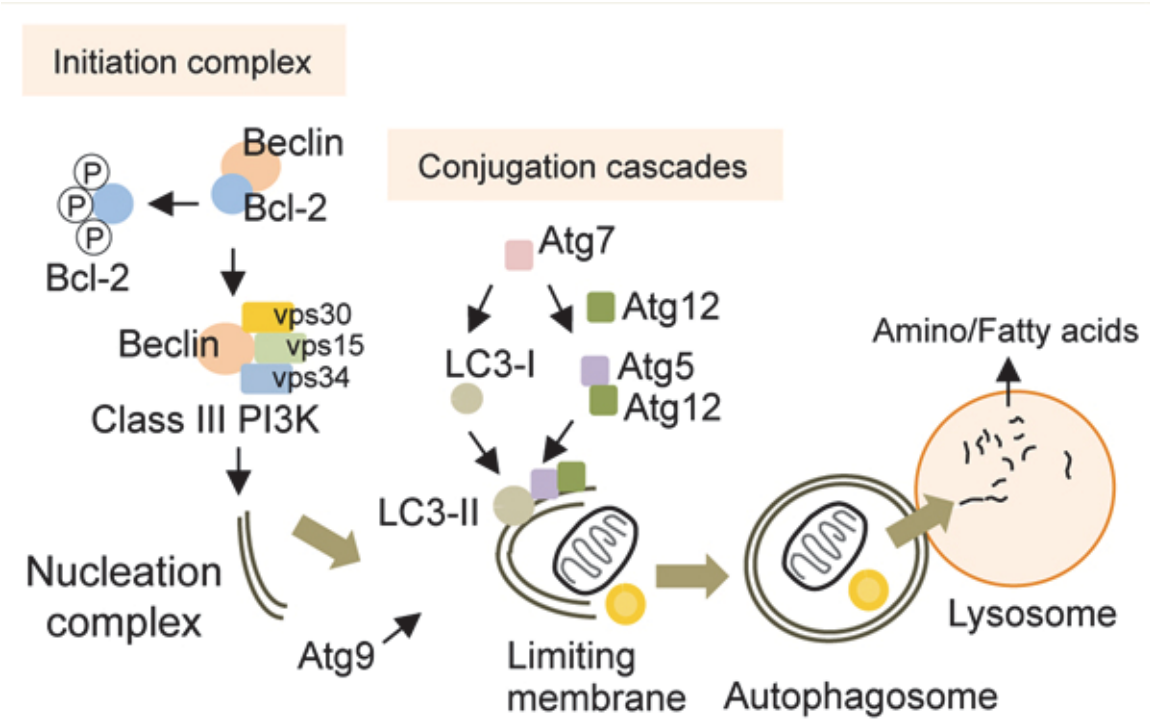

Figure 3.2 The Molecular Regulators of Autophagy
Autophagy induction requires the release of Beclin from Bcl-2, which is then free to form a complex with the Class III PI3K that contributes to the formation of the nucleation complex. Two independent conjugation cascades, the LC3-II and the Atg5-12 cascades, serve to elongate the nucleation complex to generate the limiting membrane. The sole transmembrane Atg, Atg9, delivers additional membranes for limiting membrane formation. The limiting membrane then sequesters cytosolic cargo and seals upon itself to form an autophagosome. The fusion of autophagosomes to lysosomes results in cargo degradation and release of nutrients into the cytosol. Atg: autophagy gene, LC3: light chain-3, PI3K: phosphoinositide 3-kinase, vps: vacuolar protein sorting.

3.2 Material & Methods

3.2.1 *In vitro* Model of Warm Hypoxia and H-R

In experiments using the *in vitro* model of warm IRI, successfully isolated primary human hepatocytes were cultured for 2 days at 37^0C, 5% CO_2 in Williams E media (Sigma) on rat type 1 collagen-coated plates. Hepatocytes were either maintained in normoxia or placed into hypoxia for 24 hours, or placed into hypoxia for 24 hours followed by 24 hours of reoxygenation. Hypoxia was achieved by placing cells in an airtight incubator (RS Mini Galaxy A incubator, Wolf Laboratories, UK) flushed with 5% CO_2 and 95% N_2 until oxygen content in the chamber reached 0.1%, as verified by a dissolved oxygen monitor (DOH-247-KIT, Omega Engineering, UK). No previous studies have evaluated primary human hepatocytes response to hypoxia and H-R. Therefore a well-established model of warm *in vitro* IRI was modified for the experiments described below. 0.1% oxygen was used in all experiments using the *in vitro* of IRI for 24 hours (see below). Additionally, Williams E media was pre-incubated in the hypoxic chamber in a sterile container, which allowed gas equilibration, for 8 hours before experiments were carried out, resulting in a final oxygen concentration of <0.1% as measured with the dissolved oxygen meter. Where appropriate, after 24 hours of hypoxia media was aspirated and replaced with fresh, warmed, oxygenated medium, and the cells were returned to normoxic conditions. This was defined as the beginning of reoxygenation. In experiments involving ROS inhibitors/antioxidants/autophagy inhibitors all reagents were made fresh as stock solutions and added using the correct dilutional factor to the relevant experimental wells. Specifically, 100 mM NAC (Sigma) was dissolved in molecular grade water, 1 mM rotenone (Sigma) was dissolved in chloroform, 1 mM diphenyliodonium (DPI) (Sigma) was dissolved in DMSO and 30 mM 3-MA was dissolved in DMSO and were diluted appropriately to give working

concentrations of 20 mM, 2 μM, 10 μM and 5 mM respectively. In experiments using inhibitors/antioxidants, solvent alone controls were used to ensure no vehicle effects. In addition, in experiments using inhibitors/antioxidants agents were added at the time of placement of the cells into hypoxia or into reoxygenation.

3.2.2 Flow Cytometric Assessment of ROS, Apoptosis, Necrosis and Autophagy in Primary Human Hepatocytes during Hypoxia and H-R

ROS production, apoptosis, necrosis and autophagy were determined by using a four-colour reporter assay system (Figure 3.3). ROS accumulation was determined using the fluorescent probe 2',7'-dichlorofluorescin-diacetate (Merck, Nottingham, UK, Catalogue Number 287810) [201]. This probe is cell permeable and once inside the cell is cleaved by intracellular esterases to 2',7'-dichlorofluorescin (DCF) and becomes cell impermeable. DCF is then able to react with intracellular ROS, specifically hydrogen peroxide, to give a fluorescent signal detectable on the Fluorescein Isothiocyanate (FITC) channel. The signal is directly proportional to the level of intracellular ROS present.

MitoSox Red is a mitochondrial superoxide indicator dye (Molecular Probes, Invitrogen, Catalog Number M36008) and was used as means to determine ROS in the mitochondria. Cells were treated as described above in the *in vitro* model and then loaded with 5μM MitoSox Red in HBSS (Gibco) for 30 min at 37°C in the dark. Cells were washed as described below. MitoSox Red fluorescent intensity was determined by fluorescence with excitation at 510 nm and emission at 580 nm. Mitosox was used alone in parallel experiments with DCF to determine the relative contribution of the mitochondrion to human hepatocyte ROS generation and not used in the four-colour reporter assay system described below.

Apoptosis was determined by labelling cells with Annexin-V (Molecular Probes, Invitrogen, Catalogue Number A35122), which detects exposed phosphatidylserine on the cell membrane. 7-Amino-Actinomycin D (7-AAD) (Molecular Probes, Invitrogen, Catalog Number A1310) is a vital dye that binds to DNA, only entering cells once the cell membrane is disrupted and is indicative of cellular necrosis. Autophagy formation was determined by using the fluorescent dye monodansylcadaverine (MDC) (Sigma-Aldrich, Catalogue Number 30432). This dye selectively labels autophagic vacuoles [202] and has been previously used in hepatoma cell lines [203] and primary hepatocytes [204] to detect autophagy.

Following desired experimental treatment; cell media was aspirated and replaced with HBSS without calcium and magnesium. DCF (30 μM) and MDC (1 μM) were added and the cells were incubated for 20 min in the dark at 37^0C. The cells were then trypsinsed and washed extensively in FACs buffer (phosphate-buffered saline pH 7.2 with 10% v/v heat inactivated foetal calf serum (Gibco). Cells were then labelled with Annexin-V (0.25 μg/ml) and 7-AAD (1 μg/ml) for 15 min whilst on ice and then samples were immediately subjected to flow cytometry. At least 20,000 events were recorded within the gated region of the flow cytometer for each human hepatocyte cell preparation in each experimental condition. Only the cells within the gated region were used to calculate Mean Fluorescence Intensity (MFI).

To ensure consistency of the flow cytometric data, each human hepatocyte preparation was labelled with DCF alone, Annexin-V alone, 7-AAD alone and MDC alone to ensure that cells had become labelled and that the flow cytometry data could be compensated for crossover of fluorophore emission spectra (Figure 3.4 & 3.5). The same flow cytometry protocol was used for all experiments shown within the study, i.e. voltages for all markers were constant for all human hepatocyte preparation ensuring inter and intra-experimental consistency. Specifically, for each experiment a cell only sample was used to ensure that

there was no staining of primary human hepatocytes with each specific dye/probe (Figure 3.4). This sample was also used to ensure that the MFI reading was placed in the first decade for each dye/probe. Also these cells were used to place a flow cytometric gate for subsequent samples. Human hepatocytes vary considerable in size depending upon whether they are derived from the peri-venular region of the liver or peri-portal region of the liver. Therefore Forward Scatter (FS) and Side Scatter (SS) plots shown in Figure 3.4 demonstrate a heterogeneous cell population. A gate was therefore placed in FS versus SS that included all cells. Clearly, the sample includes cell debris that by necessity is included within the large gate applied in the analysis. Also, the gate will include small hepatocytes and hepatocytes that attain lower intensity of staining with probes/dyes and do not respond to hypoxia and H-R in the same way as the highly stained species. Therefore, peaks seen adjacent to the peaks within the vertical ellipses represent cell debris and hepatocytes that have different responses to hypoxia and H-R.

In preliminary experiments, primary human hepatocytes were exposed to 5% and 1% oxygen for 24 hours, and no increase in ROS accumulation was noted (Figure 3.6). Therefore as described above the *in vitro* model utilised 0.1% oxygen throughout the studies.

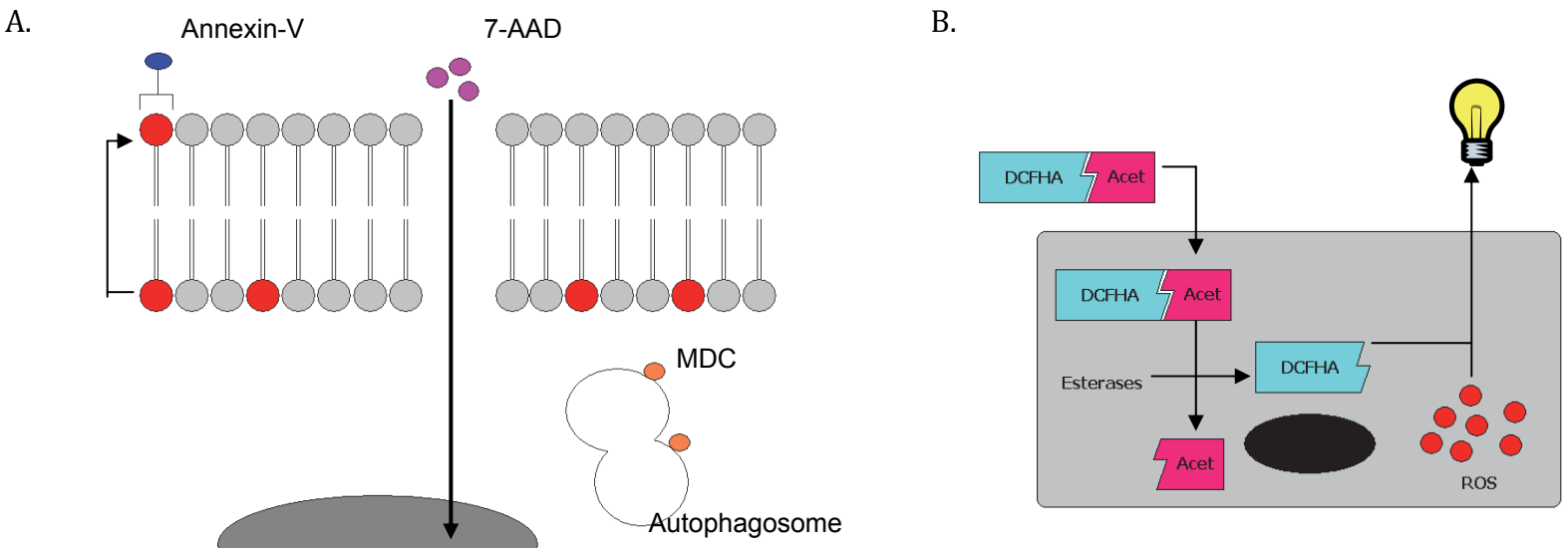

Figure 3.3 Four-Colour Reporter Assay

In the four-colour reporter assay Annexin-V, 7-AAD and MDC were combined with DCF to assess apoptosis, necrosis and autophagy respectively. (A) Apoptosis was assessed using Annexin-V. In a healthy cell phosphatidylserine (shown in red) is usually present only on the inner membrane of the cell. However when the cell is committed to apoptosis the phosphatidylserine moiety is translocated and expressed upon the outer cell membrane. This can be then detected by Annexin-V and is early marker of apoptosis and occurs temporally much earlier than caspase activation. Annexin-V gives rise to a signal on the Violet 1 channel of the flow cytometre. 7-AAD is a specific marker of necrosis. This molecule relies upon disruption of the cellular membrane to gain access to the intracellular compartment. Once inside the cell 7-AAD forms irreversible covalent bonds to DNA and gives a fluorescent signal detectable upon the PECy5 channel of the flow cytometre. The specific autophagy marker MDC can detect autophagy. MDC is able to diffuse freely across the cell membrane and bind to assembled autophagosomes. This binding is irreversible and gives rise to a signal on the Violet 2 channel of the flow cytometer.

(B) 2,7,-dichlorofluorescin-diacetate (DCFHA) is a cell permeable ester that diffuses freely across the cell membrane. Once inside the cell DCFHA is acted upon by intracellular esterases that convert DCFHA to 2,7,-dichlorofluorescin and diacetate. This renders both molecules cell impermeant. DCFHA is then able to react with ROS (hydrogen peroxide) within the cell that then gives rise to a fluorescent signal detectable upon the FITC channel of the flow cytometre.

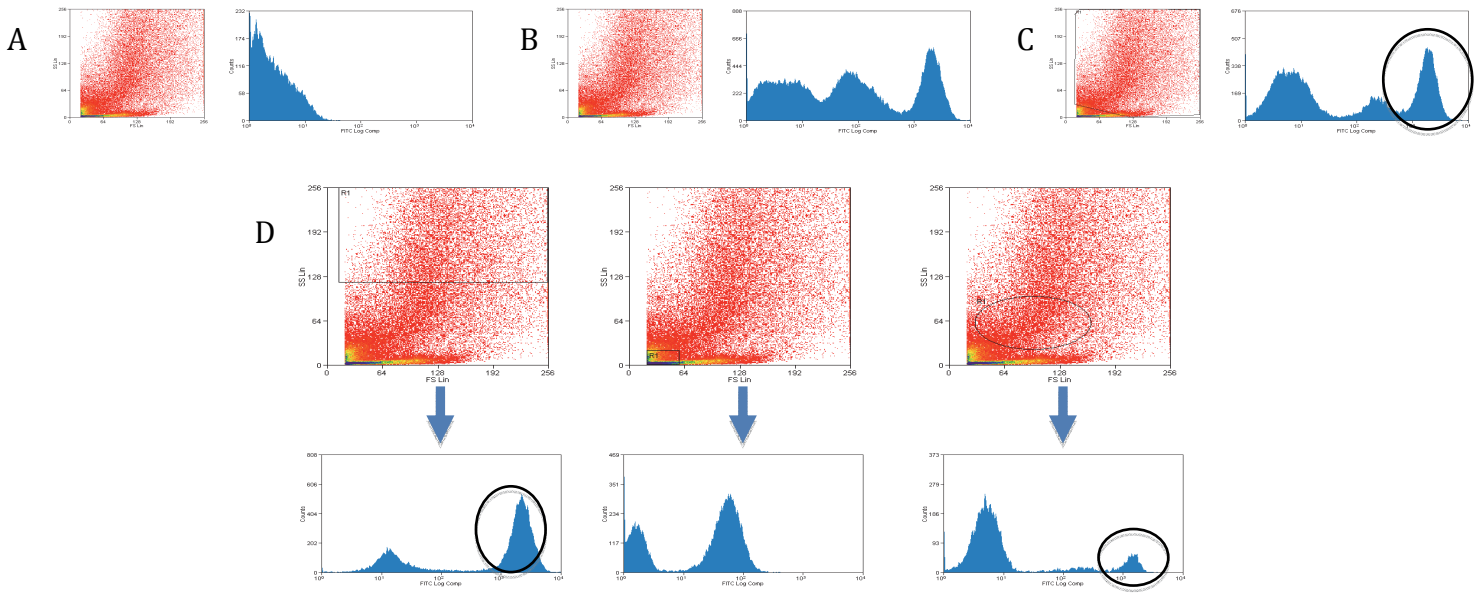

Figure 3.4 Setting up of the Flow Cytometry Protocol

The above panel shows how DCF was used in flow cytometric analysis for the assessment of ROS in primary human hepatocytes during hypoxia and H-R. Panel A shows the typical FS and SS scatter of primary human hepatocytes during H-R. Similar plots were obtained during normoxia and hypoxia. DCF is detectable upon the FITC channel of the flow cytometre. In the absence of DCF human hepatocytes show no fluorescence in the FITC channel and this signal was arbitrarily set to the first decade, as demonstrated in Panel A. As Panel B demonstrates staining of primary human hepatocyte with DCF showed typically three separate peaks upon the flow cytometre when no gate was applied. Human hepatocytes vary considerably in size ranging from 10 µm to 50 µm and including all hepatocytes within the analysis as shown in Panel C maintains all three peaks. Panel D shows how the three peaks are derived in the analysis. The left hand panel shows that when only the larger hepatocytes are included within the analysis, the majority show staining with DCF with a smaller population showing little staining. These former hepatocytes are the one of interest for subsequent studies as these show increases in intracellular ROS and have been indicated with the vertical ellipse. As the middle panel shows due to the trypinisation of human hepatocytes a large amount of debris is included within the analysis. This will represent cellular fragments that have stained with DCF and hence a fluorescent signal is seen. The right hand panel show the gating protocol that can be applied to obtain the signal from small hepatocytes. This shows that a small population of these hepatocytes increase ROS. To detect apoptosis, necrosis and autophagy similar flow cytometric analysis were used.

Figure 3.5 Compensation of the Flow Cytometric Fluorophore

To ensure that flow cytometry experiments were correctly performed and correctly compensated initially unlabelled hepatocytes were run through the flow cytometer as illustrated in Figure 3.4A. Following this the FS and SS parameter voltages were adjusted to enable appropriate gating of cells as demonstrated in Figure 3.4. In the example discussed below the compensation of Violet 1 (Annexin-V) and Violet 2 (MDC) is described. Similar compensation protocols were followed to ensure all fluorophore were correctly compensated for in the four-colour reporter assay. Following the above steps, voltages on the Violet 1 and Violet 2 parameters were adjusted to place the unlabelled cells within the first decade of the logrhythmic scale as displayed below.

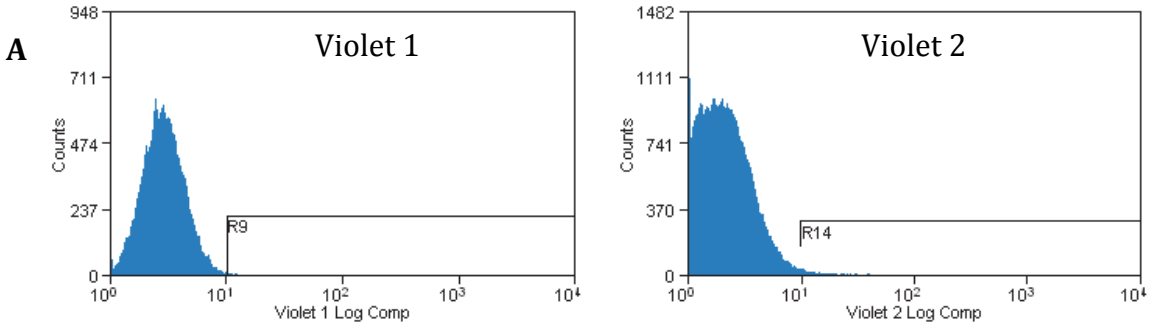

Figure 3.5A. Demonstrates the initial step up for the compensation procedure. Unlabelled hepatocytes were arbitrarily placed with the first decade of the flow cytometry plot. This was performed for both Violet 1 and Violet 2.

Following this human hepatocytes labelled with the Violet 1 fluorophore were run on the flow cytometre to check that no final adjustments to voltage were required to the Violet 1 channel. Violet 1 positive events were separate from the negative population (Figure 3.5B). Next human hepatocytes labelled with the Violet 2 fluorophore were run on the flow cytometer and check that no final adjustments to voltage are required to the Violet 2 channel. Violet 2 positive events were separate from the negative population.

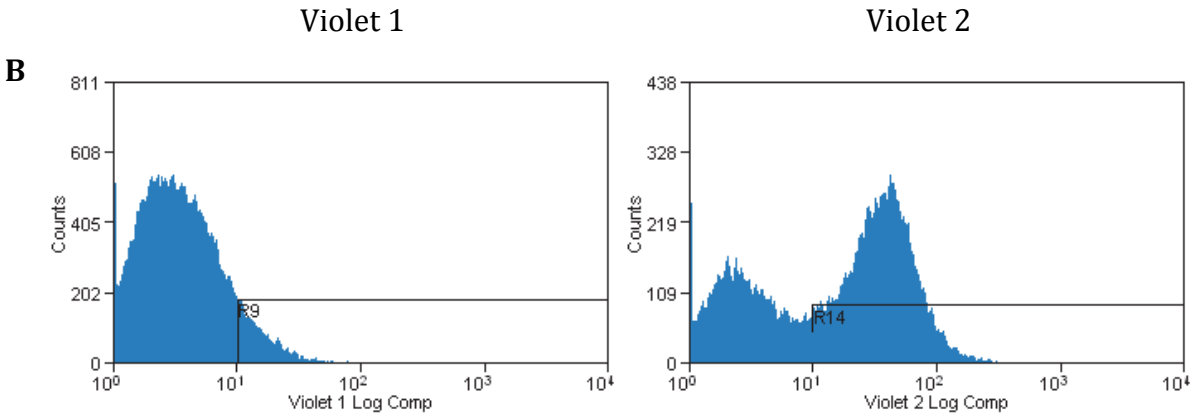

Figure 3.5B. Violet 1 and Violet 2 positive human hepatocytes were clearly distinct from the negative population demonstrated in Figure 3.5A. This ensured that the positive population of cells could be clearly distinguished from the negative cells.

The voltage settings were not then changed, as subsequent compensation would not be valid if instrument settings for fluorescence channels were changed. The same protocol and method was used to ensure correct voltages for DCF and 7-AAD.

Once the voltages were set for each of the fluorophore, compensation is applied to the data. Firstly, after gating on the human hepatocyte population of interest on the relevant FS vs. SS dot-plot (see Figure 3.4), the Violet 1 and Violet 2 data was displayed in a plot of Violet 1 vs. Violet 2 as shown below.

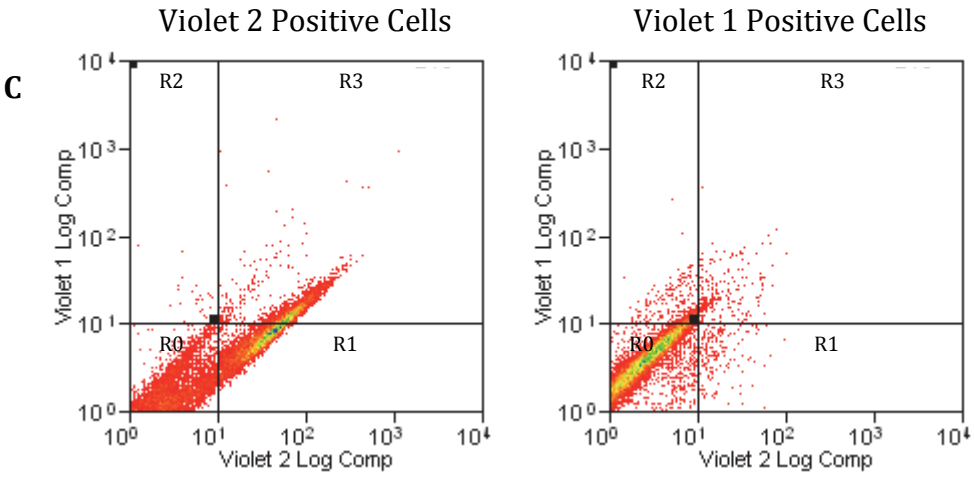

Figure 3.5C. Demonstrates the uncompensated data from Violet 1 and Violet 2 on a quadrant analysis. Violet 1 positive cells show positivity within the Violet 2 channel during normoxia. Although human hepatocytes show Violet 2 positivity under basal conditions, cells also showed positivity within the Violet 1 channel. Without compensation, cells that were not stained with the relevant fluorophore would appear positive giving rise to spurious results.

Quadrant analysis of this uncompensated data shows the negative cells in the origin (R0) with the Violet 1 and Violet 2 stained cells in the double positive quadrant (R3). This demonstrates the Violet 1 and Violet 2 spectral overlap (or bleed through) with Violet 2 and Violet 1 respectively. Compensation was applied to the data to ensure correctly stained cells were analysed as shown below (Figure 3.5D).

D

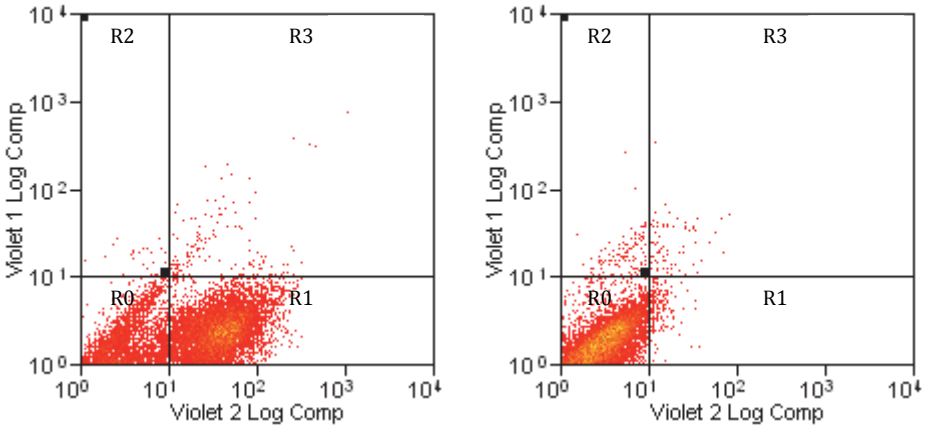

Figure 3.5D. Demonstrates the compensated Violet 1 and Violet 2 data. Compensation was applied to ensure that only cells positive for Violet 1 and Violet 2 were contained within the positive quadrant. Hence under normoxic conditions human hepatocytes show minimal positivity with Annexin-V (Violet 1) and strong positivity with MDC (Violet 2).

MFI was used to analyse data as the parameters assessed were normally distributed. Thus the Violet 2 stained human hepatocytes are now correctly compensated against Violet 1 and vice versa (Figure 3.5E).

E

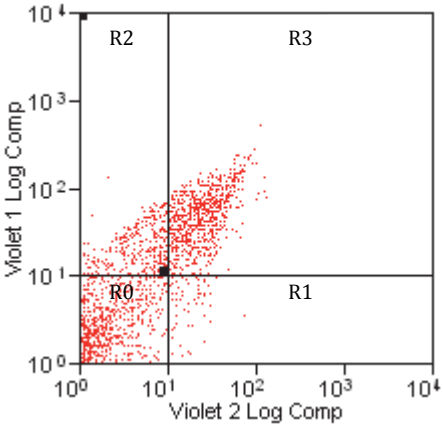

Figure 3.5E. Following correct compensation only cells that are dual positive for Annexin-V and MDC are present within R4. This data was from human hepatocytes exposed to hypoxia and show that that hypoxia induces both apoptosis and autophagy in these cells.

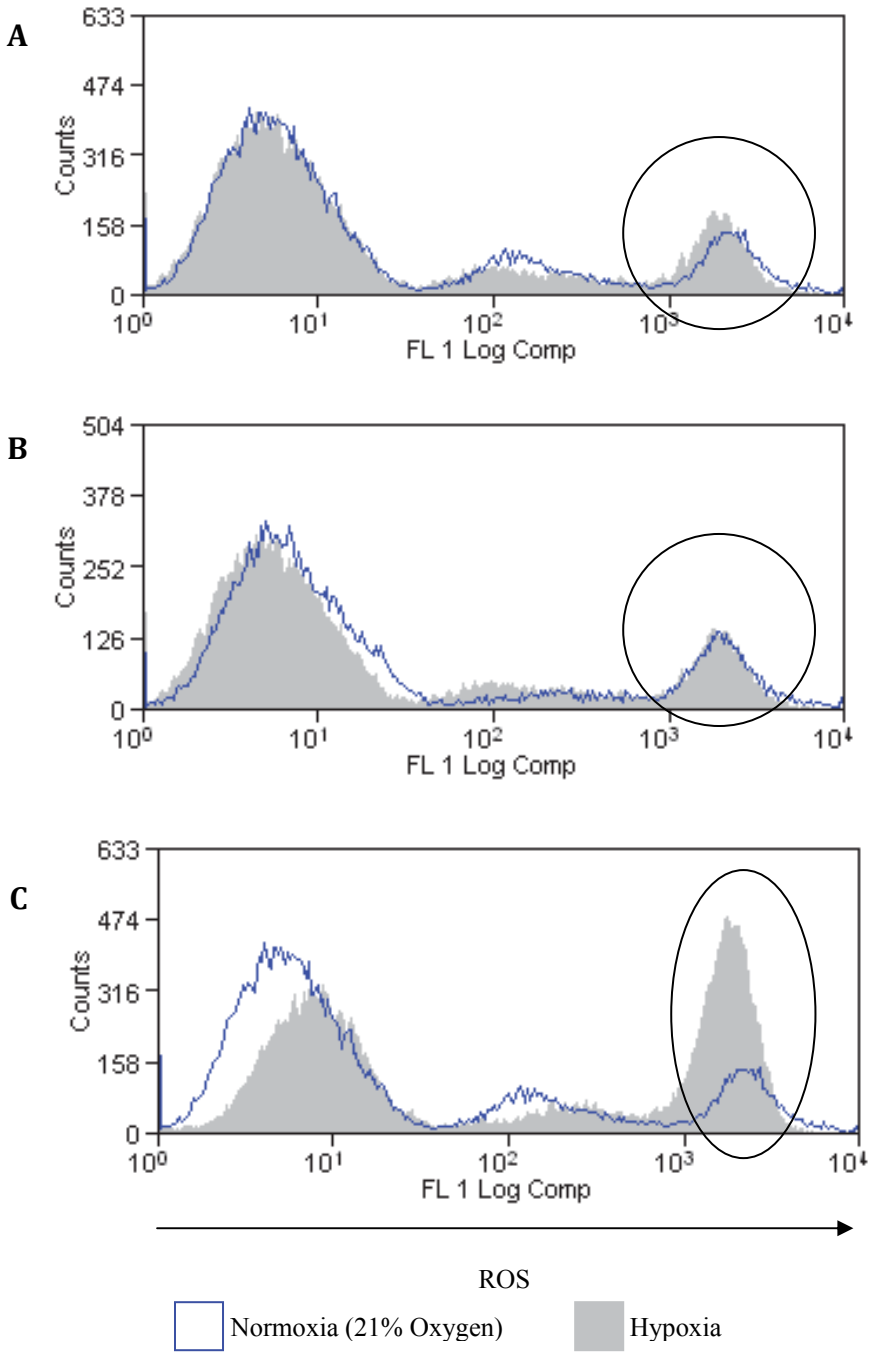

Figure 3.6 ROS Accumulation in Human Hepatocytes in Response to 5%, 1% and 0.1% Hypoxia

To date no studies have examined the effects of hypoxia upon human hepatocytes. Therefore to establish the effects of oxygen concentration upon intracellular human hepatocyte ROS production, human hepatocytes were exposed to 5%, 1% and 0.1% hypoxia for 24 hours. The accumulation of intracellular ROS was determined using DCF as detailed above. As Panel A and B demonstrate 5% and 1% oxygen respectively induced no intracellular ROS accumulation within human hepatocytes relative to normoxia whereas 0.1% oxygen (Panel C) did induce an increase. Therefore for subsequent experiments 0.1% oxygen for 24 hours was used in the *in vitro* model. (n=3).

3.2.3 Western Blotting for Atg Proteins

For Western immunoblotting studies, human hepatocytes were lysed at the end of the relevant experimental period using Nonident P-40 (NP-40) lysis buffer (20 mM Tris-HCl pH 8 (Sigma-Aldrich, Catalog Number T3253), 137 mM NaCl (Sigma-Aldrich, Catalog Number S3014), 10% glycerol (Sigma-Aldrich Catalog Number G5516), 1% Nonidet P40 (Sigma-Aldrich, Catalog Number 18896), 2 mM EDTA (Sigma-Aldrich, Catalog Number E6758). Protein concentration was determined by Bradford protein assay and 25 μg of protein was resolved on a 10% SDS-PAGE gel and transferred to a nitrocellulose membrane (Hybond; Amersham Biosciences, UK, Catalog Number RPN3032D). The blotted membrane was blocked for 1 h at room temperature in TBS pH 7.4/Tween 0.1% (Sigma-Aldrich, Catalog Number P9416) containing 5% (wt/vol) bovine serum albumin (BSA) (Sigma-Aldrich, Catalog Number A9418). All primary antibody incubations were carried out at overnight at 4^0C in TBS-Tween 0.1% containing 5% BSA (wt/vol). The incubation steps were followed by three washing steps of 5 min with TBS containing 0.1% Tween. All primary antibodies were purchased from New England Biolabs (Hitchin, UK) and used at a dilution of 1:1000 as per manufacturer's instructions. Specific primary antibodies used included: 1) Beclin-1 (catalog number. 3495) 2) LC3A (catalog number. 4599) 3) Atg5 (catalog number. 8540) 4) Atg12 (catalog number. 4180) 5) Atg7 (catalog number. 2631).

Binding of specific monoclonal antibodies was detected with a horseradish peroxidase-conjugated anti-rabbit IgG at a dilution of 1:2000 for 1 h (Sigma-Aldrich, Catalog Number A8792) Protein bands were visualized using the enhanced chemiluminescence detection system (Amersham Biosciences, Catalog Number RPN2109) followed by exposure of the membranes to Hyperfilm-ECL (Amersham Biosciences, Catalog Number 28-9068-37). Equality of protein loading on were checked by immunoblotting for β-actin (Sigma-Aldrich,

Catalog Number A2228) (dilution 1:20000). All Western immunoblots were performed at least three times from different liver preparations for each liver cell type.

3.2.4 Assessment of Mitochondrial Membrane Potential and Labelling of Autophagic Vacuoles with MDC

To measure the mitochondrial membrane potential ($\Delta\Psi m$) in human hepatocyte during normoxia, hypoxia and H-R, 5,5',6,6'-tetrachloro-1,1',3,3'-tetraethylbenzimidazolylcarbocyanine iodide (JC-1) (Molecular Probes, Invitrogen, Catalogue Number M34152), a sensitive fluorescent probe for $\Delta\Psi m$ was used [205]. Probes such as JC-1 that detect mitochondrial membrane potential are positively charged, this property allows the probes to accumulate in the electronegative interior of the mitochondria. JC-1 dye exhibits potential-dependent accumulation in mitochondria, indicated by a fluorescence emission shift from green (530 nm) to red (590 nm) [206]. Consequently mitochondrial depolarisation is indicated by a decrease in the red/green fluorescence intensity ration. The potential-sensitive colour shift is due to concentration dependent formation of red fluorescent J-aggregates. In the studies detailed below JC-1 was used in conjunction with MDC to delineate the effects of autophagy upon mitochondrial function.

Human hepatocytes were used in *in vitro* experiments as described above. At the end of the specific experimental procedure, cells were then rinsed with PBS twice and then stained with 5 μM JC-1 and/or 1 μM MDC for 30 min at 37°C. Cells were rinsed with ice-cold PBS twice, resuspended in 1 mL ice-cooled PBS, and immediately analysed with a fluorescence microscope (Nikon Eclipse TE 300, Japan). A 488 nm filter was used for the excitation of JC-1. Emission filters of 535 nm and 595 nm were used to quantify the population of mitochondria with green (JC-1 monomers) and red (JC-1 aggregates) fluorescence,

respectively. MDC staining was assessed with a filter system (V-2A excitation filter: 380/420 nm, barrier filter: 450 nm).[207] Images were captured with a CCD camera and imported into Adobe Photoshop.

3.2.5 Luminex Assay (Multiplex-30 bead assay)

The Luminex assay system is a flexible analyser based upon the principles of flow cytometry. The system allows the simultaneous measurement of numerous analytes in a single microplate well using very small biological sample volumes. The technology uses 5.6 μm polystyrene microspheres, which are internally dyed with red and infrared fluorophores. Using different amounts of the two dyes for different batches of the microspheres up to 100 different microsphere sets can be created. Each bead is unique with a spectral signature determined by a red and infrared dye mixture. The bead is filled with a specific known ratio of the two dyes. As each microsphere carries a unique signature the detection system can identify to which set it belongs. Therefore multiplexing up to 100 tests in a single reaction volume is possible. The Luminex reader combines two lasers, fluidics and real time digital signal processing to distinguish up to 100 different sets of colour-coded polystyrene beads each bearing a different assay. The reader detects individual beads by flow cytometry. The fluidics system of the reader aligns the beads into single file as they enter a stream of sheath fluid and then enter a flow cell. Once the beads are in a single file within the flow cell, each bead is individually interrogated for bead colour (analyte) and assay signal strength (R-phycoerythrin (PE) fluorescence intensity). The reader uses a 532 nm green laser (assay laser) to excite the PE dye of the assay (streptavidin-PE). The 635 nm solid-state laser (red classify laser) is used to excite the dyes inside the beads to determine their colour or region

and is also used for doublet discrimination by light scatter. The reader has four detectors one for each of the optical paths.

The human cytokine multiplex-30 bead array assay kit for Luminex was purchased from Invitrogen (Carlsbad, CA, USA) to measure the following cytokines: IL-1α, IL-1β, IL-2, IL-3, IL-4, IL-5, IL-6, IL-7, IL-8, IL-10, IL-12p40, IL-12p70, IL-13, IL-15, Interferon-γ induced protein-10 (IP-10), Monocyte chemoattractant protein-1 (MCP-1), Macrophage Interacting Protein-1α (MIP-1α), Regulated upon Activation, Normal T-cell Expressed, and Secreted (RANTES), TNF-α, IFN-α2, IFN-γ, Granulocyte macrophage- colony stimulating factor (GM-CSF) and Eotaxin. The protocol was performed as per the manufacturer's instructions. Appropriate dilutions of the human hepatocyte supernatants in assay diluents were made. The assay was performed in a 96-well filter plate, using all the assay components provided. All incubation steps were performed at room temperature and in the dark to protect the beads from light. All washes were performed using a vacuum manifold. For the detection of cytokines and chemokines, the samples were finally incubated for 30 minutes with streptavidin conjugated to the fluorescent protein, R-PE (Streptavidin-RPE, diluted 1:10). After washing to remove the unbound Streptavidin-RPE, the beads (minimum of 50 beads per cytokine) were analysed in the Luminex 100 instrument, which monitored the spectral properties of the beads while simultaneously measuring the amount of fluorescence associated with R-PE. Raw data was analyzed using Bio-Plex Manager software, v4.1 (Bio-Rad). Each undiluted plasma sample was assayed in duplicate, and cytokine standards supplied by the manufacturer were used to calculate the concentrations of the samples.

3.2.6 Statistical analysis

Data analysis was carried out using SPSS version 13.0 software. All values are presented as means ± S.E. unless otherwise noted. Statistical analysis was carried using Student's *t* test.

3.3 Results

3.3.1 Variable ROS Responses to Hypoxia and H-R of Human Hepatocytes Isolated from Patients with Different Liver Diseases

Primary human hepatocytes were isolated from normal liver wedges that were obtained from in-situ liver splits or explanted diseased livers from patients with ALD, PBC and PSC. Hepatocytes were also isolated from tissue taken from patients who had undergone hepatic resections for liver metastasis from colorectal carcinoma. Table 3.1 shows ROS accumulation within human hepatocytes isolated from normal, normal resected and explanted livers. Figure 3.7 show ROS production and accumulation in normal human hepatocytes. The response of human hepatocytes isolated from ALD, PBC, PSC and normal resected is shown in Appendix I. As discussed earlier, the mitochondrion is the main source of ROS in hepatocytes and hypoxia leads to increased generation of ROS that is further increased by H-R**.** These findings were confirmed by the use of the specific mitochondrial ROS dye MitoSox Red, which demonstrated that hypoxia and H-R resulted in an increase in mitochondrial ROS production with the increase in ROS accumulation during H-R being greater than that observed in hypoxia (Figure 3.8). Indeed, mitochondrial ROS production accounts for the vast majority of ROS production in human hepatocytes during hypoxia and H-R.

Hepatocytes isolated from normal livers, ALD and normal resected liver tissue showed this classical response to hypoxia and H-R. Interestingly, there was little basal intracellular ROS within normal hepatocytes during normoxia. However, hypoxia and H-R induced a significant increase in ROS accumulation. Hepatocytes isolated from ALD and normal resected liver tissue showed similar responses in ROS accumulation during hypoxia and H-R but had greater basal intracellular ROS content, possibly reflecting their continual exposure

to an inflammatory microenvironment. Hepatocytes isolated from biliary disease (PBC and PSC) showed very low basal levels of ROS production, similar to hepatocytes isolated from normal livers. These hepatocytes showed a 22-fold increase in ROS production during hypoxia but a reduction in ROS accumulation in H-R. This may be a reflection of increased engagement of hepatocyte cytosolic antioxidant defences in these particular disease settings or a consequence on cholestasis, which is a feature of these diseases.

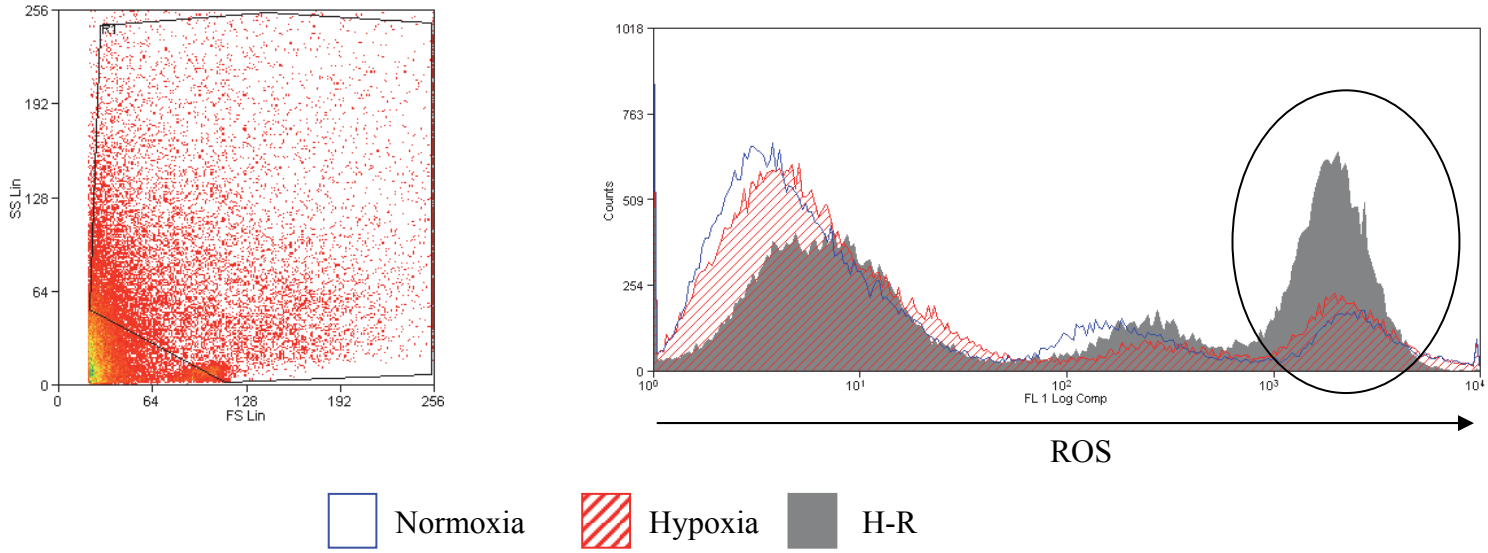

Figure 3.7 Hypoxia and H-R Mediate ROS Accumulation in Human Hepatocytes
Representative flow cytometry plots are shown to illustrate the effects of hypoxia and H-R on ROS accumulation in normal human hepatocytes. A vertical ellipse marks the area of interest within the plots. The area on the left of each ellipse represents cell debris. The reason why the cell debris is included within the plot is that human hepatocytes vary considerably in size and therefore to include all viable human hepatocytes in the analysis a large gate is required on the flow cytometer and by necessity includes the cell debris. The gate used is shown on the corresponding FS versus SS plots located on the left of each flow cytometric plot. The FS versus SS plots are from the H-R samples of each preparation but similar plots were obtained during normoxia and hypoxia. Details regarding the flow cytometric protocol are in Section 3.5. (n=4).

Table 3.1 ROS Accumulation in Human Hepatocytes during Hypoxia and H-R

	Normal	Biliary Cirrhosis	ALD	Resected
Normoxia	30.3 (13.3-53.5)	11.9 (6.2-21.1)	226.5 (217.1-247.1)	352.8 (256.4-450.5)
Hypoxia	121.9* (39.6-166.18)	255.2* (139.9-444.0)	259.5 (229.2-281.2)	377.1 (284.3-547.2)
H-R	271.1*† (217.7-370.0)	102.6* (35.2-151.0)	294.7 (278.15-311.1)	506.1 (332.2-874.0)

The mean ROS accumulation for human hepatocytes isolated from normal, diseased and normal resected liver tissue is shown in each of the three experimental conditions. Data is expressed as the MFI. Figures in parentheses represent the range of MFI readings in each experimental condition. MFI values are derived from the cells within the ellipse shown in Figure 3.7. The data is representative of 4 normal hepatocyte, 4 biliary disease, 3 ALD and 9 normal resected liver preparations. (*$p<0.05$ when compared to normoxia, †$p<0.05$ when compared to hypoxia)

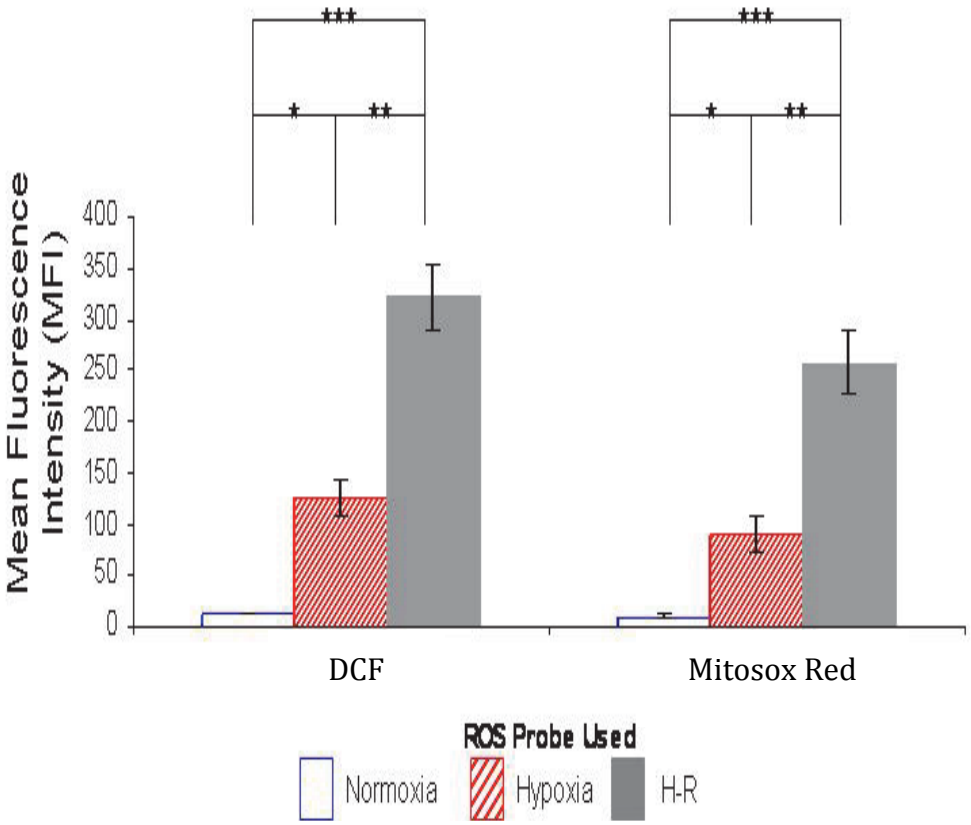

Figure 3.8 The Accumulation of ROS in Human Hepatocytes is Mitochondrial Dependent

Composite bar charts illustrate the effects of hypoxia and H-R upon ROS production in human hepatocytes isolated from benign liver diseases using DCF and Mitosox Red. DCF is measure of hydrogen peroxide production in human hepatocytes. Hydrogen peroxide is the main ROS generated within hepatocytes. Mitosox Red detects ROS generated specifically by the mitochondrion. In these experiments human hepatocytes were isolated from the same liver wedges and then used simultaneously in the *in vitro* model of hypoxia and H-R to determine DCF and Mitosox Red staining during normoxia, hypoxia and H-R. Data are expressed as MFI. Data are expressed as the mean ± S.E. Human hepatocytes used for these experiments were isolated from benign liver diseases (n=4). (*$p<0.05$ relative to normoxia, **$p<0.05$ relative to hypoxia, ***$p<0.01$ relative to normoxia, Mann-Whitney test).

3.3.2 PP and PV Human Hepatocytes Exhibit Differential ROS Accumulation during Hypoxia and H-R

As discussed earlier, FACs analysis is able to discriminate between large or PV and small or PP human hepatocytes using appropriate FS and SS gating strategies (see Figure 3.4). Accordingly, using appropriate flow cytometric gating protocols the response of large/PV and small/PP hepatocytes to hypoxia and H-R could be ascertained and defined.

Large/PV hepatocytes, isolated from benign liver resections, normal donor tissue and biliary cirrhosis (primary biliary cirrhosis and primary sclerosing cholangitis) showed a significant increase in ROS accumulation during hypoxia (Figure 3.9). Exposure of human hepatocytes to H-R further accentuated intracellular ROS accumulation. In contrast, small/PP hepatocytes, showed no increase in intracellular ROS accumulation during hypoxia and H-R. These observations show that ROS accumulation seen in the whole hepatocyte population during hypoxia and H-R (Figure 3.7) is largely due to large/PV human hepatocytes.

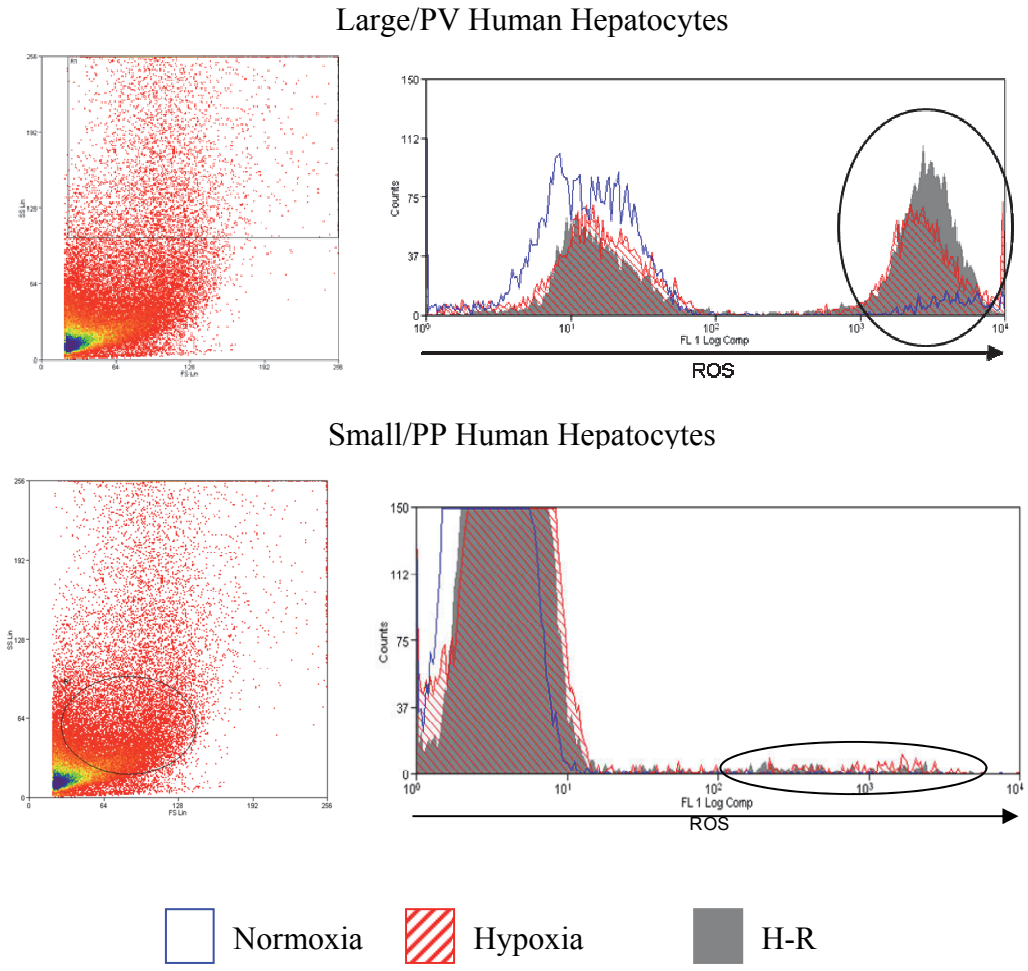

Figure 3.9 Intracellular ROS Accumulation within Large/PV and Small/PP Human Hepatocytes during Hypoxia and H-R

Demonstrates a representative flow cytometry plot of ROS accumulation in large/PV and small/PP primary human hepatocytes during normoxia, hypoxia and H-R. The plot on the left hand side of each flow cytometric plot represents a typical FS versus SS plot of primary human hepatocytes. The FS versus SS plots shown is from the H-R sample of a liver preparation but similar plots were obtained during normoxia and hypoxia. The top panel shows the gating protocol applied to human hepatocytes to analyse large/PV human hepatocytes and the bottom panel shows the protocol used to analyse small/PP human hepatocytes. The areas of interest on the flow cytometric plots are marked by the vertical ellipses. The origins of each of the peaks seen on the flow cytometry plot are discussed in detail in section 3.2.2. (n=6).

3.3.3 Cytokine and Chemokine Responses of Human Hepatocytes during Hypoxia and H-R

It is well appreciated that hepatocytes may secrete and sequester many pro-inflammatory chemokine and cytokines during inflammatory processes such as IRI [51]. There is no clear evidence as to whether hepatocytes secrete or produce pro-inflammatory chemokines and/or cytokines during IRI. Importantly, these soluble mediators are likely to shape the hepatic microenvironment and influence the type and magnitude of cell infiltrates observed during liver disease in general and IRI in particular. Of the 30 chemokines and cytokines assessed using the multiplex luminex analysis only two demonstrated significant changes during hypoxia and H-R. MCP-1 and IL-8 both showed increased levels within supernatants from human hepatocytes isolated from normal and biliary cirrhosis. Interestingly, ALD hepatocytes showed no changes in any of the 30 parameters measured. This may reflect the reduced metabolic activity of these cells (see Figure 3.10). Human hepatocytes isolated from normal resected tissue demonstrated elevated levels of both MCP-1 and IL-8 during normoxia but these decreased significantly during hypoxia and H-R.

Normal Human Hepatocytes

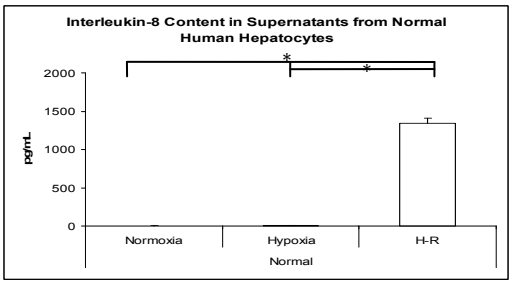

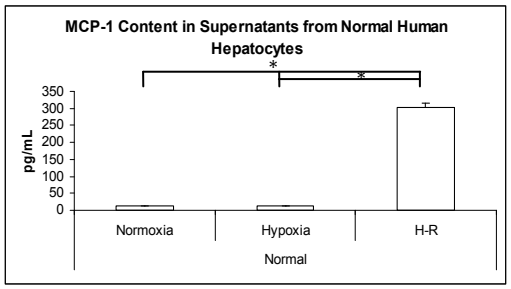

PBC Human Hepatocytes

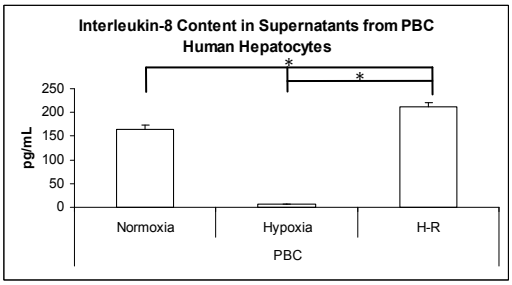

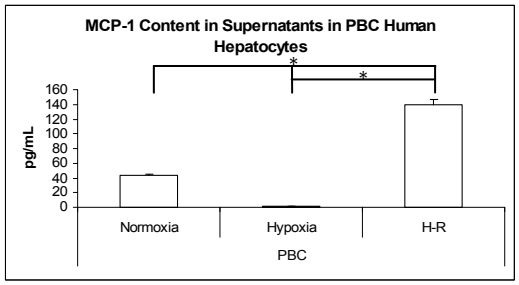

Normal Resected Human Hepatocytes

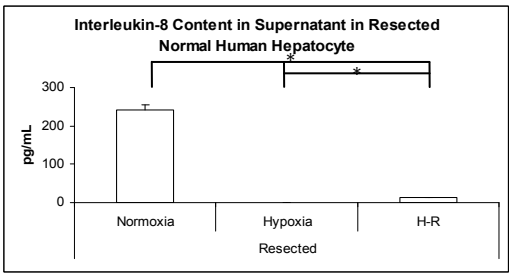

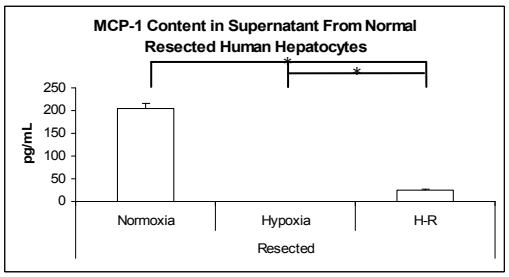

Figure 3.10 Chemokine and Cytokine Responses of Human Hepatocytes during Hypoxia and H-R

Luminex assays were utilised to assess cytokine and chemokine secretion from human hepatocytes during normoxia, hypoxia and H-R. Supernatants from normal human hepatocytes and human hepatocytes isolated from biliary liver disease and normal resected liver tissue were analysed. Of the 30 cytokines and chemokines assessed only IL-8 and MCP-1 showed significant changes. The levels of MCP-1 and IL-8 in human hepatocyte supernatants during normoxia, hypoxia and H-R are illustrated above. (*$p<0.05$, Students *t* test). (n=7-12).

3.3.4 ROS Accumulation Mediated Human Hepatocyte Apoptosis, Necrosis and Autophagy

The effect of hypoxia and H-R on human hepatocyte cell death was assessed using the four-colour reporter assay described in Section 3.2.2. Previous *in vitro* studies have shown that human hepatoma cell lines [26], murine [208] and rodent hepatocytes [209] undergo cell death during hypoxia and H-R. However, many of these studies have not assessed the relative contributions of apoptosis and necrosis to cell death in hepatocytes during oxidative stress. Moreover the function of autophagy in primary hepatocytes still remains to be determined.

Hypoxia and H-R both increased apoptosis, necrosis and autophagy of normal human hepatocytes (Figure 3.11). The level of apoptosis and necrosis in ALD, PSC, PBC and normal resected hepatocytes in shown in Appendix I and the response of autophagy in the various types of human hepatocytes is shown in Appendix V. The level of apoptosis, necrosis and autophagy during hypoxia and H-R mirrored the relative levels of intracellular ROS production within each specific hepatocyte subset. The decrease in ROS production observed in hepatocytes isolated from biliary diseases was accompanied by a concomitant decrease in apoptosis and necrosis confirming the association of ROS with apoptotic and necrotic cell death. The highest basal levels of ROS were seen in hepatocytes isolated from normal resected liver tissue. Despite the increase in intracellular ROS in normal resected hepatocytes, the level of apoptosis or necrosis did not increase suggesting an important difference in the biology and metabolic activity of these cells. It is important to note that normal resected human hepatocytes did have a higher basal level of both apoptosis and necrosis. The composite data for human hepatocyte apoptosis and necrosis during hypoxia and H-R is shown hypoxia and H-R in Appendix I.

The autophagic response as assessed by MDC staining was greater in human hepatocytes during H-R than hypoxia. Furthermore, human hepatocytes isolated from normal liver tissue and diseased liver tissue show markedly different autophagic responses during hypoxia and H-R (Appendix V). While human hepatocytes isolated from biliary cirrhosis show a similar autophagic response to those isolated from normal human hepatocytes (Appendix V) those hepatocytes isolated from ALD show very little staining with MDC during hypoxia and H-R indicating the lack of autophagy within these particular hepatocytes. Finally, human hepatocytes isolated from normal resected liver tissue that have been exposed to chemotherapy showed a very different autophagic response to hypoxia and H-R. These hepatocytes had a much higher basal autophagy level that was maintained throughout hypoxia and H-R.

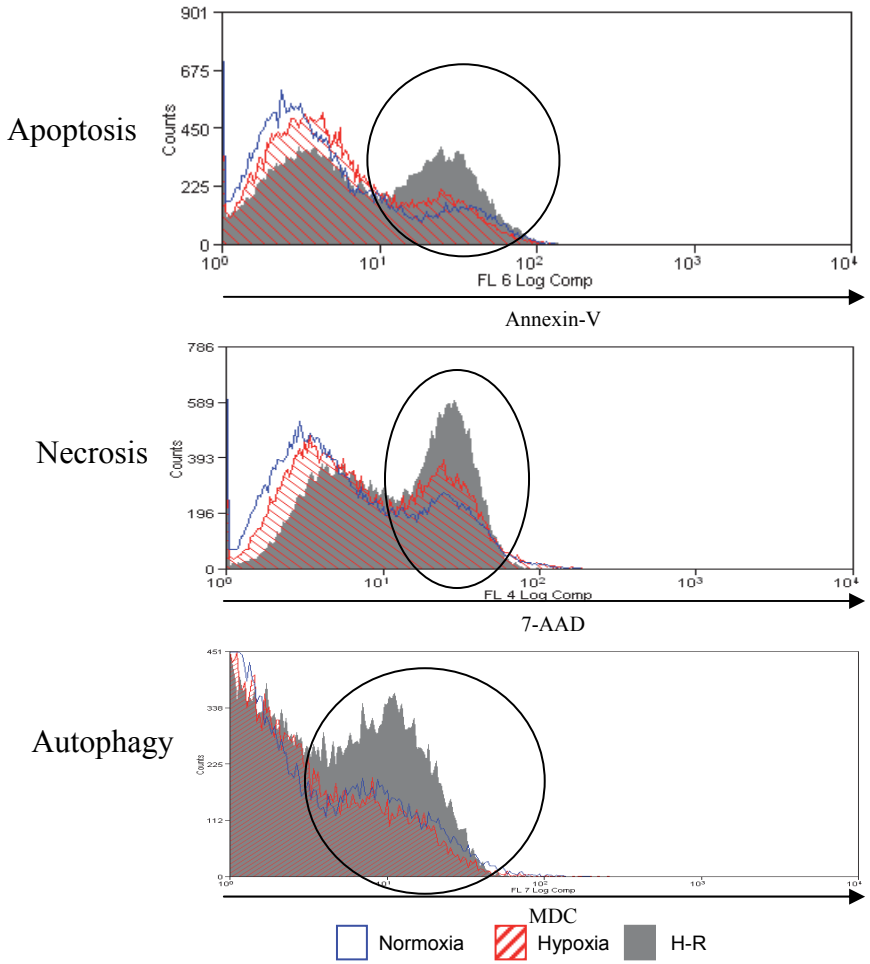

Figure 3.11 Hypoxia and H-R Induce Human Hepatocyte Apoptosis, Necrosis and Autophagy
Representative flow cytometry plots are shown to illustrate the effect of hypoxia and H-R on human hepatocytes apoptosis, necrosis and autophagy that were isolated from normal liver tissue. The vertical ellipse marks the area of interest within the plots. Data is representative of 4 normal human hepatocyte liver preparations.

3.3.5 Large/PV and not Small/PP Human Hepatocytes Undergo Apoptosis and Necrosis during Hypoxia and H-R

As the data illustrated in Figure 3.7 & 3.11 demonstrates there is an association between intracellular ROS accumulation and the induction of both apoptosis and necrosis. Despite this, the relationship between these ROS and cell death in human hepatocytes remains to be clearly established in the morphologically and metabolically distinct large/PV and small/PP hepatocytes. As Figure 3.12 demonstrates large/PV human hepatocytes, in line with their propensity to generate ROS during hypoxia and H-R (see Figure 3.9), sustained significant levels of cell death during hypoxia and H-R in the form of both apoptosis and necrosis (Figure 3.12). In contrast, small/PP hepatocytes did not undergo any apoptosis or necrosis in line with their lack of ROS generation during hypoxia and H-R.

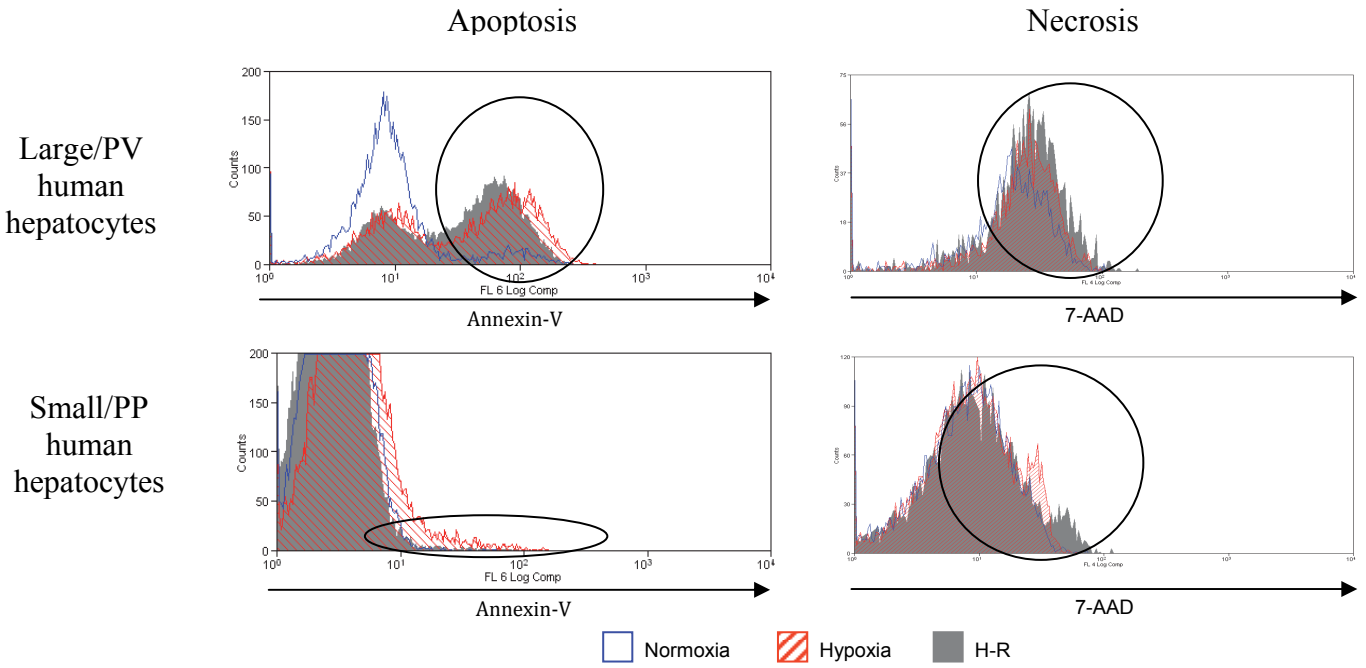

Figure 3.12 Large/PV and not Small/PP Undergo Cell Death during Hypoxia and H-R
Representative flow cytometry plots to illustrate the level of apoptosis and necrosis in small/PP and large/PV human hepatocyte during hypoxia and H-R. The flow cytometric gating protocol used to analyse primary human hepatocytes was the same as that shown in Figure 3.9. The areas of interest within the flow cytometric plots are marked by the vertical ellipses. Appendix III show a bar charts with the pooled data of five separate experiments illustrating the level of apoptosis and necrosis in small/PP and large/PV human hepatocytes during hypoxia and H-R. (n=5).

3.3.6 The Effect of ROS Inhibitors on ROS Accumulation

Anti-oxidants and inhibitors of ROS generation have been shown to abrogate human hepatoma cell death during hypoxia [26]. Figure 3.13 shows the effects of antioxidants, mitochondrial chain inhibitors and NADPH oxidase inhibitors on primary human hepatocyte ROS production during H-R. Similar results were observed in normoxia and hypoxia. NAC acts as a glutathione precursor that enters cells and interacts and detoxifies free radicals by non-enzymatic reactions. It is deacetylated to form cysteine, which supports the biosynthesis of glutathione, one of the most important components of the intracellular antioxidant system in hepatocytes [210]. NAC almost completely inhibited ROS production in all hepatocytes during H-R. Rotenone, a mitochondrial complex I inhibitor, was also able to inhibit ROS production in hepatocytes from all sources, confirming the mitochondria as a major source of endogenous ROS in human hepatocytes. The inhibition of ROS by rotenone was substantial but not as great as that observed with NAC. The production of ROS in the presence of mitochondrial inhibition implies the involvement of other mechanisms in human hepatocytes. Accordingly, the flavoenzyme NADPH oxidase was also involved in ROS production within the hepatocyte. The specific NADPH oxidase inhibitor DPI significantly decreased ROS production in all human hepatocytes. Thus although the overall effect was not as great as that of rotenone, DPI inhibition of NADPH oxidase function suggests that this enzyme is also an important source of ROS in human hepatocytes.

Mitochondrial function was also inhibited within large/PV human hepatocytes using rotenone. As Figure 3.14 demonstrates, rotenone significantly reduced ROS accumulation in large/PV human hepatocytes during normoxia, hypoxia and H-R. Rotenone had no effect upon ROS accumulation in small/PP human hepatocytes. Coupled together with the data in

Figure 3.8 these observation shows that the mitochondrion within human hepatocytes is a key ROS generator.

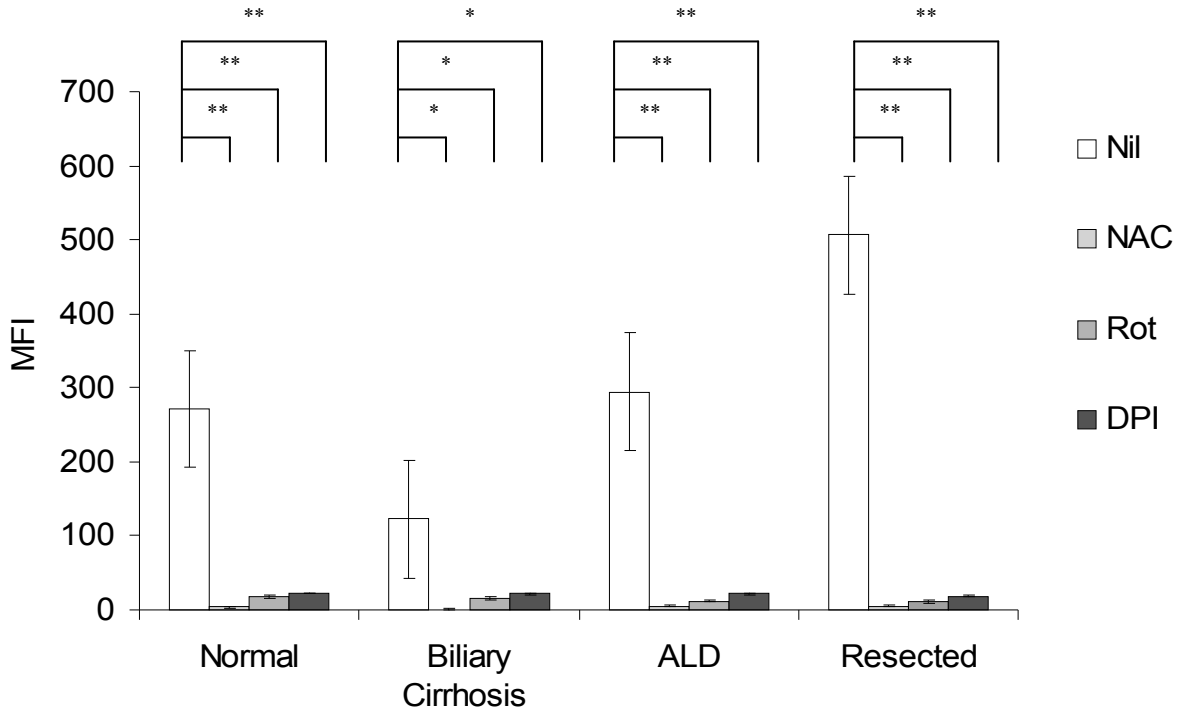

Figure 3.13 Anti-oxidants, Mitochondrial Chain Inhibitors and NADPH Oxidase Inhibitors Reduce Human Hepatocyte ROS Production during H-R

Human hepatocytes isolated from normal, diseased and normal resected livers were treated with 20 mM NAC, 2 μM rotenone (Rot) or 10 μM DPI during H-R. ROS accumulation was determined by flow cytometry as described in the Materials and Methods section. ROS production is shown as MFI and is based upon the MFI readings taken from cells within the ellipse region shown in Figure 3.7. Data are expressed as mean ± S.E. Data is representative 3 normal hepatocyte, 3 biliary disease, 3 ALD and 5 normal resected liver preparations. (*$p<0.01$, **$p<0.01$, Student's *t* test).

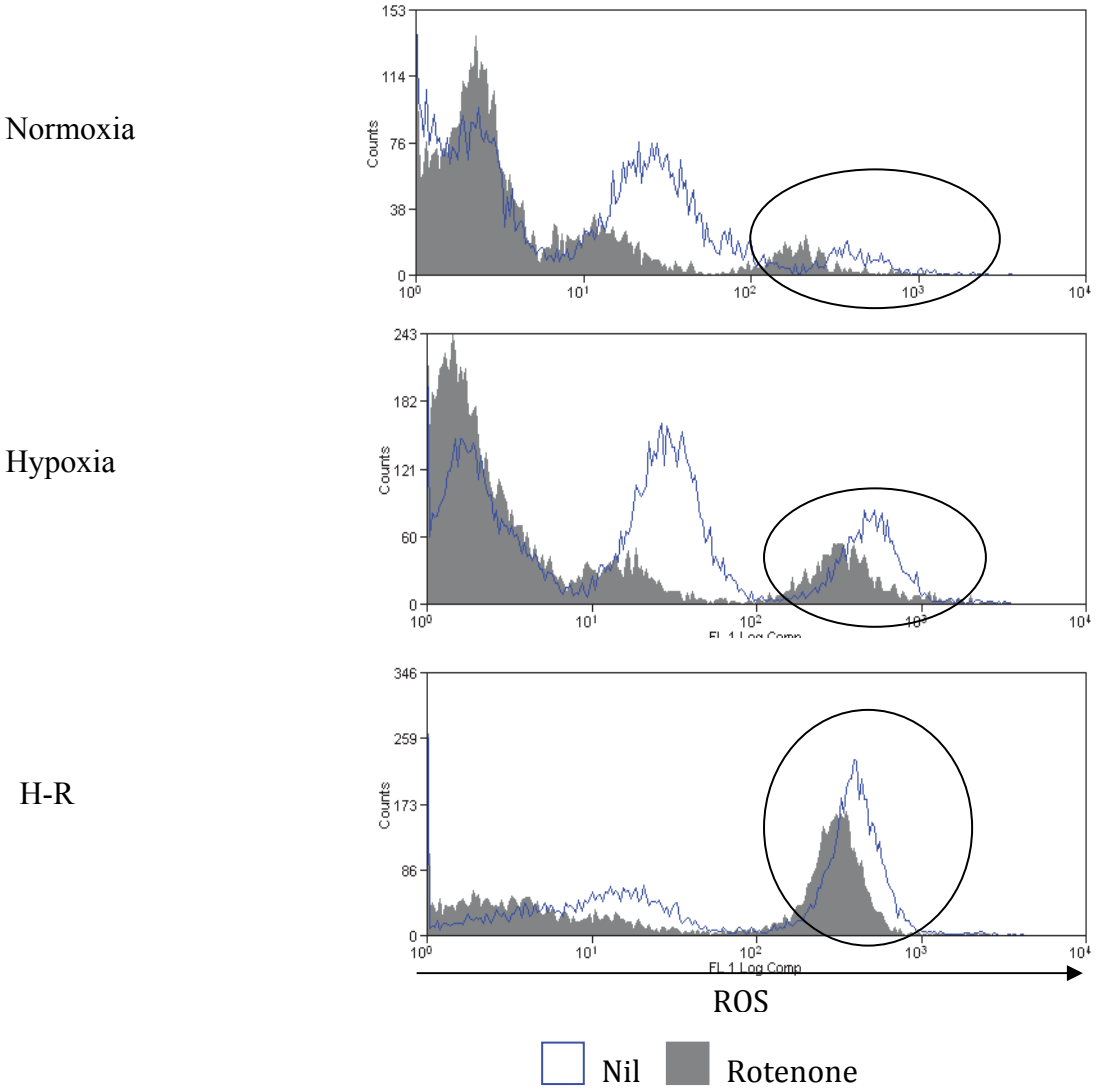

Figure 3.14 The Role of the Mitochondrion in ROS Accumulation in Large/PV Human Hepatocytes

Representative flow cytometric plots show the effect of 2 µM rotenone upon large/PV human hepatocytes ROS accumulation during normoxia, hypoxia and H-R. Human hepatocytes were treated with 2 µM rotenone at the time of placement into normoxia, hypoxia or H-R. Rotenone was dissolved in chloroform to make a stock solution of 1 mM and diluted appropriately. Vehicle alone was shown not to have any effect upon ROS production. Data is expressed as MFI and readings are based upon values taken from cells within the gated region shown in Figure 3.9. Composite data from three experiments is presented in Appendix II.

3.3.7 The effects of ROS Inhibitors on Human Hepatocyte Apoptosis, Necrosis and Autophagy

NAC, rotenone and DPI all inhibited ROS (Figure 3.13) and the effect of this decreased intracellular ROS production upon human hepatocyte apoptosis, necrosis and autophagy was assessed. Data for H-R is shown with similar results obtained during normoxia and hypoxia. The reduction in endogenous ROS in human hepatocytes treated with the various inhibitors led to significantly decreased hepatocyte apoptosis, necrosis and autophagy (Figure 3.15). The effects of NAC were the greatest, in line with its more potent effect on ROS inhibition. Rotenone and DPI also decreased apoptosis necrosis and autophagy during H-R. It is important to note that ROS inhibition abrogated apoptosis, necrosis and autophagy in human hepatocyte isolated from the different types of hepatic disease. Although ROS inhibition abrogated necrosis there was a proportion of the hepatocyte necrosis response that ROS inhibition did not reverse. These data provide clear evidence that endogenous ROS production by mitochondria and NADPH oxidase drives human hepatocyte apoptosis, necrosis and autophagy during H-R. These observations clearly demonstrate the central role of ROS in regulating all three cellular processes in human hepatocytes during normoxia, hypoxia and H-R *in vitro*.

As Figure 3.16 illustrates, NAC, rotenone and DPI significantly reduces large/PV human hepatocyte apoptosis, necrosis and autophagy during H-R. Similar results were observed during normoxia and hypoxia. These findings demonstrate that in large/PV human hepatocytes ROS production and in particular mitochondrial ROS generated during hypoxia and H-R drives cell death in the form of apoptosis and necrosis and also autophagy.

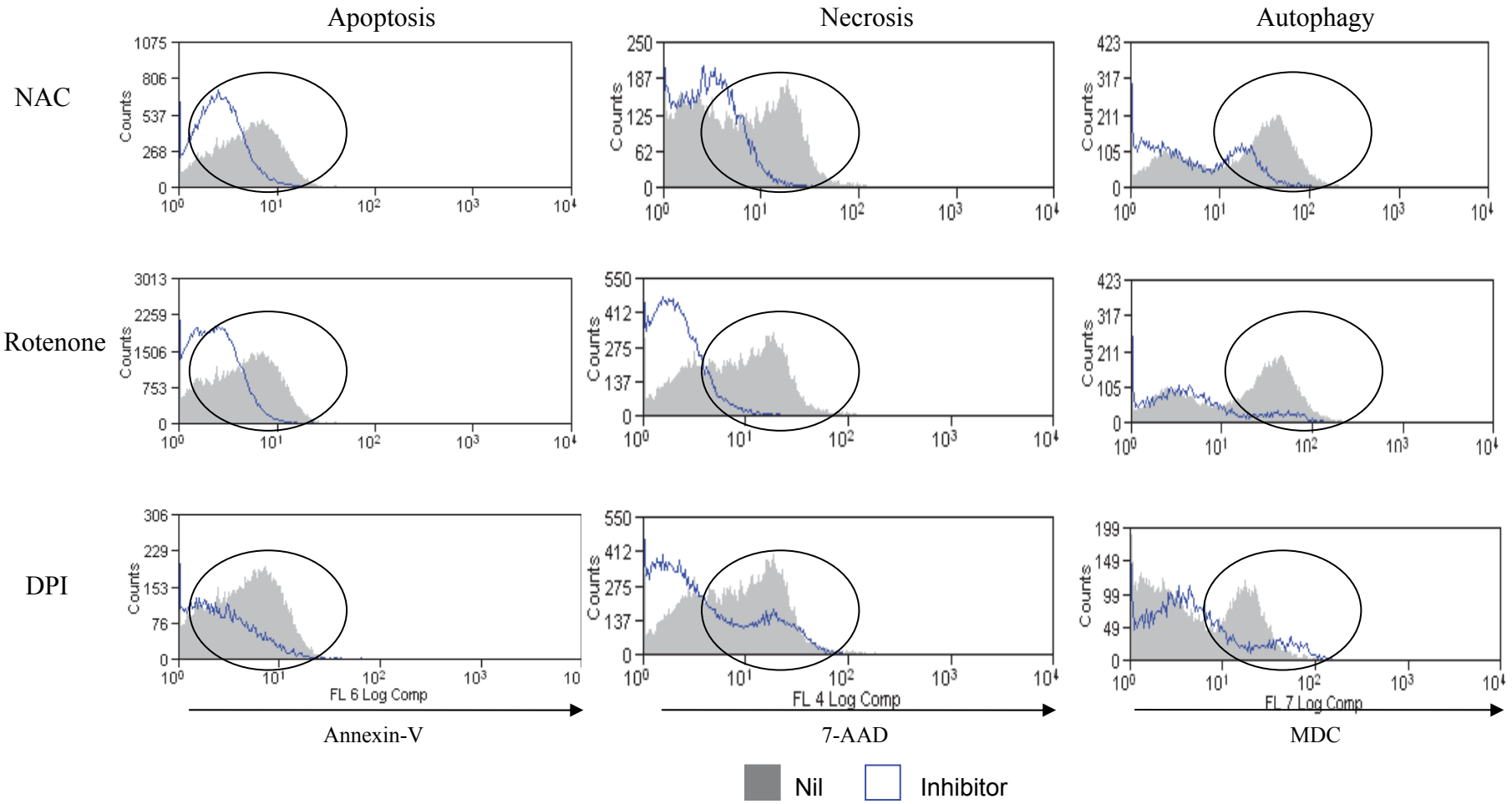

Figure 3.15 ROS Accumulation in Human Hepatocytes during H-R Mediates Apoptosis, Necrosis and Autophagy
Human hepatocytes isolated from normal liver tissue were treated with 20 mM NAC, 2 µM rotenone or 10 µM DPI during H-R and the effects upon ROS production, necrosis and apoptosis was assessed using flow cytometry. Data is representative of human hepatocytes isolated from normal livers. (n=4-7)

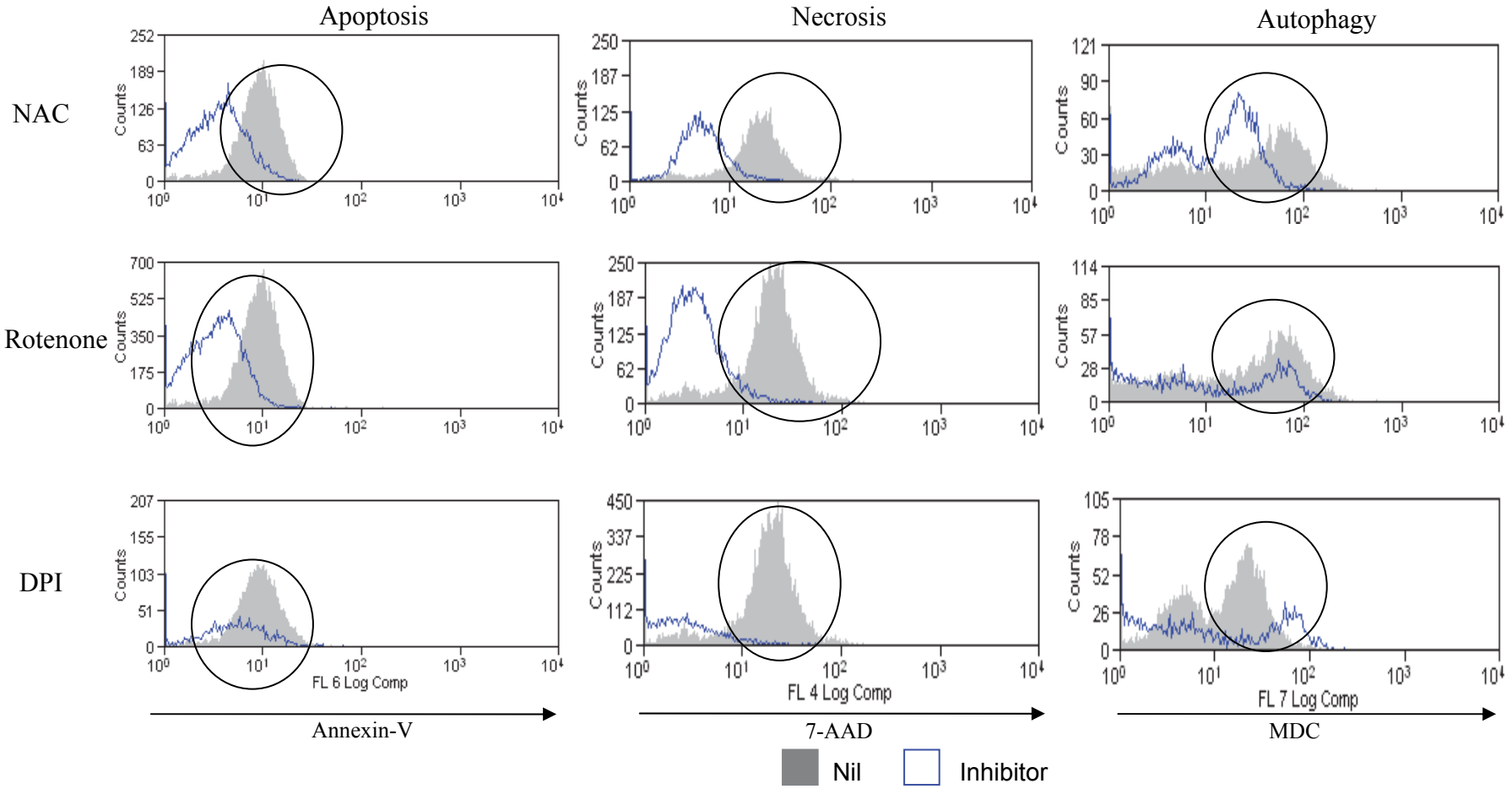

Figure 3.16 ROS Accumulation in PV Human Hepatocytes during H-R Mediates Apoptosis, Necrosis and Autophagy
Large/PV human hepatocytes isolated from normal liver tissue were treated with 20 mM NAC, 2 µM rotenone or 10 µM DPI during H-R and the effects upon ROS production, necrosis and apoptosis was assessed using flow cytometry. Data is representative of human hepatocytes isolated from normal livers. (n=4-7)

3.3.8 Inhibition of Autophagy was Associated with a Concomitant Increase in Hepatocyte Apoptosis during H-R

The specific class III PI-3K inhibitor 3-MA was used to elucidate the role of autophagy in human hepatocytes during hypoxia and H-R. As discussed above 3-MA inhibits the early formation of the autophagosome. Accordingly 3-MA significantly reduced hepatocyte autophagy during H-R. However whilst autophagy was inhibited in human hepatocytes during H-R the number of cells undergoing apoptosis increased (Figure 3.17). Similar data was obtained during normoxia and hypoxia. No significant change in the number of cells undergoing necrosis was observed during H-R with 3-MA pre-treatment (Appendix V). Interestingly inhibition of class III PI3-K also decreased ROS accumulation within human hepatocytes during H-R (Appendix V). These observations suggest that autophagy induction in human hepatocytes during hypoxia and H-R may be a cyto-protective mechanism.

As discussed earlier autophagy is regulated by a number of Atg proteins but whether these Atg proteins are modulated by hypoxia and/or H-R within primary human hepatocytes is not known. As Figure 3.18 demonstrates Beclin-1, an early regulator of autophagy, is induced by hypoxia and H-R. Interestingly, 3-MA reduces Beclin-1 protein levels during normoxia, hypoxia and H-R. Similarly Atg 5, Atg 7, Atg12 and LC3A were also increased during hypoxia and H-R. 3-MA pre-treatment of hepatocytes reduced the protein levels of these Atg proteins. Additionally, cells treated with 3-MA during normoxia, hypoxia and H-R showed the characteristic morphological appearance of the cells undergoing apoptosis (see Appendix V). Hepatocytes appeared phase bright, small and shrunken. Taken together, these observations demonstrate that autophagy promotes survival of human hepatocytes during hypoxia and H-R *in vitro*.

Much recent work has focused upon the role of mitochondrial autophagy or mitophagy during oxidative stress [211-213]. Indeed the mitochondrion is an important ROS generator during IRI and regulates cell death as demonstrated above. Accordingly, the specific mitochondrial dye JC-1 was used as measure of the mitochondrial membrane potential within human hepatocytes during hypoxia and H-R. Red fluorescence of the JC-1 probe represents normal mitochondrial membrane potential whereas green fluorescence represents low mitochondrial potential and is indicative of the onset of cell death. Furthermore, human hepatocytes were co-stained with MDC. As Figure 3.19 shows during normoxia human hepatocytes have normal mitochondrial membrane potential as demonstrated by red fluorescence with no evidence of staining with MDC. Interestingly, incubation of cells with 3-MA markedly increased the green fluorescence of human hepatocytes indicating a lowering of mitochondrial potential and the onset of cell death. Furthermore, hypoxia and H-R lower mitochondrial membrane potential further with a concomitant increase in MDC staining. Moreover, pre-treatment of cells with 3-MA during hypoxia and H-R, whilst reducing MDC staining markedly lowered mitochondrial membrane potential and increased cell death. Finally, MDC and green JC-1 staining were observed to co-localise in these samples indicating that autophagy was occurring in the mitochondrion.

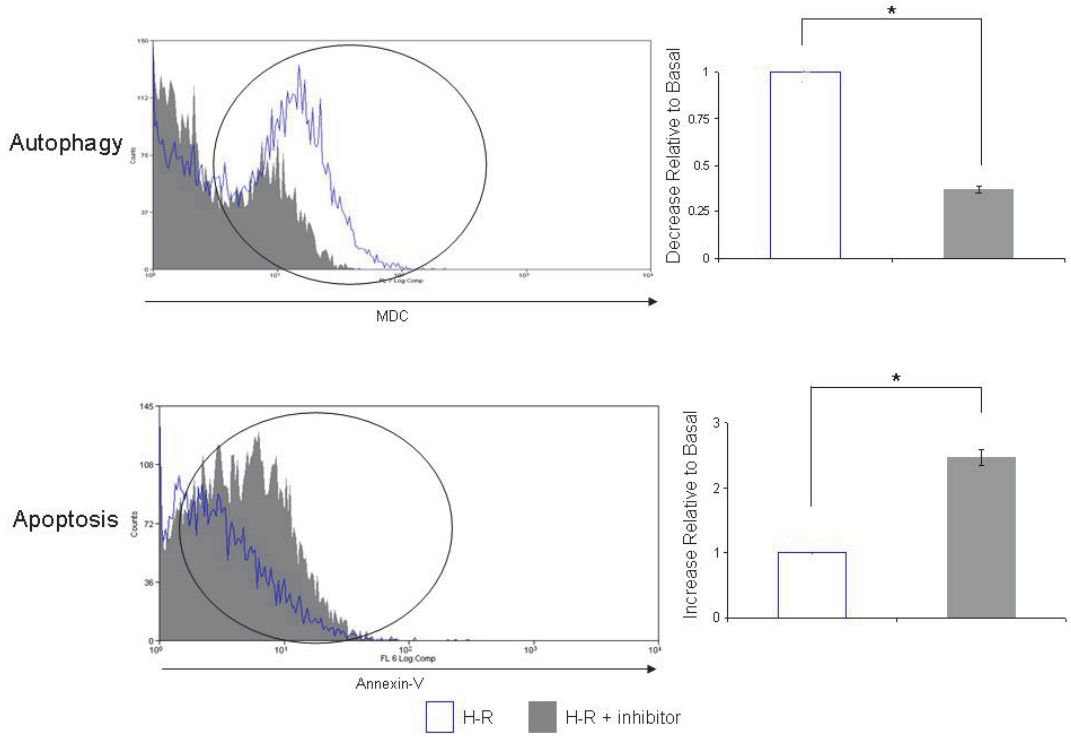

Figure 3.17 Inhibition of Autophagy Increases Apoptosis in Human Hepatocytes during Hypoxia and H-R

Representative flow cytometry plots demonstrate the effects of the pre-treatment of primary human hepatocytes with 3-MA and the resultant effects upon apoptosis and autophagy during H-R. The level of apoptosis and autophagy during H-R are shown in blue and the effects of 3-MA pre-treatment are shown in solid grey. The area of interest is marked with a vertical ellipse. The bar charts to the right of each flow cytometry plot show pooled data from three separate experiments. Data are expressed as increase or decrease relative to basal, where basal refers to the level of apoptosis or autophagy during H-R. Data are expressed as mean ± S.E. (*$p<0.05$ relative to basal, Mann-Whitney test). Human hepatocytes used for these experiments were isolated from benign liver diseases (n=3).

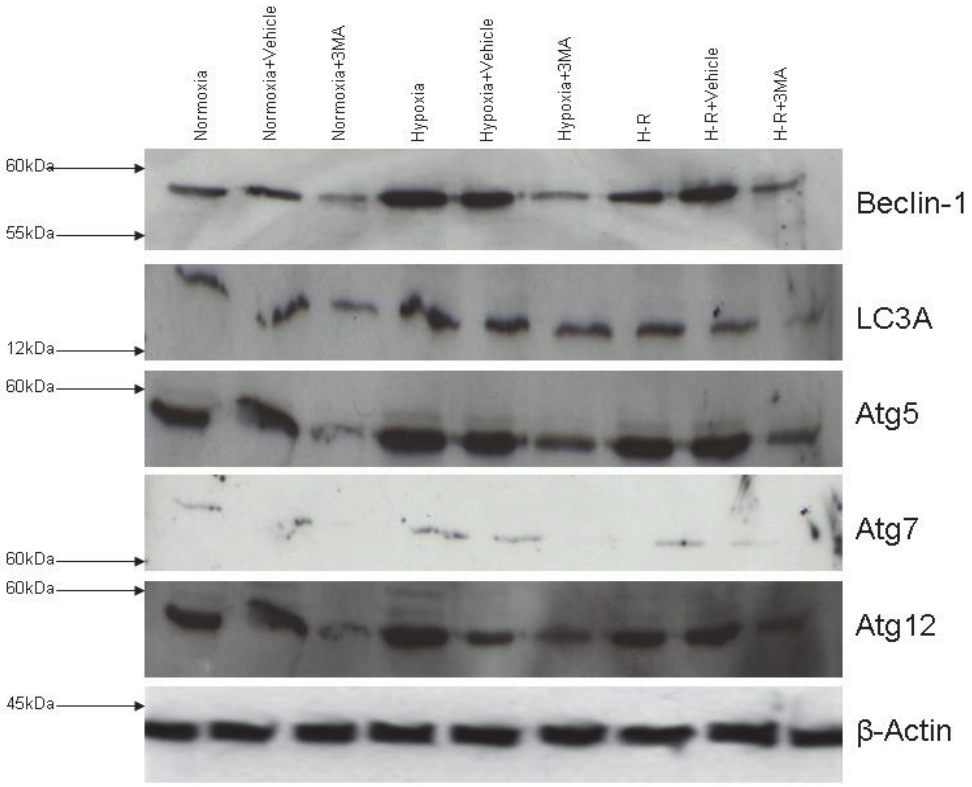

Figure 3.18 Beclin-1, LC3A, Atg5, Atg7 and Atg12 are Induced by Hypoxia and H-R in Human Hepatocytes

Illustrates the induction of various Atg proteins involved in the regulation of autophagy during normoxia, hypoxia and H-R. The effects of the PI3-K inhibitor 3-MA on Atg protein induction during normoxia, hypoxia and H-R are also shown. All Western blots were performed at least three times and presented blots are representative of all samples (n=3).

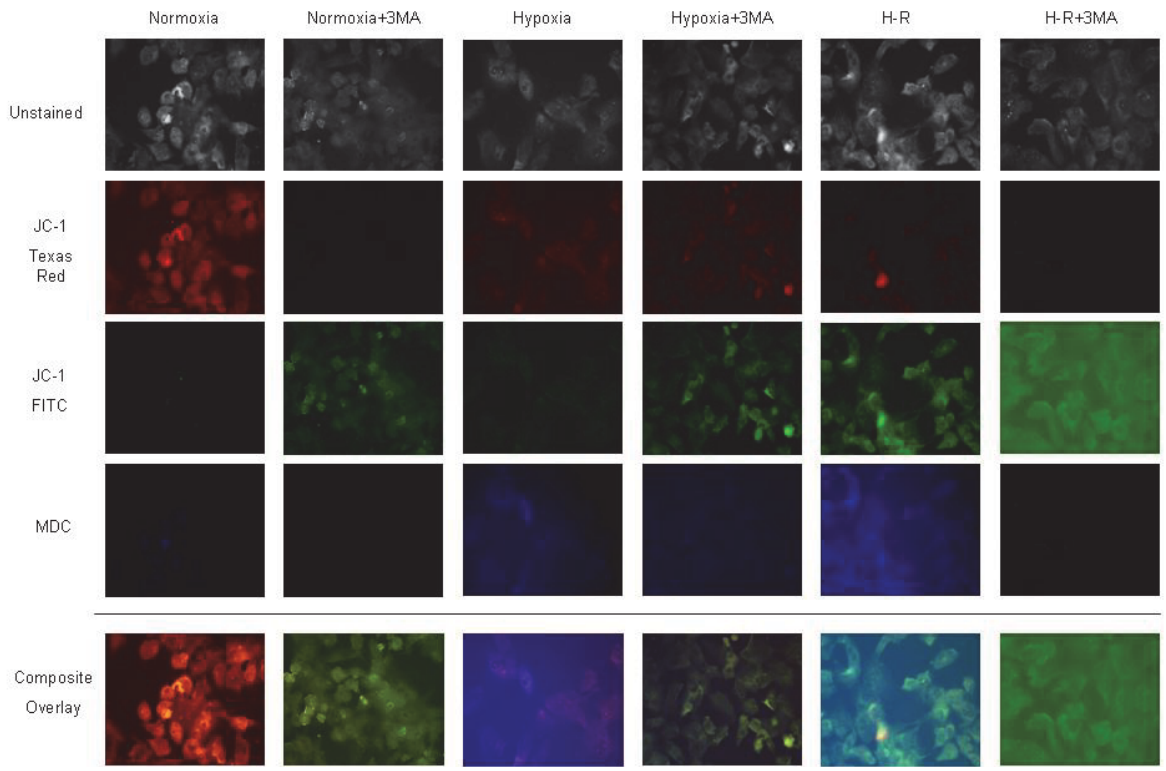

Figure 3.19 Autophagy is Primarily Carried out in Mitochondrion in Human Hepatocytes during Hypoxia and H-R
Demonstrates the effects of hypoxia and H-R upon human hepatocyte mitochondrial membrane potential and MDC staining. Mitochondrial membrane potential was determined using the specific dye JC-1. When mitochondrial membrane potential is normal JC-1 appears red but once membrane potential is lowered or lost the dye become green. MDC staining is detected within the DAPI channel and appears blue. Composite overlay images are shown at the bottom of the figure. Additionally unstained images are provided with stained images to highlight the cellular location of immunofluorescence. In normoxia, as expected there was a normal mitochondrial membrane potential and no autophagy noted. During hypoxia and H-R there was a progressive loss of red JC-1 staining and an increase in green JC-1 staining indicating loss of mitochondrial potential and onset of cell death. In addition there was an increase in MDC staining in human hepatocytes during hypoxia and H-R. Moreover, MDC staining and green JC-1 staining co-localised in human hepatocytes during hypoxia and H-R. (n=3)

3.3.9 Large/PV Human Hepatocytes Preferentially Undergo Autophagy during H-R

As discussed earlier human hepatocytes located within the PV region of the liver tend to be larger in size than their PP counterparts and as shown in Figure 3.9 large/PV human hepatocytes accumulate ROS and are more prone to cell death during oxidative stress making them the targets of hypoxic injury. As demonstrated in Figure 3.20 large/PV hepatocytes increase autophagy significantly more than small/PP human hepatocytes during H-R (Appendix V). As expected, these increased levels of autophagy are sensitive to 3-MA pre-treatment. Indeed, inhibition of autophagy in large/PV human hepatocyte significantly increased apoptosis during H-R (Figure 3.20). These findings collectively illustrate that although large/PV human hepatocytes are prone to increased intracellular ROS production during hypoxia and H-R that then induce cell death, these hepatocytes also concomitantly increase the induction of the cytoprotective mechanism of autophagy.

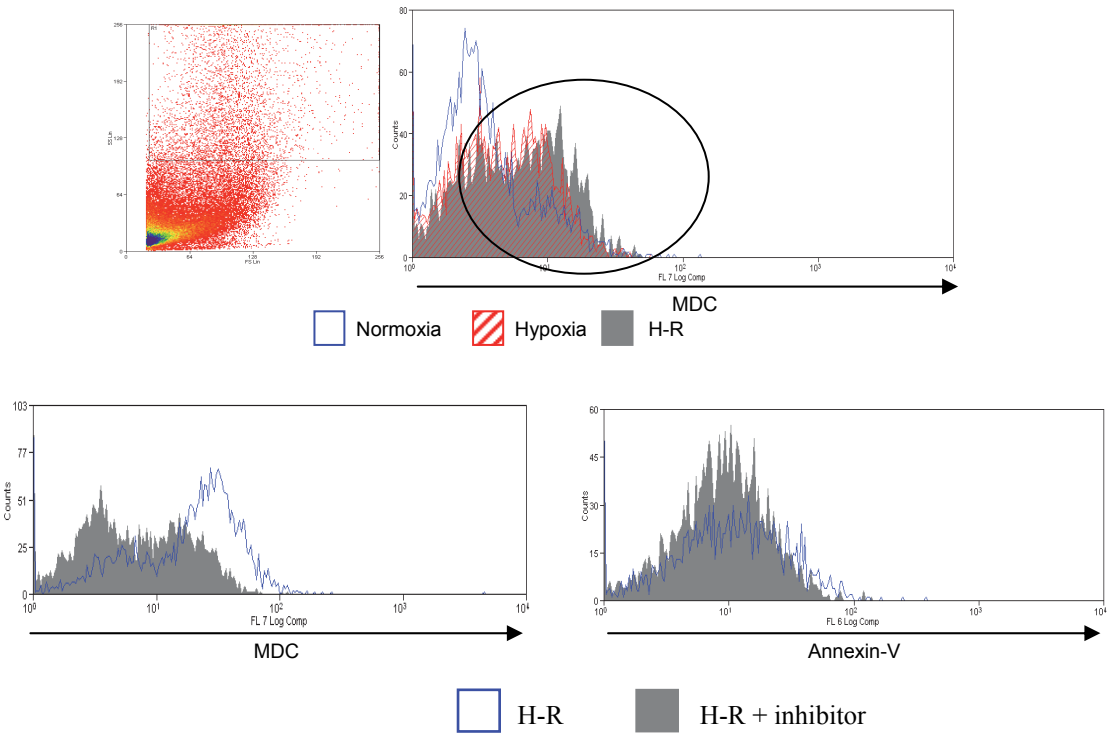

Figure 3.20 Large/PV Human Hepatocytes Requires Autophagosome to Survive H-R
The top panel demonstrates a representative flow cytometry plot to illustrate the levels of MDC staining of large/PV human hepatocytes during normoxia (blue), hypoxia (hatched red) and H-R (solid grey). The plot on the left hand side of the flow cytometric plot represents a typical FS versus SS plot, similar to that shown in Figure 3.9. The FS versus SS plot is from an H-R sample but similar plots were obtained during normoxia and hypoxia. The gating protocol applied to human hepatocytes to analyse PV/large human hepatocytes is shown on the FS versus SS plot. A vertical ellipse marks the area of interest of each flow cytometry plot. The bottom panel illustrates the effects of 3-MA pre-treatment upon large/PV human hepatocyte autophagy and apoptosis during H-R. The effects of H-R alone are shown in blue and the effects of 3-MA pretreatment are shown in solid grey.

3.4 Discussion

3.4.1 The Role of ROS in Human Hepatocytes during Hypoxia and H-R

Whilst hypoxia is a feature of hepatic IRI associated with hepatic surgery, it may also occur during chronic liver inflammation or infection. Therefore, defining the effects of hypoxia upon liver physiology and in particular hepatocyte responses to hypoxia offers important information regarding the development of future therapeutics.

Hepatocytes were conventionally considered relatively insensitive to IRI because of their extensive antioxidant defence mechanisms, and their existence within the comparatively hypoxic hepatic environment [164]. However, numerous *in vitro* and *in vivo* studies have reported deleterious effects of IRI upon hepatocytes although the effect of hypoxia and H-R upon human hepatocytes is not known. The presented data reveals that hepatocytes are susceptible to apoptotic and necrotic cell death induced in response to hypoxia and H-R. Moreover human hepatocytes isolated from different hepatic diseases show variable responses to hypoxia and H-R. Furthermore, human hepatocytes also increase the formation of autophagosomes in a ROS-dependent manner during hypoxia and H-R with the latter mechanism being cytoprotective.

Hypoxia is known to cause dysfunction of the mitochondrial electron transport chain leading to an increase in ROS (Chapter 1), which is accentuated by reoxygenation and can result in cell death [88]. Hepatocytes isolated from normal donor liver, ALD and uninvolved liver from hepatic resections exhibit this classical response to hypoxia and H-R. Interestingly, human hepatocytes isolated from ALD and normal resected liver tissues have high basal levels of ROS production which are then augmented by hypoxia and H-R whereas normal hepatocytes and hepatocytes isolated from the livers of patients with biliary cirrhosis show very little basal ROS production. These differences are likely to be due to the particular

inflammatory microenvironment and milieu that each hepatocyte population has been exposed to. For example, many mediators found in ALD patients are known to increase ROS [214] and hepatocytes isolated from hepatic resections will have been exposed to chemotherapy, a treatment known to increase intracellular ROS [215]. Hepatocytes isolated from biliary cirrhosis had lower levels of ROS during H-R possibly reflecting the upregulation of the antioxidant defences in these particular cells. The differential responses of hepatocytes isolated from different hepatic diseases are unlikely to be attributable to the method of isolation as liver tissue was procured and processed according to an identical and stringent protocol detailed in Chapter 2.

It has been suggested previously that hepatocytes are bystanders in IRI, being targeted by the inflammatory process [42]. However the presented data proposes that hepatocytes have the capacity to actively participate in the IRI process primarily through the production of ROS but also the production of pro-inflammatory cytokines. The finding emphasises the functional relevance of ROS in that increased levels of endogenous hepatocyte ROS are clearly linked to hepatocyte apoptosis and necrosis. This has particular relevance for liver diseases were hepatocytes are exposed to relative hypoxia and which may be responsible for perpetuating injury. ROS can directly activate apoptosis and necrosis thereby supporting the suggestion of Lemasters *et al* that common pathways may at least in part regulate both processes [175]. Moreover, ROS derived from mitochondria and cytosolic NADPH oxidase is crucial for regulating both apoptosis and necrosis. Inhibiting the function of mitochondria and NADPH oxidase with rotenone and DPI respectively significantly improved human hepatocyte viability during hypoxia and H-R. The final mode of cell death that hepatocytes are committed to is likely to be dictated by intracellular ATP content [216]. Interestingly, ROS inhibition had a greater effect upon reducing human hepatocyte apoptosis and only

partially inhibited hepatocyte necrosis. Although ROS does contribute to human hepatocyte necrosis, it is likely that a number of factors, including calcium overload, calpain activation and lysosome rupture commit the cell to undergo necrosis [217]. In contrast, Wang *et al* have demonstrated in Chang human hepatocytes, mitochondrial derived ROS directly activates apoptosis [218]. Accordingly, the inhibition of ROS and in particular mitochondrial ROS had a greater effect upon reducing hepatocyte apoptosis. As previously noted hepatocytes undergoing necrosis will release intracellular ROS into the liver parenchyma and induce both hepatocyte injury and endothelial cell activation [219]. Therefore these observations not only have implications for hepatic IRI but also in liver diseases where chronic hypoxia will lead to continued ROS production and on-going liver damage. On the basis of the presented data it can be speculated that in warm IRI hepatocyte ROS derived may be an important regular of hepatic injury. Furthermore human hepatocytes, with the exception of hepatocytes isolated from normal resected liver and ALD, increase the secretion of MCP-1 and IL-8. These pro-inflammatory cytokines will increase the chemotaxis of leukocytes into the liver during IRI and perpetuate hepatocyte cell death and liver injury. Importantly, whether these cytokines are synthesised or stored and released by human hepatocytes cannot be determined by the presented data.

In rat livers, treatment with antioxidants can prevent IRI [220]. In limited human studies, ischemia induced the expression ROS scavengers within the liver [16]. Despite the presence of antioxidants within hepatocytes, human hepatocytes isolated from normal, ALD and biliary cirrhosis do not appear to be protected against cell death during hypoxia and H-R. Hepatocytes isolated from normal resected liver tissue were however surprisingly resistant to ROS-mediated apoptosis and necrosis. This finding has important implications for research involving human hepatocytes and suggests that studies should be interpreted in the context

of the source of hepatocytes used and those isolated from normal resected hepatic tissues in patients with liver tumours are likely to respond differently to physiological stress. As eluded to earlier, the reason for this difference remains unknown. Furthermore which hepatocyte responses reflect the true physiological response remains to be determined. Although previous studies have shown the cytoprotective effects of anti-oxidants and ROS inhibitors, the presented data for the first time show that inhibition of mitochondrial and NADPH oxidase derived ROS reduces primary human hepatocyte apoptosis and necrosis.

A single strategy aimed at amelioration of the harmful effects brought on by IRI has not yet been adopted into general clinical practice. Experimental interventions to reduce ROS have shown potential to minimise liver injury in various models. ROS scavengers [221], thioredoxin mimetics [222] and delivery of anti-oxidant genes [223] have been shown to partially suppress the effects of IRI. However the clinical application of such compounds has been limited for toxicological and technical reasons. NAC however has clinical potential because it is well tolerated at doses that should be clinically effective. Indeed, NAC is used clinically in several setting including as a hepatoprotective agent in acute liver failure and acetaminophen toxicity. Furthermore, although NAC administration has been shown to improve hepatic microcirculation and bile flow after hepatic IRI [163], the presented data shows that NAC can also reduce all ROS production in human hepatocytes with a concomitant decrease in apoptosis and necrosis in normoxia, hypoxia and HR. Recent studies have suggested that pleiotropic compounds are required to treat IRI due to the diverse nature of IRI [224]. The data presented here suggests exogenous NAC could be a straightforward practical and beneficial strategy to ameliorate human hepatocyte cell death during IRI. Indeed, a recent study showed that NAC dependent reduction of oxidative stress reduced liver injury in a rat model of non-alcoholic steatohepatitis. [225].

Although some authors challenge the pathophysiological relevance of intracellular oxidant stress during reperfusion [226], it is clearly shown that hepatocyte ROS generated by mitochondria and NADPH oxidase can lead directly to significant hepatocyte cell death suggesting other sources of ROS, such as neutrophils and KCs whilst capable of contributing to tissue ROS accumulation in IRI may not be the only pathway leading to ROS mediated hepatocyte damage. An important caveat to the presented data is that oxidative stress in human hepatocytes after hypoxia and H-R may differ between hypoxia at 4^0C and that at 37^0C [227]. Therefore, these data can only be tentatively applied to the transplant setting as they are not wholly reflective of the *in vivo* scenario after OLT.

In summary, human hepatocytes responses to hypoxia and H-R are determined by the particular microenvironment that they have been exposed to. Endogenous human hepatocyte ROS regulates both apoptosis and necrosis and inhibitors of ROS generation significantly improve hepatocyte viability by reducing ROS generation. The use of NAC offers an opportunity to modulate hepatic IRI and improve patient outcome following OLT by possible by addition to preservation fluids. In addition it is clear that hepatocytes taken from normal, normal resected and diseased tissues may vary considerably in their functional and metabolic responses to hypoxic stress.

3.4.2 The Response of Small/PP and Large/PV Human Hepatocytes to Hypoxia and H-R

Exposure of hepatocytes to hypoxia and H-R are very frequent in several hepatic diseases as discussed above. Whilst pathological processes such as haemodynamic shock, septicemia and post liver transplantation will affect the entire liver it is likely that hepatocytes based upon their variable anatomical locations within the liver will sustain differing levels of

injury. Indeed, death of hepatocytes during hypoxia and H-R injury is a multifactorial event including alteration of the plasma membrane, rupture of blebs on the cell surface, calcium accumulation and mitochondrial damage [42]. Whilst the common mediator to these death processes as demonstrated above maybe the accumulation of ROS whether small/PP and large/PV human hepatocytes exhibit differential ROS accumulation during hypoxia and H-R is not known [228]. Studies in rodent models suggest that large/PV hepatocytes are more vulnerable to damage during hepatic injury [169]. Moreover, hepatocyte proliferation, which is an important determinant of patient survival after major hepatic resection, is suggested to occur from the small/PP to large/PV hepatocytes. Therefore, an understanding of the differential vulnerability of hepatocytes to liver injury would provide an important basis for preventing liver failure caused by cirrhosis, hepatic resection, liver transplantation and may even aid the understanding of liver regeneration [169]. The data presented here clearly shows that large/PV hepatocytes are the most susceptible to hypoxic injury. Moreover, this susceptibility is due to the greater propensity of the mitochondria of these large/PV hepatocytes to produce and accumulate intracellular ROS during hypoxia and H-R [229]. It must be noted however, that inhibiting mitochondrial function does not completely abrogate large/PV human hepatocyte apoptosis and necrosis. Indeed, as demonstrated above other enzymes, such as NADPH oxidase, are involved in ROS generation and are also involved in regulating human hepatocyte apoptosis. Accordingly inhibiting NADPH oxidase function in large/PV human hepatocytes also inhibits ROS and decreases apoptosis and necrosis during hypoxia and H-R.

The increased level of apoptosis and necrosis seen in large/PV human hepatocytes *in vitro* in the present study would concur with *in vivo* models of murine and rodent liver injury, where cell death is observed in the peri-venular regions of the liver [186]. A possible explanation

for this observation may well be that glutathione levels in rodent hepatocytes vary considerably between hepatocytes isolated from the small/PP and large/PV regions [230]. Specifically, large/PV hepatocytes have less intracellular glutathione when compared to small/PP hepatocytes. Moreover, following stimulation with amino acids larger hepatocytes generate less intracellular glutathione when compared to small hepatocytes [230]. These findings would potentially explain the increased susceptibility of large/PV human hepatocytes to hypoxic injury *in vitro*.

The data presented also shows that mitochondrial inhibition and anti-oxidants inhibit ROS accumulation in human hepatocytes during hypoxia and H-R. However, the present data builds upon this observation, showing that mitochondrial electron transport chain inhibitors specifically reduce ROS accumulation in the large/PV hepatocytes and consequently reduce apoptosis in large/PV hepatocytes during hypoxia and H-R. Many studies have suggested that liver resident macrophages or KCs located in the peri-venous region of liver are activated during ischaemia and release ROS, leading to hepatocyte damage primarily within the peri-venular region of the liver [169]. Taken together these observations suggest that the peri-venous region of the liver is the site of inflammation and ROS generation during hypoxic liver injury. However, some studies in rodent hepatocytes have suggested that small/PP hepatocytes are more vulnerable to hypoxic injury due to their higher requirement of oxygen [169]. These discrepancies are likely to represent inter-species variability of small/PP and large/PV hepatocytes.

In conclusion, large/PV human hepatocytes are the most susceptible to hypoxic damage. This suggests that therapeutics used in the treatment of liver disease may primarily act upon PV or large hepatocytes.

3.4.3 The Role of Autophagy in Human Hepatocytes During Hypoxia and H-R

While autophagy is an important mechanism by which the cell rids itself of potentially harmful constituents and helps maintain normal cellular functioning and homeostasis, its precise role during liver injury and disease remains uncertain. A consensus is now emerging that autophagy does not precede cell death but may be a physiologically protective mechanism that favours cell survival [231]. The diverse role of autophagy in liver diseases has been recently reviewed [231, 232]. Certainly in liver IRI autophagy mainly has a pro-survival activity allowing the cell to cope with hypoxia. However autophagy is also known to regulate hepatic steatosis and hepatitis virus replication [233]. The reported data is the first to demonstrate autophagy is a cytoprotective mechanism in isolated primary human cells under conditions of oxidative stress. This has potential implications for the understanding of the hepatocyte response to liver injury and development of chronic liver disease.

Previous tissue based studies have shown autophagic hepatocytes within liver allografts are increased following liver transplantation. However these studies failed to show a causal link between oxidative stress, induction of cell death and autophagy [234]. Instead it was suggested that dying hepatocytes also increased autophagy and hence autophagy was thought to represent another mode of cell death. However whether inhibition of autophagy promoted cell death or survival was not demonstrated. Recent studies have shown that the severity and duration of an ischaemic insult determine whether autophagy is induced or not. Indeed these studies have shown that autophagy can delay the decision for a cell to die via apoptosis or necrosis [235]. Using the four-colour reporter assay described here, it is evident that hepatocytes subjected to oxidative stress demonstrate features consistent with increased ROS generation, induction of autophagy and induction of apoptosis. However, crucially the

inhibition of early autophagy with the class PI3-K inhibitor, 3-MA, induces increased levels apoptosis during H-R. 3-MA was the only inhibitor of autophagy used in the presented data. siRNA knockdown or transfection of human hepatocytes was not used to manipulate the autophagy pathway as these are notoriously difficult and inefficient techniques [236-238]. Importantly, inhibiting autophagy causes the lowering of human hepatocyte mitochondrial membrane potential and leads to cell death. Previous authors have also reported that autophagy is responsible for maintaining mitochondrial potential [232]. Importantly, in the data presented above it was shown that human hepatocytes isolated from normal and diseased liver tissues have different autophagy responses during hypoxia and H-R. Specifically, human hepatocytes isolated from normal resected tissue, where livers would have been treated with chemotherapy, showed MDC staining that was consistently high throughout hypoxia and H-R. Coupled with the other findings it is clear that these hepatocytes are resistant to cell death during hypoxia and H-R. Indeed, the reduction in cell death observed in these hepatocytes maybe in part due to the induction of autophagy. This is consistent with previous work performed in human livers [239]. Moreover human hepatocytes isolated from ALD livers showed no autophagy induction during hypoxia and H-R possibly reflecting the extent of damage to these livers. To corroborate this latter point further it is clear from Figure 2.7 that these hepatocytes are metabolically less active than other isolated human hepatocytes and also these hepatocytes have relatively high intracellular ROS content even under basal conditions. Human hepatocytes isolated from biliary cirrhosis and normal benign liver showed similar autophagy responses in an analogous manner to the accumulation of ROS within these cells during hypoxia and H-R. These observations show that the varying levels of intracellular ROS within human

hepatocytes isolated from different liver diseases correlates positively with intracellular MDC staining and hence autophagy.

During hypoxic stress, autophagy appears to occur within the mitochondrion and the presented data shows that this process is likely to be mediated by Beclin-1, LC3A, Atg 5, Atg 7 and Atg 12 although other Atg proteins such as Atg 8 and Atg 9 were not assessed. These findings corroborate those in HeLa cells where inhibition of autophagy also led to an increase in apoptosis [240]. It can be seen from the experimental data presented above the induction of autophagy within human hepatocytes during oxidative stress is essential for cell survival. Previous work by Kohli *et al* in hepatocytes has shown that ROS production lies upstream of PI3-K activation [241]. Indeed, inhibition of PI3-K with 3-MA did not lead to an increase in Beclin-1, LC3A, Atg 5, Atg7 and Atg 12 protein levels which were otherwise seen during hypoxia and H-R. Coupled together these findings suggest that ROS activates PI3-K, which subsequently activates the remaining autophagy machinery. As stated above in hepatocytes, autophagy targets mitochondria for degradation, a process known as mitophagy. Indeed inhibiting ROS can regulate autophagy, apoptosis and necrosis. Inhibiting ROS inhibits all three cellular processes, but selective inhibition of human hepatocyte autophagy promotes apoptosis.

Furthermore, PV/large human hepatocytes increased levels of autophagy much more than PP/small human hepatocytes during hypoxia and H-R in line with their greater susceptibility to hypoxic injury. Moreover, inhibition of autophagy in PV/large human hepatocytes increased apoptosis during H-R, demonstrating the link between autophagy and cell survival. Central regulators of autophagy are the evolutionarily conserved Atg genes and recent studies have shown that some Atg proteins can be regulated by ROS [198]. Beclin-1, an essential regulator of early autophagy was induced by hypoxia and H-R and efficiently

inhibited by 3-MA. Indeed, recent reviews have detailed the essential role of Beclin-1 in IRI [242] as well as its central role in mediating autophagy during oxidative stress [243]. Moreover, under stress hepatocytes utilise the LC3 protein to induce mitophagy within the dysfunctional mitochondrion [244]. This latter observation is probably the role of increased LC3 seen in the *in vitro* model used here. In an experimental rat model, short term anoxia increases the expression of Atg7 in hepatocytes and protects against anoxia-reoxygenation mediated apoptosis and necrosis [245]. In the model of IRI detailed above an induction of Atg 7 was also found. Furthermore, induction of Atg5 and Atg 12 was also observed. These two Atg proteins are involved in the latter processes of autophagy. Recent studies have shown the integral role Atg 5 in regulating menadione-induced oxidative stress [246]. In this study knockdown of Atg 5 in the rat hepatocyte line RALA255-10G sensitized cells to both apoptotic and necrotic cell death. In addition Atg 12, along with other Atg proteins, is required for the protection of anoxic rat hepatocytes from cell death [247].

While the presented data does not conclusively show which signaling pathways are activated by ROS in human hepatocytes to induce autophagy, it does demonstrate that ROS is a key mediator of autophagy during oxidative stress. Furthermore in accordance with the data presented here previous authors have shown that the general anti-oxidants, catalase and NAC reduce autophagy [198]. Mitochondrial and NADPH oxidase derived ROS are critical for the induction of autophagy in human hepatocytes. In addition previous studies have shown that H-R induces increased manganese superoxide dismutase expression in hepatocytes [248]. Taken together these studies show that ROS derived from many sources within hepatocytes can regulate autophagy. Moreover this generated ROS has pro-survival effects in activating autophagy but also signals to cell death in the form of apoptosis and necrosis. The increase in antioxidant defences within hepatocytes is likely to protect from cell death and the

inhibition of autophagy may not be detrimental as autophagy can be regulated by other system besides ROS [249]. These observations provide interesting insights to the function of ROS in determining human hepatocyte fate during oxidative stress. Taken together, these observations clearly point to ROS regulating diverse and different signaling pathways within human hepatocytes during oxidative stress. These pathways appear to regulate both cell death and cell survival. It is likely that either the absolute level of intracellular ROS, the type of ROS sub-species generated or duration of ROS generation may be the critical factors in determining cell fate. The precise mechanistic pathways remain to be elucidated but may ultimately provide insights which may inform the development of therapeutic strategies aimed at limiting the cellular damage associated with liver injury. Previous authors have reported that inhibiting autophagy within rat hepatocytes leads to necrosis [250]. Moreover, in a model of ischaemic preconditioning Esposti *et al* reported that autophagy may switch necrosis and/or apoptosis on and off by modulating intracellular signaling [251]. This was not observed in the presented data and it is likely that this represents species-specific effects of autophagy as no previous studies have evaluated autophagy in human hepatocytes. It may also represent a difference between the induction of autophagy in the *in vitro* and *in vivo* setting.

The data also demonstrates that ROS production decreased within human hepatocytes after 3-MA pre-treatment during H-R. One would expect that in hepatocytes in which autophagy were inhibited damaged mitochondria would continue to form ROS and induce cell death. However, the particular model described here utilised experiments assessing cell death and ROS production at 24 hours of hypoxia and/or H-R. The significant levels of apoptosis seen after 3-MA pretreatment during H-R suggests that a significant number of hepatocytes were already dead hence intracellular ROS had reduced.

The data demonstrates that within human hepatocytes, autophagy is a cell survival mechanism during periods of oxidative stress. Moreover, taken together with previous studies, it is clear that PV/large human hepatocytes increase autophagy significantly more in H-R relative to PP/small human hepatocytes. This is in accordance with previous observations that the PV/large peri-venular human hepatocytes are more susceptible to oxidative stress. These observations suggest that the pharmacological activation of P13-K or other autophagy machinery, particularly within PV/large human hepatocytes may prove effective strategies in ameliorating human hepatocyte cell death in chronic liver disease as well as following liver transplantation.

CHAPTER 4 - THE ROLE OF CD40:CD154 IN REGULATING HUMAN HEPATOCYTE CELL DEATH DURING HYPOXIA AND H-R

4.1 Introduction

4.1.1 The CD40:CD154 Receptor Ligand Dyad

The TNFα super-family consists of at least 50 different receptors and ligands as discussed in Chapter 1. The members of this super-family are known to be integrally involved in the regulation of diverse cellular processes such as cell death, adhesion molecule expression and the regulation of lymphoid cell activation [123]. Despite the initial suggestion that CD40 exists as a dimer that trimerised after CD154 binding, it is now known that CD40 is expressed as a trimeric complex upon the cell surface of many cells [252]. CD40 is a type I trans-membrane protein receptor. The gene for CD40 is located in chromosome 20 (q12-q13.2) [253]. The B-lymphocyte is the main cell type expressing CD40 but its expression is much more diverse than first thought [254]. Other cells expressing CD40 include other immune cells, epithelial cells, fibroblasts, vascular endothelial cells and smooth muscle cells and platelets. Expression of CD40 is induced by pro-inflammatory stimuli, such as IL-1, IL-3, and IL-4, TNFα and IFNγ [254]. In general, CD40 can be up-regulated within 6-12 hours of pro-inflammatory stimulation and can remain expressed for up to 72-hours. Many transcription factors are thought to be important in the regulation of CD40 expression but NFκB is known to be a key regulator of the process. Activation of CD40 can regulate a number of diverse signalling pathways and lead to a number of different functional outcomes [255]. CD40 has no intrinsic kinase activity and following activation is reliant upon the recruitment of the TRAFs family of adapter proteins to the cell membrane that stimulate downstream signalling pathways [252, 256, 257]. The precise mechanisms involved in CD40 signalling pathways within the liver are discussed below.

CD154, a type II trans-membrane protein, has its gene located on chromosome X (q26.3-q27.1) [258]. CD154 is a 39-kD glycoprotein. Originally, CD154 was thought to function

only in stimulated CD4-positive lymphocytes [259, 260], mast cells and basophils [261]. The cellular expression of CD154 can be up-regulated by pro-inflammatory cytokines and lipo-proteins. In contrast the expression of CD154 is much more restricted than that of CD40. CD154 is expressed by platelets, T-lymphocytes and macrophages [121]. Specifically, liver resident macrophages or Kupffer cells express CD154 whilst activated platelets can release soluble CD154 after their activation [253].

Initially, the CD40:CD154 interaction was primarily investigated in connection with T-lymphocyte activation and co-stimulation, B-lymphocyte proliferation and differentiation and switching of antibodies from IgM to IgG [262]. Subsequently the CD40:CD154 receptor-ligand dyad has been shown to play a part in infection, inflammation and many other biological processes [124]. Moreover the CD40:CD154 interaction has been shown to play important roles in atherosclerosis [263], diabetes mellitus [264] and hyper IgM syndrome [265].

4.2 CD40:CD154 and the Liver

4.2.1 Introduction

The CD40:CD154 receptor-ligand dyad has particular relevance to liver disease and hepatic patho-physiology including hepatic IRI. Whilst the function and role of TNFα in liver disease has been well studied [266], the role of CD40 and CD154 remains enigmatic. Within the liver, hepatocytes, cholangiocytes, HSEC and hepatic stellate cells (HSC) express CD40 [118-120]. CD154 is expressed by CD4-positive T-lymphocytes, liver resident macrophages or Kupffer cells and platelets within the liver [124]. Platelets also release CD154 in a soluble form following their activation [253]. Thus numerous interactions between the different cells expressing CD40 and CD154 will have undoubted implications for the initiation and

progression of acute and chronic liver disease. Specifically, the consequence of the CD40:CD154 interaction upon hepatocytes, cholangiocytes, HSEC and HSC will shape the response of the liver to pro-inflammatory stimuli. The signalling pathways employed by these various cells in response to CD40 stimulation by CD154 are discussed below.

4.3 CD40 Signaling within Different Liver Cells

4.3.1 Hepatocytes

At least 70% of the liver parenchyma consists of hepatocytes. As discussed in Chapter 1 the functional unit of the liver is the acinus (see Figure 2.1) and as a consequence hepatocytes derive a zonal distribution; zone 1, zone 2 and zone 3 as discussed in Chapter 3. A growing body of evidence suggests that the zonal distribution of hepatocytes not only influences the morphology of cells but also the functional capabilities of these hepatocytes [42, 169, 178, 182, 183]. As stated above hepatocytes and in particular human hepatocytes express CD40 upon their cell surface under basal conditions in cell culture [122]. CD40 is pivotal in regulating hepatic inflammatory responses. Indeed, *in vitro* studies show that pro-inflammatory stimulation of human hepatoma cells lines increases cellular expression of CD40 [267] and *in vivo* studies demonstrate that CD40 is widely expressed upon human hepatocytes during inflammatory liver diseases [122]. Indeed CD40 positive hepatocytes are observed in both peri-portal (zone 1) and periveular areas (zone 3) areas during hepatic inflammation. Recent evidence also suggests that up-regulation of CD40 upon hepatocytes during hepatitis B virus infection may play a facilitating role in the pathogenesis of hepatocellular carcinoma [268]. Clearly, CD40 has an important role in liver pathophysiology.

Being the most abundant cell type within the liver, hepatocytes are targeted by many hepatic diseases including allograft rejection post liver transplantation, autoimmune liver disease and viral hepatitis [122, 269]. All these diseases are characterized by an inflammatory cell infiltrate associated with the loss of hepatocytes primarily by apoptotic mechanisms [119, 122, 270, 271]. CD40 activation upon hepatocytes with either soluble recombinant CD40 ligand or cross-linking monoclonal antibody initiates apoptosis, in the absence of any co-factors, via Fas-dependent mechanisms [119, 122]. However, whether other signalling pathways are activated within hepatocytes following CD40 activation is not known. In particular, whether CD40 activation can couple to the generation of ROS or lead to the activation of the Janus Kinases (JAK) is not known. The regulation of the intracellular signalling pathways and transcription factors induced as a result of CD40 activation upon hepatocytes is likely to be as complex as that for other TNFα super-family members such as TNFα.

It is known that following CD40 ligation and activation, the receptor is internalised within the cell. The cytoplasmic C terminus of the CD40 receptor, as stated above, lacks intrinsic kinase activity. Therefore, following CD40 activation, the adapter proteins of the TRAF family are recruited to the plasma membrane and are responsible for propagating signal transduction. The TRAF family of adapter proteins consist of six members; TRAF 1-6 [272]. The precise role of TRAFs and signalling events within hepatocytes remains to be fully ascertained. Following CD40 activation there is the sustained activation of Activator Protein-1 (AP-1) and the MAPKs, but not NFκB, with both AP-1 and MAPK being central to initiating apoptosis [157]. Furthermore, TRAF2 and TRAF6 have been postulated to mediate the activation of the MAPK sub-family, c-Jun NH_2-terminal kinase (JNK), which then lead to activation of the transcription factors AP-1 and NFκB and subsequent apoptosis

[256, 257, 272]**.** However, it must be remembered that these latter experiments were not conducted in hepatocytes. However, both NFκB and AP-1 have been implicated in the control of epithelial proliferation or apoptosis [122, 252, 256, 257] with cell fate being determined by the level of activation of pro- or anti-apoptotic genes with NF-κB and AP-1-sensitive promoters. Eliopoulos *et al* has further suggested TRAF2 is responsible for signal propagation with TRAF3 being a negative regulator of TRAF2 function [273]. However, CD40 activation can also increase the accumulation of intracellular ROS in lymphoid cell lines in a TRAF3 dependent manner [274]. Whether this process occurs in human hepatocytes is not known and the exact TRAF molecule that may regulate this process is not known. Obviously the accumulation of ROS secondary to CD40 activation has clear implications for hepatic IRI particularly in the context of the results presented in Chapter 3. In lymphoid cells the generation of ROS is dependent upon the recruitment of the flavoenzyme NADPH oxidase to the cell membrane, in a TRAF3 dependent process, which is then able to generate the ROS sub-species, hydrogen peroxide [274]. Therefore, the identity of the TRAF molecule critical for CD40 signalling in hepatocytes remains elusive. The possibility of different TRAFs recruitment leading to different cellular responses also remains plausible.

CD40 activation ultimately leads to the activation of the MAPKs sub-families of JNK and p38, important regulators of cell death. AP-1 activation lie downstream of MAPK activation and therefore MAPK activation is likely to be a point of convergence for the CD40 signalling pathway in hepatocytes. As Figure 4.1 illustrates the MAPK-AP-1 pathway is likely to be the common pathway that lies downstream of CD40 signals and is the point of convergence for signalling in hepatocytes and cholangiocytes (see below). Taken together, these studies highlight the complexities of the upstream CD40 signalling pathway and

suggest that CD40 can couple to AP-1 signalling pathways to regulate hepatocyte cell death. Whether CD40 ligation in human hepatocytes can also active the JAK-STAT signalling pathway, as seen in cholangiocytes (see below), remains to be ascertained. Finally, the CD40:CD154 signalling pathway has been shown to play important role in murine models of hepatic injury [19]. In these studies activation of CD40 results in hepatocyte apoptosis [19, 169]. In summary, CD154 stimulation of CD40 plays a central role in hepatocyte death in a variety of liver diseases through direct and indirect pathways that may have the potential to be utilised as therapeutic targets in human disease.

4.3.2 Cholangiocytes

Within the liver, regulation of biliary epithelial cell or cholangiocyte survival is crucial for maintaining epithelial cell integrity in the biliary tract. Immune-mediated destruction of cholangiocytes in diseases including PBC, allograft rejection and graft versus host disease occurs as a result of increased apoptosis that can be mediated by CD40:CD154 [275]. As with hepatocytes, CD40 activation in cholangiocytes leads to induction of FasL and autocrine or paracrine activation of Fas and resultant apoptosis [118]. Again in an analogous mechanism to hepatocytes, CD40-activated Fas-dependent apoptosis requires sustained activation of the transcription factors of AP-1 but also the transcription factor STAT 3 to overcome transient, short lived NFκB activation and tip the balance away from survival towards apoptosis [120]. This suggests at least some conservation of signalling pathways between the epithelial cells derived hepatocytes and cholangiocytes. Additionally, in cholangiocytes, CD40 mediated apoptosis also requires the activation of the JAK2-STAT3 pathway and the downstream activation of caspase-3 [120]. These observations suggest that CD40 initiates divergent signalling pathways that lead to apoptosis. Moreover, both primary

and malignant cholangiocytes are relatively resistant to Fas-mediated killing but show exquisite sensitivity to CD154, suggesting that the CD40 pathway is intact and fully functional in both primary and malignant cholangiocytes [118]. Furthermore, the relative insensitivity of cholangiocytes to Fas activation demonstrates the importance of CD40 augmentation of Fas dependent death in these cells. Interestingly, C4 binding protein (C4BP) can modulate CD40:sCD154 interactions by presenting a high molecular weight multimeric sCD154:C4BP complex that suppresses activation of transcription factors that critically regulate cholangiocyte apoptosis permitting survival without proliferation [275]. Figure 4.1 summarises the effects of CD40:CD154 upon cholangiocytes and hepatocytes. Importantly, these above studies have not evaluated whether CD40 activation can also drive cholangiocyte necrosis and whether CD40 can couple to other signalling pathways.

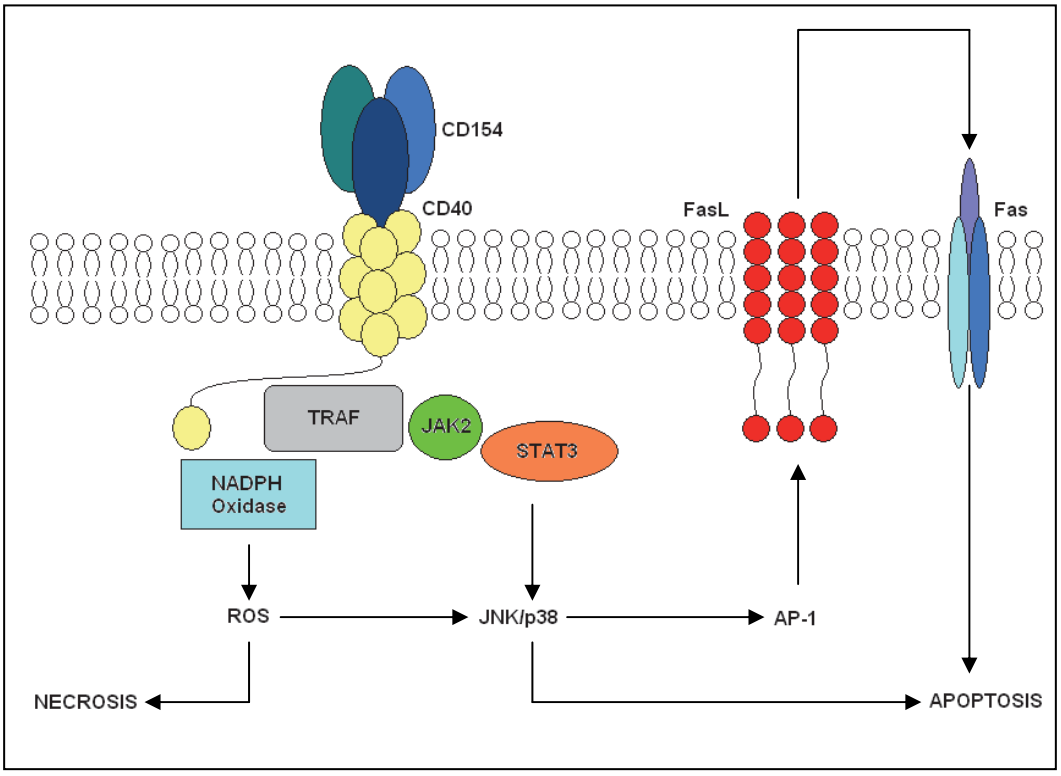

Figure 4.1 The Signalling Pathways Employed by CD40:CD154 to Induce Hepatocyte or Cholangiocytes Cell Death

The likely signalling pathway initiated by CD40:CD154 in hepatocytes and cholangiocytes. After activation by trimeric CD154, CD40 is able to recruit members of TRAF family of adaptor proteins to the cell membrane. Once at the cell membrane TRAF molecules are able to recruit the JAK2-STAT3 complex and possibly NADPH oxidase to the plasma membrane, although it is likely that both these pathways are in operation in these cell types. The upstream signalling pathways are likely to converge at the level of the MAPKs p38 and JNK. Following AP-1 assembly hepatocytes and cholangiocytes undergo apoptosis via a FasL-Fas-dependent process or via activation of the caspases.

4.3.3 Human Sinusoidal Endothelial Cells (HSEC)

The function of HSEC within the liver is diverse including the recruitment of inflammatory cells, immuno-regulation and biosynthesis. It has long been known that the activation of CD40 on endothelial cells results in increased chemokine secretion and adhesion molecule expression [276]. The role of CD40 ligation upon vascular endothelium has been extensively studied and recently reviewed [124]. In contrast to the epithelial cell types in the liver, HSEC do not undergo apoptosis in response to CD40 activation but instead proliferate. Although the mechanisms responsible for CD40-mediated proliferation of HSEC remain to be fully elucidated, NFκB activation is likely to play a key role in regulating this process as demonstrated by sustained up-regulation of NFκB activity in HSEC for >24 hours in response to CD154 [157]. In addition, inhibiting NFκB leads to marked increases in endothelial cell apoptosis at 24 hours suggesting that this prolonged NFκB activation protects HSEC from apoptosis. NFκB also binds to promoters of pro-inflammatory genes such as IL-8, MCP-1, ICAM-1, and vascular cell adhesion molecule (VCAM), and the sustained NFκB up-regulation in HSECs could explain why chemokine and adhesion molecule expression are up-regulated in endothelial cells after CD40 ligation [262]. Endothelial cell proliferation in response to CD40 could be important not only in chronic hepatic inflammation but also in angiogenesis and tumour vascularisation where 60% of hepato-cellular carcinomas express high levels of CD40 [267]. CD40 ligation on HSEC can modulate other endothelial cell functions, including expression of adhesion molecules and chemokines in a manner similar to that reported with endothelial cells from other tissues [262]. This indicates that CD40 expression by HSEC may have multiple roles beyond regulation of cell fate.

4.3.4 Hepatic Stellate Cells

The liver reacts to tissue injury with a well-defined wound-healing response that is initially directed at removing damaged tissue through infiltration of inflammatory cells, followed by a second phase that is characterized by the proliferation of myofibroblasts and increased matrix production, and a final phase of tissue remodeling and regeneration [277, 278]. Whereas acute liver injury usually resolves, chronic liver injury leads to an uncoordinated response that is characterised by parallel occurrence of inflammation and matrix production with insufficient remodeling leading to progressive scarring. HSCs are at the centre of this fibrogenic response [268]. Upon activation, HSCs change their phenotype from retinoid-storing quiescent cell to extracellular matrix-producing myofibroblasts. HSCs perpetuate their activation through autocrine and paracrine mechanisms that involve the secretion of pro-inflammatory cytokines and chemokines. There has been only limited studies of CD40 function in HSC but activated HSCs do express moderate levels of CD40 when compared with an isotype-matched control antibody [279]. Furthermore, pro-inflammatory micro-environments increase CD40 expression upon HSC, and in comparison to hepatocytes and HSEC, HSC are the major CD40-expressing cells in cirrhotic livers [279]. On fibroblasts, activation of CD40 by CD154 induces NFκB activation and cytokine secretion [280], and may up-regulate the production of extracellular matrix [281]. Ligation of CD40 on HSCs induces the activation of NFκB and JNK and enhanced IL-8 and MCP-1 secretion [279]. The secretion of MCP-1 is critically dependent upon IKK2 and TRAF2 whereas IL-8 secretion is TRAF2 independent [279]. Therefore, CD40 may be an important mediator of the cross-talk between HSCs and immune effector cells and contribute to maintaining HSCs in an activated state. HSC may fulfill a novel role in the regulation of immune response in the liver through CD40.

4.4 The Sources of CD154 within the Liver

4.4.1 Platelets

Recent evidence indicates platelets play a key role in regulating inflammatory processes via CD40:CD154 interactions [125]. Platelets express CD154 that is cryptic in unstimulated platelets but is expressed at the platelet surface upon platelet activation. When expressed at the platelet surface and exposed to CD40-expressing cells, the platelet-associated CD154 triggers a variety of pro-inflammatory and pro-coagulant responses including induction of adhesion receptors, release of cytokines and chemokines and induction of tissue metalloproteinases [253]. Platelets are also a rich source of CD154 and within seconds of activation CD154 is translocated to the platelet surface then cleaved to produce soluble CD154 [253]. Platelet-associated CD154 has been shown to have immune competence both *in vitro* and *in vivo*, observations that open new fields of research on the potential implications of platelets in the immune response and auto-immune diseases [282]. Platelets have been implicated in preservation injury during liver transplantation and in other conditions including immune mediated damage in hepatitis although the mechanisms of the effect are poorly understood [125, 283, 284]. This finding provides a novel mechanism to explain the effector function of platelets in liver injury and suggests that anti-platelet therapy may be warranted not only to prevent reperfusion injury but also to reduce liver injury in chronic hepatitis and cirrhosis in which platelets are found in close proximity to hepatocytes [283]. Whilst important in the regulation of acute and chronic liver injury, the findings that platelets are adherent to hepatocytes and HSEC very early after injury suggesting that CD154-derived from platelets may be a regulator of acute liver injury.

4.4.2 Macrophages

Macrophages are an abundant source of CD154 in the chronically inflamed liver [121, 124]. Indeed, the vanishing bile duct syndromes (VBDS), PBC and chronic allograft rejection and cholangiocyte apoptosis is associated with sustained macrophage infiltration of the liver, suggesting that these cells may mediate tissue damage and contribute to bile duct destruction. Moreover, LPS and IFNγ can induce sustained expression of CD154 on liver-derived macrophages or Kupffer cells [121]. Co-culture of these activated liver derived macrophages or Kupffer cells expressing high levels of CD154 with human cholangiocytes induces both CD40-dependent secretion of pro-inflammatory cytokines and cholangiocyte apoptosis. This is likely to amplify chronic inflammation and bile duct destruction in liver disease. These data suggest that effective targeting strategies to antagonise CD40:CD154 may have beneficial effects in patients suffering from chronic liver disease [121].

4.4.3 T-lymphocytes

The vast majority of research focusing upon CD40:CD154 function in T-lymphocytes has centred upon their role as a co-stimulatory signal in T-lymphocyte activation. Indeed, T-lymphocytes expression of CD154 is transient requiring the constant presence of cytokines such as IFNγ and contact dependent mechanisms to permit mRNA stabilisation and sustained expression of the protein [285]. Moreover, murine models deficient in CD40 and CD154 are protected from acute liver injury, with the defective priming of T-lymphocytes by dendritic cells being cited as the main mechanism of protection [19]**.** Although undoubtedly this mechanism plays a pivotal role in regulating liver injury, the effect of CD154 from platelets, macrophages and T-lymphocytes on CD40 present on the various liver cells cannot be underestimated. To this end, agonist anti-CD40 antibodies restore liver

injury following ischaemia in otherwise protected CD4-deficient mice, suggesting CD154 may well be interacting with CD40 expressed upon hepatocytes and inducing cell death. FACs analysis of liver CD4-positive T-lymphocyte revealed the selective infiltration of effector cells, which constitutively expressed a higher level of CD154 in comparison with their peripheral counterparts. These findings provide evidence that CD4-positive T-lymphocytes function in liver injury via CD154 without de novo antigen-specific activation, and innate immunity-induced CD40 up-regulation may trigger the engagement of CD154:CD40 to facilitate tissue inflammation and injury [117].

Moreover, fulminant hepatitis of various aetiologies is characterised by a hepatic influx of CD154-expressing T-lymphocytes and an up-regulation of CD40 expression upon liver-resident macrophages or Kupffer cells and hepatocytes, also implicating this pathway in the pathogenesis of fulminant hepatitis [286]**.** A significant influx of CD154-expressing T-lymphocytes into the livers of mice treated with concavalin A was associated with markedly increased expression of CD40 restricted mainly to hepatocytes in damaged areas of the liver [286]. Furthermore, *in vitro* studies demonstrated that TNFα induces CD40 expression in hepatocytes and that subsequent activation of CD40 results in hepatocyte apoptosis mediated at least in part by enhanced hepatocyte expression of FasL [122]. In conclusion, CD154 stimulation of CD40 plays a central role in hepatocyte death in fulminant and chronic liver injury through direct and indirect pathways that may have direct therapeutic implications in humans [286].

4.5 CD40:CD154 and Hepatic IRI

As well as not understanding the response of primary human hepatocytes to hypoxia and H-R it is not known which inflammatory cytokines and ligands may be responsible for

perpetuating liver injury during IRI. Many receptor-ligand dyads have been proposed to be of importance in regulating hepatocytes cell death during hypoxia and H-R as discussed in Chapter 1. The regulation of hepatic IRI by the TNFα super-family members CD40:CD154 receptor-ligand has been the subject of intense recent research. As stated above, the recent demonstrations that platelets are found adherent to hepatocytes during IRI and the fact that CD154 is also expressed by platelets and released in a soluble form following platelet activation opens up many potential mechanisms by which CD154 can induce liver injury.

Over a decade ago, the first report of the ability of CD154 to induce human hepatocyte apoptosis was made [122]. In 2005 Ke *et al* demonstrated the integral importance of CD40:CD154 receptor-ligand interaction in the regulation of hepatic IRI using both CD40 and CD154 knockout murine models [19]**.** However, the findings of this particular study should be treated with caution. Liver dendritic cells, HSEC, macrophages and hepatocytes all express CD40. Therefore, it remains to be determined as to which cell types absence of CD40 is most important to the propagation of hepatic IRI.

Given the observation that CD40 mediates human hepatocyte apoptosis, one of the possibilities is that CD40 expressed upon hepatocytes may be a key regulator of hepatic IRI. CD40 is known to mediate ROS accumulation in lymphoid cell lines were it induces proliferation [274], and in renal endothelial cells were it promotes apoptosis [287]**.** This suggests that CD40 activation by CD154 may mediate hepatocyte apoptosis through a similar mechanism. An abundance of direct and indirect evidence also suggests that the CD40:CD154 interaction might generate ROS and oxidative stress in vascular endothelial cells [124]**.** Therefore it is possible that CD40:CD154 mediated generation of ROS might play a significant role in modulating hepatic IRI. Indeed it is well appreciated that in

arthrosclerosis, CD40:CD154 forms a common link between oxidative stress and inflammation [124].

One of the mechanism by which ROS may mediate apoptosis is by the activation of the MAPK. MAPKs are evolutionarily conserved in all eukaryotic cells and consist sequentially of MAP3K, MAP2K/MEK and MAPK. ROS can activate a MAPK3K known as Apoptosis Signalling Kinase-1 (ASK1) [288]. ASK1 can then activate the MAP2K/MEK 4/7 and 3/6 which stimulate the JNK and p38 respectively [288]. Both JNK and p38 have been shown to be important in regulation of hepatic IRI [289-291]. However, injury to hepatocytes during IRI is not limited to apoptosis. Hepatocyte necrosis is also seen during and after IRI [99]. Therefore, the consequence of CD40 activation upon human hepatocytes forms an important question with regard to liver patho-physiology.

4.6 Material & Methods

4.6.1 *In Vitro* Model of hypoxia and H-R injury

The same model of *in vitro* hypoxia and H-R that was described in Chapter 3 was used for the experimental data presented below. In experiments involving the NADPH oxidase inhibitor, DPI; JNK inhibitor SP600125, or p38 inhibitor, PD169316, all reagents were made fresh as stock solutions and added using the correct dilutional factor to the relevant experimental wells. Specifically, 10 µg DPI (Sigma) was dissolved in molecular grade DMSO, 10 µg rotenone (Sigma) was dissolved in chloroform (Sigma), 50 µg SP600125 (Sigma) was dissolved in DMSO and 50 µg PD169316 (Sigma) was dissolved in DMSO and were diluted appropriately to give working concentrations of 10 µM, 2 µM, 10 µM and 10 µM respectively. In experiments using inhibitors/antioxidants, solvent alone wells were used to control for vehicle effects. In experiments using inhibitors/antioxidants hepatocytes were pre-treated with agents for up to 4 hours before placement of the cells into normoxia and hypoxia. For H-R experiments fresh inhibitor/antioxidants were added at the time of placement into reoxygenation. Recombinant human soluble CD154 (1µg/mL, Enzo Life Sciences, UK) and 1 µg/mL Cross-linker for Ligands (Enzo Life Sciences, UK) were added to cells at the time of entry into hypoxia or H-R. Where cells had been pre-treated with inhibitors/antioxidants CD154 and Cross-linker for Ligands were added after 4 hours.

4.6.2 Determination of Human Hepatocyte CD40 Expression and FasL Expression

Following appropriate incubation of human hepatocytes within normoxia, hypoxia and H-R, cells were trypinised and washed in FACs buffer (Phosphate-buffered saline (PBS) pH 7.2 with 10% v/v heat inactivated foetal calf serum (Gibco). For CD40 expression, cells were then incubated with anti-human CD40 antibody that was conjugated to the allophycocyanin

(APC) fluorophore (1:100 dilution; Caltag, UK) for 45 min at 4^0C. Mouse IgG1-APC (1:100 dilution; Caltag, UK) was used as a negative control. For FasL expression, cells were incubated with anti-human FasL antibody that was conjugated to the FITC fluorophore (1:100 dilution; Abcam, UK) for 45 min at 4^0C. Mouse IgG2a-FITC (1:100 dilution; Abcam, UK) was used as a negative control. Following this cells were washed in FACs buffer and resuspended in PBS, pH 7.2. At least 20,000 events were recorded within the gated region of the flow cytometer for each human hepatocyte cell preparation in each experimental condition. Only the cells within the gated region were used to calculate MFI as described in Chapter 3.

4.6.3 Determination of Human Hepatocyte ROS Accumulation, Apoptosis and Necrosis

ROS production, apoptosis and necrosis were determined using a three-colour reporter assay system as described in Chapter 3. In the experiments outlined below autophagy was not assessed. At least 20,000 events were recorded within the gated region of the flow cytometer for each human hepatocyte cell preparation in each experimental condition. Only the cells within the gated region were used to calculate MFI.

4.6.4 Platelet isolation and activation

Platelets were isolated by modifying a previously published method from fully consenting healthy individuals [292]. All adults were healthy volunteers that had not been taking any anti-platelet therapy. Following venesection platelet-rich plasma (PRP) was prepared by centrifuging 5 mL of heparinised blood for 5 min at 300 x *g*. The platelet layer was a distinct yellow layer within the vacutainer. Following this the PRP was withdrawn by aspiration. 10 µl of the PRP was then withdrawn and added to 10 µl of trypan blue. Following

quantification the platelet count was adjusted to 1 x 10^6 platelets/mL in Williams E media. Platelets were then seeded at the aforementioned density onto plastic plates. Following 30 min incubation at room temperature the platelets had settled, become activated and spread to form a confluent monolayer. The Williams E media was then aspirated and passed through a 0.2 μm syringe filter. This media was now arbitrarily named platelet-conditioned media (PCM). The PCM was aliquoted into Eppendorfs and frozen at -70^0C until required. Media was thawed only once and added to cells as required.

4.6.5 Determination of Soluble CD154 and Immunomagnetic Depletion of CD154 from PCM.

To confirm the presence and quantity of CD154 in the PCM, a commercial sandwich ELISA kit was used to quantify levels of CD154 (Peprotech, CA, USA, Catalogue Number 900-K145). Briefly, the capture antibody was made in PBS at a concentration of 1 μg/ml. This was then aliquoted onto the relevant wells in a 96-well plate. Following incubation at room temperature unbound antibody was washed off. Wells were then blocked using 5% BSA followed by addition of either control, standard or sample solution. Following incubation the biotinylated detection antibody was added. After incubation a solution of avidin-peroxidase conjugate was added and excess washed off. Finally the substrate of 2,2'-azino-bis(3-ethylbenzothiazoline-6-sulphonic acid) (ABTS) was added and after a 5 minute period the plate read at 405 nm with a 650 nm wavelength correction. A standard curve was constructed and used to determine the concentration of soluble CD154 in the samples.

Platelet-derived CD154 was removed from PCM via immuno-magnetic depletion. For immunomagnetic depletion of CD154, anti-human CD154 antibody (1 μg/mL; Abcam, UK) was complexed to pan-mouse IgG magnetic Dynabeads (Invitrogen, Paisley, UK) for 90 min

at room temperature. This ensured that the CD154 antibody was adequately complexed to the Dynabeads. Following this, the antibody-magnetic bead complexes were extensively washed in PBS, pH 7.2. Complexes were then incubated with PCM for a further 90 min at room temperature with continuous agitation. Finally, magnetic beads were retrieved from solutions and this media was subsequently used in experiments as CD154-depleted PCM. The content of soluble CD154 within CD154-depleted PCM was determined using the method listed above.

4.6.6. Statistical Analysis

All data are expressed as mean ± S.E. Statistical comparisons between groups were analysed by Student's *t* test. All differences were considered statistically significant at a value of $p<0.05$.

4.7 Results

4.7.1 CD40 Expression in Human Hepatocytes during Hypoxia and H-R

Primary human hepatocytes constitutively expressed CD40 on the cell membrane in cell culture as previously reported [122]. Figure 3.7 demonstrates that ROS increases during hypoxia and H-R but this increased oxidative stress did not increase CD40 expression upon human hepatocytes *in vitro* (Figure 4.2).

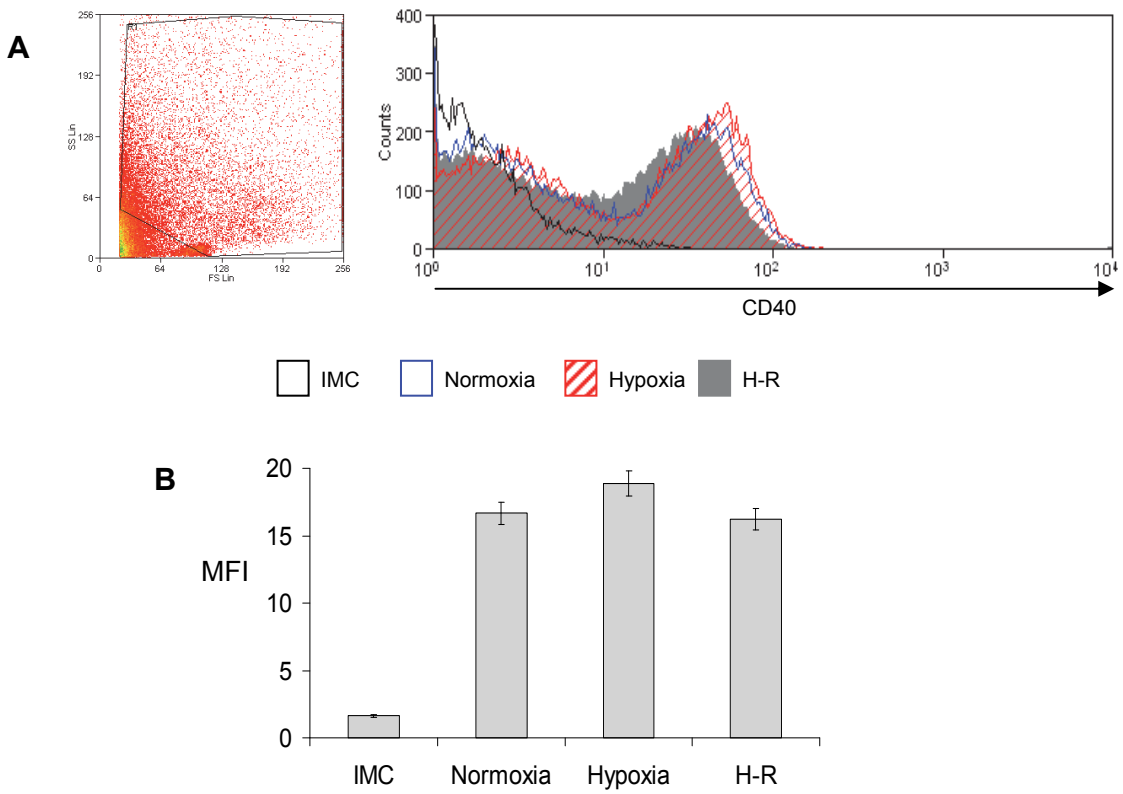

Figure 4.2 CD40 Expression upon Human Hepatocytes during Hypoxia and H-R
(A) Demonstrates a representative flow cytometry plot of CD40 expression upon primary human hepatocytes during normoxia, hypoxia and H-R. The plot on the left hand side represents a typical FS versus SS plot of primary human hepatocytes. The FS versus SS plots shown is from the H-R sample of a liver preparation but similar plots were obtained during normoxia and hypoxia.
(B) Bar chart with the pooled data of three separate experiments illustrating the level of CD40 expression on primary human hepatocytes. Data is expressed as MFI mean ± S.E. (n=4).

4.7.2 CD40:CD154 Stimulates ROS Accumulation in Human Hepatocytes in an NADPH-dependent Manner and Regulates Apoptosis and Necrosis

Intracellular ROS accumulates in hypoxic human hepatocyte that is then further increased during H-R as demonstrated in Chapter 3. Whether CD154 can augment human hepatocyte ROS production during normoxia, hypoxia and H-R is not known. Trimeric recombinant human CD154 significantly increased intracellular ROS accumulation within human hepatocytes during normoxia and H-R but not hypoxia. CD40:CD154 has been shown to mediate ROS accumulation via TRAF-dependent recruitment of the flavoenzyme NADPH oxidase in lymphoid cell lines [274]. Therefore the specific NADPH oxidase inhibitor DPI was used to assess the involvement of this pathway in ROS generation by human hepatocytes. DPI reduced hepatocyte CD154 mediated ROS production during normoxia, hypoxia and H-R (Figure 4.3 & Appendix IV).

The increased level of intracellular ROS induced by CD154 stimulation, during normoxia and H-R, increased human hepatocyte apoptosis and to a lesser extent necrosis (Figure 4.4 & Appendix IV) and this was reduced by pre-treatment of human hepatocytes with DPI. CD154 also significantly increased human hepatocyte necrosis during normoxia and H-R that was inhibited by DPI demonstrating that the CD40:CD154:ROS signalling pathway is NADPH-dependent and results in hepatocyte death in the form of apoptosis and necrosis.

Mitochondrial ROS has been implicated in hepatocyte apoptosis during hypoxia and H-R [105] and as demonstrated in Chapter 3 mitochondrial ROS is the principal form of ROS in human hepatocytes and leads to cell death. Therefore the effect of inhibiting mitochondrial ROS production upon CD154 mediated apoptosis with the complex I inhibitor, rotenone, was assessed. Inhibiting mitochondrial ROS production during normoxia and H-R did not

reduce human hepatocyte apoptosis in response to CD154 treatment but did reduce apoptosis during hypoxia (Figure 4.5 and Appendix IV).

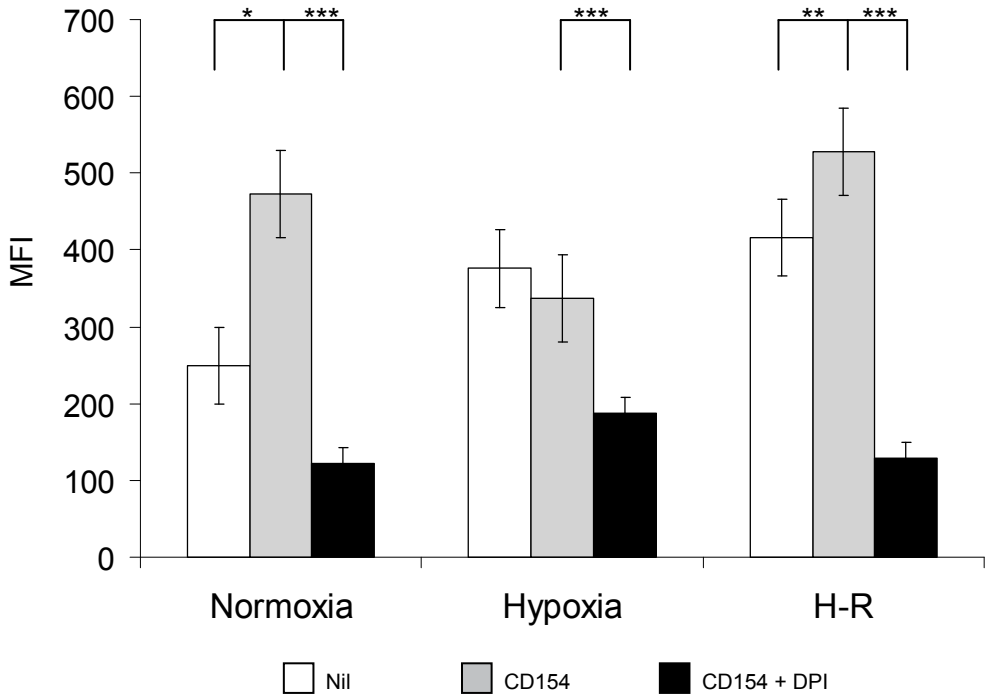

Figure 4.3 CD40:CD154 Regulates ROS Accumulation within Human Hepatocytes in a NADPH Oxidase Dependent Manner during Normoxia and H-R

The bar chart illustrates the pooled data of three separate experiments demonstrating the effects of CD154 and CD154+DPI upon human hepatocytes ROS accumulation. Data is expressed as MFI and readings are based upon values taken from cells within the gated region shown in Figure 3.7. Data is expressed as mean ± S.E. (*$p<0.01$ relative to basal, **$p<0.05$ relative to basal, ***$p<0.001$ relative to CD154). (n=3).

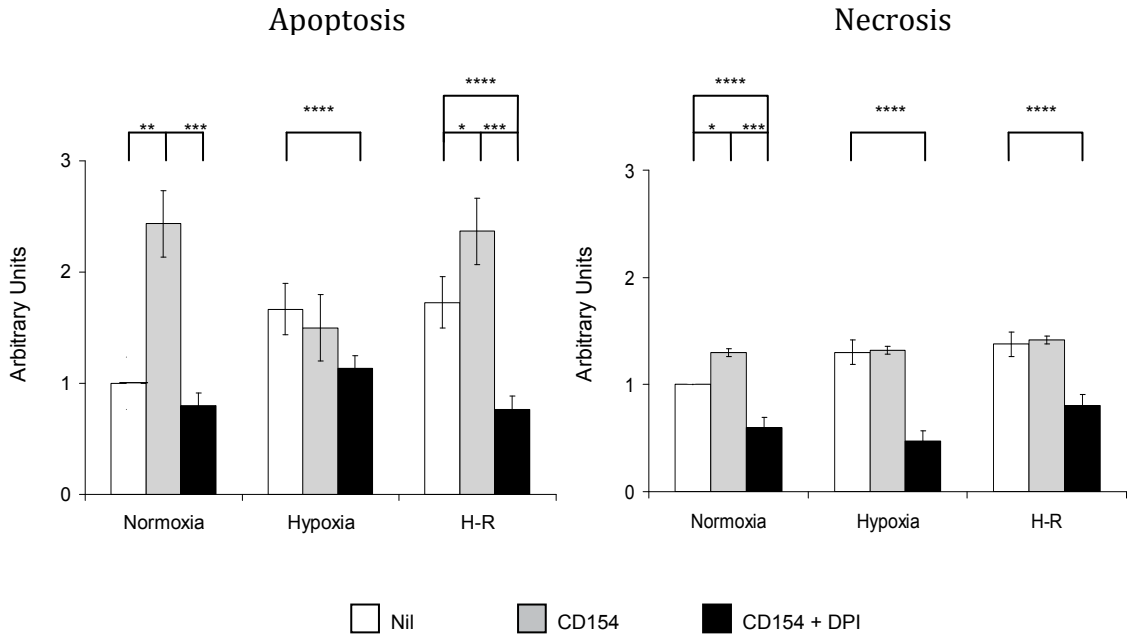

Figure 4.4 CD40:CD154 Mediated ROS Accumulation Induces Human Hepatocyte Apoptosis and Necrosis during Normoxia and H-R

Demonstrates bar charts with the pooled data of three separate experiments illustrating the effects of CD154 and CD154+DPI upon human hepatocytes apoptosis and necrosis during normoxia, hypoxia and H-R. Data is expressed as increase/decrease relative to basal, where basal refers to the level of apoptosis or necrosis during normoxia alone. Data is expressed as mean ± S.E. (**$p<0.01$ relative to basal, *$p<0.05$ relative to basal, ***$p<0.05$ relative to CD154, ****$p<0.05$ relative to basal). (n=4).

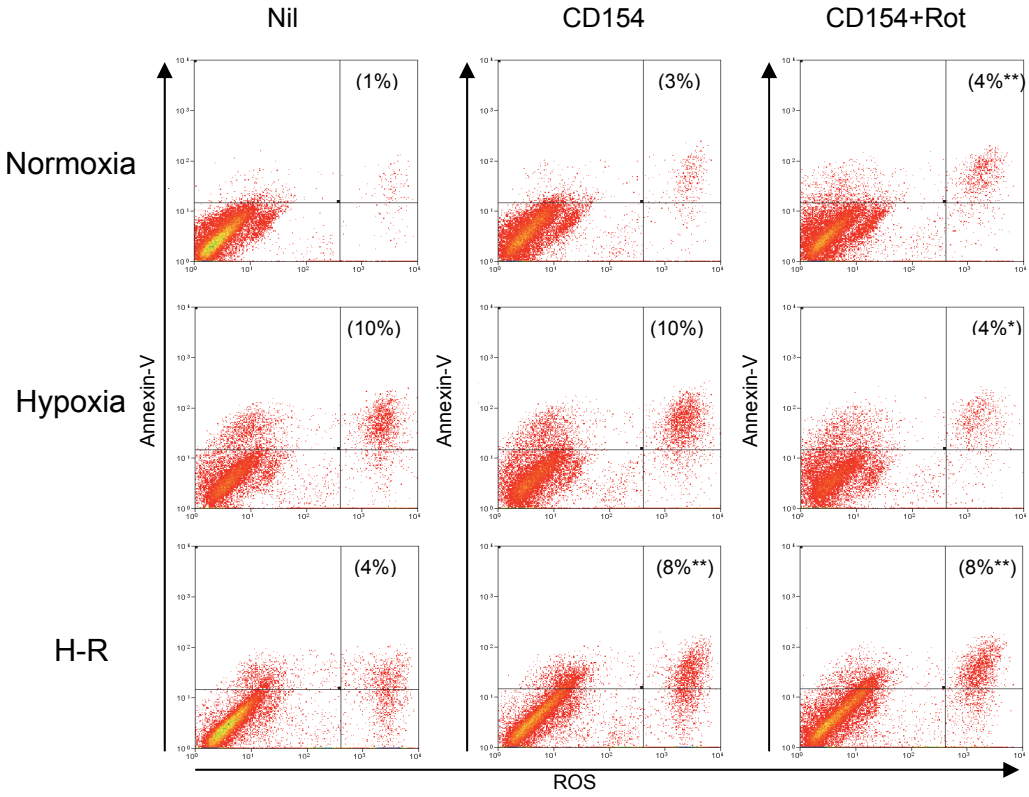

Figure 4.5 The Effect of Mitochondrial ROS Inhibition upon CD40:CD154 Mediated Human Hepatocyte Apoptosis during Normoxia, Hypoxia and H-R

Human hepatocytes were treated with CD154 or CD154 following pre-treatment with rotenone (Rot) during normoxia, hypoxia and H-R. The percentages of cells staining with both the ROS probe DCF and apoptotic marker, Annexin-V, were assessed by flow cytometry. The percentage of human hepatocytes that stain for both DCF and Annexin-V are shown in parentheses. Data are representative of 3 separate experiments (**$p<0.05$ relative to basal, *$p<0.05$ relative to CD154). (n=4).

4.7.3 JNK and p38 Regulate Apoptotic but not Necrotic Cell Death in Human Hepatocytes

ROS accumulation in human hepatocytes induced by CD40:CD154 clearly resulted in cell death but whether this was associated with involved the MAPKs was investigated. MAPKs consist of three sequentially activated kinase modules, namely mitogen-activated protein kinase kinase kinases (MAPKKK/MAP3K) followed by the mitogen-activated protein kinase kinases (MAPKK/MEKK) and finally the MAPKs. The MAPKs superfamily consists of three separate sub-families; extra-cellular regulated protein kinase (ERK), c-Jun *N*-terminal kinase (JNK) and p38. ERK is generally involved in the regulation of cell proliferation and differentiation, whereas JNK and p38 are involved in the regulation of cell death [291].

Unfortunately, primary human hepatocytes are not amenable to siRNA transfection or protein labelling. Therefore to investigate the effects of JNK and p38 inhibition upon CD40:CD154:ROS mediated human hepatocyte cell death specific JNK and p38 inhibitors were used. Inhibition of JNK and p38 in hepatocytes using the specific inhibitors SP600125 and PD169316 had no effect on ROS accumulation during normoxia, hypoxia and H-R whereas they significantly decreased CD40:CD154 mediated human hepatocyte apoptosis during normoxia, hypoxia and H-R (Figure 4.6 & Appendix V). Inhibition of p38 had a greater effect on hepatocyte apoptosis than JNK inhibition. Neither inhibitor reduced CD154 mediated hepatocyte necrosis under any of the experimental conditions (Figure 4.6). This suggests that CD40:CD154 mediated human hepatocyte apoptosis during normoxia and H-R is ROS, JNK and p38-dependent whilst necrosis is ROS-dependent but MAPK-independent.

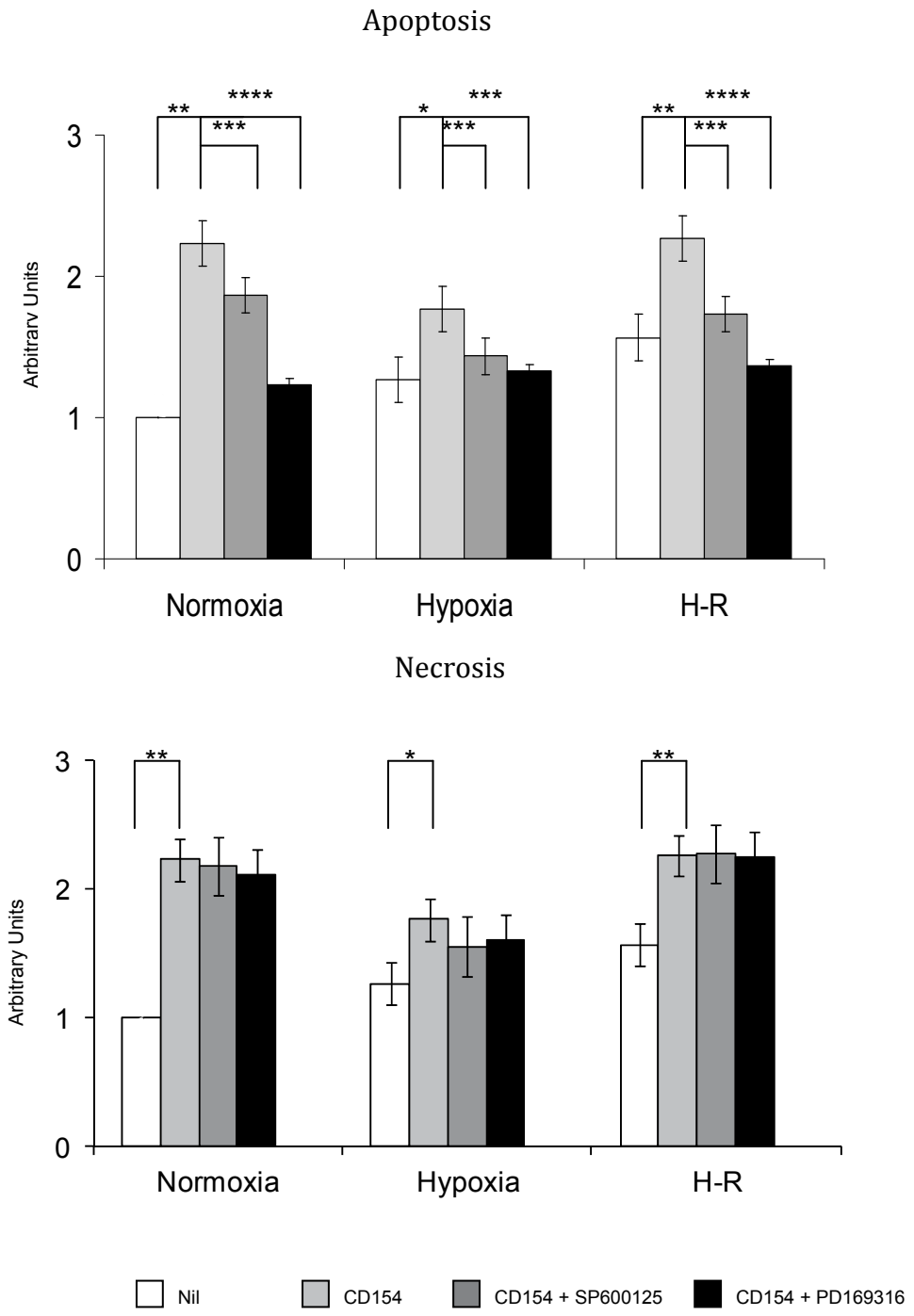

Figure 4.6 The Regulation of Human Hepatocyte Apoptosis but not Necrosis by JNK and p38

Bar charts with the pooled data of three separate experiments illustrating the effects of both SP600125 and PD169316 upon CD40:CD154 mediated human hepatocyte apoptosis and necrosis during normoxia, hypoxia and H-R. Data are expressed as increase/decrease relative to basal, where basal refers to the level of apoptosis or necrosis during normoxia alone. Data are expressed as mean ± S.E. (**$p<0.01$ relative to basal, *$p<0.05$ relative to basal, ***$p<0.05$ relative to CD154, ****$p<0.05$ relative to basal). (n=3).

4.7.4 CD40:CD154:NADPH oxidase Stimulate Hepatocyte Fas ligand Expression

Fas is a cell surface receptor of the TNF receptor superfamily which, when activated by FasL, induces apoptosis on a wide range of cells including hepatocytes [293]. Previous studies have reported that CD40 activation on human hepatocytes results in Fas-mediated apoptosis. Whether similar phenomenon operates during hypoxia or H-R alone or in association with CD154 was investigated. Neither hypoxia nor H-R increased hepatocyte cell surface FasL expression (Figure 4.7 & Appendix V). However, CD40:CD154 increased FasL expression during hypoxia and H-R, with a greater effect during hypoxia. Inhibiting NADPH oxidase function with DPI reduced CD40:CD154 mediated FasL expression during hypoxia and H-R, with a greater effect noted during H-R.

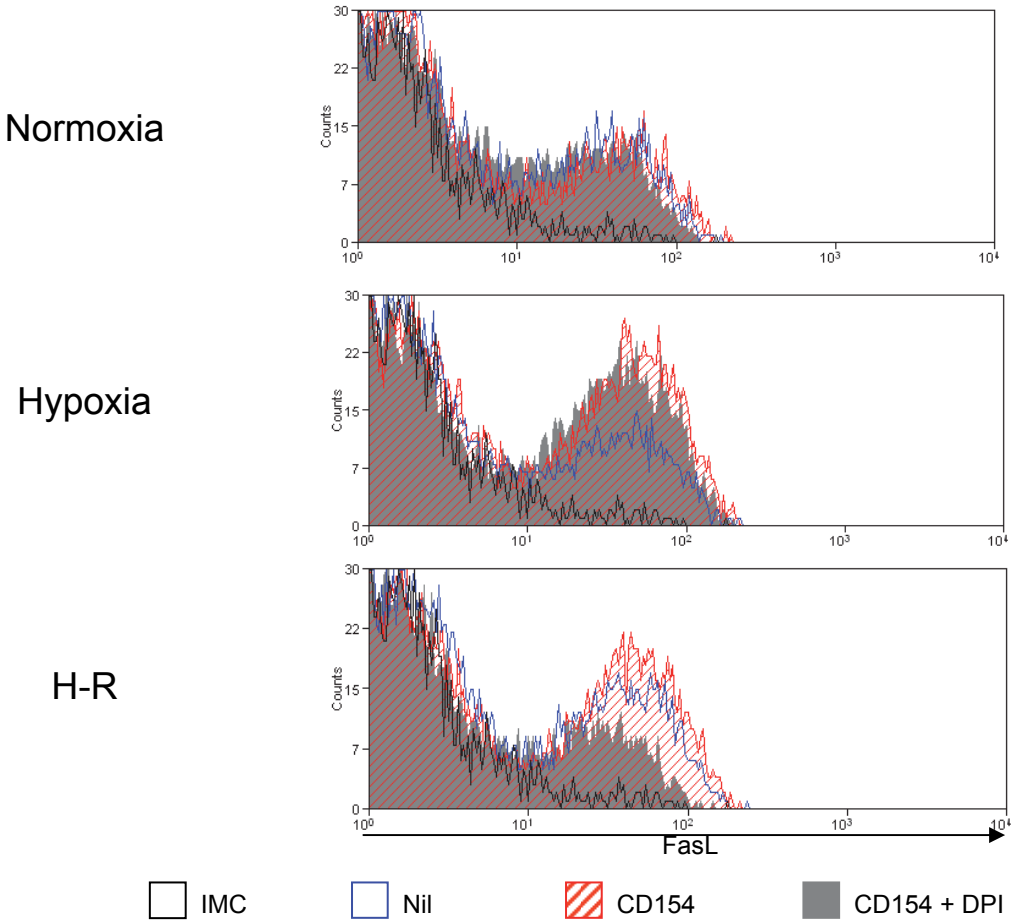

Figure 4.7 CD40:CD154 Mediated FasL Expression upon Human Hepatocytes during H-R

Demonstrates a representative flow cytometry plot of FasL expression on primary human hepatocytes during normoxia, hypoxia and H-R. Hypoxia and H-R did not increase the expression of FasL upon human hepatocytes. CD154 stimulation of human hepatocytes did increase FasL expression upon human hepatocytes during hypoxia and H-R. This increase was partially inhibited by pre-treatment of cells with DPI. Composite data is shown in Appendix V. (n=3).

4.7.5 Platelet-derived Soluble CD154 Mediates Hepatocyte Apoptosis and Necrosis

Platelets are the source for 95% of circulating soluble CD154 [283] and may be found in the liver parenchyma during inflammatory processes. Whether activated platelets may be a potential source of functionally active CD154 during hypoxia and H-R was investigated.

Immuno-magnetic depletion reduced soluble CD154 released by activated platelets by > 70% (Platelet Conditioned Media (PCM) soluble CD154 concentration 2251 ± 310 pg/mL; CD154-depleted PCM CD154 concentration 590 ± 79 pg/mL) (Figure 4.8). PCM increased hepatocyte intracellular ROS accumulation during normoxia, hypoxia and H-R (Figure 4.9). When CD154 was depleted from PCM, intracellular ROS accumulation was significantly reduced during H-R. PCM increased human hepatocyte apoptosis during H-R mirroring the increasing in intracellular ROS (Figure 4.10). However, in line with the decrease in ROS seen during H-R, CD154-depleted PCM decreased human hepatocyte apoptosis during H-R (Figure 4.10).

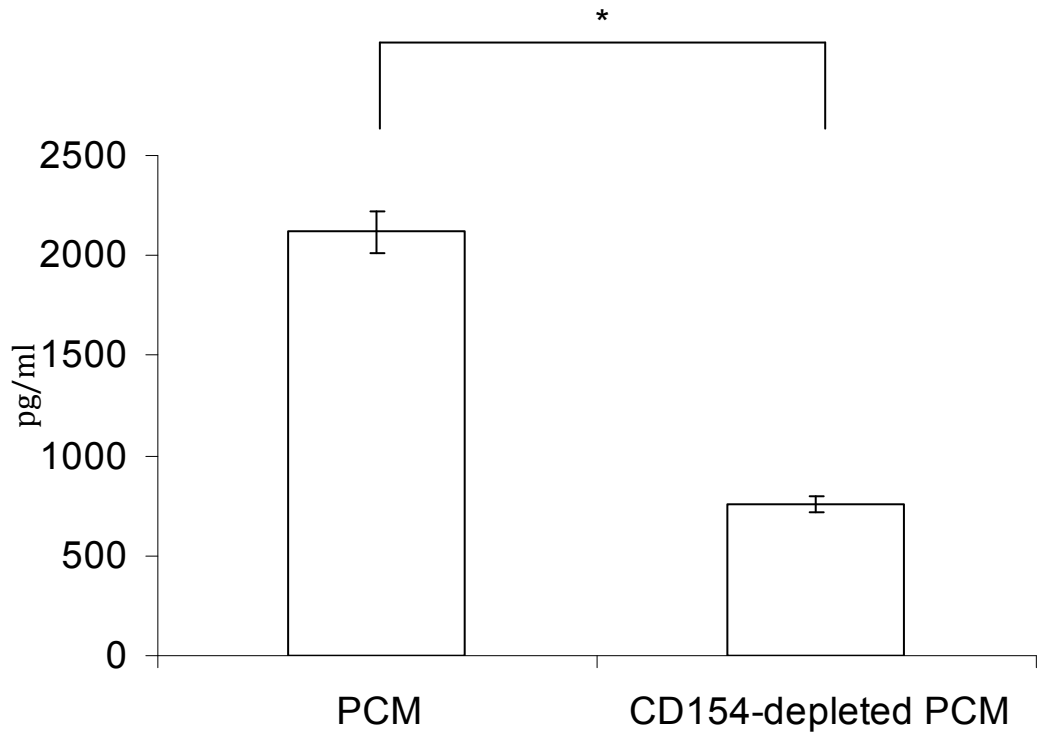

Figure 4.8 PCM and CD154-depleted PCM Soluble CD154 Content
Platelets were isolated from healthy volunteers and plated onto plastic for 30 minutes to allow activation. The supernatants were then collected and the content of soluble CD154 within the supernatants was assessed. An immuno-magnetic technique was used to deplete the soluble CD154 within the supernatants. Sandwich ELISA was used in all cases to assess the content of soluble CD154. Data are expressed as the mean ± S.E. (n=8).

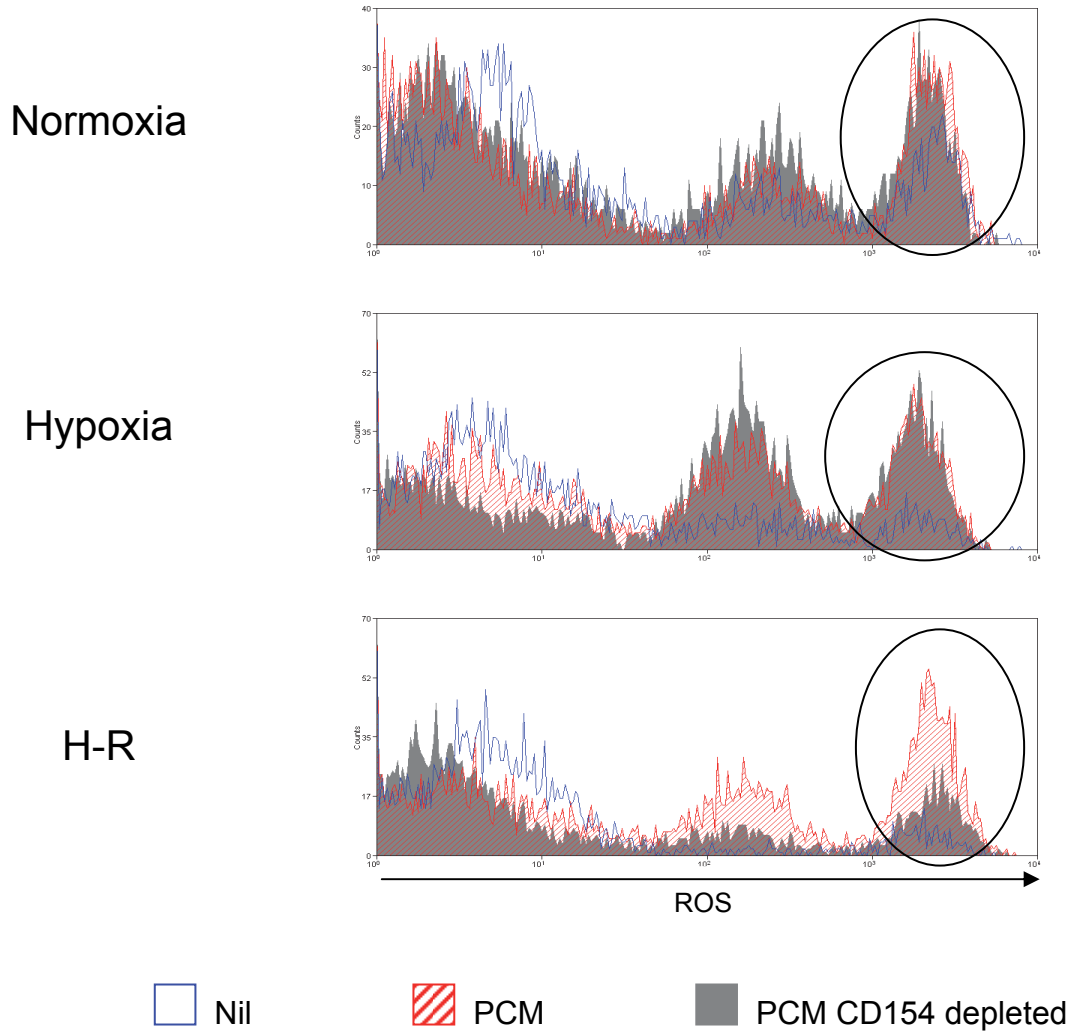

Figure 4.9 The Effects of PCM and PCM-depleted CD154 upon Human Hepatocyte ROS Production

Demonstrates representative flow cytometry plots to illustrate the effect of PCM (hatched red) and PCM CD154-depleted (solid grey) upon human hepatocyte ROS accumulation during normoxia, hypoxia and H-R. The gate used to analyse primary human hepatocytes is the same as that shown in Figures 3.7. The vertical ellipse marks the area of interest within the flow cytometric plots. (n=4).

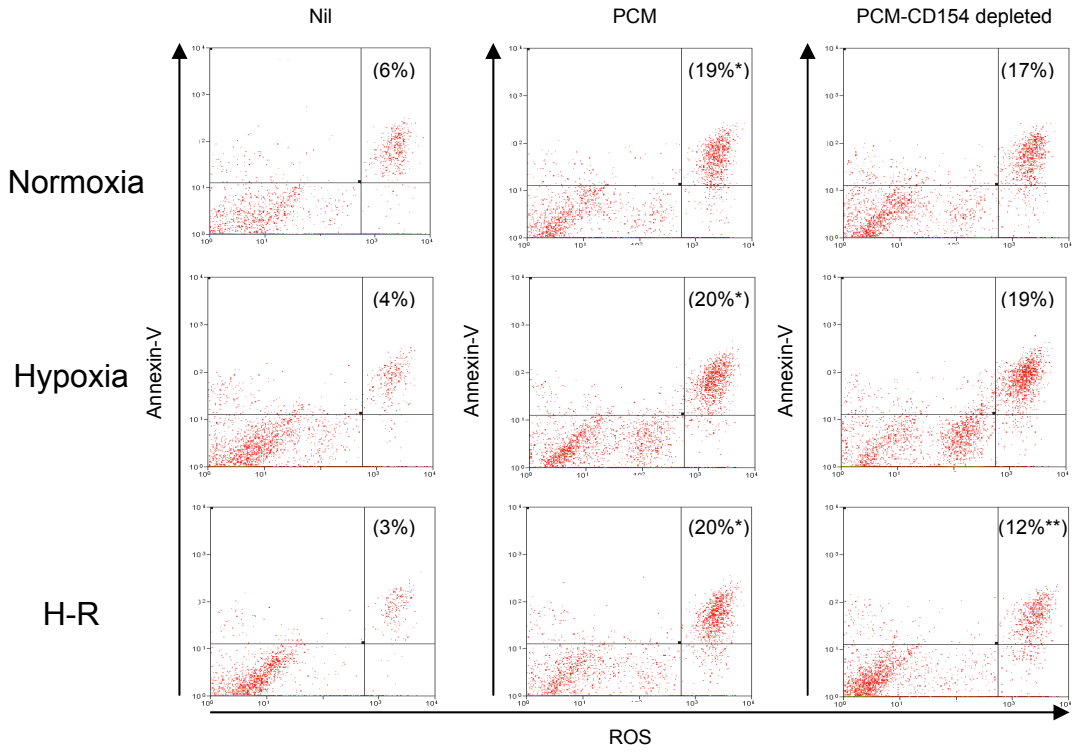

Figure 4.10 The Effects of PCM and PCM-depleted CD154 upon Human Hepatocyte Apoptosis during Normoxia, Hypoxia and H-R

Human hepatocytes were treated with PCM or PCM CD154-depleted during normoxia, hypoxia and H-R. The percentages of cells staining with both the ROS probe DCF and apoptotic marker, Annexin-V, were assessed by flow cytometry. The percentage of human hepatocytes that stain for both DCF and Annexin-V are shown in parentheses. Data is representative 3 separate experiments (*$p<0.05$ relative to basal, **$p<0.05$ relative to PCM). (n=3).

4.8 Discussion

Tissue hypoxia is a key feature of hepatic inflammation and disease and one of the central regulators of hepatic injury and cell death is the accumulation of intracellular ROS [40, 42, 43]. Building upon the model presented in Chapter 3 the data above details that ROS accumulation in human hepatocytes during hypoxia and H-R is increased by CD154 mediated activation of human hepatocyte CD40. This augmented ROS production induced by CD154 ultimately results in increased human hepatocyte cell death. This link between CD40 activation, intracellular ROS generation and cell death has implications for other inflammatory diseases characterised by local hypoxia and pro-inflammatory microenvironment such as liver cirrhosis.

CD40:CD154 receptor-ligand interactions have been associated with parenchymal injury during hypoxia and H-R in many organs [19, 125, 294] and disruption of CD40:CD154 signalling in mice improves liver function following hypoxia [19]. However until now it was thought that CD40:CD154 mediates its actions through effects on T-lymphocyte priming whereas the data presented above suggests another distinct mode of action through direct effects on hepatocyte survival. Previous reports have shown that CD40 activation mediates Fas dependent apoptosis in human hepatocytes through induction of autocrine FasL expression [122]. The new data demonstrates that CD40:CD154 can also mediate human hepatocyte apoptosis and necrosis in a NADPH Oxidase:ROS-dependent manner. This introduces a previously unknown CD40 dependent pathway to cell death and implicates CD40 in the regulation of cell survival during tissue hypoxia and H-R.

This data also supports and further emphasises an important role for intrinsic ROS accumulation in human hepatocytes as opposed to the current model which suggests that ROS is derived only from leukocytes [169]. CD40 activation did not increase ROS

accumulation or cell death in human hepatocytes during hypoxia. Although not evaluated in the data presented here several previous studies have shown that during ischaemic/hypoxic conditions hepatocytes increase intracellular antioxidant defences principally in the form of glutathione [16]. This may also explain why FasL has little effect upon increasing human hepatocyte apoptosis during hypoxia (see below). Furthermore, hypoxia alone did not increase hepatocyte cell surface CD40 implying that the lack of effect of CD154 during hypoxia was probably a consequence of the modulation of intracellular signalling pathways by antioxidants rather than changes in CD40 receptor bioavailability.

The increases in intracellular ROS induced by CD154 within human hepatocytes are dependent upon NADPH Oxidase. This finding is consistent with previous studies implicating NADPH Oxidase in intracellular ROS accumulation. Studies in WEHI 231 cells and endothelial cells have shown that following activation, CD40 recruits NADPH Oxidase to the plasma membrane via a mechanism involving TRAF3 [274, 295-297]. Once at the plasma membrane the $p40^{phox}$ subunit of NADPH oxidase can generate ROS leading to activation of a number of downstream cell death signalling pathways (Figure 4.13). In primary human hepatocytes CD40:NADPH oxidase:ROS initiated apoptosis and to a lesser extent necrotic cell death. The mode of hepatocyte cell death stimulated by hypoxia remains controversial and the data presented would corroborate this notion. Both apoptosis and necrosis have been implicated as the primary form of cell death during IRI [99] and within transplant models consistent with our findings and in support of Lemasters proposal that a common mediator regulates both forms of cell death during hypoxia and H-R [175]. On the basis of the data presented above it is clear that CD40:CD154 activation in hepatocytes has at least three downstream consequences 1) initiation of apoptosis mediated via ROS 2) initiation of apoptosis mediated via FasL induction and 3) necrosis.

CD40 activation results in apoptotic death in many cells of epithelial lineage [120, 122]. Indeed, CD40 activation induces human hepatocyte apoptosis via up-regulation of FasL expression and subsequent Fas-mediated apoptosis [122]. Moreover, in human hepatocytes, it is the sustained activation of AP-1 and MAPKs, and not NFκB, which is central to initiating apoptosis [157]. A similar signalling pathway has been reported in mediating cholangiocytes apoptosis after CD40 ligation [119]. Additionally, in cholangiocytes, CD40 mediated apoptosis also requires the activation of the JAK2-STAT3 pathway and the downstream activation of caspase-3 [120]. However, the data presented, for the first time, implicates ROS in this process of epithelial and specifically human hepatocyte, apoptosis. ROS can activate the MAPKs sub-families of JNK and p38, important regulators of cell death. Specifically, ROS can activate the MAP3K, ASK1 resulting in phosphorylation of MEK 3/6 [298] and MEK 4/7 [298] which respectively activate p38 and JNK although this has not conclusively been shown here. Inhibition of p38 [290] and JNK [289] improves hepatocyte viability after hypoxia and during H-R in rodent models. CD40:CD154 mediated human hepatocyte apoptosis is reduced by JNK inhibition and prevented by p38 inhibition. The precise mechanism of JNK mediated apoptosis is controversial. JNK can act upstream of mitochondria by activating the pro-apoptotic Bcl2 family [299] and also increases turnover of the anti-apoptotic protein c-FLIP [300]. p38 is thought to mediate apoptosis via phosphorylation of Bcl2 family members [301] and CD40-mediated-NADPH oxidase generated ROS is upstream of p38 activation in WEHI 231 cells [274]. Thus a mechanistic link between CD40:CD154 mediated ROS generation, MAPK activation and cell death is in operation in human hepatocytes during hypoxia and H-R. Taken together, these studies highlight the complexities of the upstream CD40 signalling pathway and suggest that CD40 can couple to at least ROS and AP-1 signalling pathways to regulate apoptosis. Whether

CD40 ligation in human hepatocytes can also activate the JAK-STAT pathways, as seen in cholangiocytes, remains to be ascertained.

CD40 ligation by CD154 is known to increase FasL expression resulting in autocrine/paracrine Fas-mediated apoptosis in human hepatocytes [122]. However, in contrast to *in vivo* studies [302], hypoxia and H-R did not result in increased hepatocyte FasL expression in the presented *in vitro* model of IRI. CD154 induced cell surface expression of FasL in human hepatocytes and this was in part dependent on NADPH oxidase particularly during H-R. This suggests that other mechanisms are involved in regulating ROS-independent FasL expression. As discussed above, although CD40:CD154 did not increase ROS during hypoxia, it did increase FasL expression although without a concomitant increase in apoptosis. However, the inhibition of mitochondrial ROS significantly reduced hepatocyte apoptosis during hypoxia. Fas mediated apoptosis in hepatocytes requires the downstream accumulation of mitochondrial ROS [303] and together with likely increases in hepatocyte antioxidant levels during hypoxia explains why increased FasL expression was seen in the absence of apoptosis in response to CD40 activation [42, 304]. This also suggests that different apoptotic signalling pathways may be initiated in response to CD40 activation under different conditions in distinct microenvironments.

Hypoxia, which precedes reoxygenation during preservation of an organ allograft for transplantation, can increase FasL expression thereby initiating liver damage before ROS generation during reperfusion has occurred. FasL is also increased on hepatocytes in chronically inflamed livers, a situation characterised by tissue hypoxia. Thus the mechanism described above is likely to operate in the chronic inflammation where large numbers of CD154 expressing effector cells can activate CD40 in a hypoxic environment [130].

As demonstrated in Chapter 3, ROS generation can induce human hepatocyte necrosis during hypoxia and H-R and hepatocyte necrosis has been induced experimentally during hypoxia followed by reoxygenation [175]. ROS generated by CD40:CD154 not only induces hepatocyte apoptosis but also necrosis during normoxia and H-R. This process is NADPH oxidase dependent as shown by the decrease in necrosis in the presence of DPI but in contrast to CD154-mediated hepatocyte apoptosis, necrosis is MAPK-independent. This suggests that NADPH oxidase generated ROS induces divergent signalling pathways leading to both forms of cell death (see Figure 4.13).

CD154:CD40:ROS stimulates the activation of JNK and p38, which subsequently leads to cell death. The JAK2-STAT3 signalling pathway also regulates CD40 mediated apoptosis [120] that may also be activated by ROS. In addition, FasL is up-regulated following CD40 activation. Therefore CD40 regulates multiple death signalling pathways in liver epithelial cells.

Macrophages and T-lymphocytes are an abundant source of CD154 in the chronically inflamed liver [121] and are also important mediators of liver injury during hepatic IRI. However, platelets are also a rich source of CD154 [305] and within seconds of activation CD154 is translocated to the platelet surface then cleaved to produce soluble CD154. Platelets have been implicated in preservation injury during liver transplantation and in other conditions including immune mediated damage in hepatitis although the mechanisms of the effect are poorly understood [284, 306, 307]. In the data presented here activated platelets secrete functional CD154 that is capable of inducing ROS accumulation in human hepatocytes during H-R leading to hepatocyte apoptosis. This finding provides a novel mechanism to explain the effector function of platelets in liver injury and suggests that anti-platelet therapy together with anti-oxidants may be warranted not only to prevent reperfusion

injury but also to reduce liver injury in chronic hepatitis and cirrhosis in which platelets are found in close proximity to hepatocytes [283, 308]. Although these findings suggest that platelets are a major source of CD154 capable of inducing injury as previously suggested [125] CD154 depletion from platelet-conditioned medium reduced but did not abolish human hepatocyte apoptosis suggesting either that there was residual CD154 activity in the PCM or that platelets release other active mediators of apoptosis [284].

In conclusion, these findings support the role of CD40:CD154 mediated ROS in mediating hepatocyte cell death by both apoptosis and necrosis in the hypoxic liver microenvironment. The ability of platelets as well as infiltrating T-lymphocytes and macrophages to deliver functional CD154 to hepatocytes suggests several potential mechanisms through which hepatocyte CD40 can be activated in the inflamed and hypoxic liver. The work supports the use of therapeutic intervention with anti-platelet and anti-oxidant therapy in liver disease.

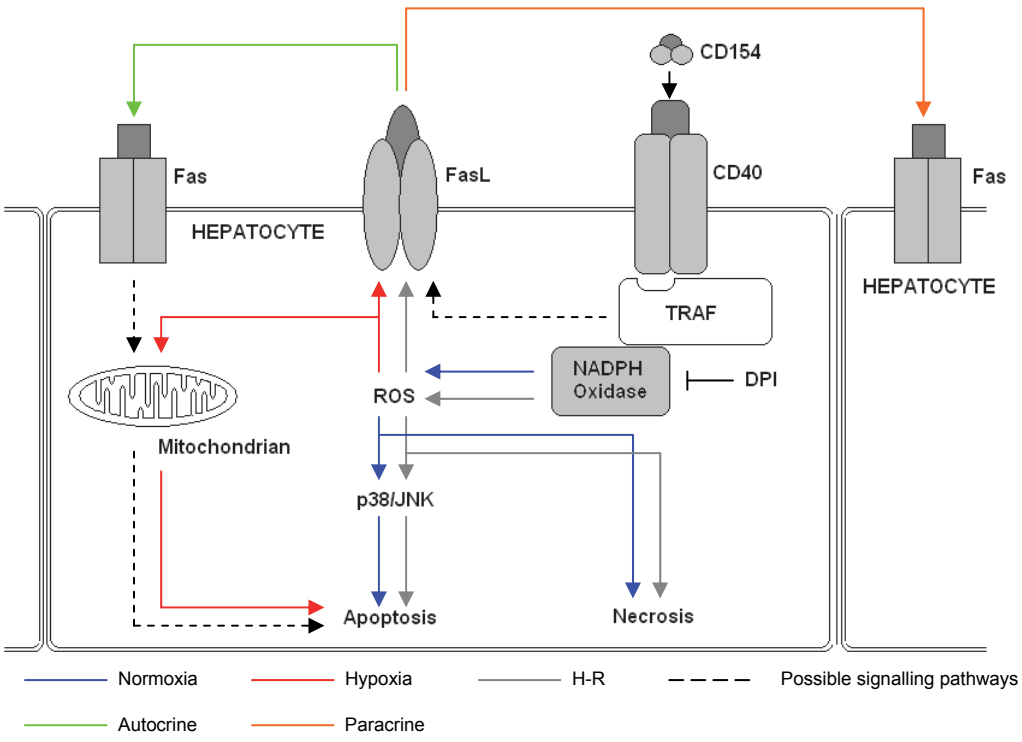

Figure 4.11 Proposed Mechanism of Regulation of Human Hepatocyte Cell Death by CD40:CD154

During normoxia (blue arrows) activation of CD40 expressed upon human hepatocyte by CD154 results in the translocation of the TRAF adaptor molecules to the cell membrane. The TRAF molecules are then responsible for the recruitment of the flavoenzyme NADPH Oxidase to the CD40:TRAF complex. Here NADPH Oxidase can induce the production of ROS, primarily in the form of hydrogen peroxide. The NADPH Oxidase inhibitor DPI can inhibit this process. The resultant accumulation of ROS can result directly in necrotic cell death or it can activate the MAPK members, JNK and p38, to induce human hepatocyte apoptosis. However, during hypoxia (red arrows) CD40 activation on human hepatocytes does not result in ROS accumulation but can induce FasL expression via mechanisms that NADPH Oxidase-dependent and ROS-independent (dotted black line). This increased FasL expression can result in autocrine (green arrow) and/or paracrine (orange arrows) Fas-mediated apoptosis. Due to the increases in intracellular antioxidants levels during hypoxia CD154 does not increase apoptosis. However, mitochondrial ROS does contribute to apoptosis during hypoxia. During H-R, CD40 activation can lead to NADPH Oxidase-ROS-JNK/p38 dependent apoptosis, NADPH Oxidase-ROS-dependent necrosis and NADPH Oxidase:ROS:FasL expression with resultant Fas-mediated apoptosis. Figure 4.13 highlights the importance of local microenvironment in shaping the effects of CD40:CD154.

CHAPTER 5 - THE *IN VIVO* REGULATION OF HEPATIC IRI BY CD40 AND CD154

5.1 Introduction

As discussed in Chapter 1, hepatic IRI is an antigen independent pro-inflammatory process. As demonstrated in Chapter 3 and 4 intracellular ROS generation is an important regulator and mediator of hepatocyte injury *in vitro*. Indeed, in *in vitro* conditions at least, CD40 activation upon human hepatocytes can augment intracellular ROS during hypoxia and H-R with resulting apoptotic and necrotic cell death. However *in vivo* hepatocytes will be subject to a different inflammatory microenvironment including exposure to and interaction with a variety of cell types. As discussed in Chapter 1 of these cells T-lymphocytes and in particular CD4-positive T-lymphocytes are central to the development of liver IRI. Furthermore, it has postulated that prolonged liver ischaemia results in an allograft becoming more susceptible to T-lymphocyte mediated immune responses [309].

The first study to demonstrate the infiltration of T-lymphocytes into the liver after ischaemia was reported in the early 1990's. Although this study by Zwacka *et al* demonstrated the presence of T-lymphocytes in the liver [310] the precise role of this cell was not fully understood until more recent studies demonstrated the central role of T-lymphocytes in mediating the liver injury seen after IRI. The role of T-lymphocytes is further emphasised by the reduction in liver injury observed after OLT by specific T-lymphocyte targeted therapies such as cyclosporine and tacrolimus [311]. More recent studies have assessed the effects of modulating specific T-lymphocytes signalling pathways to elucidate the important regulators hepatic IRI. These studies have demonstrated that disruption of the T-lymphocyte co-stimulatory signalling pathways CD40:CD154 [19] and B7:CD28 [312] all ameliorate hepatic IRI. The reduced levels of liver injury reported within these studies were associated with reduced T-lymphocyte infiltration into the liver, reduced levels of pro-inflammatory cytokine production and increased anti-apoptotic factors [19]. Hence, the role of T-

lymphocytes derived CD28, CD154 and IFNγ in liver IRI has been demonstrated in both mouse and rodent models [313]. Furthermore, CD28 [314] and CD154 [19] are integral in activating the pro-inflammatory response seen during liver IRI and are central to triggering hepatocellular injury. Indeed, murine models of *in vivo* liver IRI utilising CD154 and CD40 knockout mice have demonstrated almost complete protection of livers from IRI. Moreover, wild-type mice used in the same studies treated with anti-CD154 antibody or cytotoxic T-lymphocyte antigen-4 (CTLA-4) immunoglobulin were also protected from IRI [19, 314]. These effects were principally ascribed to the inhibition of CD4-positive T-lymphocytes function within the liver without the requirement of de novo antigen-specific activation that is dependent upon CD40:CD154 signalling [117].

The studies discussed above have exclusively focused upon the role of CD40:CD154 signalling in T-lymphocytes but as discussed in Chapter 4 the expression of CD40 and CD154 within the liver is relatively diverse. Therefore, whilst the interaction of CD40:CD154 upon the surface DC and T-lymphocytes respectively is undoubtedly important in the propagation of liver injury following ischaemia the role CD40 expressed upon hepatocytes is yet to be firmly established. Chapter 4 demonstrates that CD40 activation upon human hepatocytes leads to ROS accumulation and subsequent cell death. Whether CD40 activation upon human hepatocytes *in vivo* results in oxidative stress is not known. Investigating this *in vivo* is problematic as murine CD40 and CD154 knockout models ensure the complete absence of all liver expression of the receptor and ligand and therefore the cell type that is of importance with regard to the regulation of liver injury is difficult to assess. Selective gene or cell deletion does offer the opportunity to investigate the role of specific cells in a particular pathological process. However, before such techniques can be utilised a satisfactory model of liver IRI is required to be established.

5.2 Methods & Materials

5.2.1 Murine Model of Partial Hepatic IRI

Wild-type C57 Black 6 (C57/B6) mice were anesthetised with isofluorane inhalation. Once the animal was anesthetised, the limbs of the animal were immobilized by taping the animal's legs and arms to a clean flat surface with the abdomen facing up. The abdomen was then shaved up to the xiphoid process and was cleaned by swabbing the skin with a 70% ethanol solution. Excess hair was removed prior to the commencement of the surgical procedure.

Sharp dissection was then used to open the abdomen at the midline to expose the abdominal contents. This incision was then extended so that the entire abdomen beginning at the xiphoid process to the pelvic bones was opened (Figure 5.1). Custom made retractors were then used to retract each half of the abdominal wall and secured to produce elevation of the abdomen and aid in expose of the liver and pull the abdominal cavity open (Figure 5.1).

Two moistened cotton swabs were utilised to carefully externalise the murine intestines as gently as possible from the cavity and place them on pre-moistened (sterile 0.9% saline) gauze to expose the portal vein and associated structures. The quadrate lobe was carefully dissected from its attachment with the left lateral lobe by using blunt dissection with a pair of fine forceps. The aforementioned retractors were re-positioned to elevate the median and left liver lobes against the diaphragm to identify the connection between the left lateral and quadrate lobes. This allowed the direct visualisation of the portal triad (portal vein, hepatic artery and bile duct) (Figure 5.2). At this point an atraumatic clip was placed across the portal vein, hepatic artery, and bile duct just above the branching to the right lateral lobe (Figure 5.2).

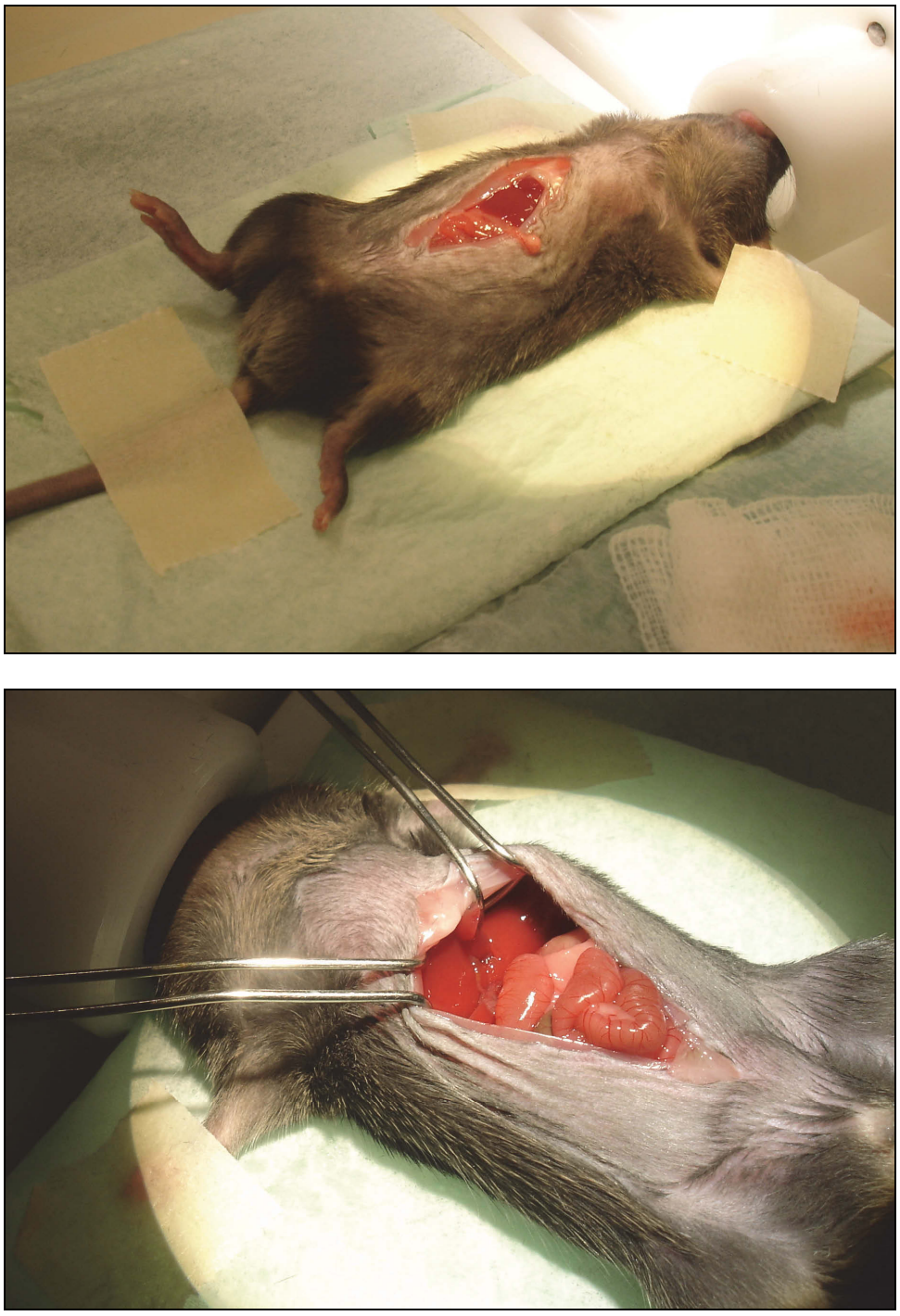

Figure 5.1 The Opening the Murine Abdomen Prior to Clamping the Hepatic Triad
(A) Following isofluorane inhalation the animal was immobilised by taping the arms and tail to a clean surface. The abdomen was clean and shaved and opened from the xiphoid to the pelvis. This allowed inspection of the intra-abdominal contents. (B) Following laparotomy retractors are placed under the abdominal muscles to aid exposure of the liver and allow subsequent liver ligament dissection.

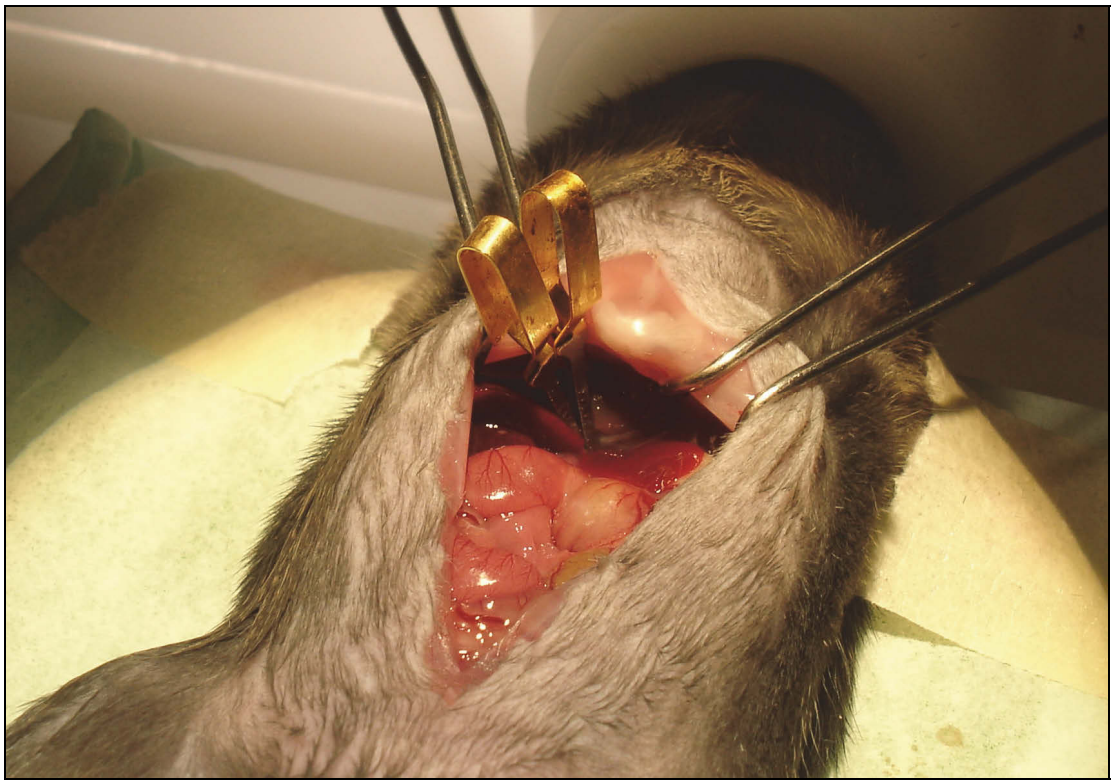

Figure 5.2 Clamping of the Portal Triad in the Murine Liver
Following opening of the abdomen the portal triad was isolated using blunt dissection. With the portal triad isolated atraumatic clips were used to stop vascular inflow into the superior to lobes of the murine liver while the inferior two lobes of the liver remained perfused. This is illustrated in the above photograph.

The median and left lateral lobes (approximately 70% of the murine liver mass) rapidly showed significant blanching. This was manifest visually as a change from the normal reddish brown colour of the liver to a pale brown or cream colour (Figure 5.2). In cases were the above blanching was not observed the atraumatic clip was removed and then reapplied. To achieve satisfactory clamping a specialised clamp holder was utilised. Following satisfactory clamp placement, the intestines were placed back into the abdominal cavity carefully and covered with a well-moistened gauze with saline. The animal was placed under a heat lamp to maintain body temperature at 37°C and monitored closely during the ischemic period making sure the covering gauze remains moist with saline. The ischaemic time used for the experiments was 90 minutes. During this time, additional anaesthesia was occasionally required. This was achieved by placing the animals back into the isofluorane chamber.

Following the 90 minute period of ischemia, the animal was placed back onto the washable plastic and the moisten gauze removed from the intestines. The retractors were placed onto the median and left liver lobes to once again gain access to the portal triad. At this point the atraumatic clamp was carefully removed. 500 μL of sterile saline was infiltrated into the peritoneal cavity to replenish any fluid loss during surgery. Successful reperfusion was visually verified as the blanched colour of the ischemic liver lobes rapidly showed the restoration of the normal reddish-brown colour within a few seconds of clamp removal. At this point suturing the muscle layer with 4/0 vicryl closed the abdomen and then the skin with 4-0 silk sutures and the animal was allowed to recover for the required reperfusion time that was 6 hours. The animals were then placed into heated chambers were free access to chow and free water. Sham operated animals were handled in exactly the same manner other than undergoing clamping of the portal triad.

Immediately following the reperfusion period of 6 hours the animals were again anaesthetised with isofluorane. The animals were then transferred to the washable plastic and the limbs once again immobilised with tape. The laparotomy wound was opened and the intestine displaced in the caudal direction and the inferior vena cava (IVC) visualised. 10 µl of heparinised saline was injected directly into the IVC and then venous blood collected into a microsyringe. The samples are allowed to clot on ice for approximately 10 minutes after which they are centrifuged at 4,000 × g for 10 minutes. Serum was removed and frozen at -80°C.

The animal was then euthanised by exsanguination. Following this a thoractomy was performed and the diaphragm divided. The liver was then removed. Representative samples of the post-ischemic liver (and/or bypass lobes) were immediately frozen in liquid nitrogen and stored at -80°C.

5.2.2 Serum Preparation and Quantification of Liver Transaminase Levels

Serum levels of alanine aminotransferase (ALT) and aspartate aminotransferase (AST) were quantitative indices of liver damage used to assess liver injury and could be quantified in serum obtained from mice subjected to liver IRI. The sample were processed and quantified at the University Medical Centre Groningen (UMCG) biochemical laboratory using standard operating protocols.

5.2.3 Histopathology

Following exsanguinations, representative pieces of ischemic, IRI or bypass lobes were quickly removed and fixed in ice cold 10% phosphate-buffered formalin for 24 hours at 4°C. The tissue is then partially dehydrated with ethanol and embedded in JB4 plastic mounting

media using standard histological methods. Five-micrometer sections cut and stained with haematoxylin and eosin (H&E).

5.2.4 Statistical Analysis

All values are presented as mean ± SEM. Data are analyzed using Students *t* test or analysis of variance where significance was set at $p<0.05$.

5.3 Results

5.3.1 CD40:CD154 Signalling Regulates Hepatic IRI *in vivo*

Depriving 70% of the murine liver of blood flow for 90 minutes followed by 6 hours of reperfusion significantly increased serum ALT and AST levels in wild-type C57B/6 (Figure 5.3). Sham operated animals did not show any increase in either serum ALT or AST levels. There was a significant reduction in ALT and AST in both CD40 and CD154 knockout mice.

Histopathological evaluation of the murine livers revealed that sham operated animals sustained no parenchymal injury as assessed by H&E staining (Figure 5.4). Wild-type C57/B6 animals however sustained marked injury of the liver particularly within the peri-venular regions of the liver that was consistent with the significantly elevated serum ALT and AST levels. Consistent with the reduced injury seen in the CD40 and CD154 knockout mice these mice sustained less injury as demonstrated by Figure 5.4.

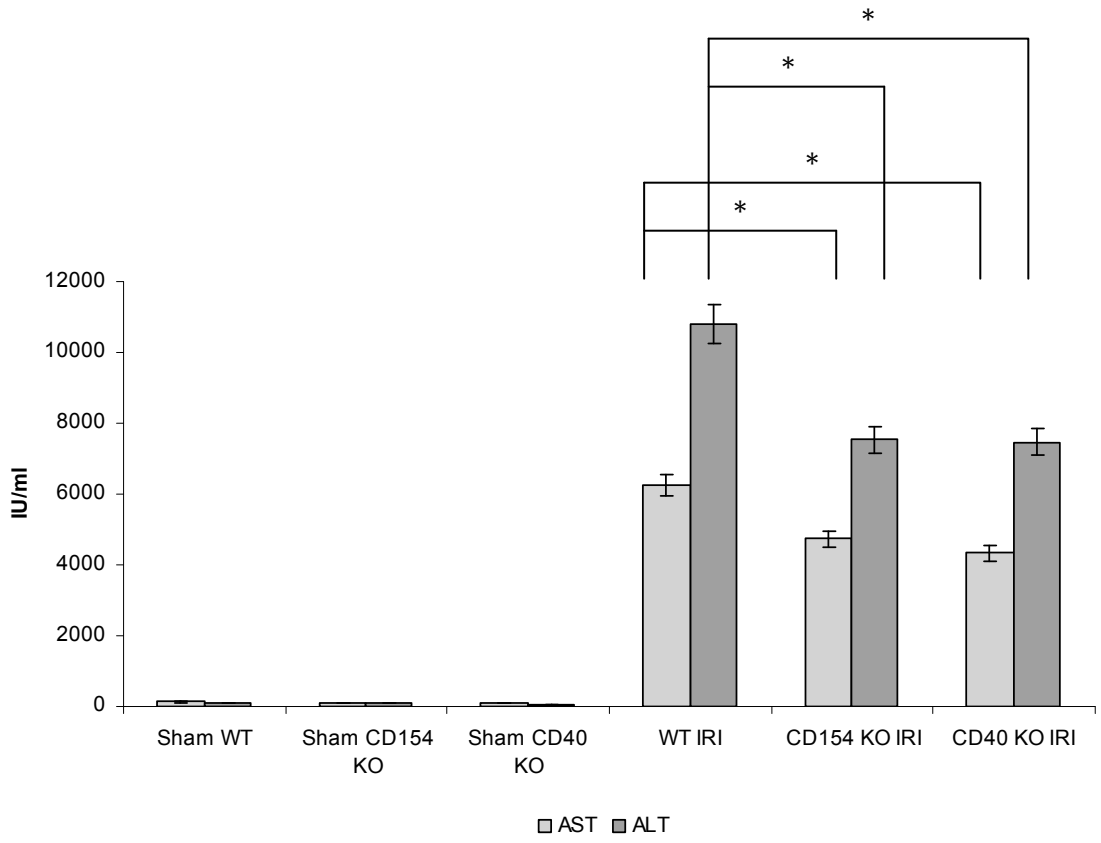

Figure 5.3 CD40 and CD154 Mice have Lower Serum AST and ALT Levels after Hepatic IRI

Following 90 minutes of liver ischaemia and 6 hours of liver reperfusion, serum was withdrawal from sham operated, wild-type, CD40 knockout and CD154 knockout mice via IVC punctuate. Serum was then used to determine the concentration of AST and ALT in the different murine groups. Data are expressed as the mean ± S.E. *$p<0.05$, Student's *t* test. (n=8-12).

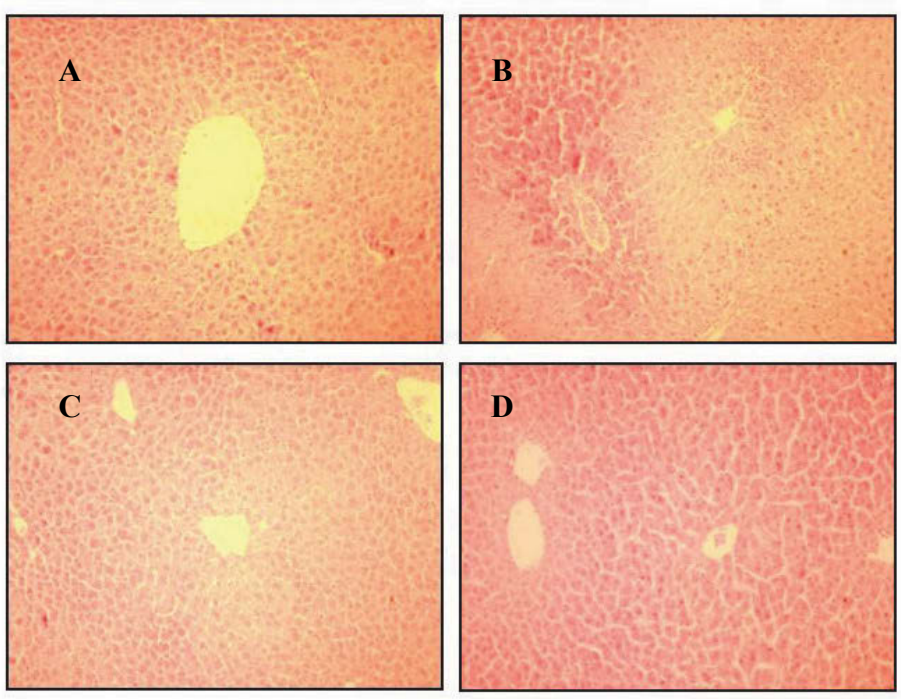

Figure 5.4 CD40 and CD154 Knockout Mice Sustain Less Hepatocellular Injury after Hepatic IRI
Panel (A) demonstrates a representative H&E stain of wild-type C57/B6 mice subjected to sham operation. There is no disruption to hepatocellular plate. Panel (B) illustrates the effects of IRI upon the liver. There is haemorrhagic necrosis and also congestion within the liver around the perivenular region. Panel (C) CD40 knockout mice and Panel (D) CD154 knockout mice show features of hepatocellular injury however there is substantially reduced injury when compared to Panel (B). (magnification 20x). (n=8-12).

5.4 Discussion

The mouse model of liver IRI utilised here has proven invaluable for the understanding of the role that the CD40:CD154 signalling pathway plays in modulating and mediating liver tissue injury *in vivo* [18]. It is clear that hepatic IRI induces significant liver injury as assessed by serum AST, serum ALT and histological examination of the liver. These changes are completely absent in sham-operated animals and significantly reduced in CD40 and/or CD154 knockout mice. The data presented above further demonstrates the key role of the CD40:CD154 interaction in mediating liver injury after IRI *in vivo*. Previous studies have ascribed the protection from liver injury in CD40 and CD154 knockout mice following IRI to a reduction in T-lymphocyte co-stimulation [19]. This particular study showed almost complete amelioration of liver injury following IRI in CD40 and CD154 knockout mice. This is in contrast to the data presented here. Although the same *in vivo* IRI model was used in the presented data a lesser degree of protection was afforded in the knockout animals in the presented data. This discrepancy in these observations is likely to be due to the difference in susceptibility of murine species to IRI. It is clear however that the CD40:CD154 receptor ligand does promote parenchymal injury after liver IRI.

The data presented in Chapter 3 and 4 clearly shows that ROS is an important mediator of hepatocyte injury during hypoxia and H-R. The assessment of ROS accumulation in tissues as opposed to cells is technically much more challenging. No studies have investigated ROS accumulation within tissue in real-time. DCF can be utilised in conjunction with intra-vital microscopy to determine intracellular ROS accumulation but this is currently only possible over short time courses in the order of 5 minutes. Therefore many *in vivo* studies have utilised surrogate markers of ROS to indirectly assess tissue hypoxia. These markers include carbonic anhydrase IX [315], pimonidazole [316] and HIF-1α [317]. Therefore although

these makers do not assess ROS accumulation they do imply ROS production. Previous studies have shown that hypoxia does increase pimonidazole staining of liver tissue after hypoxia [318, 319]. Whether CD40 activation increases parenchymal hypoxia or ischaemia cannot be stated on the basis of the presented data.

The CD40:CD154 receptor ligand dyad does mediate post-ischemic liver damage within the liver but as stated in Chapter 1 there does exist numerous differences between hepatocytes from different species. Hence although in murine livers CD40 and CD154 mediate parenchymal injury whether the same occurs in human livers in not known. More specifically, although the data presented in Chapter 3 and 4 revealed the *in vitro* and intracellular mechanisms by which ROS and CD154-mediated ROS mediate post-hypoxic hepatocyte injury whether CD40:CD154 also caused similar effects *in vivo* was not known. As discussed in Chapter 4 hepatocytes, HSEC, HSC and cholangiocytes all express CD40 while macrophages, T-lymphocytes and platelets express CD154. Which of these potential interactions is the important key interaction *in vivo* cannot be determined on the basis of the presented data. CD40:CD154 certainly regulate parenchymal injury but whether this is a result of numerous co-ordinated interaction or as a result of a specific interaction is not known. Certainly platelet depleted mice [306], T-lymphocyte knockout mice [117] and Kupffer cell/macrophage knockout mice [320] are all protected from a variety of liver injuries and this therefore suggests redundancy within the CD40:CD154 signalling system and implies numerous CD154 bearing cells can induce hepatocyte injury via CD40 activation. Hence the findings presented here should be treated with caution. In CD40 and/or CD154 knockout animals the receptor and ligand will also be absent upon macrophages, KCs, liver resident immune cells and DCs. This will also lead to defective priming of these immune cells some of which can release extracellular ROS and hence perpetuate

hepatocellular injury. The lack of effective cell activation and priming will also lead to less tissue hypoxia, less cell death and reduced serum transaminases. Coupled with *in vitro* data presented earlier an additional plausible mechanism of the action of CD40:CD154 is that reduced CD40 activation upon hepatocytes during hepatic IRI led to reduced tissue hypoxia and reduced cell death.

Importantly, antagonism of the CD40:CD154 signalling pathway is now being used in the clinic. While CD28 blockade has been successfully translated to the clinic, translation of blockade of the CD40:CD154 pathway has been less successful, in large part due to thromboembolic complications associated with anti-CD154 antibodies [321]. The efficacy of CD154 targeted therapies has been established in murine models of cardiac transplantation [125]. Indeed 3A8, a human CD40-specific monoclonal antibody, has been shown to prolong islet cell allograft survival without depleting B-lymphocytes [322]. Furthermore 3A8 in combination with CTLA4Ig and sirolimus prolonged engraftment in a well-established primate bone marrow chimerism-induction model [323].

Previous studies have also shown that within CD40 and CD154 knockout animals there is reduced intrahepatic T-lymphocyte sequestration after hepatic IRI, decreased production of Th1 pro-inflammatory cytokines and reduction of pro-apoptotic caspase proteins [19]. Coupled with the findings presented within this Chapter it is demonstrated that the CD40:CD154 receptor-ligand dyad is likely to employ diverse mechanisms to cause liver injury during IRI.

CHAPTER 6 - OVERVIEW

6.1 Overview

The initial aim of this study was to investigate the effects of CD40 activation upon hepatocyte survival *in vitro* and *in vivo*. However, it quickly became apparent that it was important to define the effects of oxidative stress upon hepatocyte susceptibility to cell death and whether ROS was involved in cellular signalling events following CD40 activation upon hepatocytes. Therefore by necessity a substantive section of the study focused upon assessing the role of oxidative stress in regulating hepatocyte cell death and survival.

The data highlights the key role of intracellular ROS accumulation in mediating human hepatocyte cell death during hypoxia and H-R and *in vivo* following liver IRI. Importantly the findings illustrate that human hepatocytes have differential vulnerability to undergo cell death in response to oxidative stress. Human hepatocytes were isolated from a variety of sources including normal, normal resected and end-stage cirrhotic liver disease. It is clear from the data those normal hepatocytes and hepatocytes isolated from biliary cirrhotic livers and ALD increase intracellular ROS during hypoxia and H-R, and undergo both apoptotic and necrotic cell death as a result. Human hepatocytes isolated from normal resected liver tissue also accumulated ROS during hypoxia and H-R but were not susceptible to cell death. These observations reveal considerable heterogeneity in the physiological responses of human hepatocytes to oxidative stress and that these responses are dependent on the source of tissue. Therefore, studies utilising human hepatocytes need to be analysed within the context of the type of liver from which cells were isolated. It is likely that the local tissue microenvironment affects the way that hepatocytes respond to oxidative stress. For instance, hepatocytes isolated from ALD livers show significantly lower albumin production, significantly lower urea synthesis and increased basal ROS levels probably reflecting the continual exposure to alcohol. These observations suggest that further studies are warranted

to discern the precise molecular mechanisms that govern the regulation of the oxidative stress responses of hepatocytes from different diseases and indeed different regions of the hepatic lobule. These differences in human hepatocyte physiology are likely to be real as a uniform stringent protocol for human hepatocyte isolation was adopted and therefore any difference observed in hepatocyte responses to the *in vitro* IRI model were unlikely to be explicable by technical variance in isolation procedure, culture conditions or manipulation of liver tissue.

Building on these above observations the present study shows that, large/PV human hepatocytes were more susceptible to cell death during hypoxia and H-R than small/PP human hepatocytes. These findings are at variance with previous studies where small/PP hepatocytes were found to be more susceptible to hypoxia [169]. There are several explanations for these observations including inter-species variability and the method employed to isolate hepatocytes. In this study hepatocytes isolated from normal liver, normal resected liver or end-stage cirrhotic liver suggested that large/PV human hepatocytes show greater intracellular ROS accumulation when compared to small/PP human hepatocytes. This observation has important implications for the pathophysiology of ischaemic liver disease. As demonstrated in Chapter 5 following *in vivo* IRI murine livers sustain injury predominantly within the peri-venular region of the liver. Therefore large/PV human hepatocytes propensity to increase intracellular ROS production during hypoxia may underlie the reason why zone 3 of the liver acinus is the area of liver damage associated with ischaemia. Furthermore, Zone 3 hepatocytes exist in a relatively hypoxic micro-environment under normal physiological conditions [99] and therefore increased levels of hypoxia may disrupt oxidative phosphorylation within large/PV human hepatocytes mitochondria leading to ROS accumulation and resultant cell death. It is important to note that ROS accumulation

in large/PV human hepatocytes is also NADPH oxidase dependent and this pathway is likely to contribute to cell death as well. Other studies examining liver injury from a variety of sources including IRI [43], viral hepatitis [324] and cirrhosis [325] all report cellular damage predominantly in the peri-venular region. Although these are important observations with regard to liver patho-physiology it is likely that the delivery of pharmacological therapeutics that target all hepatocytes will offer potential treatment to ameliorate IRI in the future [326].

ROS accumulation in human hepatocytes during oxidative stress can be derived from a variety of sources. The mitochondrion has previously been shown to be the main cellular source of ROS accumulation in the hepatocyte [71]. Consistent with these previous observations the specific mitochondrial dye MitoSox Red demonstrated that mitochondrial superoxide production is an important and abundant source of ROS in human hepatocytes during hypoxia and H-R. This observation is further corroborated with experiments using the complex I inhibitor rotenone which significantly reduced human hepatocyte ROS production. In addition inhibition of the cytosolic enzyme NADPH oxidase also reduced human hepatocyte ROS production. Therefore taken together with other studies, it is likely that hepatocyte mitochondrion [71], NADPH oxidase [327], XO [328] and peroxisomes [329] are responsible for ROS production (Figure 6.1).

This study provides evidence that extracellular signals such as exogenous TNFα ligand CD154 can augment intracellular ROS generation. Following activation of CD40 by CD154, the flavoenzyme NADPH oxidase is recruited to the plasma membrane and induces the formation of ROS [274]. TNFα recruits the TRAF-XO complex to induce ROS formation [78]. Hence the TNFα super-family of ligands and receptors may have a diverse range of mechanisms of ROS production. It is possible to speculate that these mechanisms may operate synergistically during pro-inflammatory processes such as IRI and perpetuate liver

injury although only the effects of CD154 have been assessed within this study. Moreover in this study, CD40 and/or CD154 knockout mice sustained less liver injury following hepatic IRI than wild-type mice as assessed by histology and liver serum transaminases. Although this suggests that CD40:CD154 is involved in the regulation of hepatic IRI as previously suggested [19] the presence of liver injury in the knockout mice also suggests other mechanisms are involved in mediating hepatic IRI such as those described in Chapter 1. This suggests that hepatic IRI is a multi-factorial process in accordance with recent reviews [40]. An important caveat to these observations is that the *in vitro* experiments conducted here were in human hepatocytes whereas *in vivo* experiments were conducted in a murine model. As discussed earlier there maybe significant differences between hepatocytes from different species meaning data from this study should be interpreted cautiously.

The accumulation of ROS within human hepatocytes triggers at least three separate and distinct downstream signalling functional events. Intracellular ROS accumulation during hypoxia and H-R induces cellular apoptosis, necrosis and also promotes the cyto-protective mechanism of autophagy. Therefore intracellular ROS accumulation within human hepatocytes as a result of oxidative stress paradoxically promotes both cell death and cell survival. Specifically, ROS induces autophagy in a PI3-K-Atg dependent manner promoting cell survival during hypoxia and H-R as well as inducing apoptosis and necrosis. In line with their greater propensity to produce ROS large/PV human hepatocytes are much more sensitive to induction of apoptosis, necrosis and autophagy than small/PP human hepatocytes during hypoxia and H-R. The linkage between intracellular ROS and apoptosis, necrosis and autophagy is clearly demonstrated by the pre-treatment of human hepatocytes with NAC. ROS production by human hepatocytes was completely inhibited by NAC that also completely abrogated human hepatocyte apoptosis and autophagy and significantly reduced

necrosis during hypoxia and H-R. This finding suggests that during *in vitro* IRI, intracellular ROS is the key mediator of human hepatocyte apoptosis and autophagy and also inhibits necrosis. The downstream signalling pathways activated by ROS are likely to be numerous but the MAPKs, caspases and calpains are likely to be among the most important effectors [291]. Specifically, ROS is likely to activate MAPK, caspases and calcium to regulate apoptosis [330] and the presented data shows ROS is also likely to activate PI3-K and Atg proteins to regulate autophagy. Therefore, death inducing mechanisms involving caspases, calpain, cathepsins, calcium, mitochondrial permeability transition and endoplasmic reticulum stress all regulate cell death [188] and it maybe that these downstream effectors all share a common signalling pathway. This is partly confirmed by the presented data because inhibiting ROS completely abrogated hepatocyte apoptosis. Therefore ROS is likely to be a central cellular mechanism for regulation of apoptosis.

The data demonstrates the role of the TNFR/TNF super-family members CD40 and CD154 in mediating hepatocyte cell death and injury both *in vitro* and *in vivo* following IRI. CD154 stimulation of human hepatocytes augmented ROS accumulation in a NADPH oxidase dependent manner. Intracellular ROS then induced human hepatocytes apoptosis and necrosis. The stimulation of these hepatocytes with recombinant human CD154 demonstrated that CD40 activation could augment ROS levels within human hepatocytes during normoxia and H-R. Although activated platelets can be one potential source of CD154 during pro-inflammatory liver processes, macrophages [121] and T-lymphocytes will also be important effectors cells inducing parenchymal injury. It is likely that the augmentation of intracellular ROS within hepatocytes is a common mechanism shared by pro-inflammatory signals [331]. However, CD154 activation of CD40 upon human hepatocytes was unable to augment ROS accumulation in hypoxia. Certainly CD40

expression is not altered during hypoxia and numerous studies have shown that hepatocytes are able to up-regulate intracellular antioxidant defences during hypoxia and it is likely that this buffers the increases in intracellular ROS induced by CD154 during hypoxia. Furthermore, murine model of IRI demonstrate that CD40 and CD154 regulate hepatocyte injury *in vivo* although the precise mechanism underlying this protection remains to be fully ascertained [19].

The *in vitro* IRI model does however illustrate the complexity of the CD40:CD154 signalling pathways in human hepatocytes. ROS generated by CD154 stimulation of hepatocytes appears to regulate apoptosis via two different mechanisms. CD154 activated the MAPK sub-families p38 and JNK and also induced human hepatocyte FasL expression. Therefore ROS regulation of human hepatocyte apoptosis is complex with possible redundant signalling pathways that have a high degree of cross-talk [43]. This latter mechanism maybe highly advantageous at the tissue and organ level as it would enable the elimination of diseased cells via multiple pathways. The induction of human hepatocyte necrosis by intracellular ROS is likely to be a degenerative process as previously observed [217] but can be reduced with a variety of antioxidants. Clearly apoptosis and necrosis are both induced following ROS accumulation in human hepatocytes. It is likely based upon the data that ROS-p38/JNK is integrally involved in the regulation of apoptosis whereas ROS alone induces human hepatocyte necrosis through direct toxic effects. Necrotic cell death is likely to be perpetuate the proinflammatory response during IRI through the release of cytokines and ROS itself following oncosis [219]. There are several potential mechanisms that may explain the cellular decision to undergo apoptosis or necrosis. Aside from cellular ATP content particular ROS sub-species [76] or relative and absolute levels of intracellular ROS [332] may govern the particular mode of cell death. In addition necrosis may

sequentially follow apoptosis [333]. However, taken together the presented data supports the role of both apoptosis and necrosis in mediating human hepatocyte cell death during hypoxia and H-R [52]. Taken together with previous studies it is probable that CD40 activation leads to ROS accumulation, JAK-STAT activation [120] and induction of NFκB signalling [157]. The precise outcome of these signalling pathways appears to be cell specific within the liver. Within the epithelial cell derived hepatocytes and cholangiocytes, ROS accumulation and JAK-STAT activation lead to cell death via both JNK activation and induction of FasL [118, 120, 122]. CD40 activation on HSEC however leads to proliferation and secretion of pro-inflammatory cytokines in a NFκB dependent manner [157]. Many of these studies have examined the role of a single signalling pathway in the liver cell of interest and thus the precise role of ROS in CD40 signalling in the liver remains to be fully ascertained. However, regardless as to the source of ROS it appear that at some point the cell has a decision to make about whether it will pursue cell survival or cell death in response to oxidative stress. The precise mechanism underlying these cell processes is not clear.

Finally, the current paradigm that ROS is always detrimental to hepatocyte viability [43] is not supported by the data. Intracellular ROS accumulation in other cell types has been linked to cell survival [334] and in human hepatocytes intracellular ROS accumulation induced the formation the autophagic vacuoles in a PI3-K-Atg protein dependent manner. These autophagic vacuoles inhibit apoptosis by preventing mitochondrial depolarisation probably by mitophagy and enable hepatocytes to survive extreme/severe hypoxia [212]. The data suggests that during hypoxia and H-R human hepatocytes undergo autophagy primarily in the form of mitophagy to aid cell survival [212]. It is likely that if ROS generation continues this overwhelms the cyto-protective cellular machinery and the hepatocyte then undergoes cell death in the form of both apoptosis and necrosis although the molecular switch

governing the precise mode of cell death remains to be fully ascertained. These key questions will remain unanswered until intracellular probes are developed that can assess the formation of different ROS sub-species.

In conclusion, the mitochondrion, ROS production and human hepatocyte cell death and survival are intimately linked as illustrated in Figure 6.1. Taken together these findings demonstrate that during hepatic IRI, ROS production is the key and seminal event in the initiation and propagation of the injury. Whether ROS is important in the resolution of injury and regeneration of the injured liver cannot be answered by the present study and remain an important area of research. The continued development of therapeutic strategies that ameliorate the development and production of ROS holds considerable promise for the treatment of liver disease with the caveat that ROS also appears to be an important regulator of cell survival.

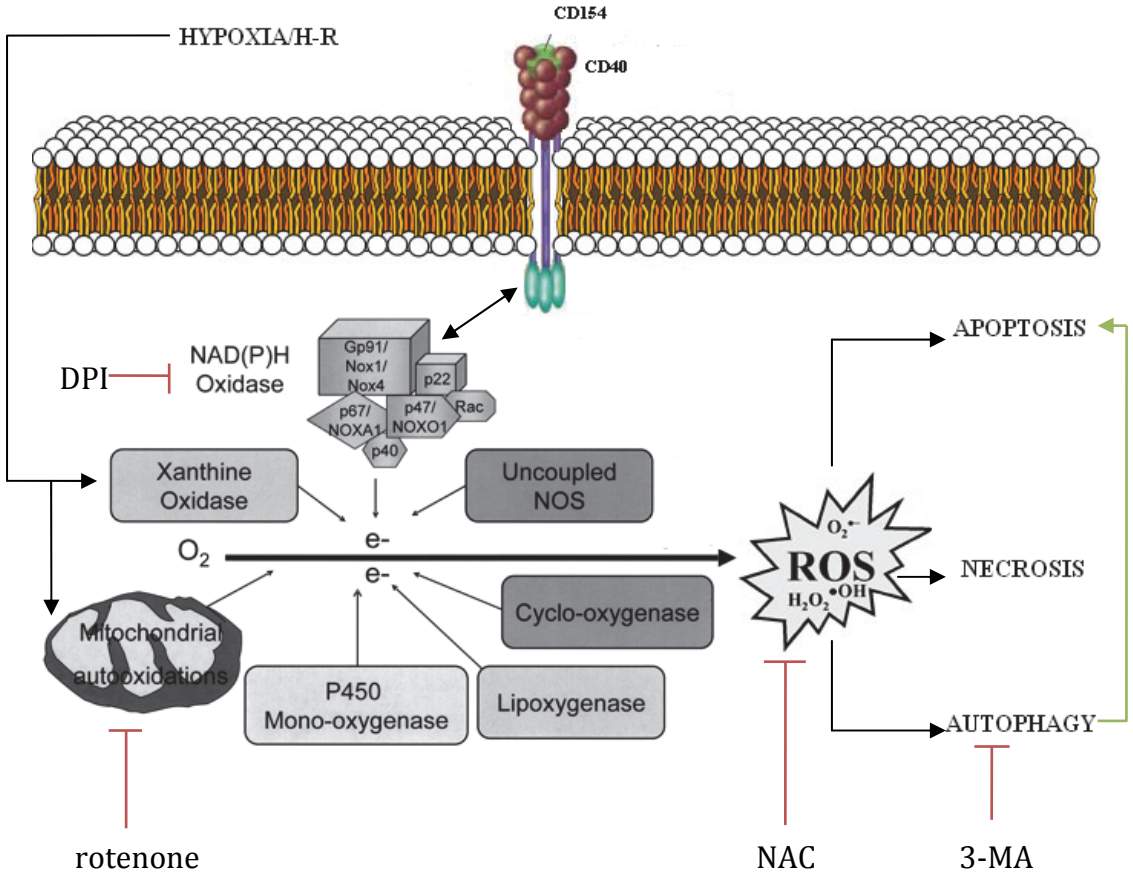

Figure 6.1 The Role of ROS and CD40:CD154 in Mediating Human Hepatocyte Cell Death and Survival

The above model illustrates the likely mechanism of action of the intracellular ROS generated within human hepatocytes during IRI. Intracellular ROS can be generated by a number of sources within hepatocytes. As discussed above hypoxia and H-R generate ROS primarily via the mitochondria but cytosolic NADPH oxidase can also stimulate ROS accumulation. Inhibition of mitochondrial electron transport chain with rotenone (red arrow) or ROS in general with NAC (red arrow) reduces cell death within human hepatocytes. Other systems within hepatocytes such as XO and cyclooxygenase can also stimulate ROS accumulation. As shown in Chapter 4 the CD40:CD154 receptor ligand interaction can stimulate ROS production in a NADPH oxidase dependent manner. Once generated ROS accumulation has at least three downstream signalling pathways. The first pathway to be activated during hypoxia and H-R is the stimulation of the pro-survival pathway of autophagy in a PI-3K-Atg dependent manner. Inhibition of the autophagic pathway with 3-MA commits the hepatocyte to cell death in the form of apoptosis (green arrow). If oxidative stress within human hepatocytes continues the autophagic response is overwhelmed and the cell is committed to cell death in the form of both apoptosis and necrosis.

6.2 Future Work

The data presented above has added further evidence for the role of oxidative stress and CD40:CD154 mediated ROS accumulation in the development of hepatic injury following IRI. Additional work would shed light on the wider role of both ROS and CD40:CD154 during IRI and may lead to the identification of important signalling pathways and therapeutic targets.

- The molecular mechanism regulating the processes of ROS-dependent human hepatocyte apoptosis, necrosis and autophagy.

  Although the link between ROS and apoptosis, necrosis and autophagy has been established by the present study the precise mechanisms governing cell fate and the decision as to when to abandon cell survival in favour of cell death remain to be fully ascertained. The use of specific inhibitors such caspase inhibitors, cathepsin inhibitors and intracellular calcium probes will further map the signalling pathways involved and add to the fundamental understanding to cell and hepatocyte biology.

- The precise nature of upstream CD40 signalling.

  The presented data show that CD40 activation upon human hepatocytes leads to cell death in a NADPH Oxidase-ROS dependent manner. However which TRAF molecule is involved in this process remains to be confirmed. The controversy surrounding this latter point makes this an important question to answer for CD40 biologists. Using immunofluorescence and cellular tagging of the different TRAF molecules would answer this question conclusively.

- The effect of cold IRI upon human hepatocyte ROS production and cell death.

  The data presented in this thesis has assessed the effects of warm IRI *in vitro* and *in vivo*. Whilst this has revealed important insights into hepatocyte responses to a

specific set of conditions *in vitro*, this model is not akin to many clinical scenarios such as OLT were cold IRI is encountered. The effect of cold IRI upon hepatocytes and livers would be of unquestionable value to clinicians. Furthermore whether CD40:CD154 signalling events are altered by hypothermia could also be assessed.

- The kinetics of Reactive Nitrogen Species generation (RNS) in determining human hepatocytes cell death during hypoxia and H-R.

Although ROS is an important regulator of IRI, RNS, which have only briefly been discussed here, are also likely to be important regulators of hepatic injury after IRI. There are commercially available RNS probes that could be used alone or in parallel with ROS probes to delineate the relationship between RNS and ROS and cell death. Peroxynitrites, formed in part by RNS, are becoming increasingly seen as important regulators of injury seen after oxidative stress and establishing their role will allow the delineation of other therapeutic targets to ameliorate hepatic IRI.

- The factors determining the increased propensity of PV/large human hepatocytes to produce ROS and induce cell death.

The data also demonstrate for the first time with human primary cells that large/PV human hepatocytes are susceptible to hypoxic injury. The precise mechanism underlying the latter observation remains to be delineated. Using FACs to separate cells and study large/PV human hepatocyte in isolation would answer these questions and add significantly to the understanding of liver biology.

Appendix I

LIVER TRANSPLANTATION 16:1303-1313, 2010

ORIGINAL ARTICLE

Reactive Oxygen Species Mediate Human Hepatocyte Injury During Hypoxia/Reoxygenation

Ricky Harminder Bhogal, Stuart M. Curbishley, Christopher J. Weston, David H. Adams, and Simon C. Afford

Centre for Liver Research, Institute for Biomedical Research, Medical School, University of Birmingham, Birmingham, United Kingdom

Increasing evidence shows that reactive oxygen species (ROS) may be critical mediators of liver damage during the relative hypoxia of ischemia/reperfusion injury (IRI) associated with transplant surgery or of the tissue microenvironment created as a result of chronic hepatic inflammation or infection. Much work has been focused on Kupffer cells or liver resident macrophages with respect to the generation of ROS during IRI. However, little is known about the contribution of endogenous hepatocyte ROS production or its potential impact on the parenchymal cell death associated with IRI and chronic hepatic inflammation. For the first time, we show that human hepatocytes isolated from nondiseased liver tissue and human hepatocytes isolated from diseased liver tissue exhibit marked differences in ROS production in response to hypoxia/reoxygenation (H-R). Furthermore, several different antioxidants are able to abrogate hepatocyte ROS–induced cell death during hypoxia and H-R. These data provide clear evidence that endogenous ROS production by mitochondria and nicotinamide adenine dinucleotide phosphate oxidase drives human hepatocyte apoptosis and necrosis during hypoxia and H-R and may therefore play an important role in any hepatic diseases characterized by a relatively hypoxic liver microenvironment. In conclusion, these data strongly suggest that hepatocytes and hepatocyte-derived ROS are active participants driving hepatic inflammation. These novel findings highlight important functional/metabolic differences between hepatocytes isolated from normal donor livers, hepatocytes isolated from normal resected tissue obtained during surgery for malignant neoplasms, and hepatocytes isolated from livers with end-stage disease. Furthermore, the targeting of hepatocyte ROS generation with antioxidants may offer therapeutic potential for the adjunctive treatment of IRI and chronic inflammatory liver diseases. ***Liver Transpl 16:1303-1313, 2010.*** © **2010 AASLD.**

Received June 2, 2010; accepted July 23, 2010.

Most studies that have investigated the mechanisms of liver damage occurring as a result of ischemia/reperfusion injury (IRI) have focused on the setting of liver transplantation. It is equally possible that relatively hypoxic conditions can occur during other episodes of hepatic inflammation or established chronic disease. Hepatocytes exposed to a hypoxic microenvironment would therefore be potentially sensitized to cell death, although no studies have yet explored this process in primary human hepatocytes.

Despite considerable advances in surgical practice and more judicious use of immunosuppression, hepatic IRI continues to adversely affect allograft function and survival after orthotopic liver transplantation (OLT). Toledo-Pereyra et al.[1] in 1975 were among the first to note the detrimental effects of IRI during experimental liver transplantation. IRI is a proinflammatory, antigen-independent process that culminates in hepatocyte injury. The potential processes regulating

Abbreviations: 7-AAD, 7-aminoactinomycin D; ALD, alcoholic liver disease; Cy5, cyanine 5; DCF, 2′,7′-dichlorofluorescin; DPI, diphenyliodonium; FITC, fluorescein isothiocyanate; FL, fluorescence; FS, forward scatter; H-R, hypoxia/reoxygenation; HSEC, hepatic sinusoidal endothelial cell; IRI, ischemia/reperfusion injury; KC, Kupffer cell; MFI, mean fluorescence intensity; NAC, N-acetylcysteine; NADPH, nicotinamide adenine dinucleotide phosphate; OLT, orthotopic liver transplantation; PE, phycoerythrin; ROS, reactive oxygen species; Rot, rotenone; SS, side scatter.

Address reprint requests to Ricky Harminder Bhogal, M.D., Centre for Liver Research, Institute for Biomedical Research, Medical School, University of Birmingham, Wolfson Drive, Birmingham, United Kingdom B15 2TT. Telephone: +44 (0)121 415 8698; FAX: +44 (0)121 415 8701; E-mail: balsin@hotmail.com

DOI 10.1002/lt.22157
View this article online at wileyonlinelibrary.com.
LIVER TRANSPLANTATION.DOI 10.1002/lt. *Published on behalf of the American Association for the Study of Liver Diseases*

hepatic IRI have been summarized in recent reviews.[2,3] Recent studies have suggested that hepatic IRI accounts for up to 10% of early allograft failures and is associated with a higher incidence of both acute and chronic rejection.[4] The primary cellular target during IRI is the hepatocyte. Hepatocyte death seen during the hypoxic and reperfusion phases of IRI occurs within a relatively hypoxic environment, and hepatic IRI can be divided into 2 phases. The early phase is thought to involve the activation of Kupffer cells (KCs), which release proinflammatory cytokines and reactive oxygen species (ROS).[5,6] The late phase is characterized by increased expression of chemokines and adhesion molecules and hepatic recruitment of effector cells, which amplify the tissue damage. The latter phenomenon is a feature common to many other hepatic diseases. There is evidence suggesting that hepatocyte injury occurs during the relatively hypoxic early phase of IRI.[7] ROS release is one of the earliest and most important components of tissue injury after the reperfusion of ischemic organs and is a major contributor to hepatocyte death during reperfusion.[8] Moreover, diseases such as alcoholic liver disease (ALD) are characterized by the chronic accumulation of ROS. The source of hepatic ROS remains controversial. Numerous studies have suggested that hepatocyte damage is triggered by KC-derived ROS,[9,10] whereas others have shown that the absence or elimination of KCs does not prevent tissue damage in IRI.[11] This suggests that other cells within the liver, including hepatocytes, may be involved in the pathophysiological production of ROS during IRI and chronic hepatic inflammation.

Early work with rat hepatocytes suggested xanthine oxidase as the main generator of ROS.[12] However, the xanthine oxidase inhibitors used in these studies are now known to inhibit mitochondrial function, and mitochondria are now accepted as the main source of ROS within hepatocytes.[13] Furthermore, the inhibition of mitochondrial complexes I and III can ameliorate ROS production in human hepatoma cell lines[14] and rat hepatocytes.[15] Other enzymes, such as the flavoenzyme nicotinamide adenine dinucleotide phosphate (NADPH) oxidase, can also produce ROS in rat hepatocytes.[16] The accumulation of excess intracellular ROS induces cell death, and during hepatic IRI, hepatocytes undergo both apoptosis and necrosis.[17] Some studies have supported apoptosis as the primary mode of death,[18] and others have supported necrosis.[19] In reality, it is uncertain whether the apoptosis and necrosis observed in liver tissue are separate processes because the terms primarily represent morphological descriptions, and it has been suggested that apoptotic cells not effectively cleared from inflammatory sites may eventually assume a necrotic appearance (so-called secondary necrosis). This led Jaeschke and Lemasters[20] to propose the term *necroapoptosis*, and it may be that the 2 forms of cell death are in part related and share some common intracellular pathways.

Despite these observations, little is known about the relative contribution of endogenous hepatocyte ROS production and its potential impact on hepatocyte cell death after hypoxia and hypoxia/reoxygenation (H-R). Much of our understanding of hepatic IRI comes from studies of rodent hepatocytes and experimental models. However, the response of human hepatocytes to hypoxia and H-R is unknown. In addition, the research performed with human hepatocytes has used cells isolated from resected liver tissue from patients with neoplastic disease.[21] Whether cells from such normal sources can be considered to truly reflect normal hepatocytes has never to our knowledge been objectively studied.

The aim of our study was to characterize the responses of human hepatocytes isolated from normal liver tissue and diseased liver tissue to hypoxia and H-R. Specifically, we delineated intracellular ROS accumulation and cell death in primary human hepatocytes isolated from normal liver tissue and diseased liver tissue during hypoxia and H-R. Using an in vitro model of warm hepatocyte IRI, we show for the first time highly variable responses of primary human hepatocytes isolated from normal liver tissue, surgically resected liver tissue, and diseased liver tissue to hypoxia and H-R. Although these findings have obvious clinical implications within the transplant setting, they are equally important for diseases in which local cellular responses to hypoxia may shape the inflammatory and regenerative microenvironment. The apparent variable responses of primary hepatocytes isolated from normal tissue, resected normal tissue, and diseased tissue are also important to workers studying hepatocyte physiology and function ex vivo.

MATERIALS AND METHODS

Isolation of Human Hepatocytes

Liver tissue was obtained from fully consenting patients undergoing transplantation for a variety of end-stage liver diseases and from patients undergoing hepatic resection for liver metastasis; normal donor tissue exceeding surgical requirements was also used. Specifically, normal donor tissue was obtained from the in situ splitting of adult livers used for pediatric OLT. These patients were 19 to 31 years old. The left lateral segment was used for pediatric OLT, and this meant that tissue could be procured from the right lobe. Human hepatocytes were isolated from explanted diseased livers from patients with ALD, primary biliary cirrhosis, or primary sclerosing cholangitis. Hepatocytes were also isolated from tissue taken from patients who had undergone hepatic resection for liver metastasis from colorectal carcinoma. Liver tissue was obtained from surgical procedures carried out at Queen Elizabeth Hospital (Birmingham, United Kingdom). Ethical approval for the study was granted by the local research ethics committee (reference number 06/Q702/61).

Importantly, all liver tissue, including explants, normal donor tissue, and normal resected tissue, was obtained from patients with the same rigorous standard protocol. Briefly, each liver specimen was in circuit

and was supplied with blood under normoxic conditions until the liver was explanted, split, or resected. The only technical difference was that normal resected tissue involved the removal of a specific portion of the liver (usually right hemihepatectomy rather than the whole organ). When liver tissue was obtained from patients undergoing hepatic resection, all the patients had received preoperative chemotherapy. After liver explantation, splitting, or resection, all specimens were placed on ice, immediately transported, and processed within the laboratory. All hepatocyte isolation was carried out within 6 hours of surgical explantation, splitting, or resection. Strict adherence to the procurement and processing protocols ensured that any differences observed between hepatocytes were results of disease or altered physiology and were not explainable by differences in the method of surgical tissue procurement or subsequent processing.

Hepatocytes were isolated from fresh liver wedges (60-156 g) with a 2-step collagenase protocol. Each liver wedge was first perfused with a nonrecirculating wash buffer [10 mM 4-(2-hydroxyethyl)-1-piperazine ethanesulfonic acid (pH 7.2), Sigma, Dorset, United Kingdom] at 37°C with a flow rate of 75 mL/minute in order to remove remaining blood within the liver. After this, the wedge was perfused with a nonrecirculating chelating solution [10 mM 4-(2-hydroxyethyl)-1-piperazine ethanesulfonic acid and 0.5 mM ethylene glycol tetraacetic acid (pH 7.2), Sigma]. This was followed by further perfusion with a nonrecirculating wash buffer to remove any remaining ethylene glycol tetraacetic acid. After this, the tissue was perfused with a recirculating enzymatic dissociation solution (Hank's balanced salt solution, Gibco, Paisley, United Kingdom) with 5 mM calcium chloride (Sigma), 5 mM magnesium chloride (Sigma), 0.5% wt/vol collagenase (Roche, Hertford, United Kingdom), 0.25% wt/vol protease (Sigma), 0.125% wt/vol hyaluronidase (Sigma), and 0.05% wt/vol deoxyribonuclease (Sigma) at 37°C with a flow rate of 75 mL/minute for 1 to 7 minutes. After manual dissociation of the liver wedge, the suspension was passed through a 250-μm nylon mesh and then a 60-μm nylon mesh. The suspension was then washed at 50*g* for 10 minutes at 4°C in a supplemented medium (Dulbecco's modified Eagle's medium, Gibco) with 10% vol/vol heat-inactivated fetal calf serum (Gibco), 2 mM glutamine (Gibco), 20,000 U/L penicillin, and 20 mg/L streptomycin (Gibco). Immediately after the washing, the cell viability was determined by trypan blue dye exclusion. Hepatocytes were plated in a supplemented medium and left for 2 hours. After this period, the medium was changed to Williams' E medium (Sigma) with 2 μg/mL hydrocortisone, 0.124 U/mL insulin, 2 mM glutamine, 20,000 U/L penicillin, and 20 mg/L streptomycin. Cells were cultured for another 2 days before use.

Model of Warm H-R Injury

In experiments, hepatocytes were grown for 2 days at 37°C with 5% CO_2 in Williams' E medium (Sigma) on rat type 1 collagen-coated plates. Hepatocytes were maintained in normoxia, placed into hypoxia for 24 hours, or placed into hypoxia for 24 hours and then reoxygenated for 24 hours. Hypoxia was achieved by the placement of cells in an airtight incubator (RS Mini Galaxy A incubator, Wolf Laboratories, United Kingdom) flushed with 5% CO_2 and 95% N_2 until the oxygen content in the chamber reached 0.1%; this was verified with a dissolved-oxygen monitor (DOH-247-KIT, Omega Engineering, United Kingdom). No previous studies had evaluated the response of primary human hepatocytes to hypoxia and H-R. Therefore, we modified a well-established model of warm in vitro IRI.[22,23] In preliminary experiments, primary human hepatocytes were exposed to 5% or 1% oxygen for 2 or 24 hours, and no increase in ROS accumulation or cell death was noted (data not shown). Therefore, we used 0.1% oxygen in all subsequent experiments for 24 hours. Additionally, Williams' E medium was preincubated in the hypoxic chamber in a sterile container (which allowed gas equilibration) for 8 hours before experiments were carried out; this resulted in a final oxygen concentration of <0.1% as measured with the dissolved-oxygen meter. When it was appropriate, after 24 hours of hypoxia, the medium was aspirated and replaced with a fresh, warmed, oxygenated medium, and the cells were returned to normoxic conditions. This was defined as the beginning of reoxygenation. In experiments involving ROS inhibitors/antioxidants, all reagents were made fresh as stock solutions and were added with the correct dilutional factor to the relevant experimental wells. Specifically, 100 mM *N*-acetylcysteine (NAC; Sigma) was dissolved in molecular-grade water, 1 mM rotenone (Rot; Sigma) was dissolved in chloroform, and 1 mM diphenyliodonium (DPI; Sigma) was dissolved in dimethyl sulfoxide; they were diluted appropriately to produce working concentrations of 20 mM, 2 μM, and 10 μM, respectively. In experiments using inhibitors/antioxidants, solvent-alone controls were used to ensure no vehicle effects. In addition, in experiments using inhibitors/antioxidants, agents were added at the time of placement of the cells into hypoxia or reoxygenation.

Flow Cytometry

ROS production, apoptosis, and necrosis were determined with a 3-color reporter assay system. ROS accumulation was determined with the fluorescent probe 2′,7′-dichlorofluorescin diacetate.[24] This probe is cell-permeable and, once inside a cell, is cleaved by intracellular esterases into 2′,7′-dichlorofluorescin (DCF; Merck, Nottingham, United Kingdom), which is then rendered cell-impermeable. DCF is then able to react with intracellular ROS (specifically hydrogen peroxide) and produce a fluorescent signal detectable on the fluorescein isothiocyanate (FITC) channel. The signal is directly proportional to the level of intracellular ROS present.

Apoptosis was determined via the labeling of cells with annexin V (Molecular Probes, Paisley, United

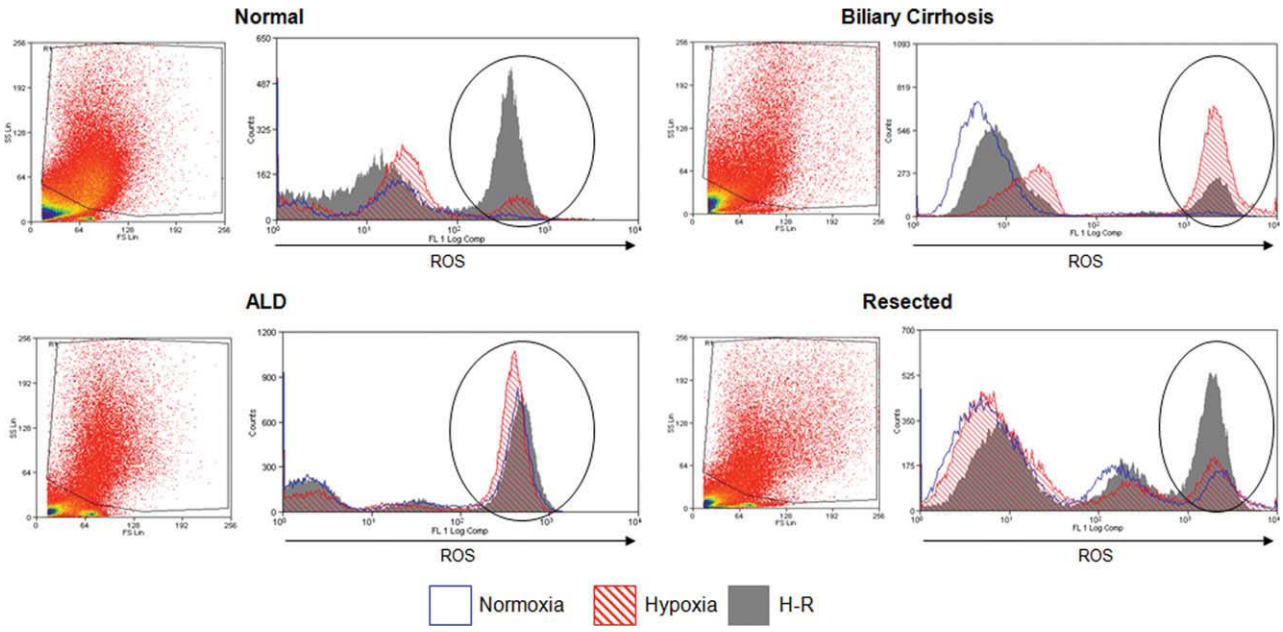

Figure 1. Hypoxia and H-R mediate ROS accumulation in human hepatocytes. Representative flow cytometry plots are shown to illustrate the effects of hypoxia and H-R on ROS accumulation in human hepatocytes isolated from normal liver tissue, diseased liver tissue, and normal resected liver tissue. Vertical ellipses mark the areas of interest within the plots. The area to the left of each ellipse represents cell debris. The reason that the cell debris is included within the plots is that human hepatocytes vary considerably in size; therefore, to include all viable human hepatocytes in the analysis, a large gate was required on the flow cytometer, and this by necessity included the cell debris. The gate is shown on the corresponding representative FS-SS plots located to the left of each flow cytometry plot. The FS-SS plots are from the H-R samples of each preparation, but similar plots were obtained during normoxia and hypoxia (data not shown). Although in the flow cytometry plot of the normal resected liver tissue there are 2 peaks to the left of the ROS peak, these both represent debris; this has been confirmed by 7-AAD staining and their size on the FS-SS plots. The data are representative of 4 normal hepatocyte preparations, 4 biliary disease preparations, 3 ALD preparations, and 9 resected normal liver preparations.

Kingdom), which detects exposed phosphatidylserine on the cell membrane. 7-Aminoactinomycin D (7-AAD; Molecular Probes) is a vital dye that binds to DNA, enters cells only once the cell membrane is disrupted, and is indicative of cellular necrosis. To ensure the consistency of the flow cytometry data, each human hepatocyte preparation was labeled with DCF alone, annexin V alone, and 7-AAD alone to ensure that the cells were labeled and that the flow cytometry data could be compensated for the crossover of fluorophore emission spectra. The same flow cytometry protocol was used for all experiments of the study; this meant that voltages for all markers were constant for all human hepatocyte preparations, so the internal consistency of the experiments was ensured.

After appropriate treatment of the cells, the medium was aspirated and replaced with Hank's balanced salt solution (Gibco) without calcium or magnesium. DCF (30 μM) was added, and the cells were incubated for 20 minutes in the dark at 37°C. Next, the cells were trypsinized and washed extensively in a fluorescence-activated cell sorting buffer [phosphate-buffered saline (pH 7.2) with 10% vol/vol heat-inactivated fetal calf serum, Gibco]. Cells were then labeled with annexin V and 7-AAD for 15 minutes while they were on ice, and samples were immediately subjected to flow cytometry. At least 20,000 events were recorded within the gated region of the flow cytometer for each human hepatocyte cell preparation under each experimental condition. Only the cells within the gated region were used to calculate the mean fluorescence intensity (MFI).

Statistical Analysis

Data analysis was carried out with SPSS software (version 13.0). All values are presented as means and standard errors unless otherwise noted. Statistical analysis was carried out with the Student *t* test.

RESULTS

Variable ROS Responses to Hypoxia and H-R of Human Hepatocytes Isolated From Patients With Different Liver Diseases

Figure 1 and Table 1 show ROS production and accumulation in primary human hepatocytes isolated from normal liver tissue, normal resected liver tissue, and diseased liver tissue. Hepatocytes isolated from normal livers, ALD liver tissue, and normal resected liver tissue showed similar and consistent responses to hypoxia and H-R. Interestingly, normal human hepatocytes had little basal intracellular ROS. However, after

TABLE 1. ROS Accumulation in Human Hepatocytes During Hypoxia and H-R

	Normal	Biliary Cirrhosis	ALD	Resected
Normoxia	30.3 (13.3-53.5)	11.9 (6.2-21.1)	226.5 (217.1-247.1)	352.8 (256.4-450.5)
Hypoxia	121.9 (39.6-166.2)*	255.2 (139.9-444.0)*	259.5 (229.2-281.2)	377.1 (284.3-547.2)
H-R	271.1 (217.7-370.0)*,†	102.6 (35.2-151.0)*	294.7 (278.2-311.1)	506.1 (332.2-874.0)

NOTE: The mean ROS accumulation for human hepatocytes isolated from normal liver tissue, diseased liver tissue, and normal resected liver tissue is shown for each of the 3 experimental conditions. Data are expressed as MFIs. Numbers in parentheses are the ranges of MFI readings for each experimental condition. The MFI values have been derived from the cells within the ellipses shown in Fig. 1. The data are representative of 4 normal hepatocyte preparations, 4 biliary disease preparations, 3 ALD preparations, and 9 normal resected liver preparations.
*$P < 0.05$ versus normoxia.
†$P < 0.05$ versus hypoxia.

exposure to hypoxia and H-R, normal human hepatocytes had significantly increased intracellular ROS accumulation. Hepatocytes isolated from ALD liver tissue and normal resected liver tissue showed similar responses with respect to ROS accumulation during hypoxia and H-R but had greater basal intracellular ROS contents; this possibly reflected their continual exposure to an inflammatory microenvironment.[25] Hepatocytes isolated from the tissue of patients with the biliary diseases, primary biliary cirrhosis and primary sclerosing cholangitis, had very low basal levels of ROS production similar to those detected in hepatocytes from normal livers, but they showed a 22-fold increase in ROS production during hypoxia and a reduction in ROS accumulation during H-R. This may be a reflection of increased engagement of hepatocyte cytosolic antioxidant defenses, which is possibly a result of cholestasis, a common feature of these diseases.

ROS Activation Mediated Hepatocyte Apoptosis and Necrosis

We next assessed the effects of hypoxia and H-R on human hepatocyte cell death. Previous in vitro studies have shown that human hepatoma cell lines[26] and murine[27] and rodent hepatocytes[28] undergo cell death during hypoxia and H-R. We have found that human hepatocytes isolated from normal liver tissue and diseased liver tissue experience increased apoptosis and necrosis during hypoxia and H-R (Fig. 2A,B). The level of human hepatocyte apoptosis and necrosis during hypoxia and H-R mirrored the level of intracellular ROS production within the particular type of hepatocyte. The decrease in ROS production observed in hepatocytes isolated from the tissue of patients with biliary diseases was accompanied by a concomitant decrease in apoptosis and necrosis; this confirmed the association of ROS with apoptotic and necrotic cell death. The highest levels of ROS were seen in hepatocytes isolated from normal resected liver tissue. Despite the increase in intracellular ROS in normal hepatocytes isolated from resected liver tissue, the level of apoptosis or necrosis did not increase; this suggested an important difference in the metabolic activity or protective mechanisms of these cells. Moreover, hepatocytes from normal resected tissue did have higher basal levels of both apoptosis and necrosis.

Effect of ROS Inhibitors on ROS Accumulation

Antioxidants and inhibitors of ROS generation have been shown to abrogate human hepatoma cell line death during hypoxia.[26] Figure 3 shows the effects of antioxidants, mitochondrial chain inhibitors, and NADPH oxidase inhibitors on primary human hepatocyte ROS production during H-R. Similar results were observed during normoxia and hypoxia (data not shown). NAC acts as a glutathione precursor; it enters cells and interacts with and detoxifies free radicals by nonenzymatic reactions. It is deacetylated to form cysteine, which supports the biosynthesis of glutathione, one of the most important components of the intracellular antioxidant system.[29] NAC almost completely inhibited ROS production in all hepatocytes during H-R. Rot, a mitochondrial complex I inhibitor, was also able to inhibit ROS production in hepatocytes isolated from all sources, and this confirmed mitochondria as a major source of endogenous ROS in human hepatocytes. The inhibition of ROS by Rot was substantial but not as great as that observed with NAC. The production of ROS in the presence of mitochondrial inhibition implies the involvement of other mechanisms in human hepatocytes. Accordingly, we found that the flavoenzyme NADPH oxidase was also involved in ROS production within the hepatocyte. The specific NADPH oxidase inhibitor DPI significantly decreased ROS production in all human hepatocytes. Thus, although the overall effect was not as great as that of Rot, NADPH oxidase is also an important source of ROS in human hepatocytes. In all cases, vehicle controls caused no inhibition of intracellular hepatocyte ROS levels (data not shown).

Effects of ROS Inhibitors on Human Hepatocyte Apoptosis and Necrosis

Because NAC, Rot, and DPI all inhibited ROS, we assessed whether this decrease in ROS affected

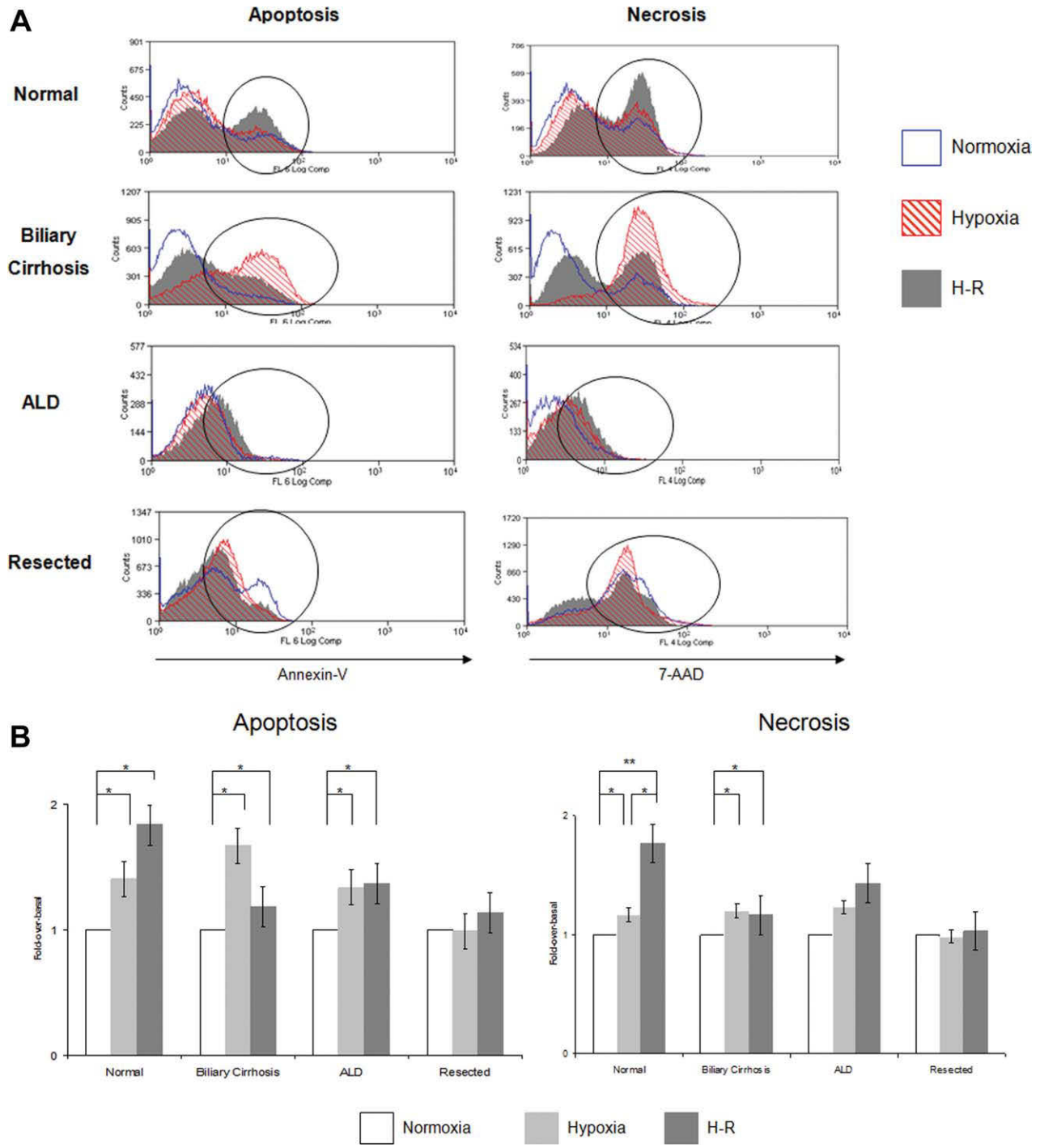

Figure 2. Hypoxia and H-R induce human hepatocyte apoptosis and necrosis. (A) Representative flow cytometry plots are shown to illustrate the effects of hypoxia and H-R on the apoptosis and necrosis of human hepatocytes isolated from normal liver tissue, diseased liver tissue, and normal resected liver tissue. The areas of interest within the plots are marked by vertical ellipses. Just as in the ROS plots shown in Fig. 1, the area to the left of each vertical ellipse represents cell debris. The data are representative of 4 normal hepatocyte preparations, 4 biliary disease preparations, 3 ALD preparations, and 9 normal resected liver preparations. (B) The bar charts show pooled data illustrating the level of apoptosis and necrosis in human hepatocytes isolated from normal tissue, diseased tissue, and normal resected tissue during hypoxia and H-R. The data are shown as fold over the basal level. The levels of apoptosis and necrosis occurring during normoxia have been taken as the basal levels. The data are expressed as means and standard errors. The data are representative of 4 normal hepatocyte preparations, 4 biliary disease preparations, 3 ALD preparations, and 9 normal resected liver preparations. *$P < 0.05$; **$P < 0.05$.

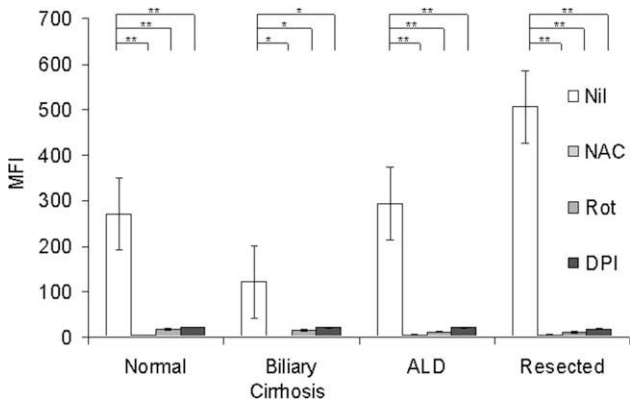

Figure 3. Antioxidants, mitochondrial chain inhibitors, and NADPH oxidase inhibitors reduce human hepatocyte ROS production during H-R. Human hepatocytes isolated from normal livers, diseased livers, and normal resected livers were treated with 20 mM NAC, 2 μM Rot, or 10 μM DPI during H-R. ROS accumulation was determined by flow cytometry as described in the Materials and Methods section. ROS production data are shown as MFIs and are based on the MFI readings taken from cells within the ellipse region shown in Fig. 1. The data are expressed as means and standard errors. The data are representative of 3 normal hepatocyte preparations, 3 biliary disease preparations, 3 ALD preparations, and 5 normal resected liver preparations. *$P < 0.01$; **$P < 0.01$.

human hepatocyte apoptosis and necrosis. Data for H-R are shown in Fig. 4; similar results were observed during normoxia and hypoxia (data not shown). The reduction in endogenous ROS levels in human hepatocytes treated with the various inhibitors led to significantly decreased hepatocyte apoptosis (Fig. 4A) and necrosis (Fig. 4B). In line with the more potent effect of NAC on ROS inhibition, the effects of NAC were the greatest. Rot and DPI also decreased apoptosis and necrosis during H-R. Moreover, ROS inhibition abrogated apoptosis in human hepatocytes isolated from tissue taken from patients with different types of hepatic diseases but only partially inhibited hepatocyte necrosis. These data provide clear evidence that endogenous ROS production by mitochondria and NADPH oxidase drives human hepatocyte apoptosis and necrosis during H-R.

DISCUSSION

Although hypoxia is a feature of hepatic IRI associated with hepatic surgery, it may also occur during chronic liver inflammation or infection. Therefore, by defining the effects of hypoxia on liver physiology, we can obtain important information regarding the development of future therapeutics.

Hepatocytes have conventionally been considered relatively insensitive to IRI because of their extensive antioxidant defense mechanisms and their existence within the comparatively hypoxic hepatic environment.[30] However, numerous in vitro and in vivo studies have reported deleterious effects of IRI on hepatocytes, although the effects of hypoxia and H-R on human hepatocytes are unknown. Our data reveal that hepatocytes are susceptible to apoptosis and necrosis induced in response to hypoxia and H-R, and we report for the first time that human hepatocytes isolated from patients with different hepatic diseases show variable responses to hypoxia and H-R.

Hypoxia is known to cause dysfunction of the mitochondrial electron transport chain and thus lead to an increase in ROS; this is accentuated by reoxygenation and can result in cell death.[31] Hepatocytes isolated from normal donor livers, ALD livers, and uninvolved livers from hepatic resections exhibit this classic response to hypoxia and H-R. Interestingly, hepatocytes isolated from ALD livers and resected liver tissue have high basal levels of ROS production, and these are then augmented by hypoxia and H-R; however, normal hepatocytes and hepatocytes isolated from the livers of patients with biliary cirrhosis show very little basal ROS production. These differences are likely due to the particular inflammatory microenvironment and milieu to which each hepatocyte population has been exposed. For example, many mediators found in ALD patients are known to increase ROS,[25] and hepatocytes isolated from hepatic resections will have been exposed to chemotherapy, a treatment known to increase intracellular ROS.[32] Hepatocytes isolated from patients with biliary cirrhosis had lower levels of ROS during H-R, and this possibly reflected the up-regulation of the antioxidant defenses in these particular cells. The differential responses of hepatocytes isolated from patients with different hepatic diseases are unlikely to be attributable to the method of isolation because the liver tissues were procured and processed according to an identical and stringent protocol. The precise cellular mechanisms underlying hepatocyte responses to hypoxia and H-R remain the subject of ongoing research within our laboratory.

It has been suggested previously that hepatocytes are bystanders in IRI and are targeted by the inflammatory process.[2] We now propose that they have the capacity to actively participate in it primarily through the production of ROS. The functional relevance of ROS is emphasized by our finding that increased levels of endogenous ROS are clearly linked to hepatocyte apoptosis and necrosis. This has particular relevance for liver diseases in which hepatocytes are exposed to relative hypoxia and may be responsible for perpetuating injury. We have demonstrated that ROS can directly activate apoptosis and necrosis and thereby support the suggestion of Jaeschke and Lemasters[20] that common pathways may at least in part regulate both processes. Moreover, ROS derived from mitochondria and cytosolic NADPH oxidase are crucial for regulating both apoptosis and necrosis, and their inhibition significantly improves human hepatocyte viability during hypoxia and H-R. The final mode of cell death is likely to be dictated by the intracellular adenosine triphosphate content.[33] Interestingly, ROS inhibition had a greater effect on reducing human hepatocyte apoptosis and only partially inhibited hepatocyte necrosis. Although ROS does contribute to human hepatocyte necrosis, it is likely that a

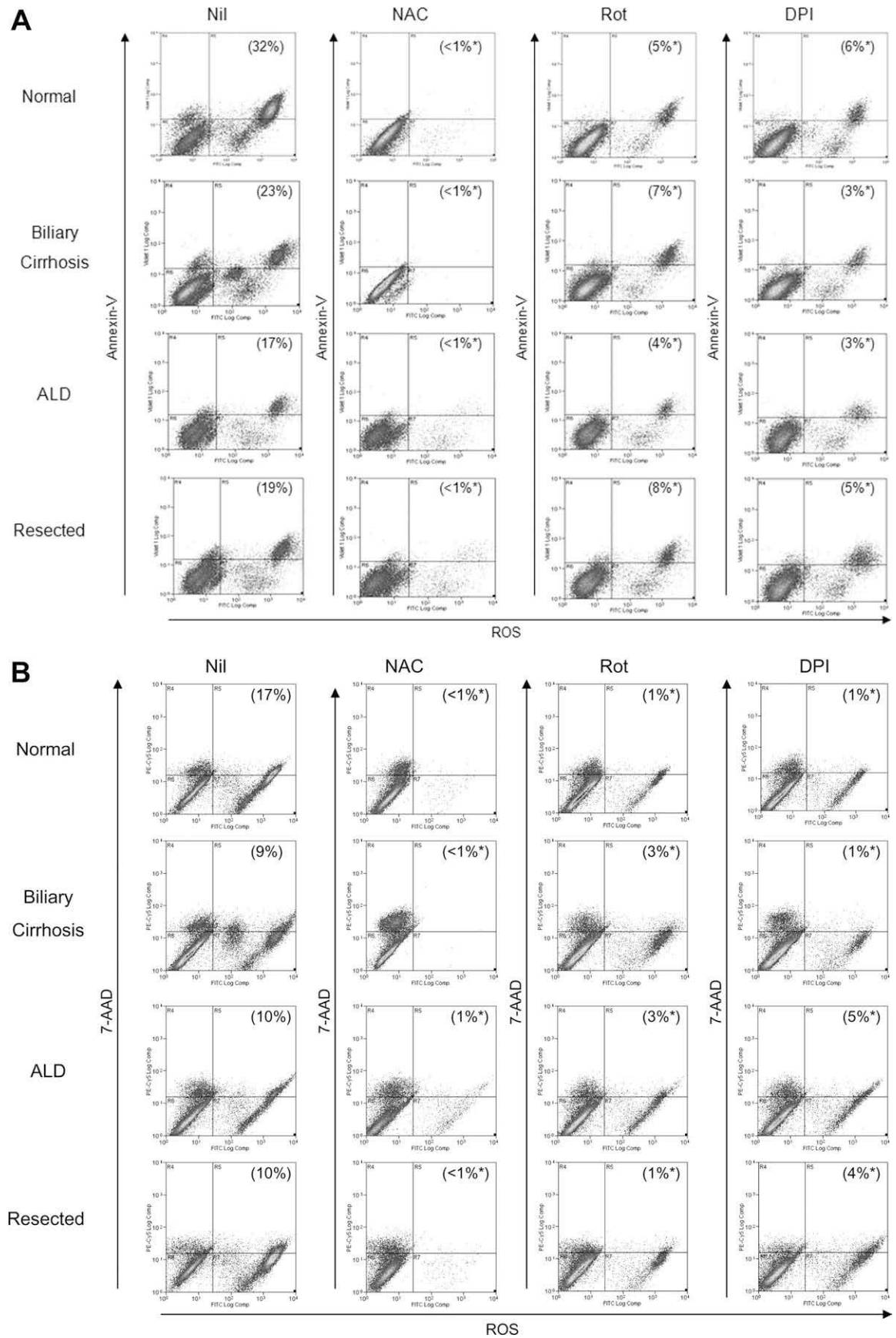
A
Nil
NAC
Rot
DPI
Normal
Biliary Cirrhosis
ALD
Resected
Annexin-V
ROS
(32%)
(<1%*)
(5%*)
(6%*)
(23%)
(<1%*)
(7%*)
(3%*)
(17%)
(<1%*)
(4%*)
(3%*)
(19%)
(<1%*)
(8%*)
(5%*)
B
Nil
NAC
Rot
DPI
Normal
Biliary Cirrhosis
ALD
Resected
7-AAD
ROS
(17%)
(<1%*)
(1%*)
(1%*)
(9%)
(<1%*)
(3%*)
(1%*)
(10%)
(1%*)
(3%*)
(5%*)
(10%)
(<1%*)
(1%*)
(4%*)

Figure 4.

number of factors, including calcium overload, calpain activation, and lysosome rupture, force the cell to undergo necrosis.[34] In contrast, Wang et al.[35] demonstrated that ROS derived from mitochondria directly activated apoptosis in Chang human hepatocytes. Accordingly, the inhibition of ROS and, in particular, mitochondrial ROS had a greater effect on reducing hepatocyte apoptosis. As previously noted, hepatocytes undergoing necrosis will release intracellular ROS into the liver parenchyma and induce both hepatocyte and endothelial cell activation.[36] Therefore, our observations have implications not only for hepatic IRI but also for liver diseases in which chronic hypoxia leads to continued ROS production and ongoing liver damage. In separate experiments, we exposed human hepatic sinusoidal endothelial cells (HSECs) to the same in vitro model of warm IRI. HSECs did not increase intracellular ROS during hypoxia and H-R and did not undergo any significant level of cell death during hypoxia and H-R (R.H.B., unpublished data, 2010). These observations show that liver epithelial and endothelial cells have different responses to hypoxia and H-R, and these differences are likely to shape the hepatic inflammatory microenvironment. On the basis of our data, we speculate that in warm IRI, hepatocyte ROS (not HSEC-derived ROS) may be important regulators of hepatic injury. The precise role of HSECs during warm IRI is beyond the scope of this particular study.

In rat livers, treatment with antioxidants can prevent IRI.[37] In limited human studies, ischemia has induced the expression of ROS scavengers within the liver.[38] Despite the presence of induced antioxidant mechanisms, human hepatocytes isolated from normal livers, the livers of patients with ALD, and the livers of patients with biliary cirrhosis do not appear to be protected against cell death during hypoxia and H-R. Hepatocytes isolated from normal resected liver tissue were, however, surprisingly resistant to ROS-mediated apoptosis and necrosis. This finding has important implications for research involving human hepatocytes and suggests that studies should be interpreted in the context of the hepatocyte source; hepatocytes isolated from resected hepatic tissues of patients with liver tumors are likely to respond differently to physiological stress. As mentioned earlier, the reason for this difference remains unknown. Furthermore, which hepatocyte response reflects the true physiological response remains to be determined. In separate experiments, NAC, Rot, and DPI were used to treat HepG2, Huh7, and PLC/PRF/5 human hepatoma cell lines during hypoxia and H-R. These inhibitors induced overwhelming cell death in these particular cell lines, and this indicated vastly different responses to hypoxia and H-R in comparison with primary hepatocytes (data not shown). Therefore, although previous studies have shown cytoprotective effects of antioxidants and ROS inhibitors, we report here for the first time that the inhibition of mitochondrial and NADPH oxidase–derived ROS reduces primary human hepatocyte apoptosis and necrosis.

A single strategy aimed at the amelioration of the harmful effects produced by IRI has not yet been adopted into general clinical practice. Experimental interventions to reduce ROS have shown potential for minimizing liver injury in various models. ROS scavengers,[39] thioredoxin mimetics,[40] and the delivery of antioxidant genes[41] have been shown to partially suppress the effects of IRI. However, the clinical application of such compounds has been limited for toxicological and technical reasons. NAC, however, has clinical potential because it is known to be well tolerated at doses that should be clinically effective. Indeed, NAC is used clinically in several settings; for example, it is used as a hepatoprotective agent for acute liver failure and acetaminophen toxicity. Furthermore, although NAC administration has been shown to improve hepatic microcirculation and bile flow after hepatic IRI,[7] we now show that NAC can also reduce all ROS production in human hepatocytes with a concomitant decrease in apoptosis and necrosis during normoxia, hypoxia, and H-R. Recent studies have suggested that pleiotropic compounds are required to treat IRI because of the diverse nature of the problem.[42] We suggest that exogenous NAC could be a straightforward, practical, and beneficial strategy for ameliorating human hepatocyte cell death during IRI. Indeed, a recent randomized study showed that the systemic infusion of NAC before liver procurement reduced graft dysfunction and early graft loss after liver transplantation.[43]

Although some authors have challenged the pathophysiological relevance of intracellular oxidant stress during reperfusion,[44] we have clearly shown that hepatocyte ROS generated by mitochondria and NADPH oxidase can lead directly to significant hepatocyte cell death; we suggest that although other sources of ROS, such as neutrophils and KCs, are capable of contributing to tissue ROS accumulation in IRI, they may not be the only pathways leading to ROS-

Figure 4. (A) ROS accumulation in human hepatocytes during H-R mediates apoptosis. Human hepatocytes isolated from normal tissue, diseased tissue, and normal resected tissue were treated with 20 mM NAC, 2 μM Rot, or 10 μM DPI during H-R, and the percentages of cells that were stained with both the ROS probe DCF and the apoptotic marker annexin V were assessed by flow cytometry. The cross-plots show ROS on the *x* axis and apoptosis on the *y* axis. The percentages of human hepatocytes that were stained with both DCF and annexin V are shown in parentheses. The data are representative of 3 normal hepatocyte preparations, 3 biliary disease preparations, 3 ALD preparations, and 5 normal resected liver preparations. $^*P < 0.001$. (B) ROS accumulation in human hepatocytes during H-R mediates necrosis. Human hepatocytes isolated from normal tissue, diseased tissue, and normal resected tissue were treated with 20 mM NAC, 2 μM Rot, or 10 μM DPI during H-R, and the percentages of cells that were stained with both the ROS probe DCF and the necrotic marker 7-AAD were assessed by flow cytometry. The cross-plots show ROS on the *x* axis and necrosis on the *y* axis. The percentages of human hepatocytes that were stained with both DCF and 7-AAD are shown in parentheses. The data are representative of 3 normal hepatocyte preparations, 3 biliary disease preparations, 3 ALD preparations, and 5 normal resected liver preparations. $^*P < 0.01$.

mediated hepatocyte damage. An important caveat to our data is that oxidative stress in human hepatocytes after hypoxia and H-R may differ between hypoxia at 4°C and hypoxia at 37°C.[45] Therefore, although these data can be applied to the transplant setting, they are not wholly reflective of the in vivo situation.

In summary, our data show that human hepatocyte responses to hypoxia and H-R are determined by their particular microenvironment. Both apoptosis and necrosis are regulated by endogenous human hepatocyte ROS, and inhibitors of ROS generation significantly improve hepatocyte viability by reducing ROS generation. The use of NAC offers an opportunity to modulate hepatic IRI and improve patient outcomes after OLT, possibly through its addition to preservation fluids. In addition, our studies demonstrate for the first time that hepatocytes taken from normal tissue, normal resected tissue, and diseased tissue may vary considerably in their functional and metabolic responses to hypoxic stress.

ACKNOWLEDGMENTS

RHB is in receipt of a Wellcome Trust Training Fellowship (DDDP.RCHX14183). The authors would like to thank the clinical team at the Queen Elizabeth Hospital, Birmingham for the procurement of liver tissue.

REFERENCES

1. Toledo-Pereyra LH, Simmons RL, Najarian JS. Protection of the ischemic liver by donor pre-treatment before transplantation. Am J Surg 1975;129:513-517.
2. Massip-Salcedo M, Rosello-Catafau J, Prieto J, Avila MA, Peralta C. The response of the hepatocyte to ischemia. Liver Int 2007;27:6-17.
3. Vardanian AJ, Busuttil RW, Kupiec-Weglinski JW. Molecular mediators of liver ischemia and reperfusion injury: a brief review. Mol Med 2008;14:337-345.
4. Fondevila C, Busuttil RW, Kupiec-Weglinski JW. Hepatic ischemia/reperfusion injury—a fresh look. Exp Mol Pathol 2003;74:86-93.
5. Jaeschke H, Farhood A. Neutrophil and Kupffer cell-induced oxidant stress and ischemia-reperfusion injury in the rat liver. Am J Physiol 1991;260(pt 1):G355-G362.
6. Jaeschke H. Molecular mechanisms of hepatic ischemia-reperfusion injury and preconditioning. Am J Physiol Gastrointest Liver Physiol 2003;284:G15-G26.
7. Zhang W, Wang M, Xie HY, Zhou L, Meng XQ, Shi J, et al. Role of reactive oxygen species in mediating hepatic ischemia-reperfusion injury and its therapeutic applications in liver transplantation. Transplant Proc 2007;39:1332-1337.
8. Decker K. Biologically active products of stimulated liver macrophages (Kupffer cells). Eur J Biochem 1990;192:245-261.
9. Jaeschke H. Reperfusion injury after warm ischemia or cold storage of the liver: role of apoptotic cell death. Transplant Proc 2002;34:2656-2658.
10. Taniai H, Hines IN, Bharwani S, Maloney RE, Nimura Y, Gao B, et al. Susceptibility of murine periportal hepatocytes to hypoxia-reoxygenation: role for NO and Kupffer cell-derived oxidants. Hepatology 2004;39:1544-1552.
11. Imamura H, Sutto F, Brault A, Huet PM. Role of Kupffer cells in cold ischemia/reperfusion injury of rat liver. Gastroenterology 1995;109:189-197.
12. Adkinson D, Hollwarth ME, Beniot JN, Parks DA, McCord JM, Granger DN. Role of free radicals in ischemia-reperfusion injury to the liver. Acta Physiol Scand Suppl 1986;548:101-107.
13. Jaeschke H, Mitchell JR. Mitochondria and xanthine oxidase both generate reactive oxygen species in isolated perfused rat liver after hypoxic injury. Biochem Biophys Res Commun 1989;160:140-147.
14. Lluis JM, Buricchi F, Chiarugi P, Morales A, Fernandez-Checa JC. Dual role of mitochondrial reactive oxygen species in hypoxia signalling: activation of nuclear factor-kB via c-SRC- and oxidant dependent cell death. Cancer Res 2007;67:7368-7377.
15. Caraceni P, Ryu HS, van Thiel DH, Borle AB. Source of oxygen free radicals produced by rat hepatocytes during postanoxic reoxygenation. Biochim Biophys Acta 1995;1268:249-254.
16. Young TA, Cunningham CC, Bailey SM. Reactive oxygen species production by the mitochondrial respiratory chain in isolated rat hepatocytes and liver mitochondria: studies using myxothiazol. Arch Biochem Biophys 2002;405:65-72.
17. Schulze-Bergkamen H, Schuchmann M, Fleischer B, Galle PR. The role of apoptosis versus oncotic necrosis in liver injury: facts or faith? J Hepatol 2006;44:984-993.
18. Sasaki H, Matsuno T, Tanaka N, Orita K. Activation of apoptosis during the perfusion phase after rat liver ischemia. Transplant Proc 1996;28:1980-1989.
19. Smith MK, Rosser BG, Mooney DJ. Hypoxia leads to necrotic hepatocyte death. J Biomed Mater Res A 2007;80:520-529.
20. Jaeschke H, Lemasters JJ. Apoptosis versus oncotic necrosis in hepatic ischemia/reperfusion injury. Gastroenterology 2003;125:1246-1257.
21. Gonzalez R, Collado JA, Nell S, Briceno J, Tamayo MJ, Fraga E, et al. Cytoprotection properties of alpha-tocopherol are related to gene regulation in cultured D-galactosamine-treated human hepatocytes. Free Radic Biol Med 2007;43:1439-1452.
22. Cao L, Li Y, Cheng F, Li S, Long D. Hypoxia/reoxygenation up-regulated the expression of death receptor 5 and enhanced apoptosis in human hepatocyte line. Transplant Proc 2006;38:2207-2209.
23. Anderson CD, Belous A, Pierce J, Nicoud IB, Knox C, Wakata A, et al. Mitochondrial calcium uptake regulates cold preservation-induced Bax translocation and early reperfusion apoptosis. Am J Transplant 2004;4:352-362.
24. Schroedl C, McClintock DS, Budinger GRS, Chandel NS. Hypoxic but not anoxic stabilization of HIF-1α requires mitochondrial reactive oxygen species. Am J Physiol Lung Cell Mol Physiol 2002;283:L922-L931.
25. Conde de la Rosa L, Moshage H, Nieto N. Hepatocyte oxidant stress and alcoholic liver disease. Rev Esp Enferm Dig 2008;100:156-163.
26. Lluis JM, Morales A, Blasco C, Colell A, Mari M, Garcia-Ruiz C, et al. Critical role of mitochondrial glutathione in the survival of hepatocytes during hypoxia. J Biol Chem 2005;280:3224-3232.
27. Haga S, Terui K, Fukai M, Oikawa Y, Irani K, Furukawa H, et al. Preventing hypoxia/reoxygenation damage to hepatocytes by p66shc ablation: up-regulation of anti-oxidant and anti-oxidant proteins. J Hepatol 2008;48:422-432.
28. Crenesse D, Schmid-Alliana A, Laurens M, Cursio R, Gugenheim J. JNK1/SAPK1 involvement in hypoxia-reoxygenation-induced apoptosis in rat hepatocytes. Transplant Proc 2001;33:260-261.
29. Cotgreave IA. N-Acetylcysteine: pharmacological considerations and experimental and clinical applications. Adv Pharmacol 1997;38:205-227.

30. Gonzalez-Flecha B, Cutrin JC, Boveris A. Time course and mechanism of oxidative stress and tissue damage in rat liver subjected to in vivo ischemia-reperfusion. J Clin Invest 1993;91:456-464.
31. Jaeshcke H, Gores GJ, Cederbaum AI, Hinson JA, Pessayre D, Lemasters JJ. Mechanisms of hepatotoxicity. Toxicol Sci 2002;65:166-176.
32. Block KI, Koch AC, Mead MN, Tothy PK, Newman RA, Gyllenhaal C. Impact of antioxidant supplementation on chemotherapeutic efficacy: a systematic review of the evidence from randomised controlled trials. Cancer Treat Rev 2007;33:407-418.
33. Rosser BG, Gores GJ. Liver cell necrosis: cellular mechanisms and clinical implications. Gastroenterology 1995; 108:252-275.
34. Golstein P, Kroemer G. Cell death by necrosis: towards a molecular definition. Trends Biochem Sci 2007;32: 37-43.
35. Wang Y, Xu Y, Wang H, Xue P, Li X, Li B, et al. Arsenic induces mitochondria-dependent apoptosis by reactive oxygen species generation rather than glutathione depletion in Chang human hepatocytes. Arch Toxicol 2009; 83:899-908.
36. Motoyama S, Minamiya Y, Saito S, Saito R, Matsuzaki I, Abo S, et al. Hydrogen peroxide derived from hepatocytes induces sinusoidal cell apoptosis in perfused hypoxic rat liver. Gastroenterology 1998;114:153-163.
37. Bilzer M, Jaeschke H, Vollmar AM, Paumgartner G, Gerbes AL. Prevention of Kupffer cell-induced oxidant injury in rat liver by atrial natriuretic peptide. Am J Physiol 1999;276(pt 1):G1137-G1144.
38. Conti A, Scala S, D'Agostino P, Alimenti E, Morelli D, Andria B, et al. Wide gene expression profiling of ischemia-reperfusion injury in human liver transplantation. Liver Transpl 2007;13:99-113.
39. Yuzawa H, Fujioka H, Mizoe A, Azuma T, Furui J, Nishikawa M, et al. Inhibitory effects of safe and novel SOD derivatives, galactosylated-SOD, on hepatic warm ischemia/reperfusion injury in pigs. Hepatogastroenterology 2005;52:839-843.
40. Sener G, Sehrili O, Ercan F, Sirvanci S, Gedil N, Kacmaz A. Protective effect of MENSA (2-mercaptoethane sulfonate) against hepatic ischemia/reperfusion injury in rats. Surg Today 2005;357:575-580.
41. He SQ, Zhang YH, Venugopal SK, Dicus CW, Perez RV, Ramsamooj R, et al. Delivery of antioxidative enzyme genes protects against ischemia/reperfusion induced injury in mice. Liver Transpl 2006;12: 1869-1879.
42. Menger MD, Vollmar B. Pathomechanisms of ischemia-reperfusion injury as the basis for novel preventive strategies: is it time for the introduction of pleiotropic compounds? Transplant Proc 2007;39:485-488.
43. D'Amico F, Vitale A, Bassi D, Bonsignore P, Scopelliti M, Boetto D, et al. Use of N-acetylcysteine during liver procurement: final report of a prospective randomized controlled study. Liver Transpl 2010; 16(6):S71.
44. Grattaglino I, Vendemiale G, Lauterburg BH. Reperfusion injury of the liver: role of mitochondria and protection by glutathione ester. J Surg Res 1999;86:2-8.
45. Mochida S, Arai M, Ohno A, Masaki N, Ogata I, Fujiwara K. Oxidative stress in hepatocytes and stimulatory state of Kupffer cells after reperfusion differ between warm and cold ischemia in rats. Liver 1994;14:234-240.

Appendix II

FEBS Letters 585 (2011) 935–941

journal homepage: www.FEBSLetters.org

Variable responses of small and large human hepatocytes to hypoxia and hypoxia/reoxygenation (H–R)

Ricky H. Bhogal *, Christopher J. Weston, Stuart M. Curbishley, Anand N. Bhatt, David H. Adams, Simon C. Afford

Centre for Liver Research, School of Infection and Immunity, Institute of Biomedical Research, The Medical School, The University of Birmingham, Edgbaston, Birmingham B15 2TT, UK

ARTICLE INFO

Article history:
Received 15 February 2011
Accepted 21 February 2011
Available online 25 February 2011

Edited by Veli-Pekka Lehto

Keywords:
Human hepatocytes
Reactive oxygen species
Apoptosis
Necrosis
Hypoxia
Liver injury

ABSTRACT

Hypoxia and hypoxia–reoxygenation (H–R) regulate human hepatocyte cell death by mediating the accumulation of reactive oxygen species (ROS). Hepatocytes within the liver are organised into peri-portal (PP) and peri-venous (PV) subpopulations. PP and PV hepatocytes differ in size and function. We investigated whether PP and PV human hepatocytes exhibit differential susceptibility to hypoxic stress. Isolated hepatocytes were used in an in vitro model of hypoxia and H–R. ROS production and cell death were assessed using flow cytometry. PV, and not PP hepatocytes, accumulate intracellular ROS in a mitochondrial dependent manner during hypoxia and H–R. This increased ROS regulates hepatocyte apoptosis and necrosis via a mitochondrial pathway. These findings have implications on the understanding of liver injury and application of potential therapeutic strategies.

1. Introduction

The functional unit of the liver is the acinus, which extends from the portal venule along the sinusoids to the terminal hepatic venule. The liver acinus in rodents extends for approximately 20 hepatocytes [1]. Peri-portal (PP) hepatocytes (zone 1) which are near the portal venule tend to be of a smaller size than peri-venous (PV) hepatocytes (zone 3) which are located near the terminal hepatic vein [2]. Indeed, some studies define and isolate PP and PV hepatocyte populations upon the basis of size [3]. Furthermore, these studies have utilised the technique of fluorescent-activated cell sorting (FACs) to consistently differentiate between PV and PP hepatocytes and study their metabolic function [4–6]. Moreover, these studies have demonstrated that these hepatocytes have distinct and separate cellular functions [3,7].

There is a large body of evidence to support the concept of morphological, biochemical and metabolic heterogeneity of small/PP and large/PV hepatocytes [7–10]. Indeed, various functions have been ascribed to specific zones of the liver acinus. Specifically, oxidative metabolism, gluconeogenesis, urea synthesis and bile formation are predominantly small/PP hepatocyte activities whereas glutamine synthesis, xenobiotic metabolism and ketogenesis are predominant functions of the large/PV hepatocytes [11,12]. Moreover, studies have shown these differences in hepatocyte function are attributable to differences in the enzyme expression [7,10].

These differences in hepatocyte function are also likely to be important determinants in the evolution of liver injury. For instance, in rodent models, it is well documented that following ischaemic liver injury, hepatocyte cell death is predominantly observed around the peri-venular region where the PV hepatocytes are located [13]. The ischaemic injury, within the liver, is regulated by the accumulation of intracellular reactive oxygen species (ROS) [14]. However, whether small/PP and large/PV hepatocytes have differential ROS accumulation during hypoxia and H–R is not known. In particular, whether small/PP or large/PV human hepatocytes exhibit differential responses to hypoxia and H–R remains to be ascertained.

Previous studies have utilised various techniques to investigate the different functions of small/PP and large/PV hepatocytes. These include retrograde digitonin perfusion of livers [8] and elutriation [7]. However, FACS analysis allows discrimination between hepatocyte subpopulations on the basis of size. Previous studies have consistently shown that the PV hepatocytes are larger in size than the PP hepatocytes [4–6]. Thus we used this latter approach to investigate whether PP or small and PV or large human hepatocytes exhibit differential responses to hypoxia and hypoxia–reoxygenation (H–R). Specifically, we investigated whether small/PP and large/PV human hepatocytes exhibit differential levels of ROS

* Corresponding author. Fax: +44 (0) 121 415 8698.
E-mail address: balsin@hotmail.com (R.H. Bhogal).

0014-5793/$36.00
doi:10.1016/j.febslet.2011.02.030

accumulation during hypoxia and H–R and whether this had an impact upon apoptosis and necrosis.

2. Materials and methods

2.1. Human hepatocyte isolation

Liver tissue was obtained from fully consenting patients undergoing transplantation, hepatic resection for benign liver disease or normal donor tissue surplus to surgical requirements. Liver tissue was obtained from surgical procedures carried out at the Queen Elizabeth Hospital, Birmingham, UK. Ethical approval for the study was granted by the Local Research Ethics Committee (LREC) (reference number 06/Q702/61). Human hepatocytes were isolated using a method that we have described previously [14]. Hepatocytes were isolated from fresh liver wedges weighing between 60 and 156 g using a two-step collagenase protocol. Liver wedges were first perfused with non-recirculating wash buffer (10 mM HEPES pH 7.2) (Sigma, Dorset, UK) at 37 °C using a flow rate of 75 mL/min in order to remove the remaining blood within the liver. After this, the wedge was perfused with a chelating solution (non-recirculating) (10 mM HEPES, 0.5 mM EGTA, pH 7.2) (Sigma). This was followed by further perfusion with [non-recirculating] wash buffer to remove any remaining EGTA. Following this the tissue was perfused with recirculating enzymatic dissociation solution (Hank's Balanced Salt Solution (HBSS) (Gibco, Paisley, UK) with calcium chloride (5 mM) (Sigma), magnesium chloride (5 mM) (Sigma), 0.5% w/v collagenase (Roche, Hertford, UK), 0.25% w/v protease (Sigma), 0.125% w/v hyaluronidase (Sigma) and 0.05% w/v DNase (Sigma)) at 37 °C using a flow rate 75 mL/min for between 1 and 7 min. Following manual dissociation of the liver wedge the suspension was passed through a nylon mesh of 250 μm followed by a nylon mesh of 60 μm. Suspensions were then washed at 50×g for 10 min at 4 °C in supplemented media (Dulbecco's Modified Eagle Medium (DMEM) (Gibco) with 10% v/v heat inactivated foetal calf serum (Gibco), 2 mM glutamine (Gibco), 20,000 units/L penicillin and 20 mg/L streptomycin (Gibco)). Immediately after washing cell viability was determined by trypan blue dye exclusion. Hepatocytes were plated out in supplemented media and left for 2 h. After this period, the media were changed to Williams E media (Sigma) containing hydrocortisone (2 μg/ml), insulin (0.124 U/ml), glutamine (2 mM), penicillin (20,000 units/L) and streptomycin (20 mg/L). Cells were cultured for further 2 days prior to use. Only viable cells are able to adhere to rat type 1 collagen-coated plates and hence all cells were viable at the commencement of the experiments.

Enzyme-linked immunosorbent assay (ELISA) of human hepatocytes and human hepatic sinusoidal endothelial cells (HSEC) for Cytokeratin 18, Cytokeratin 19 and CD31were performed.

Cells (hepatocytes or HSEC) were plated on rat type 1 collagen-coated 96-well flat-bottomed plates for 24 h following isolation. Cells were then fixed in ice cold methanol for 5 min. Non-specific binding of mAb was inhibited by pre-incubation of cells for 1 h at 37 °C with 4% goat serum (Sigma) before the addition of mouse anti-human mAb (IgG Isotype-matched control (Invitrogen) CD31 (Dako), cytokeratin 19 (Dako), cytokeratin 18 (Invitrogen) for 1 h at 37 °C. The cells were then washed thoroughly before incubation with peroxidase-conjugated goat anti-mouse secondary Ab (Dako). The enzyme-linked immunosorbent assay (ELISA) was developed using *O*-phenylenediamine substrate (OPD, Dako) according to the manufacturer's instructions and the enzymatic reaction was stopped using 0.5 mol/L H_2SO_4 (Fisher Scientific, Leicestershire, UK). Colorimetric analysis was performed by measuring absorbance values at 490 nm using a Dynatech Laboratories MRX plate reader. All treatments were performed in triplicate for each experiment.

2.2. Model of hypoxia and H–R injury

We utilised a model of warm in vitro hypoxia and H–R that we have described previously [14]. Briefly, in experiments, hepatocytes were cultured for 2 days at 37 °C, 5% CO_2 in Williams E media (Sigma) on rat type 1 collagen-coated plates. Hepatocytes were either maintained in normoxia or placed into hypoxia for 24 h, or placed into hypoxia for 24 h followed by 24 h of reoxygenation. Hypoxia was achieved by placing cells in an airtight incubator (RS Mini Galaxy A incubator, Wolf Laboratories, UK) flushed with 5% CO_2 and 95% N_2 until oxygen content in the chamber reached 0.1%, as verified by a dissolved oxygen monitor (DOH-247-KIT, Omega Engineering, UK). In preliminary experiments, human hepatocytes were exposed to 5% and 1% oxygen and no increase in ROS accumulation or cell death was noted. Therefore, we used 0.1% oxygen in all subsequent experiments for 24 h, similar to previously published studies. Additionally, Williams E media were pre-incubated in the hypoxic chamber in a sterile container, which allowed gas equilibration, for 8 h before experiments were carried out, resulting in a final oxygen concentration of <0.1% as measured with the dissolved oxygen metre. Where appropriate, after 24 h of hypoxia media were aspirated and replaced with fresh, warmed, oxygenated medium, and the cells were returned to normoxic conditions. This was defined as the beginning of reoxygenation. In experiments involving ROS inhibitors, reagents were made fresh as stock solutions and added using the correct dilutional factor to the relevant experimental wells. Specifically, 1 mM rotenone (Sigma) was dissolved in chloroform and was diluted appropriately to

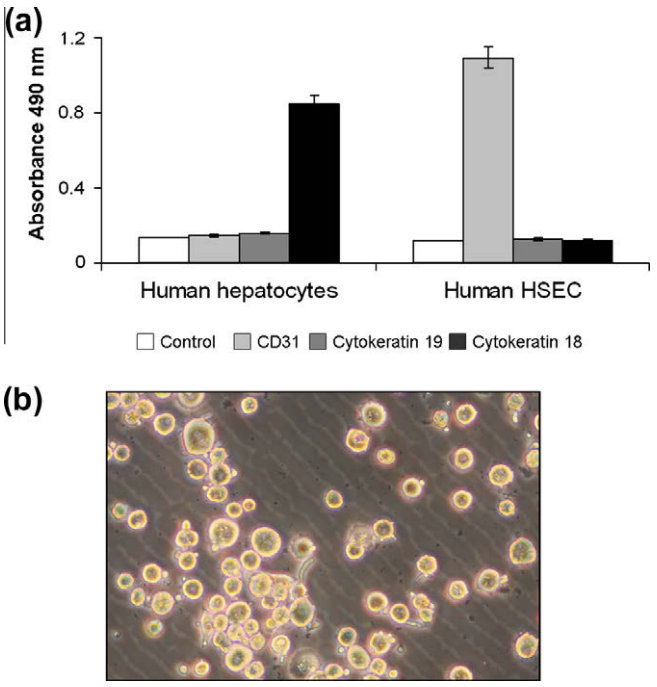

Fig. 1. The morphology and phenotype of isolated human hepatocytes. (a) Demonstrates the phenotypic features characteristic of human hepatocytes isolated using our protocol. The cell specific markers, cytokeratin 18, cytokeratin 19 and CD31 were determined using cell based ELISA as described in the Methods and Materials section. Human hepatocytes demonstrate a uniform staining for the hepatocyte specific marker, cytokeratin 18. These cells show no staining for the biliary epithelial marker, cytokeratin 19 or endothelial cell marker, CD31. In contrast, hepatic sinusoidal endothelial cells show strong positivity for the marker CD31 and no positivity for either cytokeratin 18 or cytokeratin 19. (b) Illustrates a representative image of human hepatocytes following successful isolation. These cells have been allowed to adhere to rat type 1 collagen for 2 h. There is a clear difference in size between the isolated hepatocytes. As previous authors have shown the smaller hepatocytes are likely to be derived from the peri-portal area and the larger hepatocytes are likely to be derived from the peri-venous region [4–6].

give working concentrations of 2 μM. In experiments using rotenone, solvent alone controls were used to ensure no vehicle effects (data not shown). Rotenone was added at the time of placement of the cells into conditions of hypoxia or reoxygenation.

2.3. Determination of human hepatocyte ROS accumulation and apoptosis

ROS production, apoptosis and necrosis were determined by using a three-colour reporter assay system. ROS accumulation was determined using the fluorescent probe 2′,7′-dichlorofluorescin-diacetate [14]. This probe is cell permeable and once inside the cell is cleaved by intracellular esterases to 2′,7′-dichlorofluorescin (DCF) (Merck, Nottingham, UK) which is then rendered cell impermeable. DCF is then able to react with intracellular ROS, specifically hydrogen peroxide, to give a fluorescent signal detectable on the FITC channel. The signal is directly proportional to the level of intracellular ROS present.

Apoptosis was determined by labelling cells with Annexin-V (Molecular Probes, Paisley, UK) which detects exposed

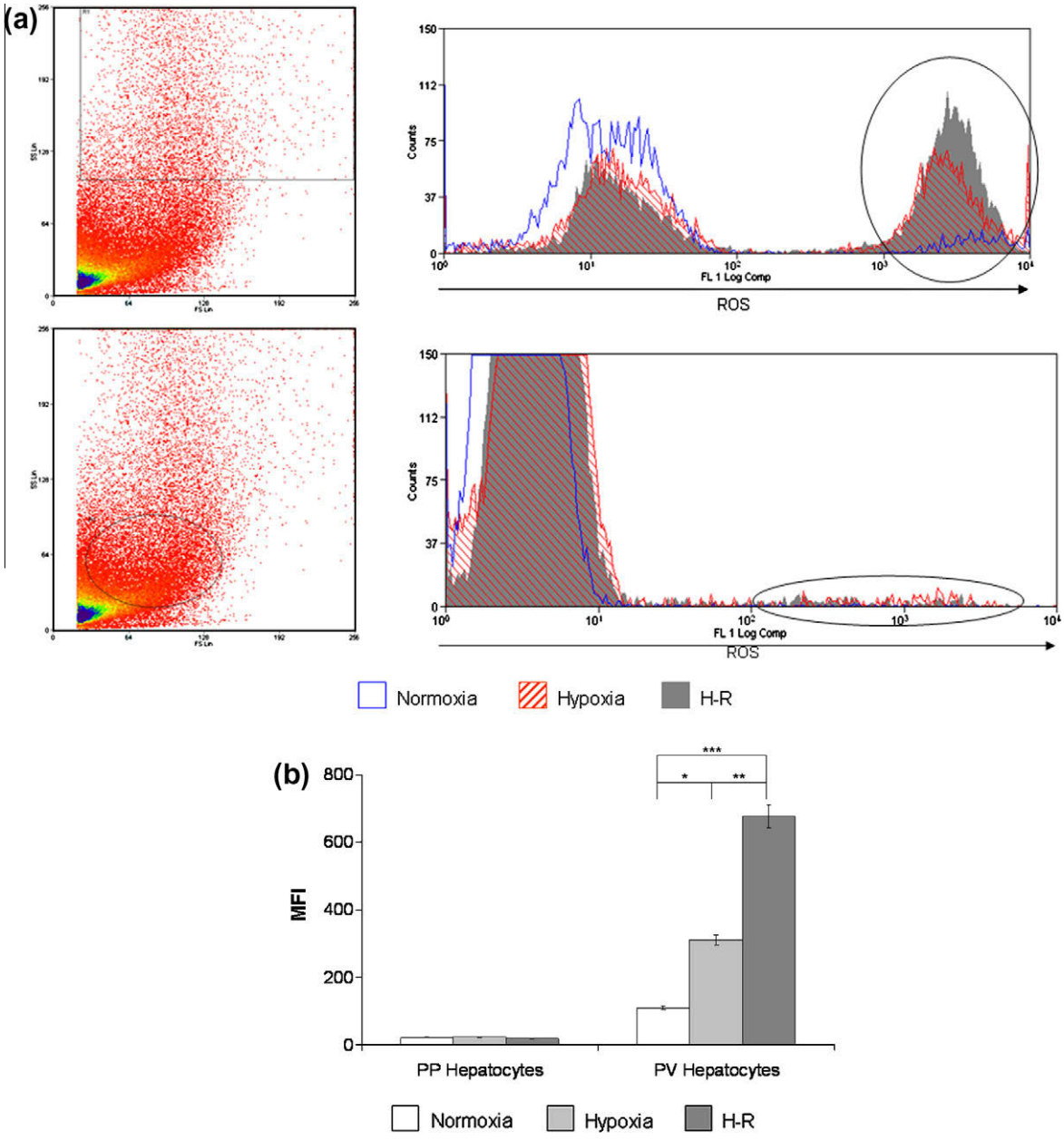

Fig. 2. Intracellular ROS accumulation within PP and PV human hepatocytes during hypoxia and H–R. (a) Demonstrates a representative flow cytometry plot of ROS accumulation in PP and PV primary human hepatocytes during normoxia, hypoxia and H–R. The plot on the left hand side of each flow cytometric plot represents a typical forward scatter (FS) versus side scatter (SS) plot of primary human hepatocytes. The FS versus SS plots shown is from the H–R sample of a liver preparation but similar plots were obtained during normoxia and hypoxia (data not shown). The top panel shows the gating protocol applied to human hepatocytes to analyse PV human hepatocytes. The areas of interest on the flow cytometric plots are marked by the vertical ellipses. The area on the left of each ellipse represents cell debris. Cell debris is included within the plot as human hepatocytes vary considerably in size and, therefore, to include all viable human hepatocytes in the analysis a large gate is required on the flow cytometre, this by necessity includes the cell debris. The bottom panel shows the gating protocol applied to human hepatocytes to analyse PP human hepatocytes ($n = 5$). (b) Shows a bar chart with the pooled data of five separate experiments illustrating the accumulation of ROS within PV and PP human hepatocytes during hypoxia and H–R. We refer to separate experiments here as human hepatocytes isolated from separate livers (normal and diseased), used in separate experiments. Data are expressed as MFI and readings are based upon values taken from cells within the gated region shown in Fig. 1a. Data are expressed as mean ± S.E. ($^{*}P < 0.01$ relative to normoxia, $^{**}P < 0.01$ relative to hypoxia, $^{***}P < 0.001$ relative to normoxia, Mann–Whitney test).

phosphatidylserine on the cell membrane. 7-Amino-Actinomycin D (7-AAD) (Molecular Probes, Paisley, UK) is a vital dye that binds to DNA, only entering cells once the cell membrane is disrupted and is indicative of cellular necrosis. To ensure consistency of the flow cytometric data, each human hepatocyte preparation was labelled with DCF alone, Annexin-V alone and 7-AAD alone to ensure that cells had become labelled and that the flow cytometry data could be compensated for crossover of fluorophore emission spectra. The same flow cytometre protocol was used for all experiments shown within the study, meaning that voltages for all markers were constant for all human hepatocyte preparation ensuring internal consistency of experiments.

Following appropriate treatment of cells, media were aspirated and replaced with HBSS (Gibco) without calcium and magnesium. DCF (30 μM) was added and the cells were incubated for 20 min in the dark at 37 °C. Next the cells were trypinsed (0.05% with EDTA, Gibco) for 5 min and washed extensively in FACs buffer (Phosphate-buffered saline pH 7.2 with 10% v/v heat inactivated foetal calf serum (Gibco). Cells were then labelled with Annexin-V and 7-AAD for 15 min whilst on ice and samples were immediately subjected to flow cytometry. At least 20,000 events were recorded within the gated region of the flow cytometre for each human hepatocyte cell preparation in each experimental condition. Only the cells within the gated region were used to calculate mean fluorescence intensity (MFI).

2.4. Statistical analysis

All data are expressed as mean ± S.E. Statistical comparisons between groups were analysed by using the Mann–Whitney test. All differences were considered statistically significant at a value of $P < 0.05$.

3. Results

3.1. Isolated human hepatocytes exhibit typical features of hepatocytes

The isolated human hepatocytes consistently showed typical morphological and phenotypic features of hepatocytes (Fig. 1). The cell preparations were uniformly positive for the specific intracellular hepatocyte marker Cytokeratin 18 whilst demonstrating no staining with the biliary epithelial cell marker Cytokeratin 19 of the hepatic sinusoidal endothelial cell (HSEC) marker CD31. In contrast control HSEC demonstrates strong positivity for CD31 and no staining with Cytokeratin 18.

In addition, the isolated hepatocytes demonstrated consistent heterogeneity in terms of size. Fig. 1b clearly shows that viable intact cells were of two different size populations. As previous studies have demonstrated the small hepatocytes are highly likely to represent cells originating from the peri-portal region of the

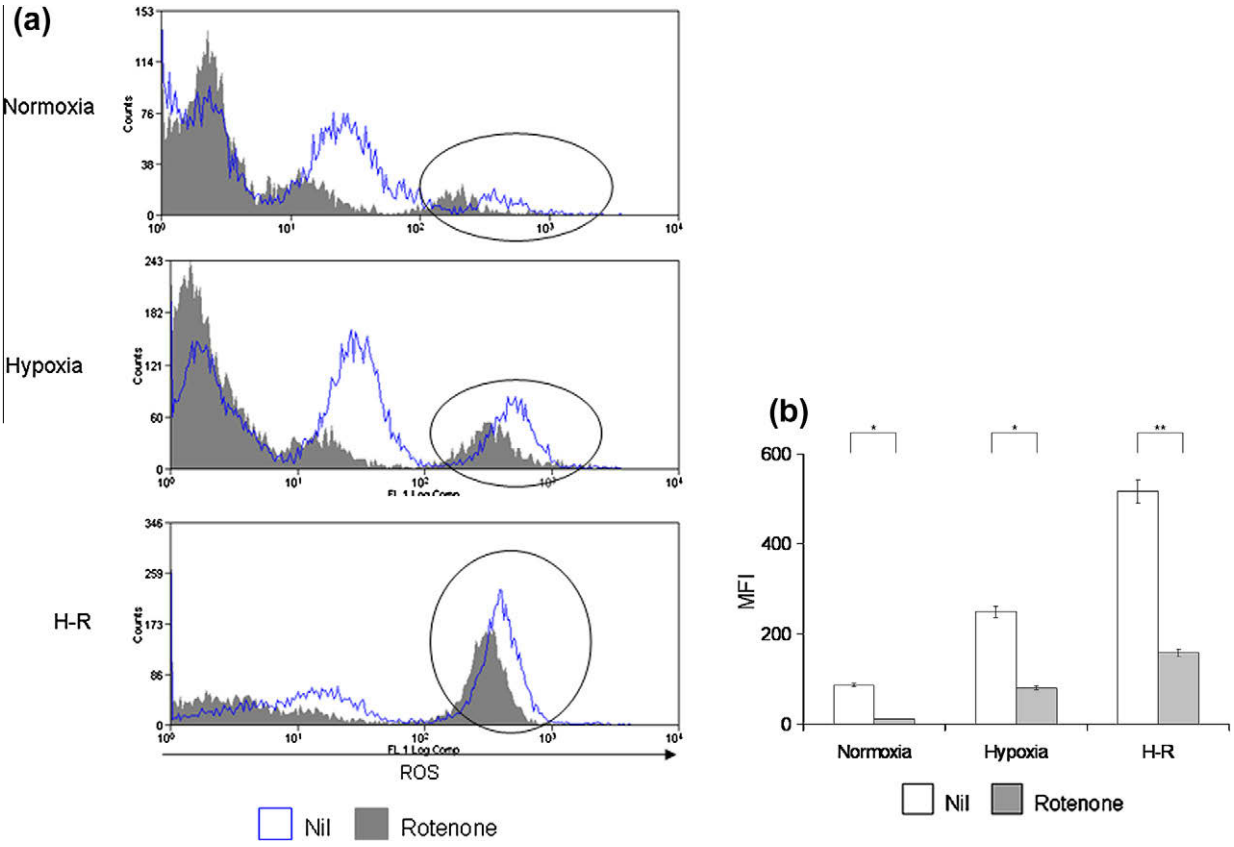

Fig. 3. Mitochondrial dependent ROS production in PV human hepatocytes during hypoxia and H–R. (a) Demonstrates representative flow cytometry plots to illustrate the effect of rotenone (solid grey) upon PV human hepatocyte ROS accumulation during normoxia, hypoxia and H–R. The areas of interest on the flow cytometric plots are marked by the vertical ellipses. The gating protocol applied to PV human hepatocytes is the same as that shown within Fig. 2a. Once again, the area on the left of each ellipse represents cell debris. Fig. 3b shows a bar chart with the pooled data of five separate experiments illustrating the effects of 2 μM rotenone upon PV human hepatocytes ROS accumulation during normoxia, hypoxia and H–R. Human hepatocytes were treated with 2 μM rotenone at the time of placement into hypoxia or H–R. Rotenone was dissolved in chloroform to make a stock solution of 1 mM and diluted appropriately. Vehicle alone was shown not to have any effect upon ROS production (data not shown). Data are expressed as MFI and readings are based upon values taken from cells within the gated region shown in Fig. 2a. Data are expressed as mean ± S.E. ($^{*}P < 0.01$ relative to basal, $^{**}P < 0.001$ relative to basal).

liver whereas the larger hepatocytes represent those from the perivenular region [4–6]. These data demonstrate that our isolation technique yielded human hepatocytes of a high purity with little or no contamination with other cell types and that using FACS we could discriminate effectively between small/PP and large/PV human hepatocytes.

3.2. Small (PP) and large (PV) human hepatocytes exhibit differential ROS accumulation during hypoxia and H–R

FACs analysis was able to discriminate between large or PV and small or PP human hepatocytes using appropriate forward scatter (FS) and side scatter (SS) plots (Fig. 2). Accordingly, using suitable flow cytometric gating protocols the response of large/PV and small/PP hepatocytes to hypoxia and H–R could be ascertained.

PV hepatocytes, isolated from benign liver resections, normal donor tissue and biliary cirrhosis (primary biliary cirrhosis and primary sclerosing cholangitis) showed significant increase in ROS accumulation during hypoxia (Fig. 2a and b). Exposure of human hepatocytes to H–R further accentuated intracellular ROS accumulation. In contrast, PP hepatocytes, showed no increase in intracellular ROS accumulation during hypoxia and H–R.

3.3. ROS production in large (PV) hepatocytes is mitochondrial dependent

Numerous previous studies have shown that the mitochondrion is the central source of ROS during hypoxia and H–R [14–16]. Therefore, mitochondrial function was inhibited within large/PV human hepatocytes using the complex I mitochondrial chain inhibitor, rotenone. As Fig. 3a and b demonstrates, rotenone

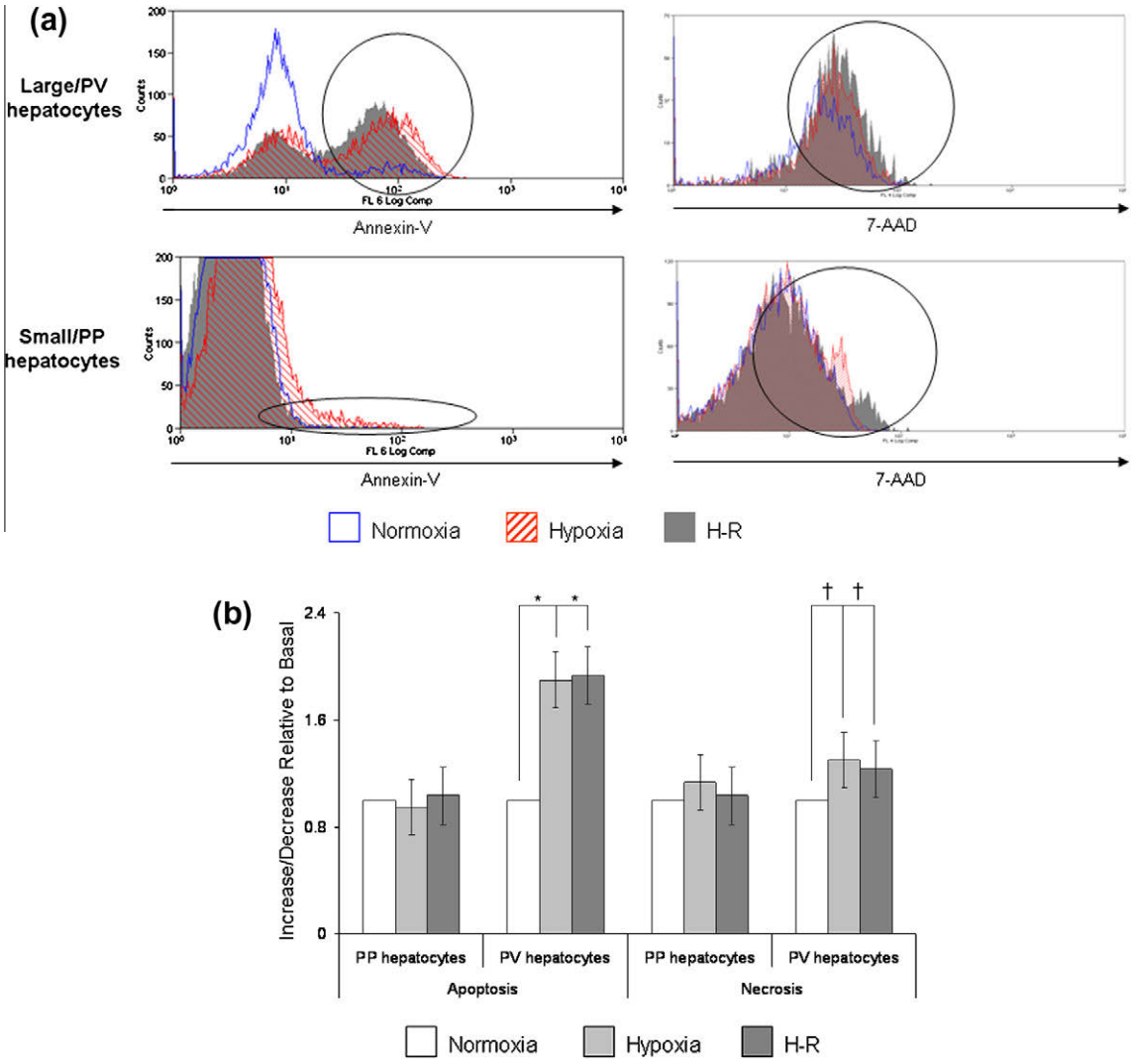

Fig. 4. PV human hepatocytes undergo apoptosis and necrosis during hypoxia and H–R. (a) Shows representative flow cytometry plots to illustrate the level of apoptosis and necrosis in PP and PV human hepatocytes during hypoxia and H–R. The gate used to analyse primary human hepatocytes are the same as that shown in Fig. 2. The area of interest within the flow cytometric plots are marked by the vertical ellipses. (b) Shows a bar chart with the pooled data of five separate experiments illustrating the level of apoptosis and necrosis in PP and PV human hepatocytes during hypoxia and H–R. Data are expressed as increase/decrease relative to basal, where basal refers to the level of apoptosis and necrosis during normoxia alone. Data are expressed as mean ± S.E. ($^{\dagger}P < 0.05$ relative to basal, $^{*}P < 0.01$ relative to basal). (c) Shows representative flow cytometry plots to illustrate the effects of rotenone upon the level of PV human hepatocyte apoptosis and necrosis during normoxia, hypoxia and H–R. The gating protocol used to analyse large human hepatocytes is the same as that shown in Fig. 2. The area of interest within the flow cytometric plots are marked by the vertical ellipses. (d) Shows a bar chart with the pooled data of five separate experiments illustrating the effect of rotenone upon the level of PV hepatocyte apoptosis and necrosis during normoxia, hypoxia and H–R. Data are expressed as increase/decrease relative to basal, where basal refers to the level of apoptosis and necrosis during normoxia alone. Data are expressed as mean ± S.E. ($^{\dagger}P < 0.05$ relative to no treatment in the same experimental condition, $^{*}P < 0.01$ relative to no treatment in the same experimental condition, $^{**}P < 0.001$ relative to no treatment in the same experimental condition).

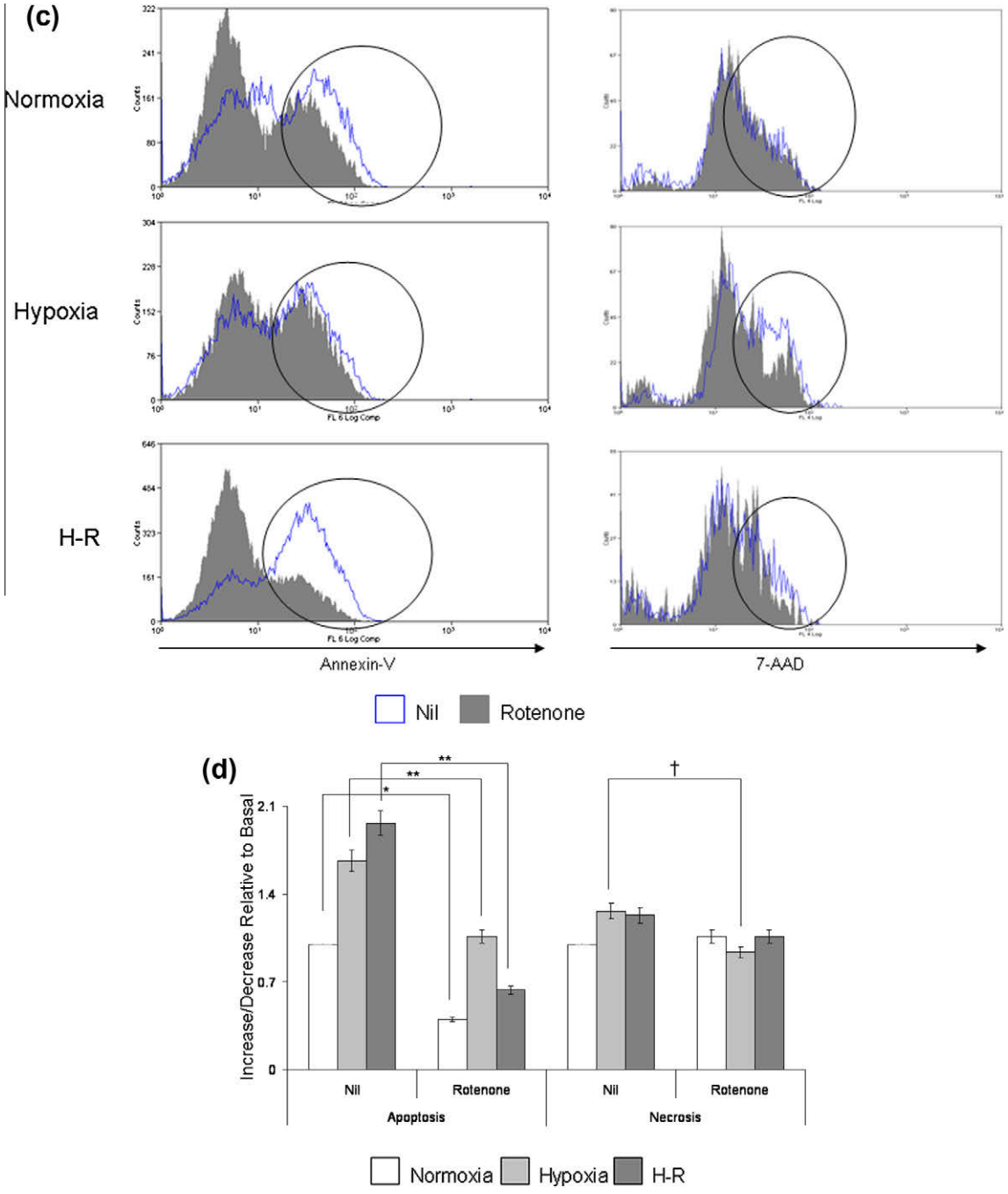

Fig. 4 (*continued*)

significantly reduced ROS accumulation in large/PV human hepatocytes during normoxia, hypoxia and H–R. Rotenone had no effect upon ROS accumulation in small/PP human hepatocytes (data not shown).

3.4. Large (PV) and not small (PP) human hepatocytes undergo apoptosis and necrosis during hypoxia and H–R

The relationship between intracellular ROS accumulation and apoptosis and necrosis has been clearly established within human hepatocytes [14]. Accordingly, we found that large/PV human hepatocytes, in line with their propensity to generate ROS during hypoxia and H–R, underwent significant levels of apoptosis and necrosis (Fig. 4a and b). In contrast, small/PP hepatocytes did not undergo any apoptosis or necrosis in line with their lack of ROS generation during hypoxia and H–R. We finally investigated whether mitochondrial generated ROS during hypoxia and H–R was responsible for regulating human hepatocyte apoptosis and necrosis. As Fig. 4c and d illustrates, rotenone significantly reduces large/PV human hepatocyte apoptosis and necrosis during normoxia, hypoxia and H–R. These findings clearly demonstrate that in PV human hepatocytes mitochondrial ROS generated during hypoxia and H–R drives cell death.

4. Discussion

Exposure of hepatocytes to pathological conditions in a microenvironment of hypoxia and H–R is very frequent in several hepa-

tic diseases and hepatic surgery. These include haemodynamic shock, septicaemia and liver transplantation. Death of hepatocytes by hypoxia and H–R injury is a multifactorial event including alteration of the plasma membrane, increase of autophagic vacuoles, rupture of blebs on the cell surface, calcium accumulation and mitochondrial damage [9]. The common mediator of these death pathways appears to be the accumulation of ROS [17]. Studies in rodent models suggest that large/PV hepatocytes are more vulnerable to damage during hepatic injury [8]. Moreover, hepatocyte proliferation, which is an important determinant of patient survival after major hepatic resection, occurs from the small/PP to large/PV hepatocytes. Therefore, an understanding of the differential vulnerability of hepatocytes to liver injury would provide an important basis for preventing loss of liver function and/or failure caused by cirrhosis, hepatic resection and liver transplantation [8]. Common factors to most liver injuries are hypoxia and the generation of ROS [14,17]. However, the susceptibility of hepatocytes, and in particular human hepatocytes, to oxidative stress has not been assessed directly. We show for the first time to our knowledge, clear evidence that large/PV hepatocytes are the most susceptible to hypoxic injury. Moreover, this susceptibility is due to the greater propensity of the mitochondria of these large/PV hepatocytes to produce and accumulate intracellular ROS [18]. It must be noted however, that inhibiting mitochondrial function does not completely abrogate large/PV human hepatocyte apoptosis and necrosis. Indeed, previous studies have shown that other enzymes involved in ROS generation are also involved in regulating human hepatocyte apoptosis [14].

The increased level of apoptosis and necrosis seen in large/PV human hepatocytes seen in vitro in the present study would concur with in vivo models of murine and rodent liver injury, where cell death is observed in the peri-venular regions of the liver [13]. A possible explanation for this observation may well be that the powerful antioxidant glutathione (in rodent models) varies considerably in concentration between hepatocytes isolated from the small/PP and large/PV regions [19]. Specifically, large/PV hepatocytes have less intracellular glutathione when compared to small/PP or small hepatocytes. Moreover, following stimulation with amino acids larger hepatocytes are able to generate less intracellular glutathione than small hepatocytes [19]. These findings could in theory explain the increased susceptibility of large/PV human hepatocytes to hypoxic injury.

Previous studies have shown that mitochondrial inhibitors and anti-oxidants inhibit ROS accumulation in human hepatocytes during hypoxia and H–R [14–16]. Our present study builds upon this observation, demonstrating that mitochondrial electron transport chain inhibitors specifically reduce ROS accumulation in the large/PV hepatocytes and consequently reduce apoptosis in this population during hypoxia and H–R. Many studies have suggested that resident liver macrophages (Kupffer cells) located in the PV region of liver are activated during ischaemia and release ROS, leading to hepatocyte damage [8]. Taken together with our study this suggests that the PV region of the liver is the preferential site of hepatic inflammation and ROS generation during hypoxic liver injury. Contrastingly, some studies in rodent hepatocytes have suggested that small/PP hepatocytes are more vulnerable to hypoxic injury due to their higher requirement of oxygen [8]. We remain uncertain about the explanation for these discrepancies which may represent inter-species differences of unknown aetiology.

In conclusion, large/PV human hepatocytes are the most susceptible to hypoxic damage. This suggests that therapeutics used in the treatment of liver disease may primarily act upon PV or large human hepatocytes. In the future, therapeutic strategies used to treat hepatic inflammation may require novel drug targeting methods that allow the delivery of the drug preferentially to the PV or large hepatocytes.

Acknowledgements

R.H.B. is in receipt of a Wellcome Trust Fellowship (DDDP.RCHX14183). The authors would like to thank the clinical team at the Queen Elizabeth Hospital, Birmingham for the procurement of liver tissue.

References

[1] Loud, A.V. (1968) A quantitative stereological description of the ultrastructure of normal rat liver parenchymal cells. J. Cell Biol. 37, 27–46.
[2] Schmuker, D.L., Mooney, J.S. and Jones, A.L. (1978) Stereological analysis of hepatic fine structure in the Fischer 344 rat. Influence of sublobular location and animal age. J. Cell Biol. 78, 319–337.
[3] Willson, R.A., Wormsley, S.B. and Muller-Eberhard (1984) A comparison of hepatocyte size distribution in untreated and Phenobarbital-treated rats as assessed by flow cytometry. Dig. Dis. Sci. 29, 753–757.
[4] Braakman, I., Keij, J., Hardonk, M.J., Meijer, D.K.F. and Groothuis, G.M. (1991) Separation of periportal and perivenous rat hepatocytes by fluorescence-activated cell sorting: confirmation with colloidal gold and exogenous marker. Hepatology 13, 73–82.
[5] Thalhammer, T., Gessl, A., Braakman, I. and Graf, J. (1989) Separation of hepatocytes of different acinar zones by flow cytometry. Cytometry 10, 772–778.
[6] Gumucio, J.J., May, M., Dvorak, C., Chianale, J. and Massey, V. (1986) The isolation of functionally heterogeneous hepatocytes of the proximal and distal half of the liver acinus in the rat. Hepatology 6, 932–944.
[7] Wilton, J.C., Chipman, K., Lawson, C.J., Strain, A.J. and Coleman, R. (1993) Periportal- and perivenous-enriched hepatocyte couplets: differences in canalicular activity and in response to oxidative stress. Biochem. J. 292, 773–779.
[8] Taniai, H., Hines, I.N., Bharwani, S., Maloney, R.E., Nimura, Y., Gao, B., et al. (2004) Susceptibility of murine periportal hepatocytes to hypoxia–reoxygenation: role for NO and Kupffer cell-derived oxidants. Hepatology 39, 1544–1552.
[9] Massip-Salcedo, M., Rosello-Catafau, J., Prieto, J., Avila, M.A. and Peralta, C. (2007) The response of the hepatocyte to ischemia. Liver Int. 27, 6–17.
[10] Bella, D.L., Hirschberger, L.L., Kwon, Y.H. and Stipanuk, M.H. (2002) Cysteine metabolism in periportal and perivenous hepatocyes: perivenous cells have greater capacity for glutathione production and taurine synthesis but not for cysteine catabolism. Amino Acids 23, 453–458.
[11] Jungerman, K. and Katz, N. (1989) Functional specialization of different hepatocyte populations. Physiol. Rev. 69, 708–763.
[12] Traber, P., Chianale, J. and Gumucio, J.J. (1988) Physiologic significance and regulation of hepatocellular heterogeneity. Gastroenterology 95, 1130–1143.
[13] Kato, Y., Tanaka, J. and Koyama, K. (2001) Intralobular heterogeneity of oxidative stress and cell death in ischemia-reperfused rat liver. J. Surg. Res. 95, 99–106.
[14] Bhogal, R.H., Curbishley, S.M., Weston, C.J., Adams, D.H. and Afford, S.C. (2010) Reactive oxygen species mediate human hepatocyte injury during hypoxia/reoxygenation. Liver Transpl. 16, 1303–1313.
[15] Lluis, J.M., Buricchi, F., Chiarugi, P., Morales, A. and Fernandez-Checa, J.C. (2007) Dual role of mitochondrial reactive oxygen species in hypoxia signalling: activation of nuclear factor-kB via c-SRC- and oxidant dependent cell death. Cancer Res. 67, 7368–7377.
[16] Lluis, J.M., Morales, A., Blasco, C., Colell, A., Mari, M., Garcia-Ruiz, C., et al. (2005) Critical role of mitochondrial glutathione in the survival of hepatocytes during hypoxia. J. Biol. Chem. 280, 3224–3232.
[17] Andrade Jr, D.R., Andrade, D.R. and Santos, S.A. (2009) Study of rat hepatocytes in primary culture submitted to hypoxia and reoxygenation: action of the cytoprotectors prostaglandin E1, superoxide dismutase, allopurinol and verapamil. Arq. Gastroenterol. 46, 333–340.
[18] Baraona, E., Jauhonen, P., Miyakawa, H. and Lieber, C.S. (1983) Zonal redox changes as a cause of selective perivenular hepatotoxicity of alcohol. Pharmacol. Biochem. Behav. 18, 449–454.
[19] Kera, Y., Penttilä, K.E. and Lindros, K.O. (1988) Glutahione replenishment capacity is lower in isolated perivenous than in periportal hepatocytes. Biochem. J. 254, 411–417.

Appendix III

OPEN ACCESS Freely available online

PLoS one

Isolation of Primary Human Hepatocytes from Normal and Diseased Liver Tissue: A One Hundred Liver Experience

Ricky H. Bhogal[1]*, James Hodson[2], David C. Bartlett[1], Christopher J. Weston[1], Stuart M. Curbishley[1], Emma Haughton[1], Kevin T. Williams[1], Gary M. Reynolds[1], Phillip N. Newsome[1], David H. Adams[1], Simon C. Afford[1]

1 Centre for Liver Research, Institute for Biomedical Research, University of Birmingham, Edgbaston, Birmingham, United Kingdom, **2** Information Technology, University Hospitals Birmingham NHS Foundation Trust, Queen Elizabeth Hospital, Edgbaston, Birmingham, United Kingdom

Abstract

Successful and consistent isolation of primary human hepatocytes remains a challenge for both cell-based therapeutics/transplantation and laboratory research. Several centres around the world have extensive experience in the isolation of human hepatocytes from non-diseased livers obtained from donor liver surplus to surgical requirement or at hepatic resection for tumours. These livers are an important but limited source of cells for therapy or research. The capacity to isolate cells from diseased liver tissue removed at transplantation would substantially increase availability of cells for research. However no studies comparing the outcome of human hepatocytes isolation from diseased and non-diseased livers presently exist. Here we report our experience isolating human hepatocytes from organ donors, non-diseased resected liver and cirrhotic tissue. We report the cell yields and functional qualities of cells isolated from the different types of liver and demonstrate that a single rigorous protocol allows the routine harvest of good quality primary hepatocytes from the most commonly accessible human liver tissue samples.

Citation: Bhogal RH, Hodson J, Bartlett DC, Weston CJ, Curbishley SM, et al. (2011) Isolation of Primary Human Hepatocytes from Normal and Diseased Liver Tissue: A One Hundred Liver Experience. PLoS ONE 6(3): e18222. doi:10.1371/journal.pone.0018222

Editor: Nathalie Wong, Chinese University of Hong Kong, China

Received November 18, 2010; **Accepted** February 27, 2011; **Published** March 29, 2011

Funding: This work has been funded by the Wellcome Trust (grant number DDDP. RCHX14183). The funders had no role in study design, data collection and analysis, decision to publish, or preparation of the manuscript.

Competing Interests: The authors have declared that no competing interests exist.

* E-mail: balsin@hotmail.com

Introduction

High quality primary human hepatocytes are a valuable resource for biomedical research, the pharmaceutical industry and therapeutic purposes [1–4]. It is becoming widely accepted that the majority of hepatocyte cell lines lack many important aspects of primary cell function and are unlikely to be used therapeutically. Primary hepatocytes are thus becoming increasingly used in drug development to evaluate key human-specific drug properties such as metabolic fate, drug-drug interactions, and drug toxicity. However the quality and metabolic/functional activity of the cells is variable. Thus human hepatocyte research would be greatly assisted if hepatocytes could be consistently isolated from human liver tissue obtained through hepatobiliary and transplant programs. Previously authors have suggested protocols for successful human hepatocyte isolation but these have applied exclusively to tissue obtained from organ donors [5–6] or from non-diseased tissue removed at surgical resection for liver tumours [1,7–10]. Recent work conducted within our laboratory has shown for the first time that human hepatocytes isolated from various cohorts of non-diseased and diseased livers exhibit different responses when used in functional studies [4]. Thus comparative studies need to be carried out in cells isolated from different hepatic diseases.

The isolation of human hepatocytes from steatotic liver tissue has been difficult [6] and although detailed protocols have been described [3] the overall results are so variable in terms of yield and quality of cells that it has been suggested it is not economically viable to attempt hepatocytes isolation from diseased liver tissue [6]. Most published studies have reported outcomes of human hepatocyte isolation from normal resected [1] and donor liver tissue [2,3]. Here we report our experience of isolating human hepatocytes from all types of livers including normal donor tissue, cut-down liver, normal resected liver tissue and cirrhotic liver disease. We do so in the hope that other researchers in this challenging field may benefit from our experience and make informed decisions on how best to isolate cells for their own studies.

Methods

Ethics Statement

Liver tissue was obtained from surgical procedures carried out at the Queen Elizabeth Hospital, Birmingham, UK. Ethical approval for the study was granted by the Local Research Ethics Committee (LREC) (reference number 06/Q702/61). Informed written consent was obtained from all participants involved in the study.

Human Hepatocyte Isolation

All liver tissue was obtained from fully consenting patients undergoing liver transplantation for a variety of end-stage liver diseases. Human hepatocytes were isolated from explanted diseased livers from patients with alcoholic liver disease (ALD), biliary cirrhosis (primary biliary cirrhosis (PBC) and primary sclerosing cholangitis (PSC) and a variety of other end-stage liver diseases (Cystic Fibrosis, Cryptogenic Fibrosis, Alpha-1-antitypsin Deficiency, Autoimmune Hepatitis and Non-alcoholic Steatohepatitis). Hepatocytes were also isolated from tissue taken from patients who had undergone hepatic resections for liver metastasis from colorectal carcinoma, hepatic resections carried out for benign disease (recurrent cholangitis, focal nodular hyperplasia and haemangiomas), cut-down specimens and normal donor tissue surplus to surgical requirements. For the purposes of the study, liver tissue obtained from resections for benign lesions was included in the normal liver group whereas liver tissue obtained from hepatic resections carried out for metastatic disease was classified as normal resected tissue as is referred to as this hereafter. All the patients included in this latter group had received pre-operative chemotherapy to reduce tumour mass prior to surgery.

For all liver tissue specimens we adopted a stringent and rigorous procurement and isolation protocol. Following explantation or resection, specimens were immediately placed on ice in a sterile sealed draw string bag and processed within 1 hour. There were however exceptions to this, in cases were hepatic resections or liver transplants were carried out at in the late evening or at night, liver tissue was kept sterile on ice overnight. The significant exception to this protocol was in the use of donor liver tissue. In all cases the donor liver was assessed for transplantation by the clinical team at the Queen Elizabeth Hospital, Birmingham and if deemed unsuitable for liver transplantation it was then used for hepatocyte isolation. Precise time between explantation or resection of the liver and commencement of the isolation procedure was recorded in each case.

In isolation procedures where donor liver or liver explants were used, liver wedges were obtained from either the segments II/III or segments V/VI. In procedures where normal resected tissue was used for isolating human hepatocytes, only patients who had undergone right hemihepatectomies were deemed suitable by our pathologist to obtain normal resected liver tissue from. This was obtained in all cases from segments V/VI. Liver wedges were cut and weighed by a trained pathologist. To eliminate interperson variability, the subsequent hepatocyte isolation procedures were carried out by a single individual (R.H.B).

Hepatocyte isolations were carried out using a modified 'two-stage' collagenase procedure developed by Berry and Friend [11]. This method has been adapted by several laboratories to isolate human hepatocytes [12–14]. After the liver wedge was cut it was placed into ice-cold Dulbecco's Modified Eagles Medium (DMEM) (Gibco, Paisley, UK). The liver was then washed through the exposed, cut, vessels with Phosphate-buffered Saline (PBS), pH 7.2. This was to remove any remaining blood from within the liver wedge and to identify two suitable vessels that could be used for cannulation and subsequent perfusion of buffers. The vessels for cannulation were chosen using two criteria. Firstly, when washing the liver through with PBS it is apparent which parts of the wedge were being 'perfused' by that particular vessel, hence the greater the liver area 'perfused' the more favourable the vessel was thought to be and secondly the two vessels should be in different parts of the liver wedge to ensure optimum perfusion of the whole wedge. Subsequently two 20 gauge cannulae (Becton-Dickinson, Oxford, UK) were sutured into the chosen vessels using a 3/0 prolene (Covidien, Hampshire, UK) purse string suture (Figure 1). The cannulae were then primed with PBS to ensure that subsequent

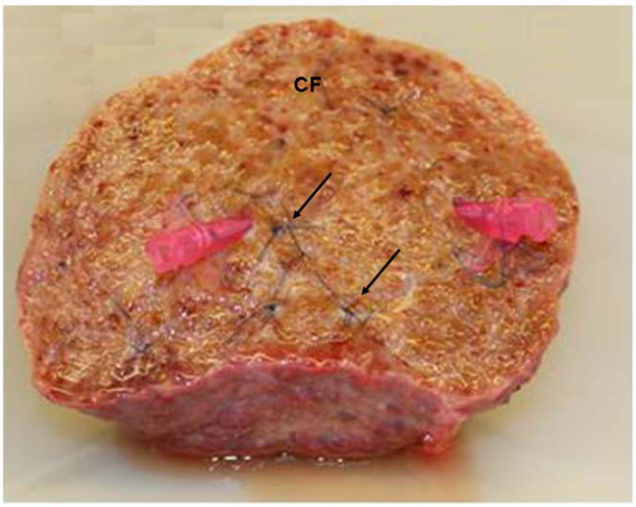

Figure 1. Preparation of the Encapsulated Liver Wedge Prior to Perfusion. Isolation of human hepatocytes was performed from liver wedges (50–413 g). Liver wedges had one cut face (CF) with the remainder of the hepatic capsule being left intact. After washing the liver through exposed vessels with PBS, 20 G cannulae were sutured into suitable vessels with 3/0 prolene purse string sutures. The remaining vessels were oversewn using continuous 3/0 prolene sutures (arrowed). The liver wedge was then ready to be used for the perfusion isolation protocol.
doi:10.1371/journal.pone.0018222.g001

fluids used for perfusion would run correctly. The final stage of preparing the liver wedge involved oversewing any major vessels that were present on the cut surface of the liver wedge, to ensure minimal loss of perfusion fluids. This also helped maintain pressure within the liver wedge throughout the isolation procedure.

The perfusion circuit was set up according to the widely established routine protocol. One end of the perfusion tube was fed into the perfusion buffer, the central segment of the tubing was within the pump (Model IP 505Du, Watson-Marlow Ltd, Falmouth, UK), and the two outlets of the tubing were connected to the sutured cannulae. The liver wedge was held over a container during the procedure. This container also contained the waste tubing which connected the container to the waste pot. At the commencement of the procedure, all rubber tubing remained 'open' allowing the free flow of perfusion and waste fluids. All buffers used in the isolation procedure were pre-warmed to 42°C in a water bath. At this stage, liver wedges were first perfused with 'non-recirculating' wash buffer (10 mM 4-(2-hydroxylethyl)-1-piperazineethanesulfonic acid (HEPES) pH 7.2) (Sigma, Dorset, UK) at room temperature using a flow rate of 75 ml/min, ensuring flushing out of blood within the liver vasculature. After this, the wedge was perfused with chelating solution (non-recirculating) (10 mM HEPES, 0.5 mM Ethylene Glycol Tetra-acetic Acid (EGTA), pH 7.2) (Sigma) in order to disrupt cell adhesion to the underlying matrix. This was followed by further perfusion with (non-recirculating) wash buffer to remove any remaining EGTA from the liver as the enzymes used to dissociate the liver are dependent upon calcium and magnesium for activation. At this point the waste tubing was clamped to allow recirculation of the enzymatic buffer. Enzyme buffer perfusion solution was made up as follows: Fresh aliquots of enzymes were removed from −20°C storage and dissolved in Hank's Balanced Salt Solution (HBSS) (Gibco, Paisley, UK) that had been supplemented with calcium chloride (5 mM) and magnesium chloride (5 mM). Following enzyme dissolution the solution was

filtered through a sterile filter (Miltenyi Biotec Ltd, Surrey, UK) back into the HBSS solution. Specifically, 0.5% w/v Collagenase A (from Clostridium Histolyticum, Roche, Hertford, UK, Lot number 70273822), 0.25% w/v Protease (Type XIV from Streptomyces Griseus, Sigma, Lot number 076K1177, 4.5 units/mg), 0.125% w/v Hyaluronidase (from bovine testes, Sigma, Lot number 025K7015, 451 units/mg) and 0.05% w/v Deoxyribonuclease (from bovine pancreas, Sigma, Lot number 107K7013, 552 units/mg) were the enzymes used. The liver wedge was perfused with the recirculating enzyme solution at 37°C using a flow rate 75 ml/min for between 1–19 min, this time was designated to be the perfusion time. The decision to stop perfusion was made when the cut surface of the liver allowed the admission of a digit. At this point the perfusion tubing and cannulae were removed and the liver was then transferred to a sterile glass dish and dissociated using manual force whilst in DMEM supplemented with 10% v/v heat inactivated foetal calf serum (Gibco), 2 mM glutamine (Gibco), 20,000 units/l Penicillin, and 20 mg/ml Streptomycin (Gibco) and 2.5 μg/ml Gentamycin. Following manual dissociation of the liver wedge the suspension was passed through a sterile nylon mesh of 250 μm (John Staniar Ltd, Manchester, UK) followed by a sterile nylon mesh of 60 μm (John Staniar Ltd). Suspensions were then washed three times at 50×g for 10 min at 4°C in supplemented media.

Immediately after washing, cell viability was determined by trypan blue dye exclusion and deemed acceptable if greater than >50% at this stage. Hepatocytes were then plated out in supplemented media. If viability was lower but total cell yield was high, Percoll density gradient centrifugation of cell suspensions was carried out to improve yield of viable cells. Percoll (Sigma) was made by adding to PBS pH 7.2 to density of 4.5 g/ml. Percoll was added to cell suspensions and washed at 300×*g* for 30 min at room temperature. Cell viability was again determined by trypan blue dye exclusion and if improved to >50% cells were plated out at 5×10^5 per well in supplemented media for 2 hours onto type 1 rat collagen coated plates to allow adherence of cells. After this period, the media was changed to Arginine-free Williams E media (Sigma) containing Hydrocortisone (2 ug/ml), Insulin (0.124 U/ml), Glutamine (2 mM), Penicillin (20,000 units/l), Streptomycin (20 mg/l) and Ornithine (0.4 mmol/l). The media was exchanged every 24 hours and for subsequent functional studies, cells were used within 2 days. Figure 2 shows the morphology of primary human hepatocyte isolated from PBC livers at different time points following successful isolation. The morphology of human hepatocytes isolated from normal tissue, biliary cirrhosis, ALD and normal resected liver tissue three days after successful isolation are also demonstrated (Figure 2b). As Figure 3 demonstrates, primary human hepatocytes showed characteristic phenotypic features of hepatocytes and were able to maintain urea and albumin synthesis up to at least one week following successful isolation. Successful human hepatocyte isolations were defined as successful plating of cells that were used in subsequent functional studies.

Liver samples from the normal liver category were histopathogically evaluated on formalin fixed paraffin-embedded sections by G.M.R. Steatosis was reported by the percentage of steatotic hepatocytes present and group accordingly: minimal/none = 0–5%, mild = 5–33%, moderate = 33–66% and severe = >66%.

Urea Synthesis Assay

Confirmation of urea synthesis by isolated human hepatocytes was performed using quantitative colorimetric urea determination (QuantiChrom™ urea assay kit-DIUR-500) (Bioassay Systems, Hayward, CA, USA).

Albumin Synthesis Assay

Albumin synthesis by isolated human hepatocytes was confirmed using a sandwich ELISA kit (Abnova, CA, USA).

Immunostaining human hepatocytes for Cytokeratin 18

Following successful isolations, cytospins of hepatocytes were made on Poly-L-lysine coated glass slides and fixed for 5 min in acetone. Cells were then incubated with 20% normal rabbit serum (Dako, Cambridge, UK) in Tris-buffered saline pH 7.4 (TBS) for 30 min. Monoclonal antibody to Cytokeratin 18 diluted 1:100 (clone DC10, Dako) or monoclonal antibody to Cytokeratin 19 diluted 1:100 (clone RCK108, Dako) or monoclonal antibody to CD326 (Epithelial Cell Adhesion Molecule (EpCAM) diluted 1:100 (clone HEA125, Progen, Heidelberg, Germany) was applied for 60 min, followed by polyclonal rabbit-anti mouse IgG antibody (1:25 dilution, Dako) for 30 min and finally anti-alkaline phosphatise (APAAP) complex (1:50 dilution in TBS) for 30 min. After each incubation step cytospins were washed x3 in TBS. Antibody binding was visualised with 0.2 mg/ml naphthol-AS-MX-phosphate dissolved in Dimethylforamide, (Sigma), 1 mg/ml Fast Red (Sigma) in 0.1 M Tris buffer (pH 8.2) and 0.25 mg/ml Levamisole (Sigma) for 15 min followed by counterstaining with Mayer's haematoxylin (Dako). Control cytospins were included where primary antibody was substituted for isotype matched immunglobulin. Slides were then mounted with Immunoblot mounting medium (Dako) and assessed for positivity.

Statistical Analysis

Univariable analysis was performed to test the effect of specific factors upon outcome measures, human hepatocyte cell viability following a preparation, total cell count after preparation and success. Success was defined as maintenance of cell adherence and morphological integrity 48 hours after plating onto type I rat collagen and their subsequent use in functional studies. The specific factors we analysed were hepatic disease type, time delay between hepatectomy and beginning of the liver perfusion, weight of liver wedge, perfusion time, the level of steatosis in the normal liver cohort, and the use of Percoll enrichment. In univariable analysis, Mann-Whitney tests were used for the time and weight variables, as they did not to follow a normal distribution, with Fisher's Exact test being used for the categorical variables. Multivariable analysis was performed by considering all specific factors simultaneously and assessing the effect upon the said outcome measures. For this analysis logistic regression models were used.

Repeated-measures ANOVA was utilised to analyse the synthesis of albumin and urea by human hepatocytes isolated from normal, PBC/PSC, ALD and normal resected liver tissue.

Results

Liver wedges were prepared as shown in Figure 1 and processed as detailed in the Methods section. Figure 2a shows representative images of primary human hepatocytes, isolated from a liver with PBC, in culture for the first week after isolation. Similar morphological changes were observed during the first week after successful cell isolation from normal, PSC, ALD and normal resected liver tissue. Figure 2b demonstrates the morphological features of primary human hepatocytes isolated from these various livers 3 days after isolation. The morphology of primary human hepatocytes after 3 days in culture was maintained for at least one week after successful isolation.

The type of livers used and the main results of all human hepatocyte isolations are shown in table 1. We processed and

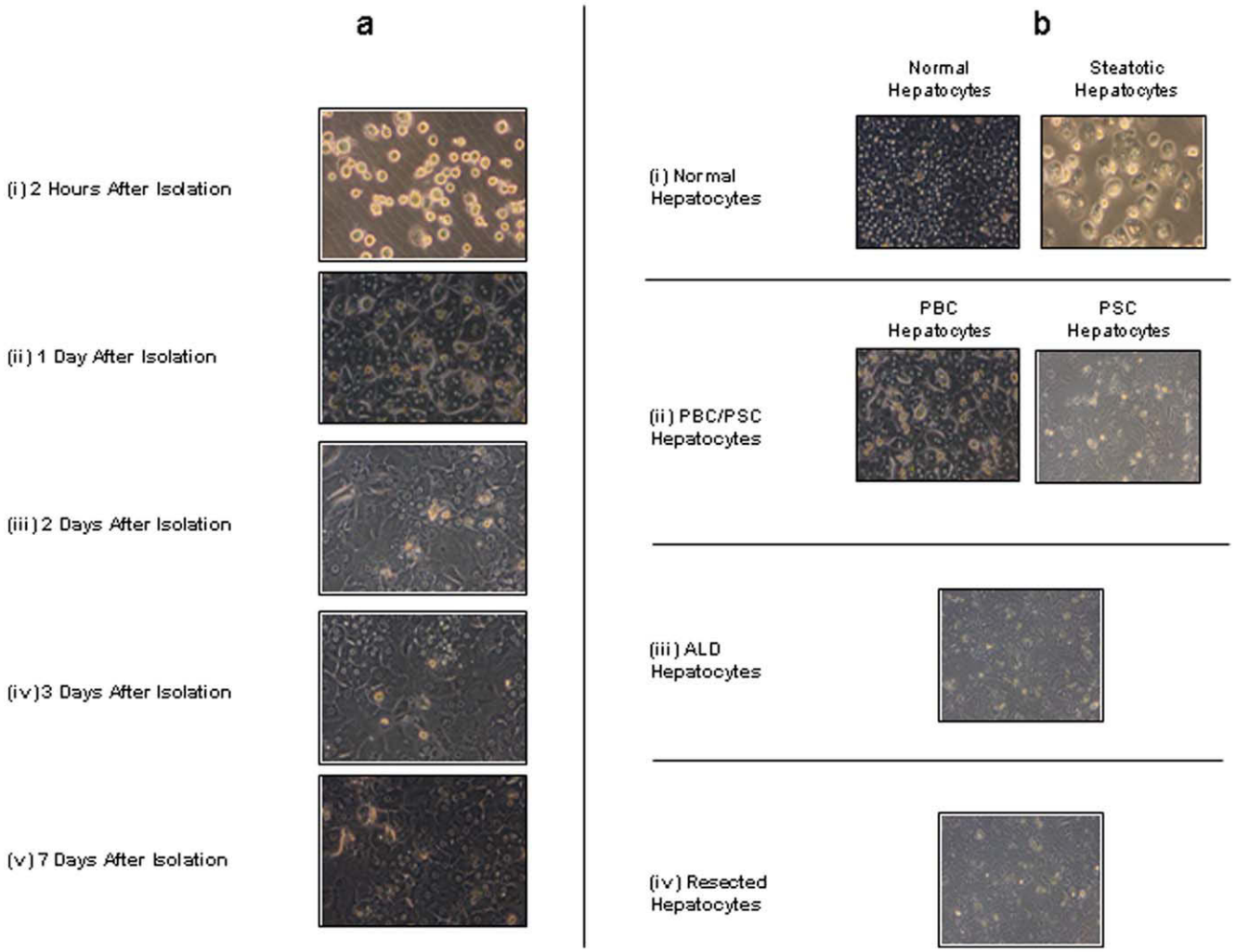

Figure 2. Morphology of Primary Human Hepatocytes after Isolation in Culture. (a) Comparison of the morphological appearance of primary human hepatocytes isolated from primary biliary cirrhosis (PBC) attached to collagen-coated plates at (i) 2 hours after isolation (magnification 20×), (ii) 1 day after isolation, (iii) 2 days after isolation, (iv) 3 days after isolation and (v) 7 days after isolation using light microscopy. The representative images show the change in morphology of primary human hepatocytes isolated from PBC livers during 1-week in culture. Immediately after isolation, cells appear ovoid and phase bright. Following 1 day in culture the cells appear binucleate and have formed a confluent monolayer. Primary human hepatocytes maintain this morphology throughout the one week culture period. Similar morphological changes were observed for human hepatocytes isolated from normal, ALD and normal resected liver tissue (data not shown). (b) Representative images of the morphology of human hepatocytes isolated from normal, PBC/PSC, ALD and normal resected liver tissue are shown in culture 3 days after successful cell isolation. Human hepatocytes demonstrated and maintained this morphology for at least one week following successful isolation. (i) Demonstrates the morphology of human hepatocytes isolated from normal liver tissue and macro-steotic liver tissue (magnification 20×). Primary human hepatocytes isolated from normal liver tissue display the typical cubic binucleate cell morphology. In contrast, primary human hepatocytes isolated from overtly macro-steatotic livers demonstrate obvious micro-vesicular steotosis. (ii) Human hepatocytes isolated from end stage biliary cirrhosis (PBC/PSC) again show the typical features of cells in culture with a cubic and binucleate morphology. (iii–iv) Cells isolated from ALD and normal resected liver show similar morphological features to human hepatocytes isolated from normal non-steatotic livers and biliary cirrhosis but also exhibit micro-vesicular steatosis.
doi:10.1371/journal.pone.0018222.g002

isolated human hepatocytes from 104 liver wedges over a two year period. A variety of liver diseases were used including, as detailed above, ALD, biliary cirrhosis (PBC and PSC), normal resected liver and normal liver tissue (donor liver tissue, resections for benign liver disease and cut-down specimens). A large proportion of livers used in our study were from cirrhotic, end stage liver diseases (54%). Normal resected liver tissue was defined as liver tissue from patients with colorectal metastasis accounted for 26% of livers used. All these latter patients had received pre-operative chemotherapy for reduction of tumour mass prior to surgery.

Isolated cells from human liver tissue were all positive for the hepatocyte cell marker, Cytokeratin 18 and were negative for the biliary epithelial cell marker, Cytokeratin 19, and the hepatic progenitor cell marker, CD326 (EpCAM) (Figure 3a). Furthermore, all hepatocytes isolated from normal and diseased liver tissue demonstrated albumin and urea synthesis in the first week after isolation (Figure 3b). Human hepatocytes isolated from normal, normal resected and biliary cirrhosis showed significantly increased albumin synthesis after two days in culture. Interestingly, human hepatocytes isolated from ALD livers demonstrated

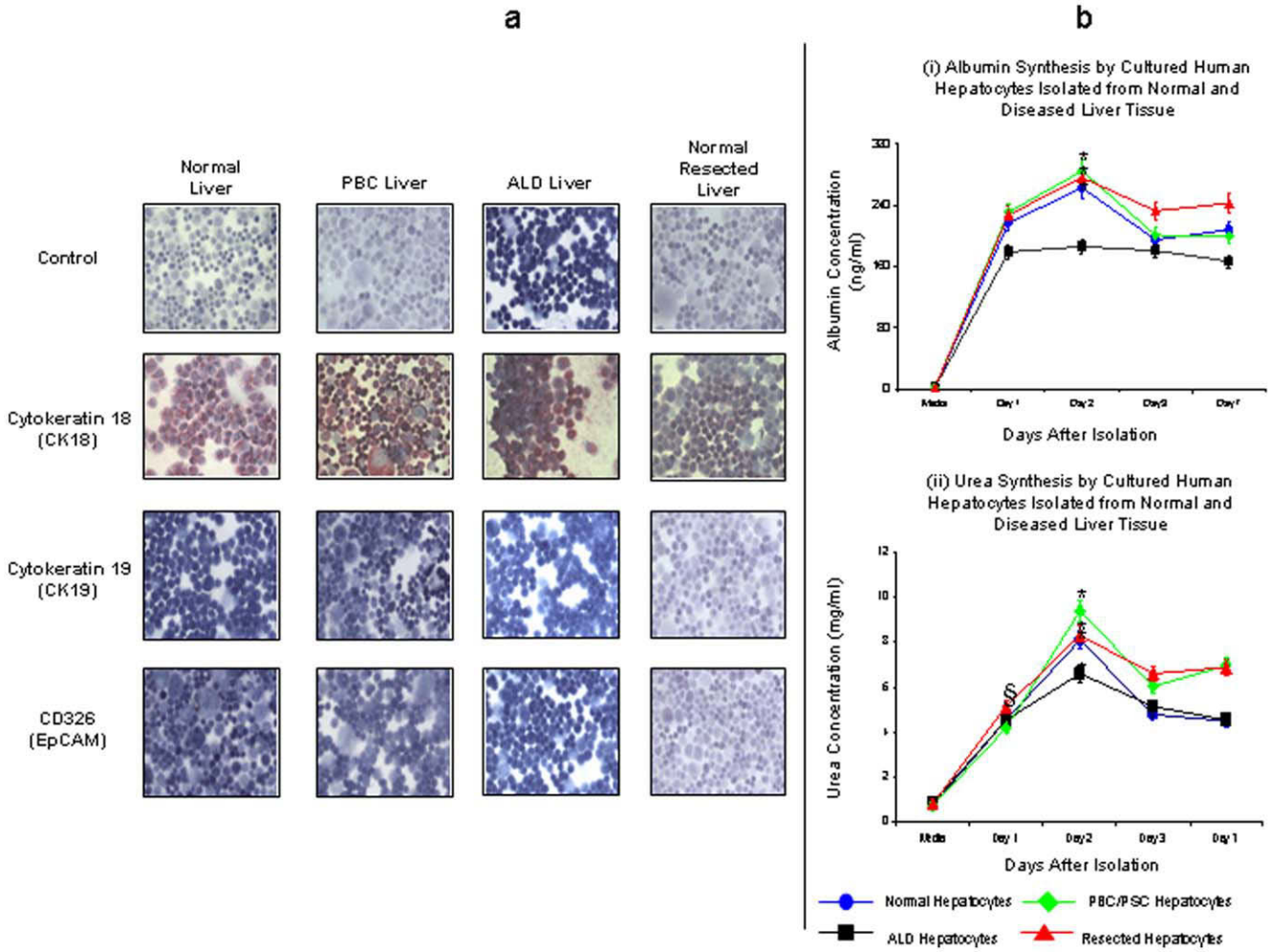

Figure 3. Immunostaining of Cytokeratin 18, Cytokeratin 19 and CD326 and Metabolic Activity of Primary Human Hepatocytes Isolated from Normal and Diseased Liver Tissue. (a) Human hepatocytes isolated from normal, PBC, ALD and normal resected liver tissue show strong staining for the intracellular hepatocyte marker Cytokeratin 18 (CK18). In contrast, isotype matched controls immunoglobulin showed no positivity. Furthermore, isolated human hepatocytes showed no staining with the biliary epithelial cell marker Cytokeratin 19 (CK19) or hepatic progenitor cell marker CD326 (EpCAM). Cytospins of human hepatocytes were made immediately after successful cell isolation, fixed in acetone for 5 min and stored at $-20^{\circ}C$ until immuno-staining was performed. (b) Following successful isolation, human hepatocytes isolated from normal, PBC/PSC, ALD or normal resected liver tissue were able to synthesise albumin (i) for at least one week demonstrating active metabolic activity in culture. Human hepatocytes isolated from normal, PBC/PSC and normal resected liver tissue show significantly greater albumin synthesis after two days in culture (*$p<0.05$). Morover, human hepatocytes isolated from ALD livers synthesised significantly less albumin than other types of human hepatocytes ($p<0.05$). In addition, human hepatocytes isolated from normal resected liver tissue synthesised significantly greater amounts of albumin than normal hepatocytes ($p<0.037$). ($n = 3–4$ separate samples). Human hepatocytes isolated from normal, PBC/PSC, ALD and normal resected liver tissue were also able to synthesise urea (ii) for at least one week following successful cell isolation. Human hepatocytes isolated from both normal and diseased liver tissue synthesised significantly lower levels of urea one day after isolation (§$p<0.001$) compared to the remainder of the culture period, but all human hepatocytes produced significantly more urea on day 2 when compared to other days (*$p<0.001$). Finally, PBC/PSC and normal resected human hepatocyte synthesis significantly greater amounts of urea when compared to the other human hepatocytes ($p<0.05$) but there was no significant difference between PBC/PSC and resected human hepatocytes. ($n = 3–4$ separate samples).
doi:10.1371/journal.pone.0018222.g003

significantly reduced levels of albumin production when compared to other hepatocytes ($p<0.05$). Urea synthesis by human hepatocytes demonstrated similar characteristics, with production of urea being significantly greater on day 2 when compared to other days in culture. Of note biliary cirrhosis and normal resected human hepatocyte produce significantly more urea in culture when compared to other human hepatocytes.

Absolute cell count after isolation was an important parameter on which to assess efficacy of the procedure. Univariable analysis revealed that disease type ($p<0.001$, Fisher's Exact test) was the only factor to have a significant bearing upon total cell count after primary isolation. Multivariable analysis showed that ALD livers have a significantly lower cell yield when compared to other liver categories ($p<0.15$ – table 1).

Overall, for all human hepatocyte isolations we report a median cell viability of 40%. Human hepatocytes isolated from biliary cirrhosis (PBC and PSC) had the highest median cell viability (55%). Univariable and Multivariable analysis showed the only factor which had an effect upon improving cell viability was the time delay between hepatectomy and beginning of the perfusion procedure ($p<0.05$, Mann-Whitney test). Complete processing within 3 hours resulted in a significantly higher cell viability (>50%), compared to time delays greater than 5 hours ($p<0.05$, Odds Ratio = 3.594). Whether the delay is 3–5 hours or more

Table 1. The Type of Livers used and the Main Results of All Human Hepatocyte Isolations.

Liver Type	Time Delay (hrs)	Weight (g)	Perfusion Time (min)	Absolute Cell Count After Perfusion $\times 10^3$	Viability (%)	Success Rate (%)
Normal (n = 21)	2.5 (1–14)	110 (66–413)	1.5 (1–11)	57 (75–200,000)	46 (0–100)	53
Donor Liver (n = 7)	4 (2–14)	117 (101–150)	1.5 (1–11)	1500 (75–200,000)	20 (0–60)	29
Normal Liver (n = 14)	2 (1–4)	105 (66–413)	2 (1–7)	505 (75–32,000)	50 (10–100)	64
Resected (n = 27)	2.5 (1–16)	90 (50–180)	1.5 (1–5)	220 (50–6,000)	50 (0–100)	53
Biliary Cirrhosis (n = 24)	2 (1–11)	106 (78–200)	1.5 (1–8.5)	720 (200–7,000)	55 (0–100)	71*
ALD (n = 24)	2.5 (1–13)	110 (64–220)	3 (1–19)	155† (20–3,000)	40 (0–100)	29
Others (n = 8)	4.5 (1–12)	101 (56–115)	5.5 (3–17)	225 (40–3,000)	7.5 (0–70)	13
TOTAL (104)	2 (1–16)	110 (50–413)	2.5 (1–19)	350 (20–200,000)	40 (0–100)	51

The time delay, weight of liver wedges, perfusion time, absolute cell count after perfusion, cell viability and success rate are shown for various liver categories; Normal (donor liver tissue, normal benign tissue and cut-down specimens), normal resected liver tissue, biliary tissue (PBC and PSC), ALD and others (cystic fibrosis 2, cryptogenic fibrosis 2, alpha-1-antitypsin deficiency 1, autoimmune hepatitis 1 and non-alcoholic steatohepatitis 2). All values are represented as medians and the values in parentheses represent the range. n, number of cases.

†$p<0.05$, multivariable analysis showing ALD livers yield significantly lower cell yields when compared to other liver diseases.

*$p<0.05$, multivariable analysis showing biliary cirrhosis yielded a higher success rate of human hepatocyte isolation when compared to other liver diseases.

doi:10.1371/journal.pone.0018222.t001

than 5 hours did not have a significant effect on the likelihood of the cell viability being greater than 50% ($p = 0.375$, Odds Ratio = 1.725). These data are summarised in Table 2. In our study we used Percoll density gradient centrifugation to enrich hepatocytes purity where cell viability was low but absolute cell count high (n = 8). These data are summarised in Table 3. Percoll enhanced purity of human hepatocyte isolates but at the expense of cell count, hence the need for a relatively high absolute cell count after the initial liver preparation.

We assigned all donor liver tissue, resections performed for benign liver disease (recurrent cholangitis, focal nodular hyperplasia and haemangiomas) and cut down specimens as 'normal' liver tissue. These livers had no signs of intrinsic liver disease. This group was analysed as a whole and as a sub-group, where donor liver tissue was compared to normal liver tissue (resections from benign liver disease and cut down specimens). Sub-group analysis was carried out to determine whether the level of steatosis had an effect upon absolute cell count, cell viability and success rate of subsequent culture. The level of steatosis in the two groups is shown in Table 4. We found no difference in absolute cell count, cell viability, and success rate between the donor liver and normal liver groups. The success of isolating human hepatocytes from this group as a whole was good (53%) but normal liver tissue obtained from hepatic resections carried out for benign disease and cut-down specimens had a statistically higher success rate (64%) when compared to donor liver tissue (20%).

Table 2. Effect of Time Delay Between Hepatectomy and Beginning of the Perfusion Procedure Upon Human Hepatocyte Cell Viability Following Isolation Procedure.

Time Delay (hrs)	Median Cell Viability (%)
<3	53
3–5	25
>5	20

doi:10.1371/journal.pone.0018222.t002

Our series is the largest reported of human hepatocyte isolations from cirrhotic livers (n = 55). We report a median success rate when isolating hepatocytes from cirrhotic livers of 45%. Table 1 shows that liver wedges from biliary cirrhosis (PBC and PSC) had the highest success rate of all livers used in our study (71%). For all liver isolations, univariate analysis showed a significant difference in time delay between hepatectomy and beginning of liver perfusion ($p<0.001$, Mann-Whitney test), perfusion time ($p<0.05$, Mann-Whitney test) and disease type ($p<0.05$, Fisher's Exact test) between the groups of successful and unsuccessful isolations. Multivariable analysis revealed disease type ($p<0.05$) and time delay between hepatectomy and beginning of perfusion ($p<0.05$) were significant factors affecting successful human hepatocyte isolation. As described above for cell viability, success is significantly dependent upon time delay ($p<0.01$), with a delay of less than 3 hours resulting in improved success rates compared to those of more than 5 hours ($p<0.05$, Odds Ratio = 3.735).

Discussion

The preparation of primary human hepatocytes is a time consuming, logistically demanding, and expensive process. The demand for high quality human hepatocytes for cell transplantation and pharmo-toxicological studies continues to rise. However, the availability of human liver tissue for laboratory investigation remains limited. Therefore, cirrhotic end-stage livers, which are more readily available to researchers, represent another potential source of human hepatocytes. We know of no other studies which evaluate and compare the outcome of human hepatocytes isolation

Table 3. Effect of Percoll upon Cell Viability and Absolute Cell Count.

Absolute Cell Count after Preparation $\times 10^3$	Viability (%)	Absolute Cell Count after Percoll $\times 10^3$	Viability after Percoll (%)
550 (200–200,000)	35 (10–50)	175 (100–400)	85 (55–90)

The effects of Percoll upon human hepatocyte isolation procedures. We used Percoll after eight human hepatocyte isolation procedures (normal resected liver tissue 1, biliary cirrhosis 5, donor liver tissue 1 and normal benign liver tissue 1). All values are represented as medians and the values in parentheses represent the range.

doi:10.1371/journal.pone.0018222.t003

from all sources, including end-stage liver disease, using one standard isolation protocol. Our experience highlights that the isolation of primary human hepatocytes from normal or diseased livers is a viable proposition given appropriate methods.

Our data confirm that isolating human hepatocytes from ALD livers is technically challenging and we had a success rate of only 29%. Thus the use of ALD livers for hepatocyte isolation is a questionable proposition. This may in part be explained by the variable disease stage of our ALD cohort which included patients with advanced cirrhosis or it may reflect toxicological damage resulting from the effects of alcohol. Excluding the 'other' disease categories, ALD livers had the longest median perfusion time again presumably reflecting that these livers were from patients with more advanced liver cirrhosis. Moreover, human hepatocytes isolated from ALD demonstrate significantly less albumin production when compared to the other human hepatocytes supporting the hypothesis that prior alcohol exposure may affect the function of these hepatocytes. Our data further highlight that tissue from patients with biliary cirrhosis (PBC or PSC) provides high yields of hepatocytes (success rate 71%). Furthermore, such hepatocytes demonstrate the highest levels of albumin and urea production. As discussed below, this success rate was similar to that we obtained using non-diseased liver tissue. In biliary cirrhosis cytoprotective agents such as ursodeoxycholic acid (UDCA) are routinely used therapeutically. The ability of UDCA to inhibit the accumulation of reactive oxygen species (ROS) [15] and its known anti-apoptotic effects may provide hepato-protection [16]. Indeed in our reported series all patients with biliary cirrhosis were taking UDCA at the time of liver transplantation. Thus UDCA may promote human hepatocytes isolation in an analogous way to that suggested for the antioxidant, N-acetylcysteine (NAC) [3]. Conversely, alcohol consumption increases ROS production which instigates hepatocyte injury during ALD [17] as well as inducing toxic metabolites and cytokines that perpetuate hepatocyte injury. It is thus possible that hepatocytes from patients with ALD are sensitised to the cellular stress induced by enzymes used in the digestion process resulting in increased hepatocyte cell death and lower cell viability and yields. The yields from end-stage cirrhotic livers other than ALD and biliary cirrhosis were very poor results (success rate 13%) and we would not recommend the routine use of such livers for cell isolation.

Table 4. The Level of Steatosis in Liver Wedges taken from Donor Liver Tissue and Normal Liver Tissue.

	Minimal/ None	Mild	Moderate	Severe
Donor liver tissue (n = 6)	1	1	3	1
Normal liver tissue (n = 12)	10	1	1	-

The level of steatosis in liver wedges taken from normal liver tissue. The level of steatosis was classified as minimal/none = 0–5%, mild = 5–33%, moderate = 33–66% and severe = ≥66% after histological analysis of paraffin embedded sections. We were unable to classify the level of steatosis in three liver wedges (1 donor liver and 2 normal livers) as the tissue from those particular livers was not available. n, number of cases.

doi:10.1371/journal.pone.0018222.t004

We report a success rate of 53% for hepatocyte isolation from normal resected livers, which is lower than that reported by other authors [7,18]. There are several potential explanations for this. Other studies used different enzyme cocktails and may have been more selective when deciding which livers to process [1]. Recent studies have used the enzyme liberase to isolate hepatocytes from normal resected liver tissue and have reported higher cell viabilities and cell yields [1]. We concur with previous authors that normal resected tissue is a good source of human hepatocytes. However, our recent study suggests that human hepatocytes isolated from normal resected liver tissue may differ functionally in their response to physiological stimuli [4]. Most authors have previously assumed that the function of human hepatocytes isolated from normal liver tissue was consistent between different sources [18]. In light of our findings further functional analyses of human hepatocytes isolated from different liver diseases should be carried out before conclusions can be drawn about their 'normality'.

The isolations we carried out using liver wedges from benign resections and cut down specimens gave good success rates (64%) compared to donor liver tissue (29%) consistent with results reported by others [7]. The donor livers used in our study had been turned down for transplantation as a result of macrosteatosis and as Figure 2b demonstrates human hepatocytes from these steatotic livers also exhibit micro-vesicular steatosis. Within the steatotic livers the rate of successful hepatocyte isolation was greater than in those with mild compared with moderate or severe steatosis (70% vs. 20%). Previous authors have also noted that high degrees of steatosis generally did not favour successful cell isolation [6,7]. Steatotic hepatocytes have higher intracellular ROS levels and are thus potentially more susceptible to damage [3]. The recent work of Sagias *et al* suggests that the addition of NAC to perfusion fluids may improve hepatocyte yields from steatotic livers. Another, contributory factor for the lower viability and yield of hepatocytes from donor liver is the longer cold ischaemic time that donor livers have been exposed to when compared to normal livers (Table 1).

Previous authors have suggested that the optimal liver wedge weight for human hepatocyte isolation is approximately 100 g. We agree with this and in the present study the majority of liver wedges were between 80–120 g. In our study a median perfusion time of 2.5 min was required to digest the livers, as judged by the admission of a digit into the liver substance. Other studies report digestion times ranging from 20–47 min (1) [19]. This could simply be a reflection of different enzyme types, concentrations or differences between batches. In our series the same enzyme batches were used for all isolations. The enzyme cocktail we used allowed isolation of cells from end-stage cirrhotic livers and it is possible that this enzyme concentration may be excessive for normal resected and donor liver tissue thereby contributing to our low yield and viability compared with other reports.

Although perfusion time was significant in the univariable analysis it fell out during multivariable analysis. The reason for this

is likely to be correlation with the time delay between hepatectomy and beginning of liver perfusion (Spearman's Rho = .377, $p<.001$) which remained significant even after adjusting for perfusion time.

Thus we provide evidence to suggest that the time delay between hepatectomy and beginning of liver perfusion should be kept to less than 3 hours. From our experience of isolating human hepatocytes from cirrhotic livers after an initial learning curve the operator becomes skilled at recognising when adequate digestion has occurred thereby avoiding overdigestion of tissue.

In conclusion, we report that the time delay between hepatectomy and beginning of liver perfusion is the most important factor in determining the likelihood of success of the procedure. Furthermore, we suggest the shortest possible digestion time is desirable. If protocols similar to ours are followed human hepatocytes can be isolated successfully from normal and diseased liver tissue.

Acknowledgments

We would like to thank Professor S.G. Hubscher for assistance with the grading of the level of steatosis in human liver tissue. We would also like to thank the clinical team at the Queen Elizabeth Hospital, Birmingham for the procurement of liver tissue.

Author Contributions

Conceived and designed the experiments: RHB SCA DHA KTW DCB. Performed the experiments: RHB DCB. Analyzed the data: JH GMR PNN. Contributed reagents/materials/analysis tools: CJW SMC EH. Wrote the paper: RHB SCA DHA CJW PNN.

References

1. Kawahara T, Toso C, Douglas DN, Nourbakhsh M, Lewis JT, et al. (2010) Factors affecting hepatocyte isolation, engraftment, and replication in an in vivo model. Liver Transpl 16(8): 974–982.
2. Hughes RD, Mitry RR, Dhawan A, Lehec SC, Girlanda R, et al. (2006) Isolation of hepatocytes from livers from non-heart-beating donors for cell transplantation. Liver Transpl 12(5): 713–717.
3. Sagias FG, Mitry RR, Hughes RD, Lehec SC, Patel AG, et al. (2010) N-acetylcysteine improves the viability of human hepatocytes isolated from severely steatotic donor liver tissue. Cell Transplant. DOI:10.3727/096368910X514620.
4. Bhogal RH, Curbishley SM, Weston CJ, Adams DH, Afford SC (2010) Reactive oxygen species mediate human hepatocyte injury during hypoxia-reoxygenation. Liver Transpl 16(11): 1303–1313.
5. Li AP (2007) Human hepatocytes: isolation, cryopreservation and applications in drug development. Chem Biol Interact 168(1): 16–29.
6. Alexandrova K, Griesel C, Barthold M, Heuft HG, Ott M, et al. (2005) Large-scale isolation of human hepatocytes for therapeutic application. Cell Transplant 14(10): 845–853.
7. Vordnan FW, Katenz E, Schwartlander R, Morgul MH, Raschzok N, et al. (2008) Isolation of primary human hepatocytes after partial hepatectomy: criteria for identification of the most promising liver specimen. Artif Organs 32(2): 205–213.
8. Lecluyse EL, Alexandre E (2010) Isolation and culture of primary hepatocytes from resected human liver tissue. Methods Mol Biol 640: 57–82.
9. Gonzalez R, Collado JA, Nell S, Briceno J, Tamayo MJ, et al. (2007) Cytoprotection properties of alpha-tocopherol are related to gene regulation in cultured D-galactosamine-treated human hepatocytes. Free Radic Biol Med 43(10): 1439–1452.
10. Dhawan A, Mitry RR, Hughes RD (2005) Hepatocyte transplantation for metabolic disorders, experiences at King's College hospital and review of literature. Acta Gastroenterol Belg 68(4): 457–460.
11. Berry MN, Friend DS (1969) High-yield preparation of isolated rat liver parenchymal cells: a biochemical and fine structural study. J Cell Biol 43(3): 506–520.
12. Li AP, Roque MA, Beck DJ, Kaminski DL (1992) Isolation and culturing of hepatocytes from human livers. J Tissue Cult Meth 14: 139–146.
13. Pichard L, Raulet E, Fabre G, Ferrini JB, Ourlin JC, et al. (2006) Human hepatocyte culture. Meth Mol Biol 320: 283–293.
14. Mitry RR, Hughes RD, AW MM, Terry C, Mieli-Vergani G, et al. (2003) Human hepatocyte isolation and relationship of cell viability to early graft function. Cell Transplant 12(1): 69–74.
15. Rodrigues CM, Fan G, Wong PY, Kren BT, Steer CJ (1998) Ursodeoxycholic acid may inhibit deoxycholic acid-induced apoptosis by modulating mitochondrial transmembrane potential and reactive oxygen species production. Mol Med 4: 165–178.
16. Guicciardi ME, Gores GJ (1998) Is ursodeoxycholate an antiapoptotic drug? Hepatology 28: 1077–1084.
17. Schaffert CS, Duryee MJ, Hunter CD, Hamilton BC, 3rd, DeVeney AL, et al. Alcohol metabolites and lipopolysaccharide: roles in the development and/or progression of alcoholic liver disease. World J Gastroenterol 2009 15(10): 1209–1218.
18. Hewes JC, Riddy D, Morris RW, Woodrooffe AJ, Davidson BR, et al. (2006) A prospective study of isolated human hepatocytes function following liver resection for colorectal liver metastases: the effects of prior exposure to chemotherapy. J Hepatol 45(2): 263–270.
19. Laba A, Ostrowska A, Patrzalek D, Paradowski L, Lange A (2005) Characterization of human hepatocytes isolated from non-transplantable livers. Arch Immunol Ther Exp (Warsz) 53(5): 442–453.

Appendix IV

OPEN ACCESS Freely available online

PLoS one

Activation of CD40 with Platelet Derived CD154 Promotes Reactive Oxygen Species Dependent Death of Human Hepatocytes during Hypoxia and Reoxygenation

Ricky H. Bhogal*, Christopher J. Weston, Stuart M. Curbishley, David H. Adams, Simon C. Afford

Centre for Liver Research, School of Infection and Immunity, Institute of Biomedical Research, The Medical School, The University of Birmingham, Edgbaston, Birmingham, United Kingdom

Abstract

Background: Hypoxia and hypoxia-reoxygenation (H-R) are pathogenic factors in many liver diseases that lead to hepatocyte death as a result of reactive oxygen species (ROS) accumulation. The tumor necrosis factor super-family member CD154 can also induce hepatocyte apoptosis via activation of its receptor CD40 and induction of autocrine/paracrine Fas Ligand/CD178 but the relationship between CD40 activation, ROS generation and apoptosis is poorly understood. We hypothesised that CD40 activation and ROS accumulation act synergistically to drive human hepatocyte apoptosis.

Methods: Human hepatocytes were isolated from liver tissue and exposed to an *in vitro* model of hypoxia and H-R in the presence or absence of CD154 and/or various inhibitors. Hepatocyte ROS production, apoptosis and necrosis were determined by labelling cells with 2′,7′-dichlorofluorescin, Annexin-V and 7-AAD respectively in a three-colour reporter flow cytometry assay.

Results: Exposure of human hepatocytes to recombinant CD154 or platelet-derived soluble CD154 augments ROS accumulation during H-R resulting in NADPH oxidase-dependent apoptosis and necrosis. The inhibition of c-Jun *N*-terminal Kinase and p38 attenuated CD154-mediated apoptosis but not necrosis.

Conclusions: CD154-mediated apoptosis of hepatocytes involves ROS generation that is amplified during hypoxia-reoxygenation. This finding provides a molecular mechanism to explain the role of platelets in hepatocyte death during ischemia-reperfusion injury.

Citation: Bhogal RH, Weston CJ, Curbishley SM, Adams DH, Afford SC (2012) Activation of CD40 with Platelet Derived CD154 Promotes Reactive Oxygen Species Dependent Death of Human Hepatocytes during Hypoxia and Reoxygenation. PLoS ONE 7(1): e30867. doi:10.1371/journal.pone.0030867

Editor: Gordon Langsley, Institut National de la Santé et de la Recherche Médicale - Institut Cochin, France

Received September 2, 2011; **Accepted** December 29, 2011; **Published** January 25, 2012

Funding: Mr. RH Bhogal's work has been funded by a Wellcome Trust Fellowship (DDDP.RCXH14183). The authors would also like to thank the Birmingham Biomedical Research Unit (BRU) and the National Institute Health Research (NIHR) for continued funding and help with research. The funders had no role in study design, data collection and analysis, decision to publish, or preparation of the manuscript.

Competing Interests: The authors have declared that no competing interests exist.

* E-mail: balsin@hotmail.com

Introduction

Hepatocyte death is central to most liver diseases and is frequently associated with tissue hypoxia. Hypoxia can also occur as a result of ischaemia associated with hepatic surgery or liver transplantation where reoxygenation follows hypoxia and may further exacerbate tissue injury and promote liver inflammation. Central mediators of hepatocyte cell death during hypoxia are the reactive oxygen species (ROS) [1]. ROS, which include superoxide anions, hydrogen peroxide, hypohalus acid and hydroxyl radicals, accumulate in the many liver diseases and have also been implicated in the preservation/reperfusion injury that follows liver transplantation [2].

Under physiological conditions hepatocytes exist in a relatively hypoxic micro-environment [3] which promotes the generation of ROS. Consequently hepatocytes have several cellular mechanisms, including high intracellular glutathione levels, which counteract increases in ROS and thereby limit parenchymal injury [4,5]. It has long been assumed that extracellular ROS, released by Kupffer cells (KCs) and infiltrating neutrophils are the main contributors to hepatocyte injury [6]. However, we recently reported that intracellular ROS can also regulate human hepatocyte cell death during hypoxia and hypoxia-reoxygenation (H-R) [2]. In this micro-environment, hepatocytes will be exposed to an array of pro-inflammatory mediators including cytokines which may augment intracellular ROS production and amplify liver injury.

CD40 and its ligand CD154, members of the tumor necrosis factor-(TNF) receptor/ligand superfamily are known to regulate hepatocyte apoptosis [7] and have been implicated in hepatocyte death during hypoxia [8]. CD40 is a type I trans-membrane protein receptor and expressed as a trimeric complex upon the cell surface of many cells including hepatocytes, endothelial cells and cholangiocytes. CD154, a type II trans-membrane protein, is expressed by $CD4^+$ T-lymphocytes, macrophages, mast cells and basophils. It is also expressed by platelets and released in a soluble form following platelet activation. Studies in CD40 and CD154 deficient mice have implicated this pathway in hypoxic liver injury

[8,9]. The mechanism was assumed to involve defective CD40:CD154 priming of T-lymphocytes. However, we have previously reported that activation of CD40 on hepatocytes or cholangiocytes can induce Fas Ligand (FasL/CD178) expression and autocrine/paracrine Fas-mediated apoptosis [7,10]. CD40:CD154 interactions have also been shown to mediate ROS accumulation in the WEHI231 lymphoid cell line [11] leading us to hypothesise that CD40 activation could be implicated in ROS-mediated hepatocyte death.

Following ligation by trimeric CD154, CD40 is activated and internalized. CD40 has no active intracellular kinase domain and binds to members of the tumor necrosis factor receptor-associated factor (TRAF) family which are responsible for activating downstream signaling pathways. In lymphoid cells, TRAFs recruit the cystolic enzyme nicotinamide adenine dinucleotide phosphate oxidase (NADPH oxidase) to the plasma membrane providing a potential mechanism to generate ROS [11]. We now report that in primary human hepatocytes, CD40 ligation leads to NADPH-dependent intracellular ROS generation and hepatocyte death in hypoxic conditions demonstrating for the first time how TNF receptor activation and ROS can co-operate to mediate epithelial cell injury in chronic inflammation and hypoxia/reperfusion injury.

Materials and Methods

Ethics Statement

Liver tissue was obtained from surgical procedures carried out at the Queen Elizabeth Hospital, Birmingham, UK. Ethical approval for the study was grant by the Local Research Ethics Committee (LREC) (Leicestershire and Rutland Ethics Committee - reference number 06/Q702/61). Informed written consent was obtained from all participants involved in the study.

Human Hepatocyte Isolation

Liver tissue was obtained from fully consenting patients undergoing transplantation, hepatic resection for liver metastasis, hepatic resection for benign liver disease or normal donor tissue surplus to surgical requirements. Human hepatocytes were isolated using a method that we have described previously [2,12].

Model of hypoxia and H-R injury

We used a model of *in vitro* hypoxia and H-R that we have described previously [2]. In experiments involving the NADPH oxidase inhibitor, DPI; JNK inhibitor SP600125, or p38 inhibitor, PD169316, all reagents were made fresh as stock solutions and added using the correct dilutional factor to the relevant experimental wells. Specifically, 10 μg DPI (Sigma) was dissolved in molecular grade dimethyl sulfoxide (DMSO), 10 μg rotenone (Sigma) was dissolved in chloroform (Sigma), 50 μg SP600125 (Sigma) was dissolved in DMSO and 50 μg PD169316 (Sigma) was dissolved in DMSO and were diluted appropriately to give working concentrations of 10 μM, 2 μM, 10 μM and 10 μM respectively. In experiments using inhibitors/antioxidants, solvent alone wells were used to control for vehicle effects. In experiments using inhibitors/antioxidants hepatocytes were pre-treated with agents for up to 4 hours before placement of the cells into normoxia and hypoxia. For H-R experiments fresh inhibitor/antioxidants were added at the time of placement into reoxygenation. Recombinant human soluble CD154 (1 μg/mL, Enzo Life Sciences, UK) and 1 μg/mL Cross-linker for Ligands (Enzo Life Sciences, UK) were added to cells at the time of entry into hypoxia or H-R. Where cells had been pre-treated with inhibitors/antioxidants CD154 and Cross-linker for Ligands were added after 4 hours.

Determination of Human Hepatocyte CD40 Expression and FasL Expression

Following appropriate incubation of human hepatocytes within normoxia, hypoxia and H-R, cells were trypinised and washed in FACs buffer (Phosphate-buffered saline (PBS) pH 7.2 with 10% v/v heat inactivated foetal calf serum (Gibco). For CD40 expression, cells were then incubated with anti-human CD40 antibody that was conjugated to the APC fluorophore (1:100 dilution; Caltag, UK) for 45 min at 4°C. Mouse IgG1-APC (1:100 dilution; Caltag, UK) was used as a negative control. For FasL expression, cells were then incubated with anti-human FasL antibody that was conjugated to the FITC fluorophore (1:100 dilution; Abcam, UK) for 45 min at 4°C. Mouse IgG2a-FITC (1:100 dilution; Abcam, UK) was used as a negative control. Following this cells were washed in FACs buffer and resuspended in PBS, pH 7.2. At least 20,000 events were recorded within the gated region of the flow cytometer for each human hepatocyte cell preparation in each experimental condition. Only the cells within the gated region were used to calculate Mean Fluorescence Intensity (MFI) as described in our previous study [2].

Determination of Human Hepatocyte ROS Accumulation, Apoptosis and Necrosis

ROS production, apoptosis and necrosis were determined using a three-colour reporter assay system as previously described [2]. At least 20,000 events were recorded within the gated region of the flow cytometer for each human hepatocyte cell preparation in each experimental condition. Only the cells within the gated region were used to calculate MFI.

Platelet isolation and activation

Platelets were isolated by modifying a previously published method from fully consenting healthy individuals [13]. Platelet-rich plasma (PRP) was prepared by centrifuging 5 mL of heparinised blood for 5 min at $300\times g$. Following this the PRP was withdrawn and the platelet count adjusted to 1×10^6 platelets/mL in Williams E media. Platelets were then seeded onto plastic. Following 30 min incubation at room temperature the platelets had settled, become activated and spread to form a confluent monolayer. The Williams media was then aspirated and passed through a 0.2 μm syringe filter. The PCM was aliquoted and frozen at −70°C until required. Media was thawed and added to cells as required.

Determination of Soluble CD154 and Immunomagnetic Depletion of CD154 from PCM

To confirm the presence and quantity of CD154 in the PCM levels were quantified by ELISA and platelet-derived CD154 was removed via immuno-magnetic depletion. Briefly, soluble human CD154 was measured in both PCM and CD154-depleted PCM using a sandwich ELISA kit (Peprotech, UK). For immunomagnetic depletion of CD154, anti-human CD154 antibody (1 μg/mL; Abcam, UK) was complexed to pan-mouse IgG magnetic Dynabeads (Invitrogen, Paisley, UK) for 90 min at room temperature. Following this, the antibody-magnetic bead complexes were extensively washed. Complexes were then incubated with PCM for a further 90 min at room temperature. Finally, magnetic beads were retrieved from solutions and this media was subsequently used in experiments as CD154-depleted PCM.

Statistical Analysis

All data are expressed as mean ± S.E. Statistical comparisons between groups were analysed by Student's *t* test. All differences were considered statistically significant at a value of $p<0.05$.

Results

CD40 expression in human hepatocytes during hypoxia and H-R

Primary human hepatocytes constitutively expressed CD40 on the cell membrane as previously reported [14] but this did not increase in response to hypoxia or H-R *in vitro* (Figure 1).

CD40:CD154 stimulates ROS accumulation in human hepatocytes in an NADPH-dependent manner and regulates apoptosis and necrosis

We have recently reported that intracellular ROS accumulate in hypoxic human hepatocytes and that this is increased further during H-R [2]. Here we investigated whether CD154 could augment human hepatocyte ROS production during normoxia, hypoxia and H-R. Trimeric recombinant human CD154 significantly increased intracellular ROS accumulation within human hepatocytes during normoxia and H-R but not hypoxia. Because CD40:CD154 has been shown to mediate ROS accumulation via TRAF-dependent recruitment of the flavoenzyme NADPH oxidase in lymphoid cell lines [11] we used the specific NADPH oxidase inhibitor Diphenyliodonium (DPI) to assess the involvement of this pathway in ROS generation by human hepatocytes. DPI reduced hepatocyte CD154 mediated ROS production during normoxia, hypoxia and H-R (Figure 2a & 2b).

The increased levels of intracellular ROS induced by CD154 stimulation, during normoxia and H-R, increased human hepatocyte apoptosis and to a lesser extent necrosis (Figure 2c & 2d) and this were reduced by pre-treatment with DPI. CD154 also significantly increased human hepatocyte necrosis during normoxia and H-R that was inhibited by DPI demonstrating that that the CD40:CD154:ROS signaling pathway is NADPH-dependent and results in hepatocyte death.

Mitochondrial ROS has been implicated in hepatocyte apoptosis during hypoxia and H-R [2] leading us to test the effect of inhibiting mitochondrial ROS production upon CD154 mediated apoptosis with the complex I inhibitor, rotenone. Inhibiting mitochondrial ROS production during normoxia and H-R did not reduce human hepatocyte apoptosis in response to CD154 treatment but did reduce apoptosis during hypoxia (Figure 2e).

JNK and p38 regulate apoptotic but not necrotic cell death in human hepatocytes

We next investigated whether CD40:CD154 generated ROS and hepatocyte death was associated with activation of mitogen-

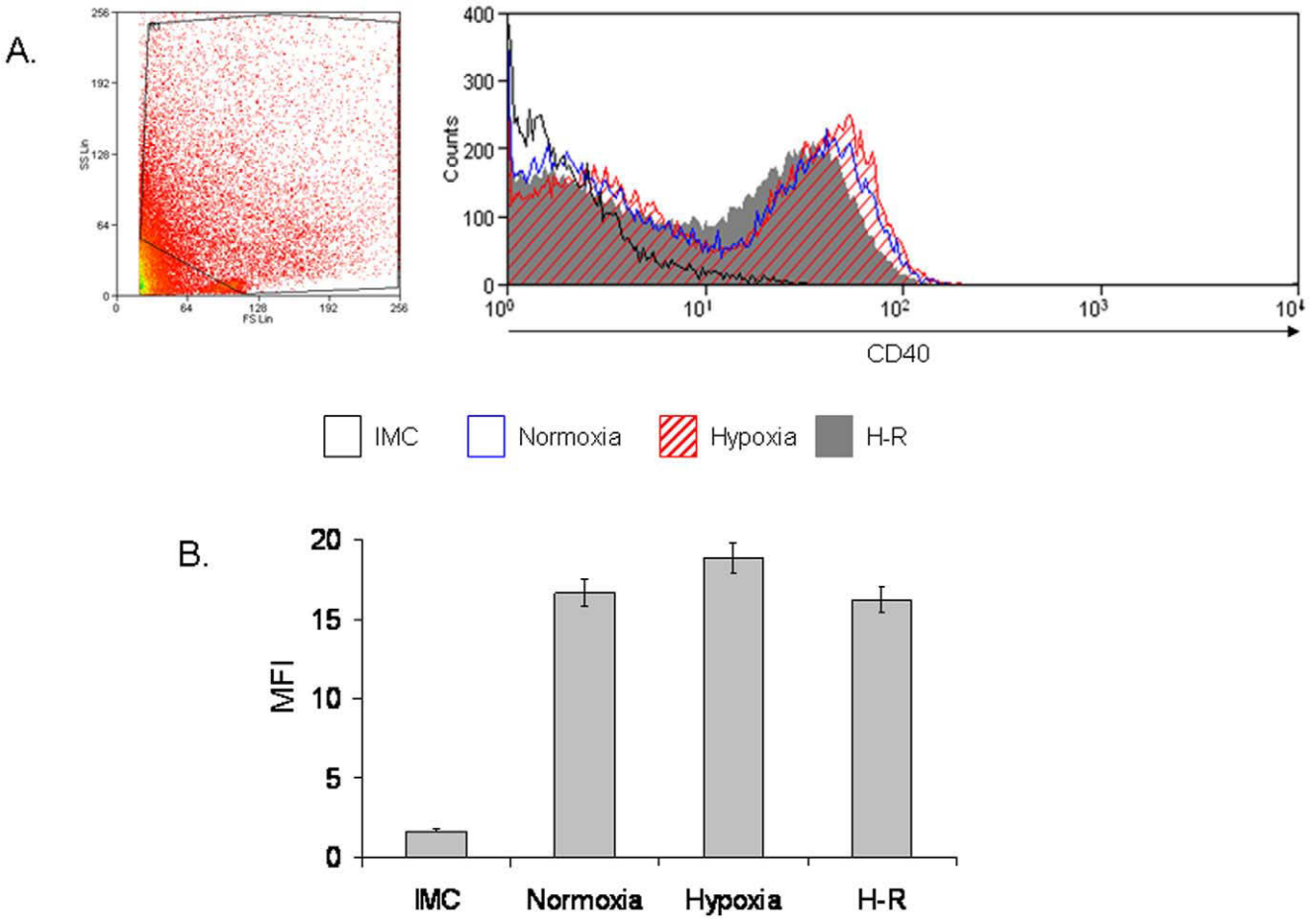

Figure 1. CD40 Expression on Primary Human Hepatocytes. Figure 1a demonstrates a representative flow cytometry plot of CD40 expression on primary human hepatocytes during normoxia, hypoxia and H-R. The plot on the left hand side represents a typical forward scatter (FS) versus side scatter (SS) plot of primary human hepatocytes. The FS versus SS plots shown is from the H-R sample of a liver preparation but similar plots were obtained during normoxia and hypoxia (data not shown). Figure 1b shows a bar chart with the pooled data of three separate experiments illustrating the level of CD40 expression on primary human hepatocytes. Data are expressed as MFI and readings are based upon values taken from cells within the gated region in Figure 1a.
doi:10.1371/journal.pone.0030867.g001

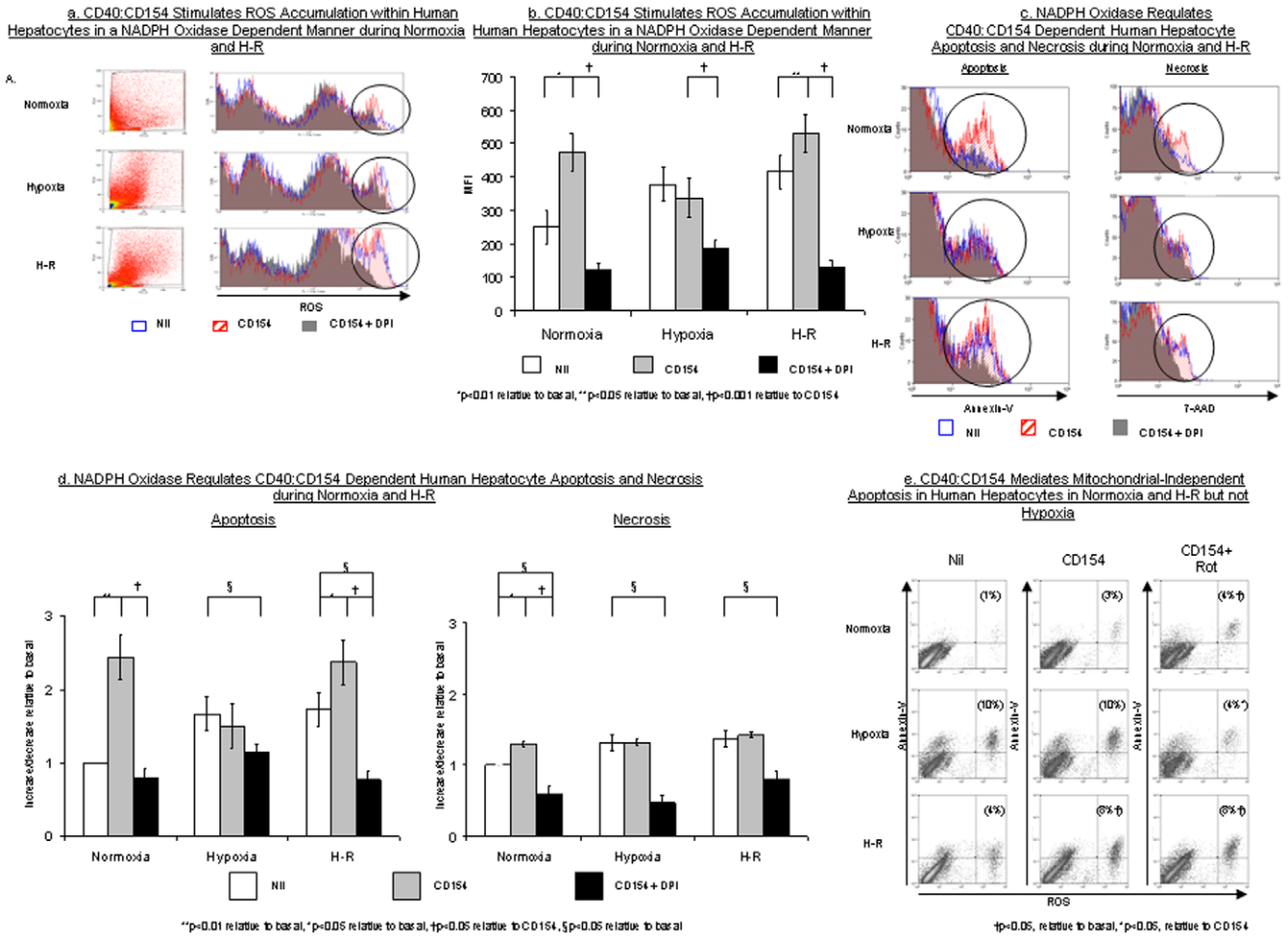

Figure 2. CD40:CD154 regulates ROS accumulation, apoptosis and necrosis within human hepatocytes in a NADPH Oxidase dependent manner during normoxia and H-R. Figure 2a demonstrates representative flow cytometry plots to illustrate the effect of CD154 (hatched red) and CD154 in presence of DPI (solid grey) upon human hepatocyte ROS accumulation during normoxia, hypoxia and H-R. Typical FS versus SS plots of primary human hepatocytes during normoxia, hypoxia and H-R are shown to the left of each flow cytometric plot. The FS versus SS plots shown is from the H-R alone sample of a liver preparation but similar plots were obtained during normoxia and hypoxia (data not shown). The areas of interest on the flow cytometric plots are marked by the vertical ellipses. The area on the left of each ellipse represents cell debris. Cell debris is included within the plot as human hepatocytes vary considerably in size and therefore to include all viable human hepatocytes in the analysis a large gate is required on the flow cytometer, this by necessity includes the cell debris. Figure 2b. shows a bar chart with the pooled data of three separate experiments illustrating the effects of CD154 and CD154+DPI upon human hepatocytes ROS accumulation. Data is expressed as MFI and readings are based upon values taken from cells within the gated region shown in Figure 2a. Data are expressed as mean ± S.E. (*$p<0.01$ relative to basal, **$p<0.05$ relative to basal, †$p<0.001$ relative to CD154). Figure 2c demonstrates representative flow cytometry plots to illustrate the effect of CD154 (hatched red) and CD154 in presence of DPI (solid grey) upon human hepatocyte apoptosis and necrosis during normoxia, hypoxia and H-R. Again, the area of interest within the flow cytometric plots is marked by the vertical ellipse. The same gate has been applied to primary human hepatocytes for these plots as those shown in Figure 2a. Figure 2d. shows a bar chart with the pooled data of three separate experiments illustrating the effects of CD154 and CD154+DPI upon human hepatocytes apoptosis and necrosis during normoxia, hypoxia and H-R. Data is expressed as increase/decrease relative to basal, where basal refers to the level of apoptosis or necrosis during normoxia alone. Data are expressed as mean ± S.E. (**$p<0.01$ relative to basal, *$p<0.05$ relative to basal, †$p<0.05$ relative to CD154, §$p<0.05$ relative to basal). Figure 2e. Human hepatocytes were treated with CD154 or CD154 following pre-treatment with rotenone (Rot) during normoxia, hypoxia and H-R. The percentage of cells staining with both the ROS probe DCF and apoptotic marker, Annexin-V, were assessed by flow cytometry. The percentage of human hepatocytes that stain for both DCF and Annexin-V are shown in parentheses. Data are representative of 3 separate experiments (†$p<0.05$ relative to basal, *$p<0.05$ relative to CD154).

doi:10.1371/journal.pone.0030867.g002

activated protein kinases (MAPKs). MAPKs consist of three sequentially activated kinase modules, namely mitogen-activated protein kinase kinase kinases (MAPKKK/MAP3K) followed by the mitogen-activated protein kinase kinases (MAPKK/MEKK) and finally the MAPKs. The MAPKs superfamily consists of three separate sub-families; extra-cellular regulated protein kinase (ERK), c-Jun *N*-terminal kinase (JNK) and p38. ERK is generally involved in the regulation of cell proliferation and differentiation, whereas JNK and p38 are involved in the regulation of cell death [15].

Unfortunately, primary human hepatocytes are not amenable to siRNA transfection or protein labeling [16,17,18]. Therefore to investigate the effects of JNK and p38 inhibition upon CD154:ROS mediated human hepatocyte apoptosis we used specific JNK and p38 inhibitors [19,20,21]. Inhibition of JNK and p38 in hepatocytes using the specific inhibitors SP600125 and

PD169316 had no effect on ROS accumulation during normoxia, hypoxia and H-R (data not shown) whereas they significantly decreased CD40:CD154 mediated human hepatocyte apoptosis during normoxia, hypoxia and H-R (Figure 3a, 3b & 3c). Inhibition of p38 had a greater effect on hepatocyte apoptosis than JNK inhibition. Neither inhibitor reduced CD154 mediated hepatocyte necrosis under any of the experimental conditions (Figure 3). This suggests that CD40:CD154 mediated human hepatocyte apoptosis during normoxia and H-R is ROS, JNK and p38-dependent whilst necrosis is ROS-dependent but MAPK-independent.

CD40:CD154:NADPH oxidase interactions stimulate hepatocyte Fas ligand expression

Fas is a cell surface receptor of the TNF Receptor superfamily which, when activated by FasL, induces apoptosis on a wide range of cells including hepatocytes [7]. Because we have previously reported the CD40 activation on human hepatocytes results in Fas-mediated apoptosis, we investigated whether hypoxia or H-R alone or in association with CD154 induced FasL expression. Neither hypoxia nor H-R increased hepatocyte cell surface FasL expression (Figure 4a). However, CD40:CD154 increased FasL expression during hypoxia and H-R, with a greater effect during hypoxia. Inhibiting NADPH oxidase function with DPI reduced CD40:CD154 mediated FasL expression during hypoxia and H-R, with a greater effect noted during H-R (Figure 4b & 4c).

Platelet-derived soluble CD154 mediates hepatocyte apoptosis and necrosis

Finally, because platelets are the source for 95% of circulating soluble CD154 and activated platelets may be found in the liver parenchyma during damage [22] we determined whether activated platelets may be a potential source of functionally active CD154 during hypoxia and H-R.

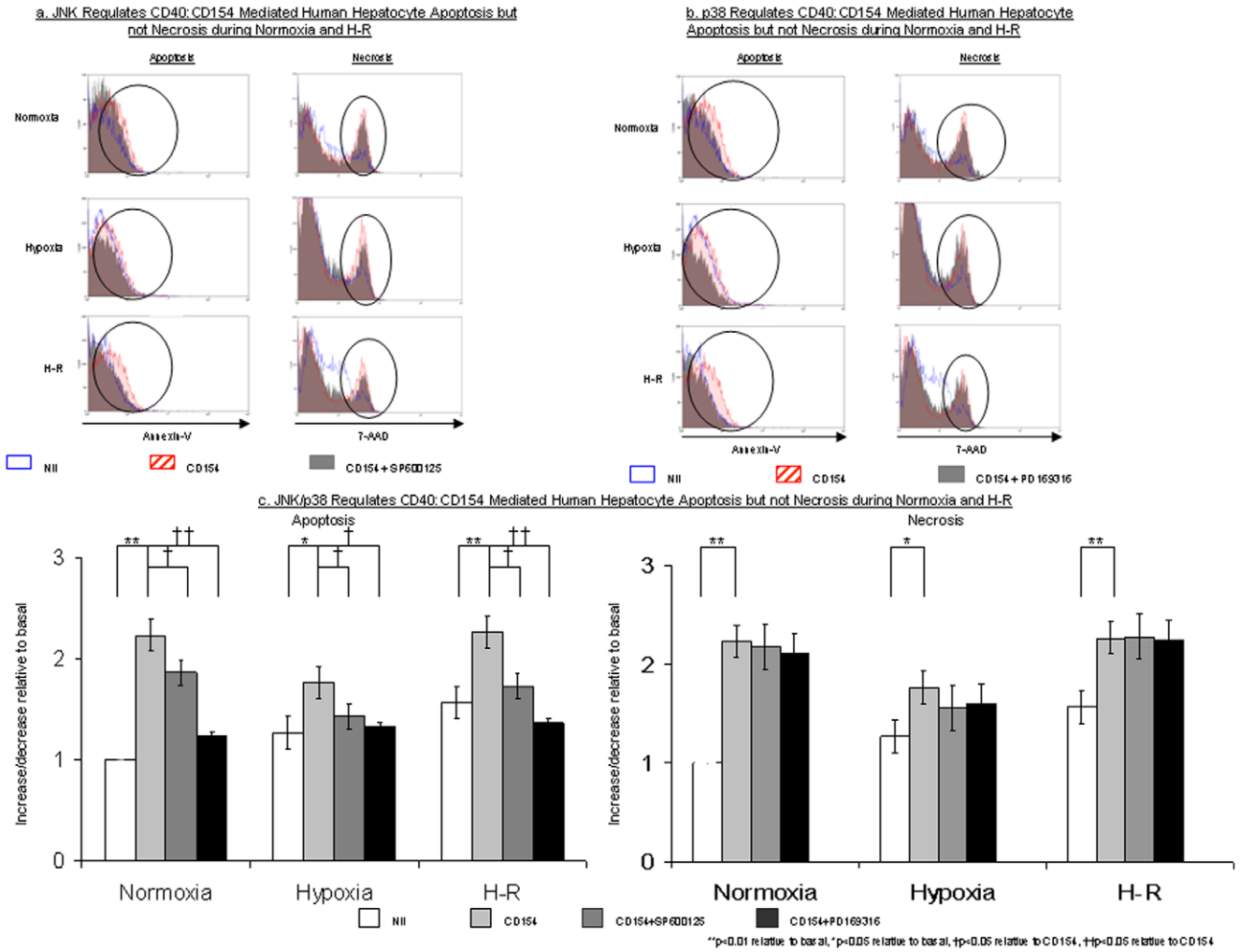

Figure 3. JNK and p38 regulate CD40:CD154 mediated human hepatocyte apoptosis but not necrosis. Figure 3a show representative flow cytometry plots to illustrate the effect of the JNK inhibitor SP600125 upon CD40:CD154 mediated apoptosis and necrosis during normoxia, hypoxia and H-R. The gate used to analyse primary human hepatocytes is the same as that shown in Figures 1 & 2. The area of interest within the flow cytometric plots are marked by the vertical ellipses. Figure 3b illustrates the effects of the p38 inhibitor P169316 upon CD40:CD154 mediated apoptosis and necrosis during normoxia, hypoxia and H-R. Figure 3c shows a bar chart with the pooled data of three separate experiments illustrating the effects of both SP600125 and PD169316 upon CD40:CD154 mediated human hepatocyte apoptosis and necrosis during normoxia, hypoxia and H-R. Data are expressed as increase/decrease relative to basal, where basal refers to the level of apoptosis or necrosis during normoxia alone. Data are expressed as mean ± S.E. (**$p<0.01$ relative to basal, *$p<0.05$ relative to basal, †$p<0.05$ relative to CD154, ††$p<0.05$ relative to basal).
doi:10.1371/journal.pone.0030867.g003

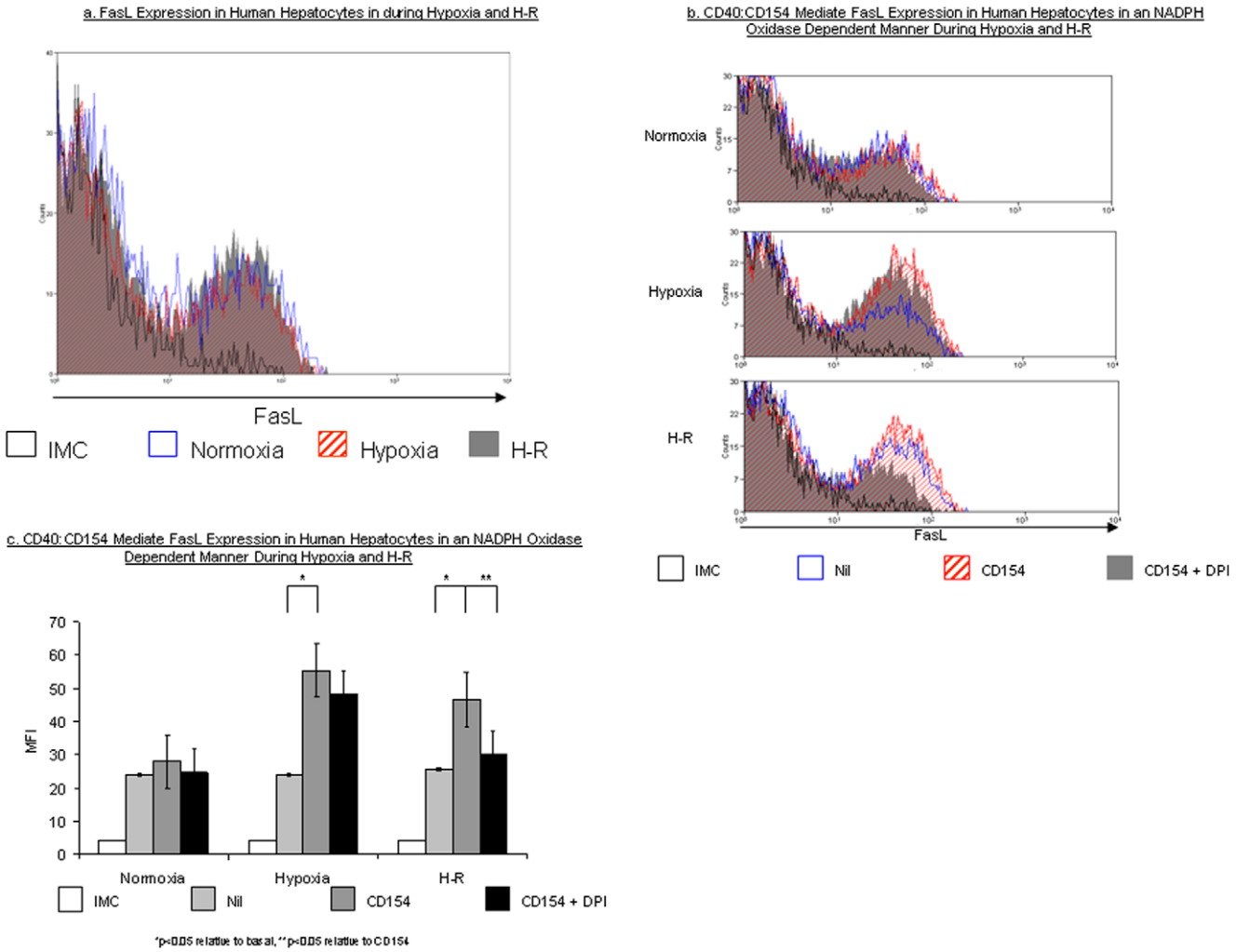

Figure 4. FasL Expression on Primary Human Hepatocytes. Figure 4a demonstrates a representative flow cytometry plot of FasL expression on primary human hepatocytes during normoxia, hypoxia and H-R. The gate used to analyse primary human hepatocytes is the same as that shown in Figures 1 & 2. Figure 4b. demonstrates representative flow cytometry plots to illustrate the effect of CD154 (hatched red) and CD154 in presence of DPI (solid grey) upon human hepatocyte FasL expression during normoxia, hypoxia and H-R. Figure 4c. shows a bar chart with the pooled data of three separate experiments illustrating the effects of CD154 upon human hepatocyte FasL expression during normoxia, hypoxia and H-R. Data are expressed as MFI and readings are based upon values taken from cells within the gated region in Figure 1a. Data are expressed as mean ± S.E. (*$p<0.05$ relative to basal, **$p<0.05$ relative to CD154).
doi:10.1371/journal.pone.0030867.g004

Immuno-magnetic depletion reduced soluble CD154 released by activated platelets by >70% (Platelet Conditioned Media (PCM) soluble CD154 concentration 2251±310 pg/mL; CD154-depleted PCM CD154 concentration 590±79 pg/mL). PCM increased hepatocyte intracellular ROS accumulation during H-R (Figure 5a). When CD154 was depleted from PCM, intracellular ROS accumulation was significantly reduced during H-R. PCM increased human hepatocyte apoptosis during H-R mirroring the increasing in intracellular ROS (Figure 5b). However, in line with the decrease in ROS seen during H-R, CD154-depleted PCM decreased human hepatocyte apoptosis during H-R (Figure 5b).

Discussion

Tissue hypoxia is a feature of hepatic inflammation and disease [23] and we have recently shown the accumulation of intracellular ROS is a critical mediator of hepatocyte death during hypoxia and H-R [2]. In the present report we show that ROS accumulation in human hepatocytes during hypoxia and H-R is increased by CD154 mediated activation of hepatocyte CD40 resulting in increased cell death. This link between CD40 activation, intracellular ROS generation and cell death has implications for other inflammatory diseases characterised by local hypoxia.

CD40:CD154 receptor-ligand interactions have been associated with parenchymal injury during hypoxia and H-R in many organs [8,24,25] and disruption of CD40:CD154 signaling in mice improves liver function following hypoxia [8]. However until now it was thought that CD40:CD154 mediates its actions through effects on T-lymphocyte priming whereas our data suggest another mode of action through direct effects on hepatocyte survival. We have previously reported that CD40 activation mediates Fas dependent apoptosis in human hepatocytes through induction of autocrine FasL expression [7]. We now demonstrate that CD40:CD154 can also mediate human hepatocyte apoptosis and necrosis in a NADPH Oxidase:ROS-dependent manner. This introduces a previously unknown CD40 dependent pathway to cell

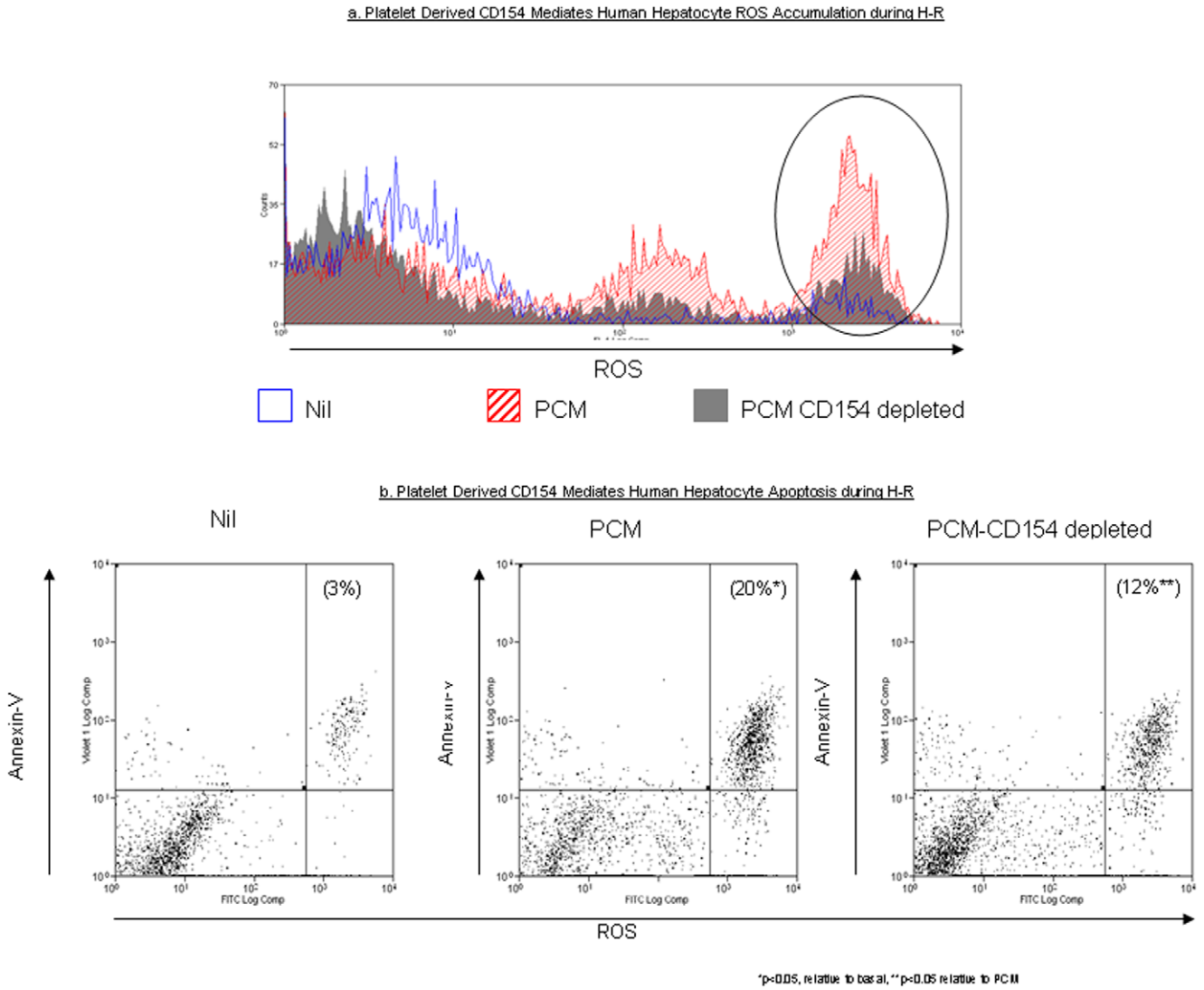

Figure 5. The effects of PCM and PCM CD154-depleted upon human hepatocyte ROS accumulation and cell death. Figures 5a demonstrates representative flow cytometry plots to illustrate the effect of PCM (hatched red) and PCM CD154-depleted (solid grey) upon human hepatocyte ROS accumulation during H-R. The gate used to analyse primary human hepatocytes is the same as that shown in Figures 1 & 2. The area of interest within the flow cytometry plots is marked by the vertical ellipse. The area on the left of each ellipse again represents cell debris. Figure 5b, human hepatocytes were treated with PCM or PCM CD154-depleted during H-R and the percentage of cells staining with both the ROS probe DCF and apoptotic marker, Annexin-V, were assessed by flow cytometry.. The percentage of human hepatocytes that stain for both DCF and Annexin-V are shown in parentheses. Data is representative 3 separate experiments (*$p<0.05$ relative to basal, **$p<0.05$ relative to PCM).
doi:10.1371/journal.pone.0030867.g005

death and implicates CD40 in the regulation of cell survival during tissue hypoxia and H-R.

Our data also support an important role for intrinsic ROS accumulation in hepatocytes as opposed to the current model which suggests that ROS is derived from leukocytes [6]. CD40 activation did not increase ROS accumulation or cell death in human hepatocytes during hypoxia and this is probably a consequence of the increased antioxidant levels induced in hepatocytes during hypoxia [26]. This may also explain why FasL has little effect during hypoxia (see below). Furthermore, hypoxia alone did not increase hepatocyte cell surface CD40 implying that the lack of effect of CD154 during hypoxia was probably a consequence of the modulation of intracellular signaling pathways by antioxidants rather than changes in CD40 receptor bioavailability.

Our data clearly show that increases in intracellular ROS induced by CD154 are dependent upon NADPH Oxidase, this is consistent with previous studies implicating NADPH in ROS accumulation in hypoxic human hepatocytes during normoxia, hypoxia and H-R [2]. Studies in WEHI 231 cells and endothelial cells have shown that following activation, CD40 recruits NADPH Oxidase to the plasma membrane via a mechanism involving TRAF3 [11,27,28,29]. Once at the plasma membrane the $p40^{phox}$ subunit of NADPH oxidase can generate ROS leading to activation of a number of downstream cell death signaling pathways (Figure 6). In our primary human hepatocyte model, CD40:NADPH oxidase:ROS initiated apoptosis and to a lesser extent necrotic cell death. The mode of hepatocyte cell death stimulated by hypoxia remains controversial. Both apoptosis and necrosis have been implicated in transplant models [30] consistent

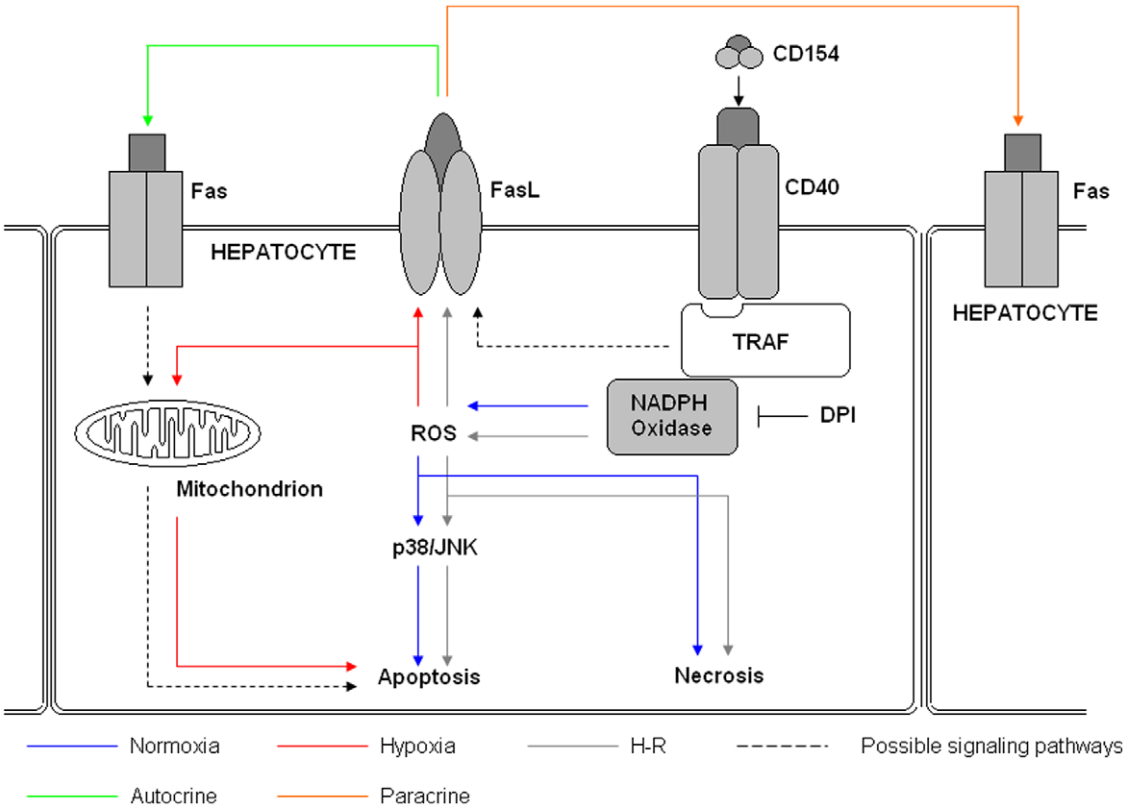

Figure 6. Proposed mechanism of CD40-CD154 mediated apoptosis and necrosis in human hepatocytes during normoxia, hypoxia and H-R. During normoxia (blue arrows) activation of CD40 expressed upon human hepatocyte by CD154 results in the translocation of the TRAF adaptor molecules to the cell membrane. The TRAF molecules are then responsible for the recruitment of the flavoenzyme NADPH Oxidase to the CD40:TRAF complex. Here NADPH Oxidase can induce the production of ROS, primarily in the form of hydrogen peroxide. This process can be inhibited by the NADPH Oxidase inhibitor DPI. The resultant accumulation of ROS can result directly in necrotic cell death or it can activate the MAPK members, JNK and p38, to induce human hepatocyte apoptosis. However, during hypoxia (red arrows) CD40 activation on human hepatocytes does not result in ROS accumulation but can induce FasL expression via mechanisms that NADPH Oxidase-dependent and ROS-independent (dotted black line). This increased FasL expression can result in autocrine (green arrow) and/or paracrine (orange arrows) Fas-mediated apoptosis. Due to the increases in intracellular antioxidants levels during hypoxia CD154 does not increase apoptosis. However, mitochondrial ROS does contribute to apoptosis during hypoxia. During H-R, CD40 activation can lead to NADPH Oxidase-ROS-JNK/p38 dependent apoptosis, NADPH Oxidase-ROS-dependent necrosis and NADPH Oxidase:ROS:FasL expression with resultant Fas-mediated apoptosis. Figure 6 highlights the importance of local microenvironment in shaping the effects of CD40:CD154.
doi:10.1371/journal.pone.0030867.g006

with our findings and in support of Lemasters proposal that a common mediator regulates both forms of cell death during hypoxia and H-R [31]. We propose that CD40:CD154 activation in hepatocytes has at least three downstream consequences 1) initiation of apoptosis mediated via ROS 2) initiation of apoptosis mediated via FasL induction and 3) necrosis.

CD40 activation results in apoptotic death in many cells of epithelial lineage [7,14]. Indeed, CD40 activation induces human hepatocyte apoptosis via up-regulation of FasL expression and subsequent Fas-mediated apoptosis [7]. Moreover, in human hepatocytes, it is the sustained activation of Activator Protein-1 (AP-1) and MAPKs, and not NF-kappaB, which is central to initiating apoptosis [32]. A similar signalling pathway has been reported in mediating cholangiocytes apoptosis after CD40 ligation [33]. Additionally, in cholangiocytes, CD40 mediated apoptosis also requires the activation of the JAK2-STAT3 pathway and the downstream activation of caspase-3 [14]. However, our study is the first to implicate ROS in this process of epithelial and specifically human hepatocyte, apoptosis. ROS can activate the MAPKs sub-families of JNK and p38, important regulators of cell death. Specifically, ROS can activate the MAP3K, apoptosis signaling kinase 1 (ASK1) resulting in phosphorylation of MEK 3/6 [34] and MEK 4/7 [34] which respectively activate p38 and JNK. Inhibition of p38 [35] and JNK [36] improves hepatocyte viability after hypoxia and during H-R in rodent models. We now show that CD40:CD154 mediated human hepatocyte apoptosis is reduced by JNK inhibition and prevented by p38 inhibition. The precise mechanism of JNK mediated apoptosis is controversial. JNK can act upstream of mitochondria by activating the pro-apoptotic Bcl2 family [37] and also increases turnover of the anti-apoptotic protein c-FLIP [38]. p38 is thought to mediate apoptosis via phosphorylation of Bcl2 family members [39] and CD40-mediated-NADPH oxidase generated ROS is upstream of p38 activation in WEHI 231 cells [11]. Thus our data report for the first time a mechanistic link between CD40:CD154 mediated ROS generation, MAPK activation and cell death. Taken together, these studies highlight the complexities of the upstream CD40 signaling pathway and suggest that CD40 can couple to at least ROS and AP-1 signaling pathways to regulate apoptosis. Whether CD40 ligation in human hepatocytes can also active the JAK-STAT pathways, as seen in cholangiocytes, remains to be ascertained.

CD40 ligation by CD154 is known to increase FasL expression resulting in autocrine/paracrine Fas-mediated apoptosis in human hepatocytes [7]. However, in contrast to *in vivo* studies [40], hypoxia and H-R did not result in increased hepatocyte FasL expression in our study. We confirmed that CD154 induced cell surface expression of FasL in human hepatocytes and showed for the first time that this is in part dependent on NADPH oxidase particularly during H-R. This suggests that other mechanisms are involved in regulating ROS-independent FasL expression. As discussed above, although CD40:CD154 did not increase ROS during hypoxia, it did increase FasL expression although without a concomitant increase in apoptosis. However, the inhibition of mitochondrial ROS significantly reduced hepatocyte apoptosis during hypoxia. Fas mediated apoptosis in hepatocytes requires the downstream accumulation of mitochondrial ROS [41] and together with likely increases in hepatocytes antioxidant levels during hypoxia explains why we saw increased FasL expression in the absence of apoptosis in response to CD40 activation [4,5]. This also suggests that different apoptotic signaling pathways may be initiated in response to CD40 activation under different conditions in distinct microenvironments.

Our data suggest that hypoxia, which precedes reoxygenation during preservation of an organ allograft for transplantation, can increase FasL expression thereby initiating liver damage before ROS generation during reperfusion has occurred. FasL is also increased on hepatocytes in chronically inflamed livers a situation characterized by tissue hypoxia. Thus the mechanism we describe is likely to operate in the chronic inflammation where large numbers of CD154 expressing effector cells can activate CD40 in a hypoxic environment [42].

We have previously reported that ROS generation can regulate human hepatocyte necrosis during hypoxia and H-R [2] and hepatocyte necrosis has been induced experimentally during hypoxia followed by reoxygenation [31]. We show that ROS generated by CD40:CD154 not only induces hepatocyte apoptosis but also necrosis during normoxia and H-R. This process is NADPH Oxidase dependent as shown by the decrease in necrosis in the presence of DPI but in contrast to CD154-mediated hepatocyte apoptosis, necrosis is MAPK-independent. This suggests that NADPH oxidase generated ROS regulates divergent signaling pathways leading to both forms of cell death.

Therefore, coupled with previous work regarding CD40 mediated death of liver epithelial cells it is clear that the signaling pathways regulating this process are diverse. Clearly, in the present manuscript we demonstrate that CD154:CD40:ROS is an important activator of JNK and p38 which subsequently leads to cell death. However the JAK2-STAT3 is also important CD40 mediated apoptotic pathway [14] that may also be activated by ROS. Furthermore FasL is also up-regulated following CD40 activation. Therefore CD40 regulates multiple death signaling pathways in liver epithelial cells.

We have shown that macrophages and T-lymphocytes are an abundant source of CD154 in the chronically inflamed liver [43]. However platelets are also a rich source of CD154 [22] and within seconds of activation CD154 is translocated to the platelet surface then cleaved to produce soluble CD154. Platelets have been implicated in preservation injury during liver transplantation and in other conditions including immune mediated damage in hepatitis although the mechanisms of the effect are poorly understood [44,45,46]. We now show that activated platelets secrete functional CD154 that is capable of inducing ROS accumulation in human hepatocytes during H-R leading to hepatocyte apoptosis. This finding provides a novel mechanism to explain the effector function of platelets in liver injury and suggests that anti-platelet therapy together with anti-oxidants may be warranted not only to prevent reperfusion injury but also to reduce liver injury in chronic hepatitis and cirrhosis in which platelets are found in close proximity to hepatocytes [47,48]. Although our findings suggest that platelets are a major source of CD154 capable of inducing injury as previously suggested [25] CD154 depletion from platelet-conditioned medium reduced but did not abolish human hepatocyte apoptosis suggesting either that there was residual CD154 activity in the PCM or that platelets release other active mediators of apoptosis [44].

In conclusion, we have shown that CD40:CD154 mediated generation of ROS contributes to hepatocyte cell death by both apoptosis and necrosis in the hypoxic liver microenvironment. The ability of platelets as well as infiltrating T-lymphocytes and macrophages to deliver functional CD154 to hepatocytes suggests several potential mechanisms through which hepatocyte CD40 can be activated in the inflamed and hypoxic liver. The work supports therapeutic intervention with anti-platelet and anti-oxidant therapy in liver disease.

Author Contributions

Conceived and designed the experiments: RHB CJW SMC. Performed the experiments: RHB. Analyzed the data: RHB CJW SMC DHA SCA. Wrote the paper: RHB DHA SCA.

References

1. Vardanian AJ, Busuttil RW, Kupiec-Weglinski JW (2008) Molecular mediators of liver ischemia and reperfusion injury: a brief review. Mol Med 14: 337–345.
2. Bhogal RH, Curbishley SM, Weston CJ, Adams DH, Afford SC (2010) Reactive oxygen species mediate human hepatocyte injury during hypoxia/reoxygenation. Liver Transpl 16: 1303–1313.
3. Broughan TA, Naukam R, Tan C, Van De Wiele CJ, Refai H, et al. (2008) Effects of hepatic zonal oxygen levels on hepatocyte stress responses. J Surg Res 145: 150–160.
4. Massip-Salcedo M, Rosello-Catafau J, Prieto J, Avila MA, Peralta C (2007) The response of the hepatocyte to ischemia. Liver Int 27: 6–16.
5. Garcia-Ruiz C, Fernandez-Checa JC (2007) Redox regulation of hepatocyte apoptosis. J Gastroenterol Hepatol 22 Suppl 1: S38–42.
6. Taniai H, Hines IN, Bharwani S, Maloney RE, Nimura Y, et al. (2004) Susceptibility of murine periportal hepatocytes to hypoxia-reoxygenation: role for NO and Kupffer cell-derived oxidants. Hepatology 39: 1544–1552.
7. Afford SC, Randhawa S, Eliopoulos AG, Hubscher SG, Young LS, et al. (1999) CD40 activation induces apoptosis in cultured human hepatocytes via induction of cell surface fas ligand expression and amplifies fas-mediated hepatocyte death during allograft rejection. J Exp Med 189: 441–446.
8. Ke B, Shen XD, Gao F, Tsuchihashi S, Farmer DG, et al. (2005) The CD154-CD40 T-cell co-stimulation pathway in liver ischemia and reperfusion inflammatory responses. Transplantation 79: 1078–1083.
9. Shen X, Wang Y, Gao F, Ren F, Busuttil RW, et al. (2009) CD4 T cells promote tissue inflammation via CD40 signaling without de novo activation in a murine model of liver ischemia/reperfusion injury. Hepatology 50: 1537–1546.
10. Humphreys EH, Williams KT, Adams DH, Afford SC (2010) Primary and malignant cholangiocytes undergo CD40 mediated Fas dependent apoptosis, but are insensitive to direct activation with exogenous Fas ligand. PLoS One 5: e14037.
11. Ha YJ, Lee JR (2004) Role of TNF receptor-associated factor 3 in the CD40 signaling by production of reactive oxygen species through association with p40phox, a cytosolic subunit of nicotinamide adenine dinucleotide phosphate oxidase. J Immunol 172: 231–239.
12. Bhogal RH, Hodson J, Bartlett DC, Weston CJ, Curbishley SM, et al. (2011) Isolation of primary human hepatocytes from normal and diseased liver tissue: a one hundred liver experience. PLoS One 6: e18222.
13. Lalor P, Nash GB (1995) Adhesion of flowing leucocytes to immobilized platelets. Br J Haematol 89: 725–732.
14. Ahmed-Choudhury J, Williams KT, Young LS, Adams DH, Afford SC (2006) CD40 mediated human cholangiocyte apoptosis requires JAK2 dependent activation of STAT3 in addition to activation of JNK1/2 and ERK1/2. Cell Signal 18: 456–468.
15. King LA, Toledo AH, Rivera-Chavez FA, Toledo-Pereyra LH (2009) Role of p38 and JNK in liver ischemia and reperfusion. J Hepatobiliary Pancreat Surg 16: 763–770.

16. Kohrmann M, Haubensak W, Hemraj I, Kaether C, Lessmann VJ, et al. (1999) Fast, convenient, and effective method to transiently transfect primary hippocampal neurons. J Neurosci Res 58: 831–835.
17. Gardmo C, Kotokorpi P, Helander H, Mode A (2005) Transfection of adult primary rat hepatocytes in culture. Biochem Pharmacol 69: 1805–1813.
18. Park JS, Surendran S, Kamendulis LM, Morral N (2011) Comparative nucleic acid transfection efficacy in primary hepatocytes for gene silencing and functional studies. BMC Res Notes 4: 8.
19. Bumpus NN (2011) Efavirenz and 8-hydroxyefavirenz induce cell death via a JNK- and BimEL-dependent mechanism in primary human hepatocytes. Toxicol Appl Pharmacol 257: 227–234.
20. Chai J, He Y, Cai SY, Jiang Z, Wang H, et al. (2011) Elevated hepatic MRP3/ABCC3 expression in human obstructive cholestasis is mediated through TNFalpha and JNK/SAPK signaling pathway. Hepatology.
21. Lee YJ, Shukla SD (2007) Histone H3 phosphorylation at serine 10 and serine 28 is mediated by p38 MAPK in rat hepatocytes exposed to ethanol and acetaldehyde. Eur J Pharmacol 573: 29–38.
22. Andre P, Prasad KS, Denis CV, He M, Papalia JM, et al. (2002) CD40L stabilizes arterial thrombi by a beta3 integrin–dependent mechanism. Nat Med 8: 247–252.
23. Chaparro M, Sanz-Cameno P, Trapero-Marugan M, Garcia-Buey L, Moreno-Otero R (2007) Mechanisms of angiogenesis in chronic inflammatory liver disease. Ann Hepatol 6: 208–213.
24. Xu H, Montgomery SP, Preston EH, Tadaki DK, Hale DA, et al. (2003) Studies investigating pretransplant donor-specific blood transfusion, rapamycin, and the CD154-specific antibody IDEC-131 in a nonhuman primate model of skin allotransplantation. J Immunol 170: 2776–2782.
25. Xu H, Zhang X, Mannon RB, Kirk AD (2006) Platelet-derived or soluble CD154 induces vascularized allograft rejection independent of cell-bound CD154. J Clin Invest 116: 769–774.
26. Conti A, Scala S, D'Agostino P, Alimenti E, Morelli D, et al. (2007) Wide gene expression profiling of ischemia-reperfusion injury in human liver transplantation. Liver Transpl 13: 99–113.
27. Ha YJ, Seul HJ, Lee JR (2011) Ligation of CD40 receptor in human B lymphocytes triggers the 5-lipoxygenase pathway to produce reactive oxygen species and activate p38 MAPK. Exp Mol Med 43: 101–110.
28. Xia M, Li G, Ma J, Ling W (2010) Phosphoinositide 3-kinase mediates CD40 ligand-induced oxidative stress and endothelial dysfunction via Rac1 and NADPH oxidase 2. J Thromb Haemost 8: 397–406.
29. Ueno T, Watanabe H, Fukuda N, Tsunemi A, Tahira K, et al. (2009) Influence of genetic polymorphisms in oxidative stress related genes and smoking on plasma MDA-LDL, soluble CD40 ligand, E-selectin and soluble ICAM1 levels in patients with coronary artery disease. Med Sci Monit 15: CR341–348.
30. Smith MK, Mooney DJ (2007) Hypoxia leads to necrotic hepatocyte death. J Biomed Mater Res A 80: 520–529.
31. Jaeschke H, Lemasters JJ (2003) Apoptosis versus oncotic necrosis in hepatic ischemia/reperfusion injury. Gastroenterology 125: 1246–1257.
32. Ahmed-Choudhury J, Russell CL, Randhawa S, Young LS, Adams DH, et al. (2003) Differential induction of nuclear factor-kappaB and activator protein-1 activity after CD40 ligation is associated with primary human hepatocyte apoptosis or intrahepatic endothelial cell proliferation. Mol Biol Cell 14: 1334–1345.
33. Afford SC, Ahmed-Choudhury J, Randhawa S, Russell C, Youster J, et al. (2001) CD40 activation-induced, Fas-dependent apoptosis and NF-kappaB/AP-1 signaling in human intrahepatic biliary epithelial cells. FASEB J 15: 2345–2354.
34. Mebratu Y, Tesfaigzi Y (2009) How ERK1/2 activation controls cell proliferation and cell death: Is subcellular localization the answer? Cell Cycle 8: 1168–1175.
35. Kobayashi M, Takeyoshi I, Yoshinari D, Matsumoto K, Morishita Y (2002) P38 mitogen-activated protein kinase inhibition attenuates ischemia-reperfusion injury of the rat liver. Surgery 131: 344–349.
36. Uehara T, Xi Peng X, Bennett B, Satoh Y, Friedman G, et al. (2004) c-Jun N-terminal kinase mediates hepatic injury after rat liver transplantation. Transplantation 78: 324–332.
37. Lei K, Davis RJ (2003) JNK phosphorylation of Bim-related members of the Bcl2 family induces Bax-dependent apoptosis. Proc Natl Acad Sci U S A 100: 2432–2437.
38. Chang L, Kamata H, Solinas G, Luo JL, Maeda S, et al. (2006) The E3 ubiquitin ligase itch couples JNK activation to TNFalpha-induced cell death by inducing c-FLIP(L) turnover. Cell 124: 601–613.
39. Bu SZ, Huang Q, Jiang YM, Min HB, Hou Y, et al. (2006) p38 Mitogen-activated protein kinases is required for counteraction of 2-methoxyestradiol to estradiol-stimulated cell proliferation and induction of apoptosis in ovarian carcinoma cells via phosphorylation Bcl-2. Apoptosis 11: 413–425.
40. Cursio R, Filippa N, Miele C, Colosetti P, Auberger P, et al. (2005) Fas ligand expression following normothermic liver ischemia-reperfusion. J Surg Res 125: 30–36.
41. Ding WX, Ni HM, DiFrancesca D, Stolz DB, Yin XM (2004) Bid-dependent generation of oxygen radicals promotes death receptor activation-induced apoptosis in murine hepatocytes. Hepatology 40: 403–413.
42. Nakajima H, Mizuta N, Fujiwara I, Sakaguchi K, Ogata H, et al. (2008) Blockade of the Fas/Fas ligand interaction suppresses hepatocyte apoptosis in ischemia-reperfusion rat liver. Apoptosis 13: 1013–1021.
43. Alabraba EB, Lai V, Boon L, Wigmore SJ, Adams DH, et al. (2008) Coculture of human liver macrophages and cholangiocytes leads to CD40-dependent apoptosis and cytokine secretion. Hepatology 47: 552–562.
44. Lisman T, Porte RJ (2010) The role of platelets in liver inflammation and regeneration. Semin Thromb Hemost 36: 170–174.
45. Sullivan BP, Wang R, Tawfik O, Luyendyk JP (2010) Protective and damaging effects of platelets in acute cholestatic liver injury revealed by depletion and inhibition strategies. Toxicol Sci 115: 286–294.
46. Ohtaki Y, Yamaguchi K, Yu Z, Kumamoto H, Shimauchi H, et al. (2009) Hepatic platelet accumulation in Fas-mediated hepatitis in mice. Int Immunopharmacol 9: 1071–1078.
47. Khandoga A, Biberthaler P, Messmer K, Krombach F (2003) Platelet-endothelial cell interactions during hepatic ischemia-reperfusion in vivo: a systematic analysis. Microvasc Res 65: 71–77.
48. Hong SW, Jung KH, Zheng HM, Lee HS, Suh JK, et al. (2010) The protective effect of resveratrol on dimethylnitrosamine-induced liver fibrosis in rats. Arch Pharm Res 33: 601–609.

Appendix V

Autophagy 8:4, 545–558; April 2012; © 2012 Landes Bioscience

Autophagy

A cyto-protective mechanism which prevents primary human hepatocyte apoptosis during oxidative stress

Ricky H. Bhogal,* Christopher J. Weston, Stuart M. Curbishley, David H. Adams and Simon C. Afford

Centre for Liver Research; The Institute for Biomedical Research; The Medical School; University of Birmingham; Birmingham, West Midlands UK

Keywords: autophagy, human hepatocytes, hypoxia, apoptosis, reactive oxygen species, necrosis

The role of autophagy in the response of human hepatocytes to oxidative stress remains unknown. Understanding this process may have important implications for the understanding of basic liver epithelial cell biology and the responses of hepatocytes during liver disease. To address this we isolated primary hepatocytes from human liver tissue and exposed them ex vivo to hypoxia and hypoxia-reoxygenation (H-R). We showed that oxidative stress increased hepatocyte autophagy in a reactive oxygen species (ROS) and class III PtdIns3K-dependent manner. Specifically, mitochondrial ROS and NADPH oxidase were found to be key regulators of autophagy. Autophagy involved the upregulation of BECN1, LC3A, Atg7, Atg5 and Atg 12 during hypoxia and H-R. Autophagy was seen to occur within the mitochondria of the hepatocyte and inhibition of autophagy resulted in the lowering a mitochondrial membrane potential and onset of cell death. Autophagic responses were primarily observed in the large peri-venular (PV) hepatocyte subpopulation. Inhibition of autophagy, using 3-methyladenine, increased apoptosis during H-R. Specifically, PV human hepatocytes were more susceptible to apoptosis after inhibition of autophagy. These findings show for the first time that during oxidative stress autophagy serves as a cell survival mechanism for primary human hepatocytes.

Introduction

Tissue hypoxia is a feature common to many liver diseases including cirrhosis and cancer. It also occurs as a consequence of hemodynamic shock and liver surgery. At the subcellular level hepatocyte hypoxia causes depletion of glycolytic substrates, loss of adenosine triphosphate and intracellular acidosis. Moreover, following liver surgery/transplantation, the restoration of blood flow, although restoring normal oxygen saturation and acid-base balance paradoxically induces and augments hepatocellular injury.[1] The key mediator of these events is accumulation of intracellular reactive oxygen species (ROS).[2] Furthermore, ROS can regulate both human hepatocyte apoptosis and necrosis during hypoxia and hypoxia-reoxygenation (H-R).[2]

While hepatocyte apoptosis and necrosis have been shown to occur during hypoxia, the role of hepatocyte autophagy remains controversial. It is now widely recognized that autophagy is required for protein and organelle turnover and is typically a homeostatic cellular response to starvation. Furthermore, autophagy degrades both long-lived cytoplasmic proteins and surplus or dysfunctional organelles by lysosome-dependent mechanisms.[3] Nearly all hepatocyte-derived proteins are long-lived and autophagy is thought to be the primary process for hepatic protein catabolism.[4] Recent studies suggest that autophagy is another distinct and separate form of cell death that hepatocytes sustain when exposed to oxidative stress but it has been conclusively shown that cells undergoing autophagy are not committed irreversibly to death.[5] The role of autophagy in liver disease has been comprehensively presented in recent reviews.[6,7]

Autophagy is an active process which involves sequestration of parts of the cytoplasm in double-membrane vesicles which then fuse with lysosomes forming the autophagosome. The cytoplasmic material engulfed is then hydrolysed permitting recycling of amino acids and other macromolecular precursors.

In contrast to classical apoptosis, the cellular machinery that regulates autophagy is known to be lysosomal proteinase-dependent and caspase-independent. In particular the Atg proteins and phosphatidylinositol 3-kinase (PtdIns3K) are crucial for autophagosome assembly. The initial step of autophagosome formation requires class III PtdIns3K and BECN1/Atg6 protein.[8] The assembly of the autophagosome can be inhibited pharmacologically by 3-methyladenine (3-MA), a specific class III PtdIns3K inhibitor.[9,10] The formation and expansion of the autophagosome requires two protein conjugation systems that involve several of members of the Atg protein superfamily,[11] namely the Atg8/LC3-PE and Atg12–Atg5 conjugation systems. These conjugation events are regulated and involve Atg3, Atg4, Atg10.[12] In particular Atg8 serves as a substrate for the Atg4 family of cysteine proteases.[11] Many Atg proteins can be regulated by ROS.[11] Once activated Atg8 is

*Correspondence to: Ricky H. Bhogal; Email: balsin@hotmail.com
Submitted: 03/28/11; Revised: 11/19/11; Accepted: 12/12/11
http://dx.doi.org/10.4161/auto.19012

able to associate with autophagosomes and remain there until fusion with lysosomes.[3,6]

Under starvation, cellular generation of ROS is essential for autophagosome formation and autophagic degradation. Because we have observed that hepatocyte ROS generation is enhanced during hypoxia, we wished in the present study, to define and assess the role of hepatocyte autophagy during hypoxia and H-R. We demonstrate for the first time that autophagy is essential for protection of human hepatocytes against oxidative stress and ROS-mediated cell death.

Results

Intracellular ROS accumulation is associated with increased autophagy within human hepatocytes. Consistent with our previous studies we show that exposure of human hepatocytes to hypoxia and H-R increased human hepatocyte accumulation of intracellular ROS as detected by DCF (**Fig. 1A**). These findings were confirmed by the use of the mitochondrial ROS dye Mitosox where we found that hypoxia and H-R also resulted in an increase in mitochondrial ROS production (**Fig. 1B**). Indeed, mitochondrial ROS production accounts for the vast majority of ROS production in human hepatocytes during hypoxia and H-R. This increase in intracellular ROS accumulation during hypoxia and H-R was also associated with an increase in the number of cells undergoing autophagy as demonstrated by increased staining of human hepatocytes with MDC (**Fig. 2**). The autophagic response was greater during H-R than hypoxia. Furthermore, human hepatocytes isolated from normal liver tissue and diseased liver tissue show markedly different autophagic responses during

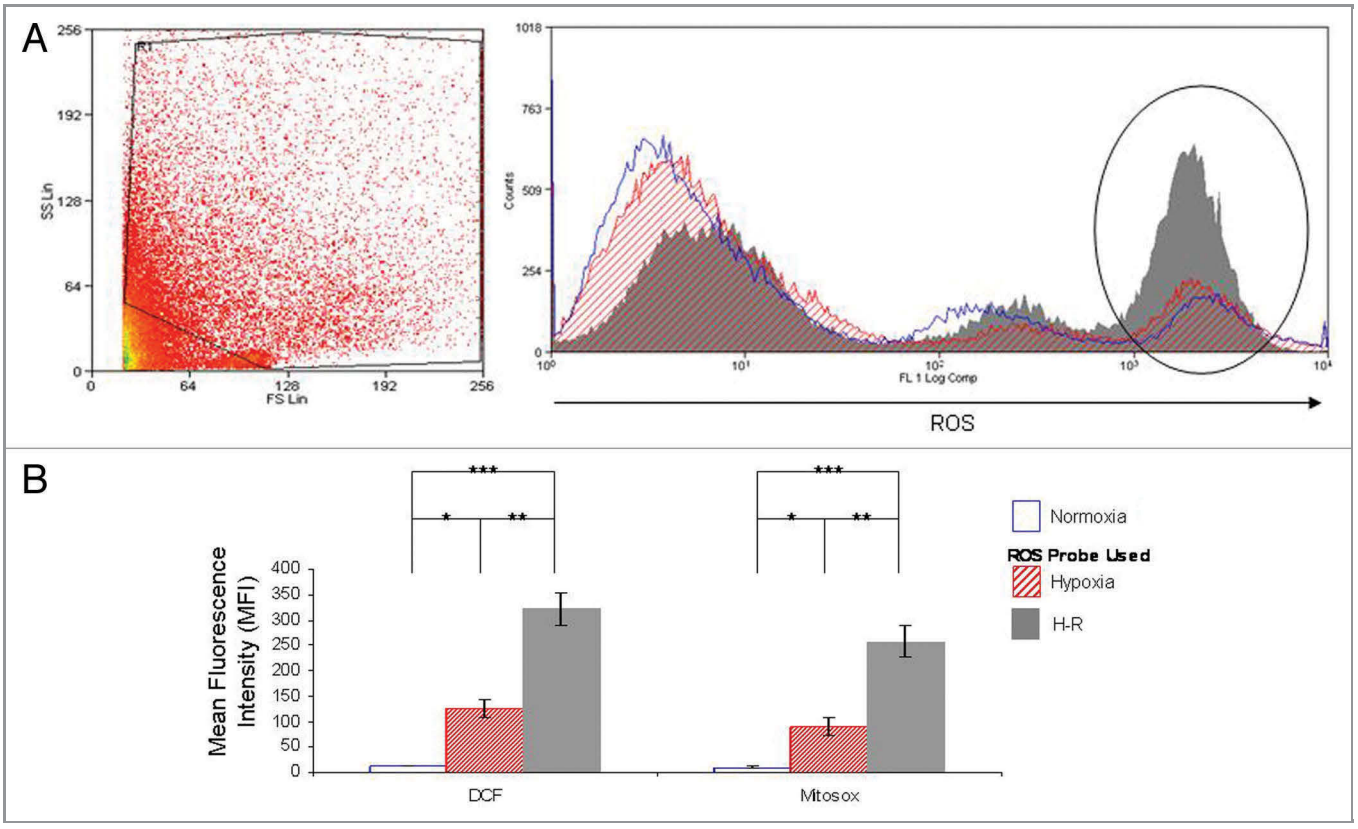

Figure 1. Intracellular ROS accumulation in primary human hepatocytes is mitochondrial dependent during hypoxia and H-R. (A) demonstrates representative flow cytometry plots to illustrate the effects of normoxia (blue), hypoxia (hatched red) and H-R (solid gray) upon human hepatocyte ROS production as assessed by DCF staining. A typical FS vs. SS plots of primary human hepatocytes during H-R is shown to the left of the flow cytometric plot. Human hepatocytes are known to vary considerably in size and hence a large gate is required to include all cells in the analysis. Refer to the Methods and Materials section for further details of the gating procedure and protocol. Similar FS vs. SS plots were obtained during normoxia and hypoxia (data not shown). The areas of interest on the flow cytometric plots are marked by vertical ellipses. The area on the left of each ellipse represents cell debris. Cell debris is included within the plot as human hepatocytes vary considerably in size and therefore to include all viable human hepatocytes in the analysis a large gate is required on the flow cytometer, this by necessity includes the cell debris. The representative plot is of normal human hepatocytes that have been isolated from benign liver diseases (n = 7). (B) shows composite bar charts to illustrate the effects of hypoxia and H-R upon ROS production in human hepatocytes isolated from benign liver diseases using DCF and Mitosox. DCF is measure of hydrogen peroxide production in human hepatocytes. Hydrogen peroxide is the main ROS generated within hepatocytes. Mitosox detects ROS generated specifically by the mitochondrion. In these experiments human hepatocytes were isolated from the same liver wedges and then used simultaneously in our in vitro model of hypoxia and H-R to determine DCF and Mitosox staining during normoxia, hypoxia and H-R. Data are expressed as mean fluorescence intensity (MFI) and the values are derived from the gates shown in (A). Human hepatocytes used for these experiments were isolated from benign liver diseases (n = 3–4). (*$p < 0.05$ relative to normoxia, **$p < 0.05$ relative to hypoxia, ***$p < 0.01$ relative to normoxia, Mann-Whitney test).

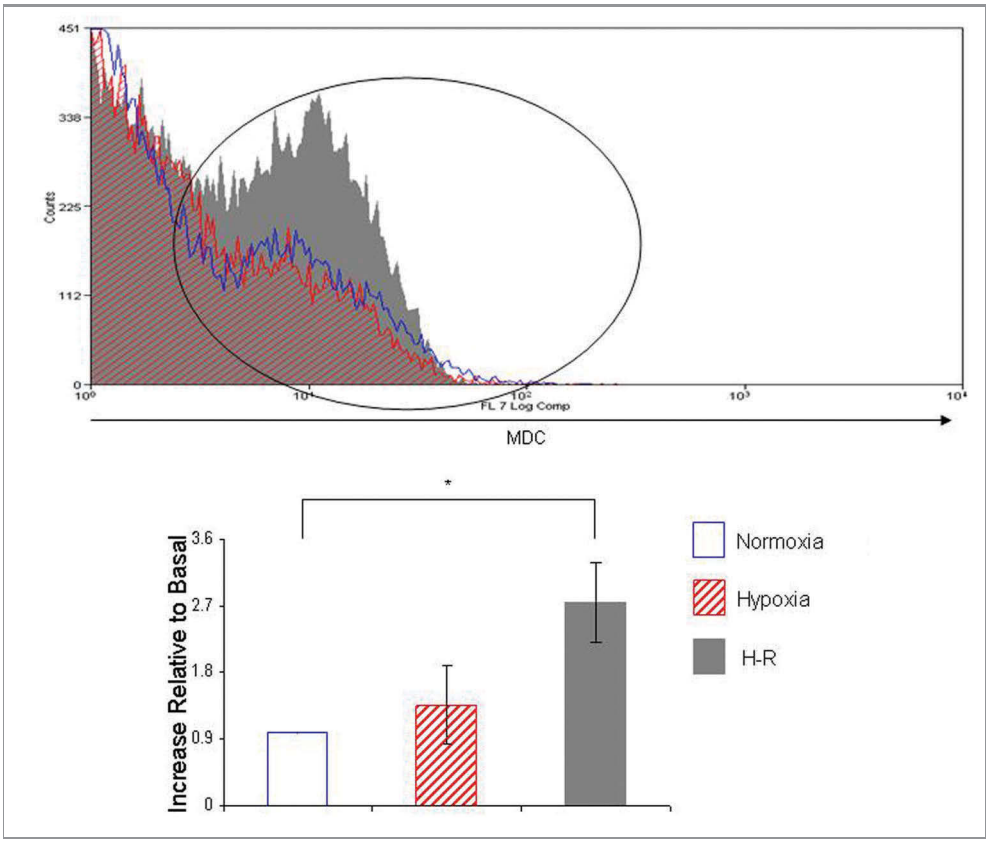

Figure 2. Intracellular ROS accumulation is associated with increased autophagy during hypoxia and H-R in human hepatocytes. This figure demonstrates a representative flow cytometry plot to illustrate the effect of normoxia (blue), hypoxia (hatched red) and H-R (solid gray) upon autophagy within human hepatocytes isolated from benign liver disease. Again, the areas of interest within the flow cytometry plots are marked by vertical ellipses. The same gate has been applied to primary human hepatocytes for these plots as those shown in **Figure 1A**. The bar chart shows pooled data of five separate experiments illustrating the effects of hypoxia and H-R upon human hepatocyte autophagy (n = 5). Data are expressed as increase relative to basal, where basal refers to the level of autophagy during normoxia alone. Data are expressed as mean ± SE (*$p < 0.05$ relative to basal, Mann-Whitney test).

hypoxia and H-R (**Fig. 3**). While human hepatocytes isolated from biliary cirrhosis show a similar autophagic response to those isolated from normal human hepatocytes (**Fig. 2**) those hepatocytes isolated from alcoholic liver disease (ALD) show very little staining with MDC during hypoxia and H-R indicating the lack of autophagy within these particular hepatocytes. Finally, human hepatocytes from normal resected liver tissue that have been exposed to chemotherapy showed a very different autophagic response to hypoxia and H-R. These hepatocytes had a much higher basal autophagy level that was maintained throughout hypoxia and H-R. For the remainder of the experiments presented in this study we used human hepatocytes isolated from normal benign liver tissue.

Mitochondrial and NADPH oxidase mediate autophagy in human hepatocytes during H-R. It has been previously shown that ROS are critical regulators of autophagy.[11] Accordingly, during H-R, inhibition of ROS production inhibits autophagy in primary human hepatocytes (**Fig. 4**). Specifically, inhibition of mitochondrial complex I with rotenone and cytoplasmic NADPH oxidase with diphenyliodonium significantly reduced MDC staining of human hepatocytes, as assessed by flow cytometry. Moreover, the general antioxidant *N*-acetylcysteine, which has the greatest effect upon human hepatocyte ROS production,[2] almost completely inhibited autophagy in human hepatocytes. These observations clearly demonstrate the central role of ROS in regulating autophagy in human hepatocytes.

Inhibition of autophagy was associated with a concomitant increase in hepatocyte apoptosis during H-R. We utilized the specific class III PtdIns3K inhibitor 3-MA to elucidate the role of autophagy in human hepatocytes. 3-MA significantly reduced hepatocyte autophagy during H-R while the number of cells undergoing apoptosis increased (**Fig. 5**). Similar data was obtained during normoxia and hypoxia (data not shown). No significant change in the number of cells undergoing necrosis was observed during H-R with 3-MA pretreatment (**Fig. 6**). Similar data was obtained during hypoxia (data not shown). Interestingly inhibition of class III PtdIns3K also decreased ROS accumulation within human hepatocytes during H-R (**Fig. 6**).

Given that autophagy is regulated by a number of Atg proteins we investigated whether these Atg proteins were modulated by hypoxia and/or H-R. As **Figure 7** demonstrates BECN1, an early regulator of autophagy, is induced by hypoxia and H-R. Interestingly, 3-MA reduces BECN1 protein levels during normoxia, hypoxia and H-R. Similarly we found that Atg 5,

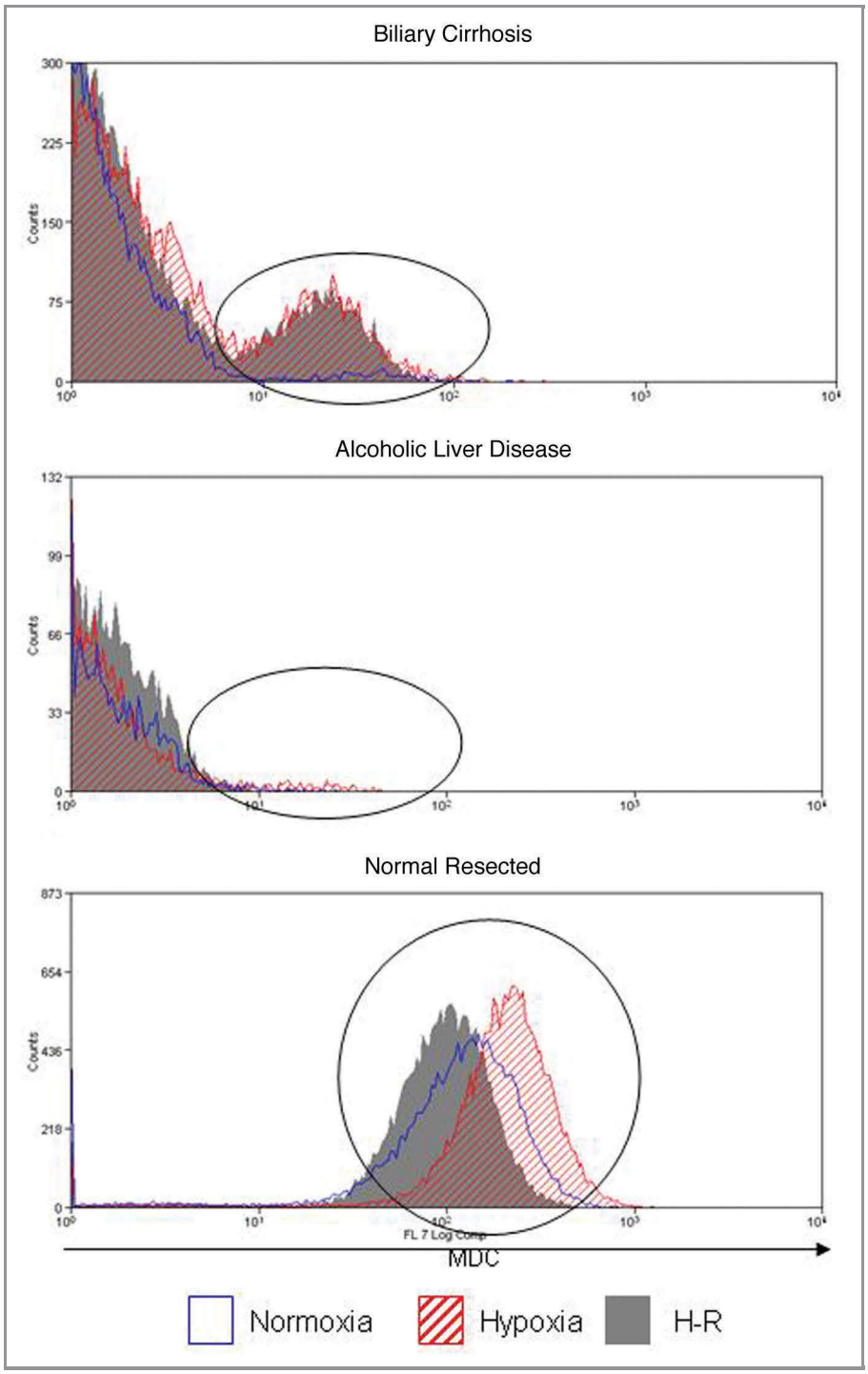

Figure 3. Differential levels of autophagy induction in human hepatocytes isolated from different liver diseases. This figure illustrates the level of autophagy in human hepatocytes isolated from different liver diseases. The FS and SS plots for these hepatocytes are the same as those shown in **Figure 1A** (n = 3–6).

Atg 7, Atg12 and LC3A were also increased during hypoxia, and H-R and 3-MA pre-treatment of hepatocytes reduced the protein levels of these Atg proteins. Additionally, cells treated with 3-MA during normoxia, hypoxia and H-R showed the characteristic morphological appearance of the cells undergoing apoptosis. Hepatocytes appeared phase bright, small and shrunken (**Fig. 8**). These observations clearly demonstrate that autophagy promotes survival of human hepatocytes during hypoxia and H-R in vitro.

Much recent work has focused upon the role of mitochondrial autophagy or mitophagy during oxidative stress.[13-15] Indeed the mitochondrion is an important ROS generator during IRI and is known to regulate human hepatocyte apoptosis and necrosis.[2]

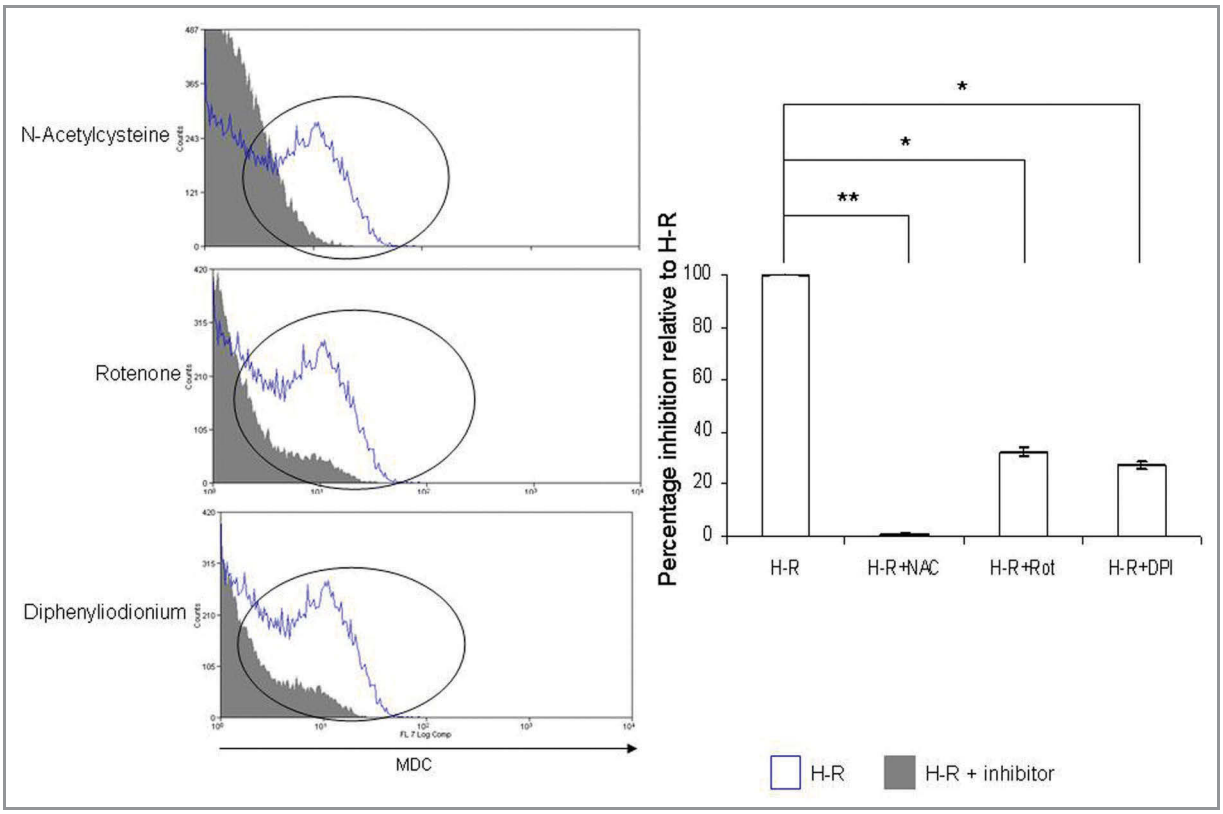

Figure 4. Mitochondrial and NADPH oxidase mediate autophagy in human hepatocytes during H-R. This figure demonstrates representative flow cytometry plots to illustrate the effects of NAC, rotenone and DPI upon human hepatocyte autophagy during H-R. The staining of cells with MDC during H-R is shown in blue and the effects of NAC, rotenone and DPI are shown in solid gray. Similar data were obtained during normoxia and hypoxia (data not shown). Again, the area of interest within the flow cytometry plots is marked by a vertical ellipse. The same gate has been applied to primary human hepatocytes for these plots as those shown in **Figure 1A**. The bar chart shows pooled data of three separate experiments illustrating the effects of NAC, rotenone, DPI upon human hepatocyte autophagy during H-R. Similar data were obtained during normoxia and hypoxia (data not shown). Data are expressed as percentage inhibition relative to H-R, where the level of autophagy during H-R alone represents 100%. Data are expressed as mean ± SE (*$p < 0.05$ relative to H-R alone, **$p < 0.01$ relative to H-R alone, Mann-Whitney test). Human hepatocytes used for these experiments were isolated from benign liver diseases (n = 3–5).

Accordingly, we used the specific mitochondrial dye JC-1 as a measure of the mitochondrial membrane potential within hepatocytes during hypoxia and H-R. Red fluorescence represents normal mitochondrial membrane potential whereas green fluorescence represents low mitochondrial potential. In addition, human hepatocytes were co-stained with MDC. As **Figure 9** shows, during normoxia human hepatocytes have normal mitochondrial membrane potential with no staining for MDC. Interestingly, incubation of cells with 3-MA markedly increased the green fluorescence of human hepatocytes indicating a lowering of mitochondrial potential and is indicative of cell death. Furthermore, hypoxia and H-R lower mitochondrial membrane potential further with a concomitant increase in MDC staining. Moreover, pre-treatment of cells with 3-MA during hypoxia and H-R, while reducing MDC staining markedly lowered mitochondrial membrane potential and increased cell death. Finally, MDC and green JC-1 staining were observed to colocalize in these samples indicating that autophagy was occurring in the mitochondrion.

Large peri-venular human hepatocytes preferentially undergo autophagy during H-R. Our group has recently reported that human hepatocytes located within the peri-venular (PV) region of the liver, which tend to be larger in size than their peri-portal (PP) counterparts, are the targets of hypoxic injury.[16] Here we demonstrate that large/PV hepatocytes (**Fig. 10**) increase autophagy significantly more than PP/small human hepatocytes during H-R (**Fig. 11**). As expected, these increased levels of autophagy are sensitive to 3-MA pre-treatment. However, inhibition of autophagy in large/PV human hepatocyte significantly increased apoptosis during H-R (**Fig. 4A**).

Discussion

While autophagy is an important mechanism by which the cell rids itself of potentially harmful constituents and helps maintain normal cellular functioning and homeostasis, its precise role during liver injury and disease where hepatocytes are involved remains uncertain. A consensus is now emerging that autophagy does not precede cell death but may be a physiologically protective mechanism which favors cell survival.[17] The diverse role of autophagy in liver diseases has been recently reviewed.[6,18,19] Certainly in liver IRI autophagy mainly has a prosurvival activity allowing the cell to cope with hypoxia. However autophagy is also

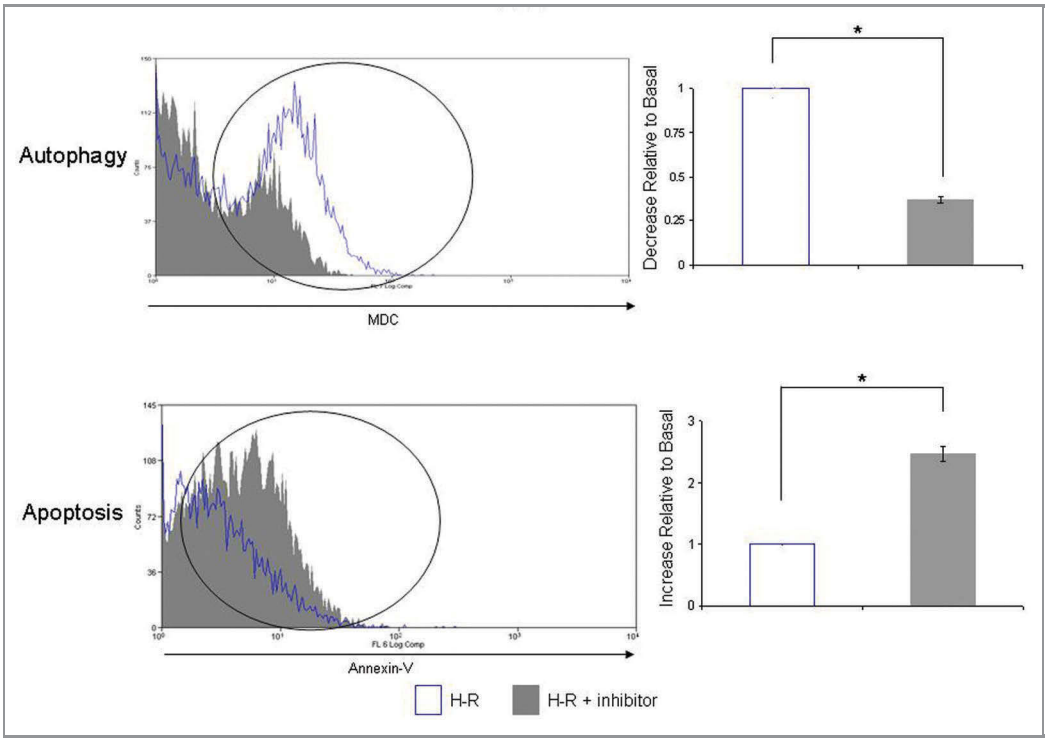

Figure 5. Inhibition of autophagy increases apoptosis in human hepatocytes during H-R. This figure illustrates representative flow cytometry plots to demonstrate the effects of the pre-treatment of primary human hepatocytes with 3-MA and the resultant effects upon apoptosis and autophagy during H-R. The level of apoptosis and autophagy during H-R are shown in blue and the effects of 3-MA pre-treatment are shown in solid gray. The area of interest is marked with a vertical ellipse. The same gate has been applied to primary human hepatocytes for these plots as those shown in **Figure 1A**. The bar charts to the right of each flow cytometry plot show pooled data from three separate experiments. Data are expressed as increase or decrease relative to basal, where basal refers to the level of ROS production, apoptosis, necrosis or autophagy during H-R. Data are expressed as mean ± SE (*$p < 0.05$ relative to basal, Mann-Whitney test). Human hepatocytes used for these experiments were isolated from benign liver diseases (n = 3).

known to regulate hepatic steatosis and hepatitis virus replication.[18] To our knowledge this is the first study to conclusively demonstrate autophagy in isolated primary human cells under conditions of hypoxic stress. This has potential implications for our understanding of the hepatocyte response to liver injury and development of chronic liver disease.

Previous tissue-based studies have shown autophagic hepatocytes within allografts are increased following liver transplantation. However these studies failed to show a causal link between oxidative stress, induction of cell death and autophagy.[5] Instead it was suggested that dying hepatocytes also increased autophagy. However whether inhibition of autophagy promoted cell death or survival was not demonstrated. Recent studies have shown that the severity and duration of an ischemic insult determine whether autophagy is induced or not. Indeed these studies have shown that autophagy can delay the decision for a cell to die via apoptosis or necrosis.[20] We clearly show, using our novel four-color reporter assay, that hepatocytes subjected to oxidative stress demonstrated features consistent with increased ROS generation, autophagy and apoptosis. However, crucially we show that inhibition of early autophagy with the class PtdIns3K inhibitor, 3-MA, induces increased levels apoptosis during H-R. For our presented study we used 3-MA only and not siRNA knockdown or transfection of human hepatocytes as these are notoriously difficult and inefficient techniques.[21-23] Importantly, inhibiting autophagy causes the lowering of mitochondrial membrane potential and leads to cell death. Previous authors have also reported that autophagy is responsible for maintaining mitochondrial potential.[19] Importantly, in the present study we have shown that human hepatocytes isolated from normal and diseased liver tissues have different autophagy responses during hypoxia and H-R. Specifically, human hepatocytes isolated from normal resected tissue, where livers would have been treated with chemotherapy, showed MDC staining that was consistent throughout hypoxia and H-R. Coupled with the findings of our previous study[2] it can be seen that these hepatocytes are also resistant to cell death during hypoxia and H-R. Indeed, the reduction in cell death maybe in part due to the induction of autophagy. This is consistent with previous work performed in human livers.[24] Moreover human hepatocytes isolated from ALD livers showed no autophagy response during hypoxia and H-R possibly reflecting the extent of damage to these livers. Human hepatocytes isolated from biliary cirrhosis and normal benign liver showed similar autophagy responses in an analogous manner to the accumulation of ROS within these cells.[2] These observations show that the varying levels of intracellular ROS within human hepatocytes isolated from different liver diseases correlates positively with intracellular MDC staining and hence autophagy.

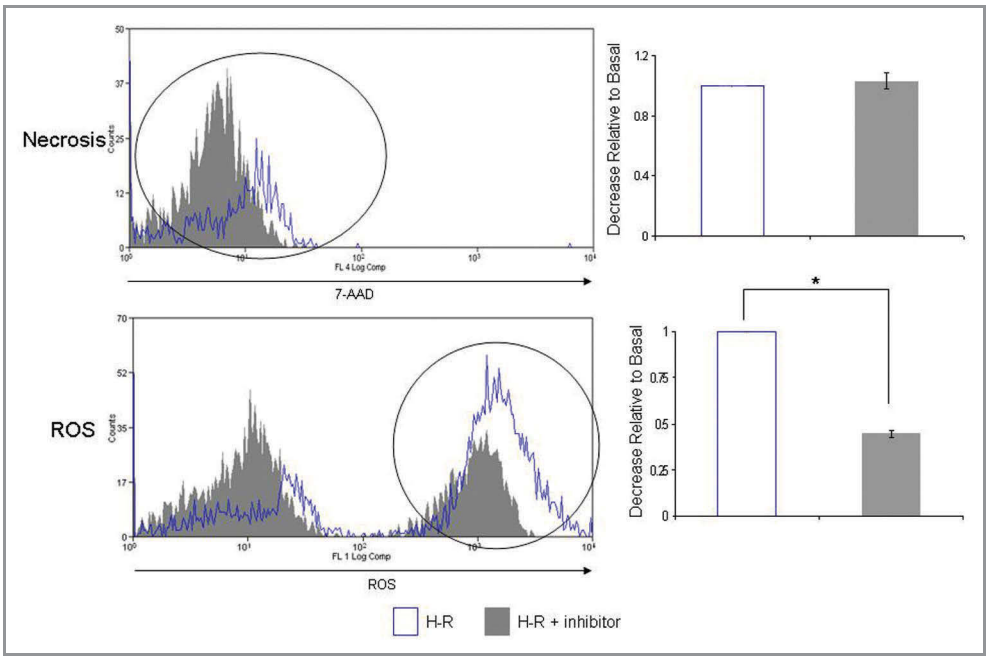

Figure 6. Inhibition of autophagy reduces ROS production in human hepatocytes during H-R but does not affect necrosis. This figure illustrates representative flow cytometry plots to demonstrate the effects of the pre-treatment of primary human hepatocytes with 3-MA and the resultant effects upon intracellular ROS production and necrosis during H-R. The level of intracellular ROS production and necrosis during H-R are shown in blue and the effects of 3-MA pre-treatment are shown in solid gray. The area of interest is marked with a vertical ellipse. The same gate has been applied to primary human hepatocytes for these plots as those shown in **Figure 1A**. The bar charts to the right of each flow cytometry plot show pooled data from three separate experiments. Data are expressed as increase or decrease relative to basal, where basal refers to the level of ROS production, apoptosis, necrosis or autophagy during H-R. Data are expressed as mean ± SE (*$p < 0.05$ relative to basal, Mann-Whitney test). Human hepatocytes used for these experiments were isolated from benign liver diseases (n = 3).

This finding also suggests that autophagy is differential induced in different liver diseases and may have important implications for disease pathogenesis.

During hypoxic stress, autophagy appears to occur within the mitochondrion and our data shows that this process is likely to be mediated by BECN1, LC3A, Atg 5, Atg 7 and Atg 12. Our findings corroborate those in HeLa cells where inhibition of autophagy also led to an increase in apoptosis.[25] We illustrate, for the first time, that the induction of autophagy within human hepatocytes during oxidative stress is essential for cell survival. Previous work by Kohli et al. in hepatocytes has shown that ROS production lies upstream of PtdIns3K activation.[26] Indeed, inhibition of PtdIns3K with 3-MA did not lead to an increase in BECN1, LC3A, Atg 5, Atg7 and Atg 12 protein levels which were otherwise seen during hypoxia and H-R. Coupled together these findings suggest that ROS activates PtdIns3K which subsequently activates the remaining autophagy machinery (**Fig. 12**). As stated above in hepatocytes autophagy targets mitochondria for degradation, a process known as mitophagy. The finding that the mitochondrion is the main ROS generator within human hepatocytes would also fit with this observation particularly in light of our previous findings that ROS can regulate autophagy, apoptosis and necrosis. Inhibiting ROS inhibits all three cellular processes, but selective inhibiting autophagy promotes apoptosis.

Furthermore, we demonstrate that the PV/large human hepatocytes increased levels of autophagy much more than PP/small human hepatocytes in line with their greater susceptibility to hypoxic injury. Moreover, inhibition of autophagy in PV/large human hepatocytes increased apoptosis during H-R, clearly demonstrating the link between autophagy and cell survival.

Central regulators of autophagy are the evolutionarily conserved Atg genes and recent studies have shown that some Atg proteins can be regulated by ROS.[11] BECN1, an essential regulator of early autophagy was induced by hypoxia and H-R and efficiently inhibited by 3-MA. Recent reviews have detailed the essential role of BECN1 in IRI[27] as well as its central role in mediating autophagy during oxidative stress.[28] Moreover, under stress hepatocytes utilize the LC3 protein to induce mitophagy within the dysfunctional mitochondrion.[29] This latter observation is probably the role of increased LC3 seen in our in vitro model. In an experimental rat model, short-term anoxia increases the expression of Atg7 in hepatocytes and protects against anoxia-reoxygenation mediated apoptosis and necrosis.[1] We also found an induction of Atg 7 during our model of IRI. Furthermore, we found induction of Atg5 and Atg 12. These two Atg proteins are involved in the latter processes of autophagy. Recent studies have shown the integral role Atg 5 in regulating menadione-induced oxidative stress.[30] In this study knockdown of Atg 5 in the rat hepatocyte line RALA255-10G sensitized cells to both apoptotic and necrotic cell death. In addition Atg 12, along with other Atg proteins, is required for the protection of anoxic rat hepatocytes from cell death.[31]

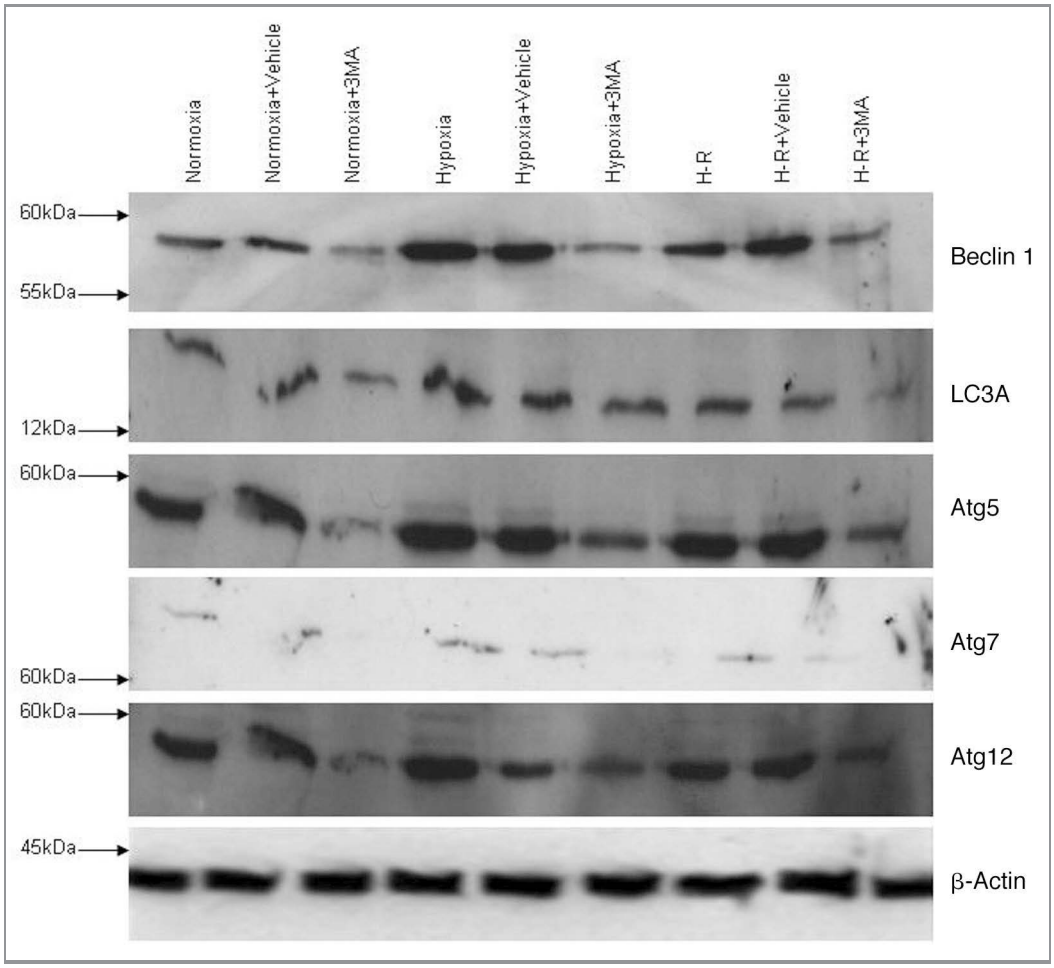

Figure 7. BECN1, LC3A, Atg 5, Atg 7 and Atg 12 are induced by hypoxia and H-R in human hepatocytes. This figure illustrates the induction of various Atg proteins involved in the regulation of autophagy during hypoxia and H-R. The effects of the PtdIns3K inhibitor 3-MA on Atg protein induction during hypoxia and H-R are also shown. All western blots were performed at least three times and presented blots are representative of all samples (n = 3).

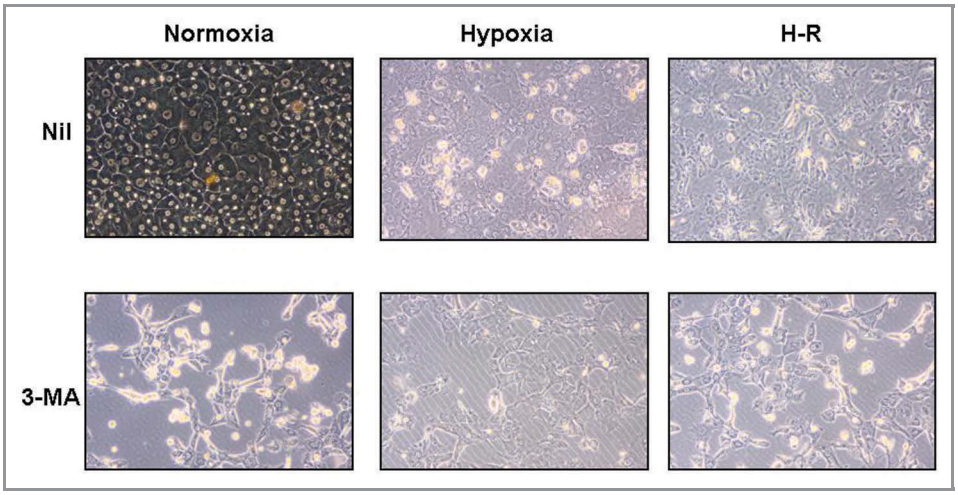

Figure 8. Inhibition of autophagy increases apoptosis in human hepatocytes during H-R. This figure shows representative light microscopy images of primary human hepatocytes during normoxia, hypoxia and H-R in the presence and absence of 3-MA. In normoxia human hepatocytes are typical cuboid morphology with many cells having the characteristic binucleate appearance. During hypoxia and H-R, cells lose this appearance and many cells appear small shrunken in the confluent monolayer of cells, indicative of apoptotic bodies. Following 3-MA pretreatment in either normoxia, hypoxia or H-R many more cells appear phase bright, small and shrunken. In addition there is disruption to the monolayer of hepatocytes. These light microscopy images have been taken after 24 h incubation in hypoxia and H-R with and without the presence of 3-MA. (Magnification x20).

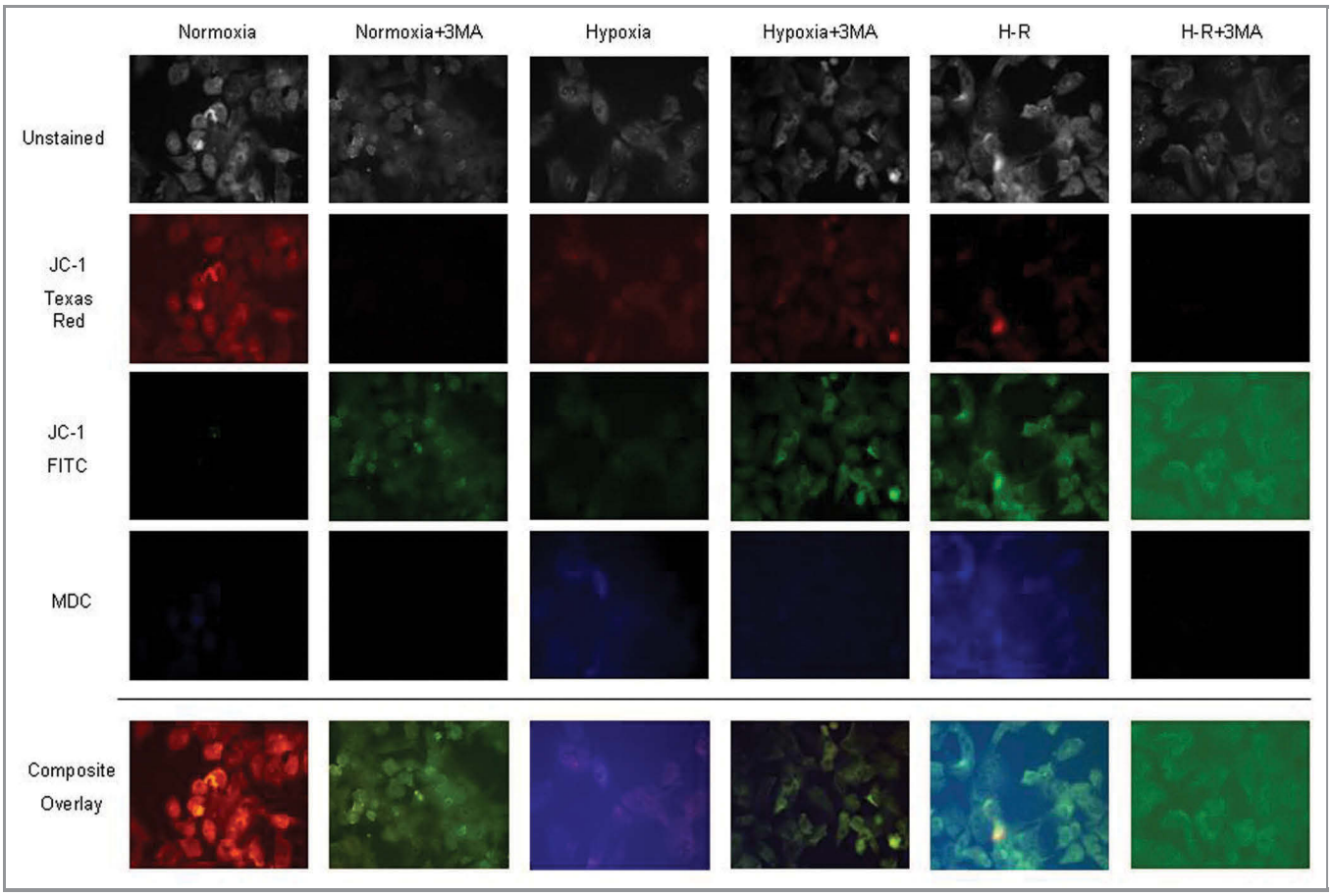

Figure 9. Autophagy is primarily performed in mitochondrion in human hepatocytes during hypoxia and H-R. This figure demonstrates the effects of hypoxia and H-R upon human hepatocyte mitochondrial membrane potential and MDC staining. Mitochondrial membrane potential was determined using the specific dye JC-1. When mitochondrial membrane potential is normal JC-1 appears red but once membrane potential is lowered or lost the dye become green. MDC staining is detected within the DAPI channel and appears blue. Composite overlay images are shown at the bottom of the figure. Additionally unstained images are provided with stained images to highlight the cellular location of immunofluorescence. In normoxia, as expected there was a normal mitochondrial membrane potential and no autophagy noted. During hypoxia and H-R there was a progressive loss of red JC-1 staining and an increase in green JC-1 staining indicating loss of mitochondrial potential and onset of cell death. In addition there was an increase in MDC staining in human hepatocytes during hypoxia and H-R. Moreover, MDC staining and green JC-1 staining co-localized in human hepatocytes during hypoxia and H-R.

While our study does not conclusively show which signaling pathways are activated by ROS in human hepatocytes to induce autophagy, it does clearly demonstrate that ROS is a key mediator of autophagy during oxidative stress. Furthermore in accordance with our study, previous authors have shown that the general antioxidants, catalase and *N*-acetylcysteine reduce autophagy.[11] We now show that mitochondrial and NADPH oxidase derived ROS are critical for the induction of autophagy in human hepatocytes. In addition previous studies have shown that H-R induces increased manganese superoxide dismutase expression in hepatocytes.[32] Taken together these studies show that ROS derived from many sources within hepatocytes can regulate autophagy. Moreover this generated ROS has prosurvival effects in activating autophagy but also signals to cell death in the form of apoptosis and necrosis (**Fig. 12**). The increase in antioxidant defenses within hepatocytes is likely to protect from cell death and the inhibition of autophagy may not be detrimental as autophagy can be regulated by other system besides ROS.[33] These observations provide interesting insights to the function of ROS in determining human hepatocyte fate.[2] Taken together, these observations clearly point to ROS regulating diverse and different signaling pathways within human hepatocytes during oxidative stress. These pathways appear to regulate both cell death and cell survival. It is likely that either the absolute level of intracellular ROS, the type of ROS sub-species generated or duration of ROS generation may be the critical factors in determining cell fate. The precise mechanistic pathways remain to be elucidated but may ultimately provide insights which inform the development of therapeutic strategies aimed at limiting the cellular damage and loss associated with liver injury. Previous authors have reported that inhibiting autophagy within rat hepatocytes leads to necrosis.[34] Moreover, in a model of ischemic preconditioning Esposti et al. reported that autophagy may switch necrosis and/or apoptosis on and off by modulating intracellular signaling.[35] We did not find this and it is likely that this represents species-specific effects of autophagy as no previous studies have evaluated

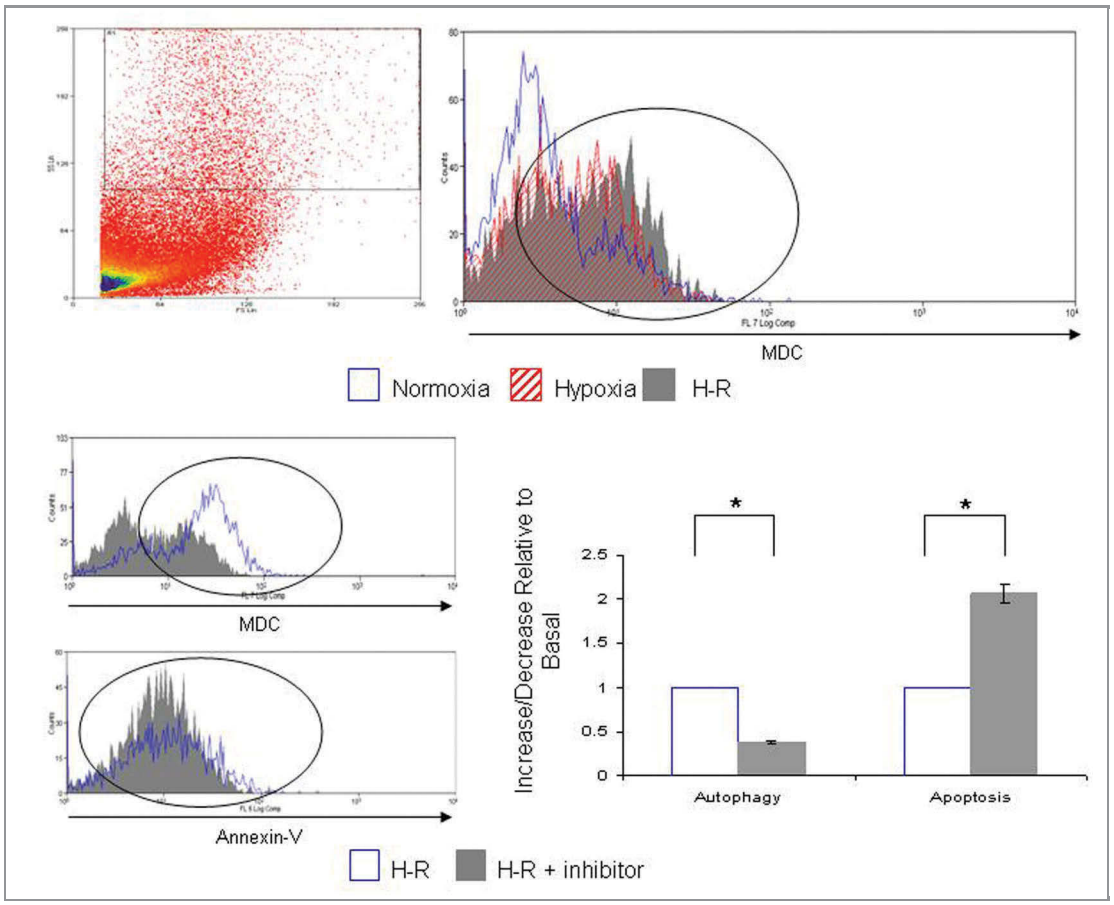

Figure 10. Autophagic response in large human hepatocytes during hypoxia and H-R. The top panel demonstrates a representative flow cytometry plot to illustrate the levels of MDC staining of PV/large human hepatocytes during normoxia (blue), hypoxia (hatched red) and H-R (solid gray). The plot on the left hand side of the flow cytometric plot represents a typical FS vs. SS plot, similar to that shown in **Figure 1A**. The FS vs. SS plot is from a H-R sample but similar plots were obtained during normoxia and hypoxia (data not shown). The gating protocol applied to human hepatocytes to analyze PV/large human hepatocytes is shown on the FS vs. SS plot. The area of interest of each flow cytometry plot is marked by a vertical ellipse. The bottom panel illustrates the effects of 3-MA pre-treatment upon PV/large human hepatocyte autophagy and apoptosis during H-R. The effects of H-R alone are shown in blue and the effects of 3-MA pretreatment are shown in solid gray. The bar chart shows composite data from four separate experiments. Data are expressed as mean ± SE (*$p < 0.05$ relative to basal, Mann-Whitney test).

autophagy in human hepatocytes. It may also represent a difference between the induction of autophagy in the in vitro and in vivo setting.

Our study demonstrates that ROS production decreased within human hepatocytes after 3-MA pre-treatment during H-R. One would expect that in hepatocytes in which autophagy was inhibited damaged mitochondria would continue to form ROS and induce cell death. However, the particular model utilized in our experiments examines cell death and ROS production at 24 h of hypoxia and/or H-R. The significant levels of apoptosis seen after 3-MA pretreatment during H-R suggests that a significant number of hepatocytes were already dead, hence intracellular ROS had reduced. Importantly, our study showed no significant effect of vehicle controls on human hepatocyte ROS production during H-R.

We provide evidence that within human hepatocytes, autophagy is a cell-survival mechanism during periods of oxidative stress. Moreover, taken together with previous studies, we show that the PV/large human hepatocytes increase autophagy significantly more in H-R relative to PP/small human hepatocytes. This is in accordance with our previous observations that the PV/large peri-venular human hepatocytes are more susceptible to oxidative stress. These observations suggest that the pharmacological activation of P13-K or other autophagy machinery, particularly within PV/large human hepatocytes may prove effective strategies in ameliorating human hepatocyte cell death in chronic liver disease as well as following liver transplantation.

Materials and Methods

Human hepatocyte isolation. Liver tissue was obtained via the Hepatobiliary and Transplant surgery program at the Queen Elizabeth Hospital Birmingham UK, from fully consenting patients undergoing transplantation, hepatic resection for liver metastasis, hepatic resection for benign liver disease or normal donor tissue surplus to surgical requirements. Ethical approval for

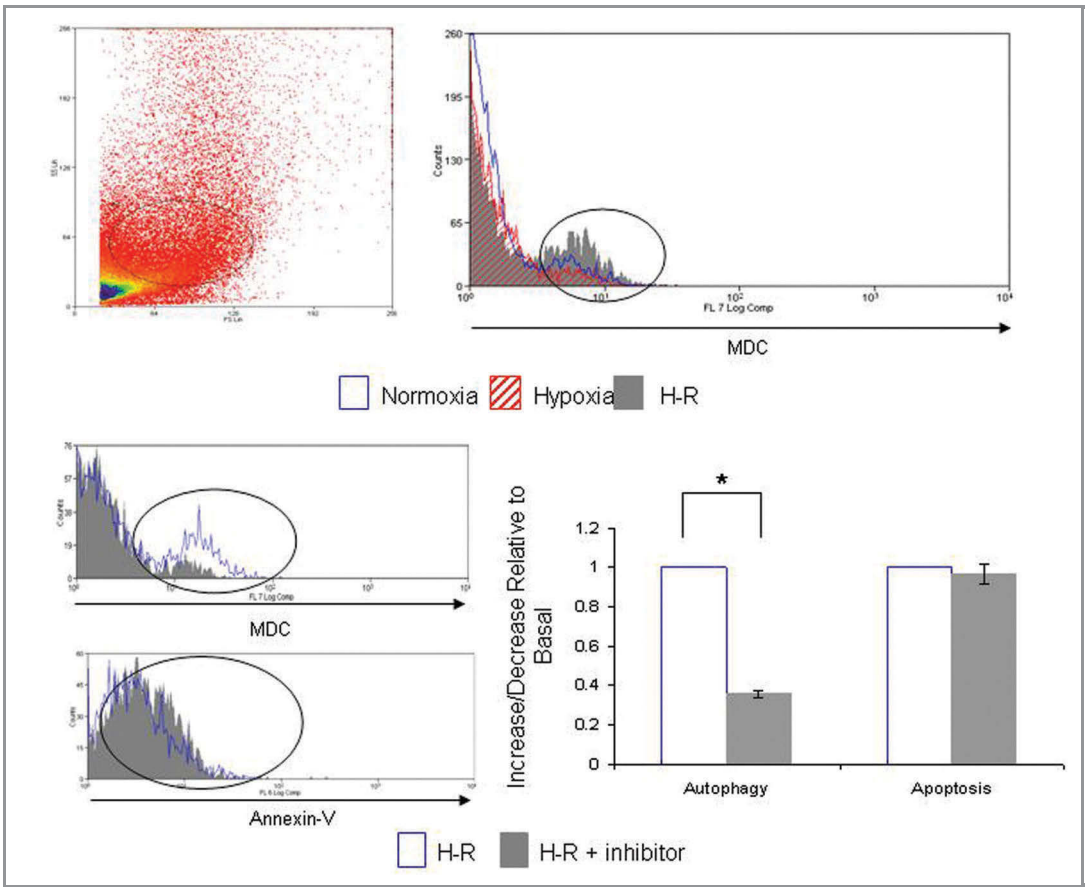

Figure 11. Autophagic response in small human hepatocytes during hypoxia and H-R. This figure demonstrates a representative flow cytometry plot to illustrate the levels of MDC staining of PP/small human hepatocytes during normoxia (blue), hypoxia (hatched red) and H-R (solid gray). The FS vs. SS plot is from a H-R sample but similar plots were obtained during normoxia and hypoxia (data not shown). The gating protocol applied to human hepatocytes to analyze PP/small human hepatocytes is shown on the FS vs. SS plot. The areas of interest on the flow cytometric plots are marked by vertical ellipses. The bottom panel illustrates the effects of 3-MA pre-treatment upon PP/small human hepatocyte autophagy and apoptosis during H-R. The effects of H-R alone are shown in blue and the effects of 3-MA pretreatment are shown in solid gray. The bar chart shows composite data from four separate experiments. Data are expressed as mean ± SE (*$p < 0.05$ relative to basal, Mann-Whitney test).

the study was grant by the Local Research Ethics Committee (LREC) (reference number 06/Q702/61). Human hepatocytes were isolated using the method that we have described previously.[36] Normal benign livers were classified as livers where resection was performed for recurrent cholangitis, haemangioma and focal nodular hyperplasia. Biliary cirrhosis livers included livers with both primary biliary cirrhosis and primary sclerosing cholangitis. Normal resected liver tissue was tissue taken from surgical resections performed for metastatic disease. Tissue was taken well away from the tumor site and all such patients had received pre-operative chemotherapy.

Model of hypoxia and H-R. In experiments, human hepatocytes were grown for 2 d at 37°C, 5% CO_2 in Williams E media (Sigma-Aldrich, W4125) on rat type 1 collagen-coated plates. Hepatocytes were either maintained in normoxia or placed into hypoxia for 24 h, or placed into hypoxia for 24 h followed by 24 h of reoxygenation. Hypoxia was achieved by placing cells in an airtight incubator (RS Mini Galaxy A incubator, Wolf Laboratories) flushed with 5% CO_2 and 95% N_2 until oxygen content in the chamber reached 0.1%, as verified by a dissolved oxygen monitor (DOH-247-KIT, Omega Engineering, UK). In preliminary experiments, human hepatocytes were exposed to 5% and 1% oxygen and no increase in ROS accumulation or cell death was noted. Therefore, we used 0.1% oxygen in all subsequent experiments. Additionally, Williams E media was pre-incubated in the hypoxic chamber in a sterile container, which allowed gas equilibration, for 8 h before experiments were performed, resulting in a final oxygen concentration of $< 0.1\%$ as measured with the dissolved oxygen meter. Where appropriate, after 24 h of hypoxia media was aspirated and replaced with fresh, warmed, oxygenated medium, and the cells were returned to normoxic conditions. This was defined as the beginning of reoxygenation. In experiments involving ROS inhibitors/antioxidants all reagents were made fresh as stock solutions and added using the correct dilution factor to the relevant experimental wells. Specifically, N-acteylcysteine (Sigma-Aldrich, A9165) was dissolved in molecular grade water (Sigma-Aldrich, W4502) to a concentration of 100 mM, rotenone (Sigma-Aldrich, R8875) was dissolved in chloroform (Sigma-Aldrich, C2432) to a concentration of 1 mM and diphenyliodonium (Sigma-Aldrich, 43088) was

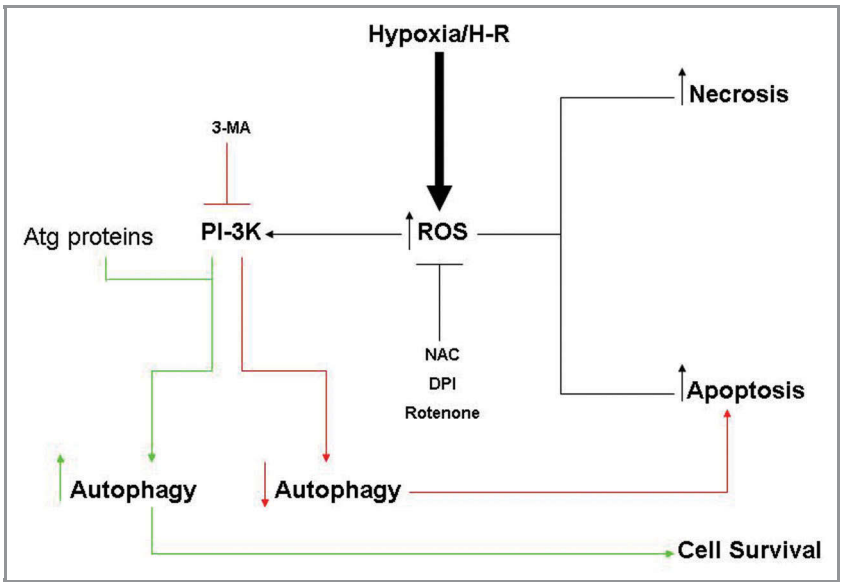

Figure 12. The proposed regulation of autophagy in human hepatocytes during hypoxia and H-R. Hypoxia and H-R leads to the generation of ROS in human hepatocytes predominantly in a mitochondrial dependent manner. As our previous work has demonstrated this increased ROS during hypoxia and H-R can lead to both apoptosis and necrosis2 (black arrows). However, the increased ROS can also activate autophagy which can be inhibited by the ROS inhibitors NAC, rotenone or DPI leading to reduced levels of apoptosis, necrosis and autophagy. As Kohli et al. have demonstrated in hepatocytes, ROS can activate PI3-K34, the essential first step in the assembly of the autophagosome. Once activated a number of Atg proteins including BECN1, LC3A, Atg5, Atg7 and Atg12 are involved in maturation of the autophagosome. It appears that the autophagy process predominantly removes dysfunctional mitochondria in human hepatocytes during hypoxia and H-R which in turns aids cell survival (green arrows). Inhibiting PtdIns3K with 3-MA ensures that the autophagosome does not develop and that Atg proteins are not induced in human hepatocytes during hypoxia and H-R (red arrows). Consequently, human hepatocytes are not able to carry out autophagy and thus mitochondria lose their membrane potential and are committed to cell death in the form of apoptosis.

dissolved in dimethyl sulfoxide (DMSO) (Sigma-Aldrich, D2650) to give a stock concentration of 1 mM, and these stocks were diluted appropriately to give working concentrations of 20 mM, 2 μM and 10 μM respectively. In experiments using ROS inhibitors/antioxidants, solvent alone controls were used to ensure no vehicle effects. In addition, in experiments using ROS inhibitors/antioxidants agents were added 4 h before the placement of the cells into hypoxia or into reoxygenation.

In experiments involving the use of 3-MA (Merck, Nottingham, 189490), stock solutions were made and added to the correct final dilution factor in the relevant tissue culture wells. 3-MA is a specific class III PtdIns3K inhibitor and specifically inhibits the early phases of autophagy. Specifically, 2 mg 3-MA was dissolved in molecular grade DMSO (Sigma-Aldrich) and were diluted appropriately to give working concentrations of 5 mM. In experiments using 3-MA, solvent alone wells were included as vehicle only controls. Hepatocytes were pre-treated with 3-MA for up to 4 h before placement of the cells into normoxia and hypoxia. For H-R experiments fresh 3-MA was added at the time of placement into reoxygenation.

Determination of human hepatocytes ROS accumulation, apoptosis, necrosis and autophagy. ROS production, apoptosis, necrosis and autophagy were determined by using a four-color reporter assay system. ROS accumulation was determined using the fluorescent probe 2',7'-dichlorofluorescin-diacetate (Merck, 287810).[37] This probe is cell permeable and once inside the cell is cleaved by intracellular esterases to 2',7'-dichlorofluorescin (DCF) and becomes cell impermeable. DCF is then able to react with intracellular ROS, specifically hydrogen peroxide, to give a fluorescent signal detectable on the FITC channel. The signal is directly proportional to the level of intracellular ROS present.

MitoSox Red is a mitochondrial superoxide indicator dye (Molecular Probes, Invitrogen, M36008) and was used as an alternative means to determine ROS in the mitochondria. Cells were treated as described above in the in vitro model and then loaded with 5 μM MitoSox Red in Hank's Balanced Salt Solution (HBSS) (Gibco, 14180046) for 30 min at 37°C in the dark. Cells were washed as described below. MitoSox Red fluorescent intensity was determined by fluorescence with excitation at 510 nm and emission at 580 nm.

Apoptosis was determined by labeling cells with Annexin-V (Molecular Probes, Invitrogen, A35122) which detects exposed phosphatidylserine on the cell membrane. 7-Amino-Actinomycin D (7-AAD) (Molecular Probes, Invitrogen, A1310) is a vital dye that binds to DNA, only entering cells once the cell membrane is disrupted and is indicative of cellular necrosis. Autophagy formation was determined by using the fluorescent dye monodansylcadaverine (MDC) (Sigma-Aldrich, 30432). This dye selectively labels autophagic vacuoles[38] and has been previously used in hepatoma cell lines[39] and primary hepatocytes[40] to detect autophagy. Following treatment, cell media was aspirated and replaced with HBSS without calcium and magnesium. DCF (30 μM) and MDC (1 μM) was added and the cells were incubated for 20 min in the dark at 37°C. The cells were then trypsinized and washed extensively in FACs buffer (phosphate-buffered saline pH 7.2 with 10% v/v heat inactivated fetal calf serum (Gibco) Sigma-Aldrich, F6178). Cells were then labeled with Annexin-V (0.25 μg/ml) and 7-AAD (1 μg/ml) for 15 min while on ice and then samples were immediately subjected to flow cytometry. At least 20,000 events were recorded within the gated region of the flow cytometer for each human hepatocyte cell preparation in each experimental condition. Only the cells within the gated region were used to calculate Mean Fluorescence Intensity (MFI).

To ensure consistency of the flow cytometric data, each human hepatocyte preparation was labeled with DCF alone, Annexin-V alone, 7-AAD alone and MDC alone to ensure that cells had become labeled and that the flow cytometry data could be compensated for crossover of fluorophore emission spectra. The same flow cytometry protocol was used for all experiments shown

within the study, i.e. voltages for all markers were constant for all human hepatocyte preparation ensuring inter- and intra-experimental consistency. Specifically, for each experiment a cell-only sample was used to ensure that there was no staining of primary human hepatocytes with each specific dye/probe. This sample was also used to ensure that the MFI reading was placed in the first decade for each dye/probe. Also these cells were used to place a flow cytometric gate for subsequent samples. Human hepatocytes vary considerable in size depending upon whether they are derived from the peri-venular region of the liver or peri-portal region of the liver. Therefore forward scatter (FS) and side scatter (SS) as shown in **Figure 1A** demonstrate a heterogeneous cell population. A gate was therefore placed in FS vs. SS that included all cells. Clearly, the sample includes cell debris that by necessity is included within the large gate applied in the analysis. Also, the gate will include small hepatocytes and hepatocytes that attain lower intensity of staining with probes/dyes and do not respond to hypoxia and H-R in the same way as the highly stained species. Therefore, peaks seen adjacent to the vertical ellipses of interest represent cell debris and hepatocytes that have different responses to hypoxia and H-R.

Western blotting. For western immunoblotting studies, human hepatocytes were lysed at the end of the relevant experimental period using NP-40 lysis buffer (20 mM TRIS-HCl pH 8 (Sigma-Aldrich, T3253), 137 mM NaCl (Sigma-Aldrich, S3014), 10% glycerol (Sigma-Aldrich, G5516), 1% Nonidet P40 (Sigma-Aldrich, 18896), 2 mM EDTA (Sigma-Aldrich, E6758). Protein concentration was determined by Bradford protein assay and 25 μg of protein was resolved on a 10% SDS-PAGE gel and transferred to a nitrocellulose membrane (Hybond; Amersham Biosciences, RPN3032D). The blotted membrane was blocked for 1 h at room temperature in Tris-buffered saline (TBS) pH 7.4/Tween 0.1% (Sigma-Aldrich, P9416) containing 5% (wt/vol) bovine serum albumin (BSA) (Sigma-Aldrich, A9418). All primary antibody incubations were performed at overnight at 4°C in TBS-Tween 0.1% containing 5% BSA (wt/vol). The incubation steps were followed by three washing steps of 5 min with TBS containing 0.1% Tween. All primary antibodies were purchased from New England Biolabs and used at a dilution of 1:1000 as per manufacturer's instructions. Specific primary antibodies used included: (1) BECN1 (3495), (2) LC3A (4599), (3) Atg5 (8540), (4) Atg12 (4180) and (5) Atg7 (2631).

Binding of specific mAb was detected with a horseradish peroxidase-conjugated anti-rabbit IgG at a dilution of 1:2000 for 1 h (Sigma-Aldrich, A8792) Protein bands were visualized using the enhanced chemiluminescence detection system (Amersham Biosciences, RPN2109) followed by exposure of the membranes to Hyperfilm-ECL (Amersham Biosciences, 28-9068-37). Equality of protein loading on were checked by immunoblotting for β-actin (Sigma-Aldrich, A2228) (dilution 1:20000). All Western immunoblots were performed at least three times from different liver preparations for each liver cell type.

Assessment of mitochondrial membrane potential and labeling of autophagic vacuoles with MDC. To measure the mitochondrial membrane potential ($\Delta\Psi$m), 5,5',6,6'-tetrachloro-1,1',3,3'-tetraethylbenzimidazolylcarbocyanine iodide (JC-1) (Molecular Probes, Invitrogen, M34152), a sensitive fluorescent probe for $\Delta\Psi$m was used.[41] Human hepatocytes were used in in vitro experiments as described above. At the end of the specific experimental procedure, cells were then rinsed with PBS twice and then stained with 5 μM JC-1 and/or 1 μM MDC for 30 min at 37°C. Cells were rinsed with ice-cold PBS twice, resuspended in 1 mL ice-cooled PBS, and immediately analyzed with a fluorescence microscope (Nikon Eclipse TE 300). A 488 nm filter was used for the excitation of JC-1. Emission filters of 535 nm and 595 nm were used to quantify the population of mitochondria with green (JC-1 monomers) and red (JC-1 aggregates) fluorescence, respectively.[42]

MDC staining was assessed with a filter system (V-2A excitation filter: 380/420 nm, barrier filter: 450 nm).[43] Images were captured with a CCD camera and imported into Adobe Photoshop.

Statistical analysis. All data are expressed as mean ± SE. Statistical comparisons between groups were analyzed by Mann-Whitney test. All differences were considered statistically significant at a value of $p < 0.05$.

Disclosure of Potential Conflicts of Interest

No potential conflicts of interest were disclosed.

Acknowledgments

R.H.B. is in receipt of Wellcome Trust Training Fellowship (DDDP.RCH1X1483). The authors would also like to thank the NIHR and BRU for their continued support of research. The authors are also grateful to the clinical team at the Queen Elizabeth Hospital, Birmingham for the procurement of liver tissue.

References

1. Kim JS, He L, Qian T, Lemasters JJ. Role of the mitochondrial permeability transition in apoptotic and necrotic death after ischemia/reperfusion injury to hepatocytes. Curr Mol Med 2003; 3:527-35; PMID:14527084; http://dx.doi.org/10.2174/1566524033479564
2. Bhogal RH, Curbishley SM, Weston CJ, Adams DH, Afford SC. Reactive oxygen species mediate human hepatocyte injury during hypoxia/reoxygenation. Liver Transpl 2010; 16:1303-13; PMID:21031546; http://dx.doi.org/10.1002/lt.22157
3. Yorimitsu T, Klionsky DJ. Autophagy: molecular machinery for self-eating. Cell Death Differ 2005; 12(Suppl 2):1542-52; PMID:16247502; http://dx.doi.org/10.1038/sj.cdd.4401765
4. Mortimore GE, Pösö AR, Lardeux BR. Mechanism and regulation of protein degradation in liver. Diabetes Metab Rev 1989; 5:49-70; PMID:2649336; http://dx.doi.org/10.1002/dmr.5610050105
5. Lu Z, Dono K, Gotoh K, Shibata M, Koike M, Marubashi S, et al. Participation of autophagy in the degeneration process of rat hepatocytes after transplantation following prolonged cold preservation. Arch Histol Cytol 2005; 68:71-80; PMID:15827380; http://dx.doi.org/10.1679/aohc.68.71
6. Czaja MJ. Functions of autophagy in hepatic and pancreatic physiology and disease. Gastroenterology 2011; 140:1895-908; PMID:21530520; http://dx.doi.org/10.1053/j.gastro.2011.04.038
7. Rautou PE, Mansouri A, Lebrec D, Durand F, Valla D, Moreau R. Autophagy in liver diseases. J Hepatol 2010; 53:1123-34; PMID:20810185; http://dx.doi.org/10.1016/j.jhep.2010.07.006
8. Bursch W, Ellinger A, Kienzl H, Török L, Pandey S, Sikorska M, et al. Active cell death induced by the anti-estrogens tamoxifen and ICI 164 384 in human mammary carcinoma cells (MCF-7) in culture: the role of autophagy. Carcinogenesis 1996; 17:1595-607; PMID:8761415; http://dx.doi.org/10.1093/carcin/17.8.1595
9. Ohsumi Y, Mizushima N. Two ubiquitin-like conjugation systems essential for autophagy. Semin Cell Dev Biol 2004; 15:231-6; PMID:15209383; http://dx.doi.org/10.1016/j.semcdb.2003.12.004

10. Ichimura Y, Kirisako T, Takao T, Satomi Y, Shimonishi Y, Ishihara N, et al. A ubiquitin-like system mediates protein lipidation. Nature 2000; 408:488-92; PMID:11100732; http://dx.doi.org/10.1038/35044114
11. Scherz-Shouval R, Sagiv Y, Shorer H, Elazar Z. The COOH terminus of GATE-16, an intra-Golgi transport modulator, is cleaved by the human cysteine protease HsApg4A. J Biol Chem 2003; 278:14053-8; PMID:12473658; http://dx.doi.org/10.1074/jbc.M212108200
12. Kabeya Y, Mizushima N, Yamamoto A, Oshitani-Okamoto S, Ohsumi Y, Yoshimori T. LC3, GABARAP and GATE16 localize to autophagosomal membrane depending on form-II formation. J Cell Sci 2004; 117:2805-12; PMID:15169837; http://dx.doi.org/10.1242/jcs.01131
13. Youle RJ, Narendra DP. Mechanisms of mitophagy. Nat Rev Mol Cell Biol 2011; 12:9-14; PMID:21179058; http://dx.doi.org/10.1038/nrm3028
14. Scherz-Shouval R, Elazar Z. Regulation of autophagy by ROS: physiology and pathology. Trends Biochem Sci 2011; 36:30-8; PMID:20728362; http://dx.doi.org/10.1016/j.tibs.2010.07.007
15. Mijaljica D, Prescott M, Devenish RJ. Mitophagy and mitoptosis in disease processes. Methods Mol Biol 2010; 648:93-106; PMID:20700707; http://dx.doi.org/10.1007/978-1-60761-756-3_6
16. Bhogal RH, Weston CJ, Curbishley SM, Bhatt AN, Adams DH, Afford SC. Variable responses of small and large human hepatocytes to hypoxia and hypoxia/reoxygenation (H-R). FEBS Lett 2011; 585:935-41; PMID:21356211; http://dx.doi.org/10.1016/j.febslet.2011.02.030
17. Levine B, Kroemer G. Autophagy in aging, disease and death: the true identity of a cell death impostor. Cell Death Differ 2009; 16:1-2; PMID:19079285; http://dx.doi.org/10.1038/cdd.2008.139
18. Huett A, Goel G, Xavier RJ. A systems biology viewpoint on autophagy in health and disease. Curr Opin Gastroenterol 2010; 26:302-9; PMID:20571384; http://dx.doi.org/10.1097/MOG.0b013e32833ae2ed
19. Yin XM, Ding WX, Gao W. Autophagy in the liver. Hepatology 2008; 47:1773-85; PMID:18393362; http://dx.doi.org/10.1002/hep.22146
20. Loos B, Genade S, Ellis B, Lochner A, Engelbrecht AM. At the core of survival: autophagy delays the onset of both apoptotic and necrotic cell death in a model of ischemic cell injury. Exp Cell Res 2011; 317:1437-53; PMID:21420401; http://dx.doi.org/10.1016/j.yexcr.2011.03.011
21. Köhrmann M, Haubensak W, Hemraj I, Kaether C, Lessmann VJ, Kiebler MA. Fast, convenient, and effective method to transiently transfect primary hippocampal neurons. J Neurosci Res 1999; 58:831-5; PMID:10583914; http://dx.doi.org/10.1002/(SICI)1097-4547(19991215)58:6<831::AID-JNR10>3.0.CO;2-M
22. Gardmo C, Kotokorpi P, Helander H, Mode A. Transfection of adult primary rat hepatocytes in culture. Biochem Pharmacol 2005; 69:1805-13; PMID:15885657; http://dx.doi.org/10.1016/j.bcp.2005.03.028
23. Park JS, Surendran S, Kamendulis LM, Morral N. Comparative nucleic acid transfection efficacy in primary hepatocytes for gene silencing and functional studies. BMC Res Notes 2011; 4:8; PMID:21244687; http://dx.doi.org/10.1186/1756-0500-4-8
24. Domart MC, Esposti DD, Sebagh M, Olaya N, Harper F, Pierron G, et al. Concurrent induction of necrosis, apoptosis, and autophagy in ischemic preconditioned human livers formerly treated by chemotherapy. J Hepatol 2009; 51:881-9; PMID:19765849; http://dx.doi.org/10.1016/j.jhep.2009.06.028
25. Cui Q, Tashiro S, Onodera S, Ikejima T. Augmentation of oridonin-induced apoptosis observed with reduced autophagy. J Pharmacol Sci 2006; 101:230-9; PMID:16861822; http://dx.doi.org/10.1254/jphs.FPJ06003X
26. Kohli R, Pan X, Malladi P, Wainwright MS, Whitington PF. Mitochondrial reactive oxygen species signal hepatocyte steatosis by regulating the phosphatidylinositol 3-kinase cell survival pathway. J Biol Chem 2007; 282:21327-36; PMID:17540768; http://dx.doi.org/10.1074/jbc.M701759200
27. Wang JH, Ahn IS, Fischer TD, Byeon JI, Dunn WA, Jr., Behrns KE, et al. Autophagy suppresses age-dependent ischemia and reperfusion injury in livers of mice. Gastroenterology 2011; 141:2188-2199.e6; PMID:21854730; http://dx.doi.org/10.1053/j.gastro.2011.08.005
28. Tanida I. Autophagy basics. Microbiol Immunol 2011; 55:1-11; PMID:21175768; http://dx.doi.org/10.1111/j.1348-0421.2010.00271.x
29. Kim I, Lemasters JJ. Mitochondrial degradation by autophagy (mitophagy) in GFP-LC3 transgenic hepatocytes during nutrient deprivation. Am J Physiol Cell Physiol 2011; 300:C308-17; PMID:21106691; http://dx.doi.org/10.1152/ajpcell.00056.2010
30. Wang Y, Singh R, Xiang Y, Czaja MJ. Macroautophagy and chaperone-mediated autophagy are required for hepatocyte resistance to oxidant stress. Hepatology 2010; 52:266-77; PMID:20578144; http://dx.doi.org/10.1002/hep.23645
31. Kim JS, Nitta T, Mohuczy D, O'Malley KA, Moldawer LL, Dunn WA, Jr., et al. Impaired autophagy: A mechanism of mitochondrial dysfunction in anoxic rat hepatocytes. Hepatology 2008; 47:1725-36; PMID:18311843; http://dx.doi.org/10.1002/hep.22187
32. Pardo M, Tirosh O. Protective signalling effect of manganese superoxide dismutase in hypoxia-reoxygenation of hepatocytes. Free Radic Res 2009; 43:1225-39; PMID:19905985; http://dx.doi.org/10.3109/10715760903271256
33. Tong J, Yan X, Yu L. The late stage of autophagy: cellular events and molecular regulation. Protein Cell 2010; 1:907-15; PMID:21204017; http://dx.doi.org/10.1007/s13238-010-0121-z
34. Zucchini-Pascal N, de Sousa G, Rahmani R. Lindane and cell death: at the crossroads between apoptosis, necrosis and autophagy. Toxicology 2009; 256:32-41; PMID:19041923; http://dx.doi.org/10.1016/j.tox.2008.11.004
35. Esposti DD, Domart MC, Sebagh M, Harper F, Pierron G, Brenner C, et al. Autophagy is induced by ischemic preconditioning in human livers formerly treated by chemotherapy to limit necrosis. Autophagy 2010; 6:172-4; PMID:20009565; http://dx.doi.org/10.4161/auto.6.1.10699
36. Bhogal RH, Hodson J, Bartlett DC, Weston CJ, Curbishley SM, Haughton E, et al. Isolation of primary human hepatocytes from normal and diseased liver tissue: a one hundred liver experience. PLoS One 2011; 6:e18222; PMID:21479238; http://dx.doi.org/10.1371/journal.pone.0018222
37. Schroedl C, McClintock DS, Budinger GR, Chandel NS. Hypoxic but not anoxic stabilization of HIF-1alpha requires mitochondrial reactive oxygen species. Am J Physiol Lung Cell Mol Physiol 2002; 283:L922-31; PMID:12376345
38. Biederbick A, Kern HF, Elsässer HP. Monodansylcadaverine (MDC) is a specific in vivo marker for autophagic vacuoles. Eur J Cell Biol 1995; 66:3-14; PMID:7750517
39. Zhang JQ, Li YM, Liu T, He WT, Chen YT, Chen XH, et al. Antitumor effect of matrine in human hepatoma G2 cells by inducing apoptosis and autophagy. World J Gastroenterol 2010; 16:4281-90; PMID:20818811; http://dx.doi.org/10.3748/wjg.v16.i34.4281
40. Mizushima N. Methods for monitoring autophagy. Int J Biochem Cell Biol 2004; 36:2491-502; PMID:15325587; http://dx.doi.org/10.1016/j.biocel.2004.02.005
41. Salvioli S, Ardizzoni A, Franceschi C, Cossarizza A. JC-1, but not DiOC6(3) or rhodamine 123, is a reliable fluorescent probe to assess delta psi changes in intact cells: implications for studies on mitochondrial functionality during apoptosis. FEBS Lett 1997; 411:77-82; PMID:9247146; http://dx.doi.org/10.1016/S0014-5793(97)00669-8
42. Gravance CG, Garner DL, Baumber J, Ball BA. Assessment of equine sperm mitochondrial function using JC-1. Theriogenology 2000; 53:1691-703; PMID:10968415; http://dx.doi.org/10.1016/S0093-691X(00)00308-3
43. Munafó DB, Colombo MI. A novel assay to study autophagy: regulation of autophagosome vacuole size by amino acid deprivation. J Cell Sci 2001; 114:3619-29; PMID:11707514

APPENDIX VI

PUBLICATIONS

MANUSCRIPTS

I. RH Bhogal, SM Curbishley, CJ Weston, DH Adams, SC Afford (2010) Reactive oxygen species regulate human hepatocyte cell death during hypoxia and reoxygenation. Liver Transplantation 16(11): 1303-1313

II. RH Bhogal, SM Curbishley, CJ Weston, AN Bhatt, DH Adams & SC Afford (2011) Variable responses of large and small human hepatocytes to hypoxia and hypoxia-reoxygenation (H-R). FEBS Letters 585(6): 935-941

III. RH Bhogal, J Hodson, DC Bartlett, SM Curbishley, CJ Weston, EL Haughton, GM Reynolds, PN Newsome, DH Adams & SC Afford (2011) Human hepatocyte isolation from normal and diseased livers: a one-hundred liver experience. PLoS One 6(3): e18222

IV. GK Wilson, CL Brimacombe, GM Reynolds, NF Fletcher, IA Rowe, Z Stamataki, RH Bhogal, M Simoes, M Ashcroft, SC Afford, R Mitry, A Dhawan, SG Hubscher & JA McKeating (2012) A dual role for hypoxia inducible factor-1α in the hepatitis C virus lifecycle and hepatoma cell migration. Journal of Hepatology 56(4): 803-809

V. R.H. Bhogal, CJ Weston, SM Curbishley, DH Adams & SC Afford (2012) Activation of CD40 with platelet derived CD154 promotes reactive oxygen species dependent death of human hepatocytes during hypoxia and reoxygenation. PLoS One 7(1): e30867

VI. RH Bhogal, SM Curbishley, CJ Weston, DH Adams & SC Afford (2012) Autophagy: A cyto-protective mechanism which prevents primary human hepatocyte apoptosis during oxidative stress. Autophagy 8(4): [Epub ahead of print]

BOOK CHAPTERS

I. R.H. Bhogal & S.C. Afford (2010) Immunology Cell Communication and Signalling Systems in Liver Disease. In: Signalling Pathways in Liver Diseases. Editors J.F. Dufour & Pierre-Alain Clavien. DOI 10.1007/978-3-642-00150-5. (Publisher Springer Berlin Heidelberg)

PRESENTATIONS TO LEARNED SOCITIES

I. European Transplant Fellow Workshop, Edinburgh, United Kingdom, 18th September 2009 (oral presentation)

II. British Inflammation Research Association, Birmingham, United Kingdom, 22nd January 2010 (poster presentation)

III. British Transplant Society, London, United Kingdom, 17th March 2010 (poster presentation)

IV. Association of Surgeons in Training, Hull, United Kingdom, 25th-27th March 2010 (poster presentation)

V. American Transplant Congress, San Diego, United States of America, 5th May 2010 (poster presentation)

VI. International Liver Transplant Society, Hong Kong, China, 17th June 2010 (oral presentation)

VII. American Association for the Study of the Liver, Boston, United States of America, 29th October 2010 (poster presentation)

VIII. Society of Academic Research in Surgery, Dublin, Ireland, 5-6th January 2011 (oral presentation)

IIX. Academy of Medical Sciences, London, United Kingdom, 23rd February 2011 (oral presentation)

IX. British Transplant Society, Bournemouth, United Kingdom, 9th March 2011 (poster presentation)

X. American Transplant Congress, Philadelphia, United States of America, 3rd March 2011 (oral presentation)

XI. International Liver Transplantation Society, Valencia, Spain, 24th May 2011 (poster presentation)

XII. Association of Surgeon in Training, Sheffield, United Kingdom, 17th May 2011 (poster presentation)

IIVX. European Society of Transplantation, Glasgow, United Kingdom, 5th September 2011 (oral presentation)

IVX. Society of Academic Research Surgery, Nottingham, United Kingdom, 5th September 2011 (oral presentation)

XV. British Transplant Society, Glasgow, United Kingdom, 22nd February 2012 (oral presentation)

XVI. International Liver Transplantation Society, San Francisco, United States of America, 16th May 2012 (poster presentation).

CORRESPONDANCE

I. R.H. Bhogal, R Sutaria, BK Gunson & SR Bramhall (2010) Letter: Similar liver transplantation survival with selected cardiac death donors and brain death donors. British Journal of Surgery 97: 1309-1312

II. R.H. Bhogal & SC Afford (2010) Letter: Blockade of Janus Kinase-2 signalling ameliorates mouse liver damage due to ischemia and reperfusion. Liver Transplantation 16(9): 1112-1113

III. R.H. Bhogal, R Sutaria & S.C. Afford (2010) Letter: Bacterial Lipopolysaccharide promotes profibrotic activation of intestinal fibroblasts. British Journal of Surgery 97(11): 1742

IV. R.H. Bhogal & SC Afford (2010) Letter: Blockade of Janus Kinase-2 signalling ameliorates mouse liver damage due to ischemia and reperfusion. Liver Transplantation 16(12): 1443

V. RH Bhogal & SC Afford (2010) Letter: Factors affecting hepatocyte isolation, engraftment, and replication in an *in vivo* model. Liver Transplantation 16(12): 1444

VI. RH Bhogal & SC Afford (2011) Letter: Anti-oxidants do not prevent bile acid-induced cell death in rat hepatocytes. Liver International 31(2): 273-274

VII. RH Bhogal, R Sutaria & SC Afford (2011) Letter: Hepatic liver ischemia/reperfusion injury: Processes in inflammatory networks – a review. Liver Transplantation 17(1): 95

VIII. R.H.Bhogal, B. Stephenson & SC Afford (2011) Letter: Preoperative fasting protects mice against hepatic ischemia/reperfusion injury: mechanisms and effects on liver regeneration. Liver Transplantation 17(11): 1364

PUBLISHED ABSTRACTS

I. RH Bhogal, DH Adams, SC Afford (2009) Regulation of hepatic hypoxia-reoxygenation injury by CD40-CD154. European Society of Transplantation (ESOT)

II. RH Bhogal, KT Williams, SM Curbishley, CJ Weston, DH Adams & SC Afford (2010) Hepatocyte responses to CD40 ligation by CD154 during hypoxia-reoxygenation. American Transplant Congress (ATC).

III. RH Bhogal, DH Adams & SC Afford (2010) The effects of hypoxia and reoxygenation on hepatocytes reactive oxygen species generation and sensitivity to CD40 mediated cell death. British Transplantation Society (BTS).

IV. RH Bhogal, CJ Weston, SJ Curbishley, DH Adams & SC Afford (2010) CD154-CD40 Stimulated Reactive Oxygen Species (ROS) Accumulation and Mitogen-Activated Protein Kinase (MAPKs) Regulates Human Hepatocytes During Reoxygenation. Liver Transplantation Vol 16 Issue S1

V. RH Bhogal & SC Afford (2010) Platelet Derived CD154 Mediates Human Hepatocyte Death During Ischaemia-Reperfusion Injury. Association of Surgeons in Training (ASiT).

VI. RH Bhogal, D MacDonald, CJ Weston, SM Curbishley, DH Adams & SC Afford (2010) Differential effects of hypoxia and hypoxia-reoxygenation on human hepatocyte and human sinusoidal endothelial cells. American Association for the Study of the Liver (AASLD)

VII. RH Bhogal, CJ Weston, SM Curbishley, DH Adams & SC Afford (2011) Primary human hepatocytes fate is modulated by intracellular reactive oxygen species generation and CD154 during hypoxia-reoxygenation injury. Society of Academic Surgery (SARS).

VIII. RH Bhogal, DH Adams & SC Afford (2011) Perivenous and not periportal human hepatocytes are the targets of ischemia-reperfusion injury following liver transplantation. British Transplant Society (BTS).

IIX. RH Bhogal, SM Curbishley, CJ Weston, AN Bhatt, DH Adams & SC Afford (2011) Peri-venous human hepatocytes are the targets for hepatic ischaemia-reperfusion injury. American Transplant Congress (ATC).

IX. RH Bhogal, SM Curbishley, CJ Weston, AN Bhatt, SC Afford & DH Adams (2011) Peri-venous human hepatocytes responses to pro-inflammatory stimuli shape the liver microenvironment after hepatic ischaemia-reperfusion injury. International Liver Transplantation Society (ILTS).

X. RH Bhogal, DH Adams & SC Afford (2011) Pro-inflammatory Stimuli and not Reactive Oxygen Species Regulate Adhesion Molecule Expression Upon Human Liver Sinusoidal Endothelial Cells During Hepatic Ischaemia-Reperfusion Injury. Association of Surgeons in Training (ASiT).

XI. RH Bhogal, DH Adams & SC Afford (2011) Autophagy Protects Human Hepatocytes from Cell Death During Hypoxia and Hypoxia-Reoxygenation. ESOT Basic Science Meeting.

XII. EH Humphreys, GM Muirhead, RH Bhogal, B Eksteen, SC Afford, YH Oo & DH Adams (2011) The effects of TH17 cytokines on liver parenchymal cells in shaping the microenvironment for local generation of TH17/Tc17 inflammatory liver disease. British Association for the Study of Liver Disease (BASL)

XIII. EH Humphreys, GM Muirhead, RH Bhogal, B Eksteen, SC Afford, YH Oo & DH Adams (2011) The effects of TH17 cytokines on liver parenchymal cells in shaping the microenvironment for local generation of TH17/Tc17 inflammatory liver disease. American Association for the Study of Liver Disease (AASLD)

IX. RH Bhogal, DH Adams & SC Afford (2012) Autophagy Protects Human Hepatocytes from Cell Death During Hypoxia and Hypoxia-Reoxygenation. Society Academic Research Surgery (SARS).

XV. RH Bhogal, SC Afford & DH Adams (2012) The inhibition of CD40-CD154 signalling inhibits liver injury in vitro and *in vivo*. International Liver Transplantation Society (ILTS).

XVI. RH Bhogal, DH Adams & SC Afford (2012) The inhibition of CD40-CD154 signalling protects the liver against ischaemia-reperfusion injury *in vitro* and *in vivo*. The British Transplantation Society (BTS).

AWARD & PRIZES

I. 2009 European Society Of Transplantation (ESOT) Prize for best basic science presentation at The European Fellow Transplant Workshop (EFTW)

II. 2010 Association of Surgeons in Training (ASiT) Poster Prize for best poster at the national annual ASiT meeting

III. 2011 British Transplant Society (BTS) Travelling Bursary to present research abstract at the BTS national congress

IV. 2011 British Transplant Society (BTS) Travelling Bursary to present research abstract at the American Transplant Congress (ATC)

V. 2011 St John's Ambulance Travelling Fellowship in Transplantation

VI. 2012 British Transplant Society Travelling Bursary to present research abstract at the BTS national congress

LIST OF REFERENCES

1. Monassier, J.P., *Reperfusion injury in acute myocardial infarction: from bench to cath lab. Part II: Clinical issues and therapeutic options.* Arch Cardiovasc Dis, 2008. **101**(9): p. 565-75.
2. Ritter, L., *Ischemia-reperfusion injury after stroke: from mechanisms to a nursing process.* Nurs Sci Q, 2008. **21**(1): p. 41-2.
3. Sadis, C., et al., *Nicotine protects kidney from renal ischemia/reperfusion injury through the cholinergic anti-inflammatory pathway.* PLoS One, 2007. **2**(5): p. e469.
4. Cerqueira, N.F., et al., *Systemic evaluation on ischemia and reperfusion injury of splanchnic organs in rats.* Acta Cir Bras, 2009. **24**(4): p. 290-5.
5. Arumugam, T.V., et al., *Toll-like receptors in ischemia-reperfusion injury.* Shock, 2009. **32**(1): p. 4-16.
6. Jaeschke, H., *Reactive oxygen and ischemia/reperfusion injury of the liver.* Chem Biol Interact, 1991. **79**(2): p. 115-36.
7. Jaeschke, H., *Molecular mechanisms of hepatic ischemia-reperfusion injury and preconditioning.* Am J Physiol Gastrointest Liver Physiol, 2003. **284**(1): p. G15-26.
8. Tilney, N.L. and R.D. Guttmann, *Effects of initial ischemia/reperfusion injury on the transplanted kidney.* Transplantation, 1997. **64**(7): p. 945-7.
9. Farrell, A.M., *Adding value? EU governance of organ donation and transplantation.* Eur J Health Law, 2010. **17**(1): p. 51-79.
10. Stahl, J.E., et al., *Consequences of cold-ischemia time on primary nonfunction and patient and graft survival in liver transplantation: a meta-analysis.* PLoS One, 2008. **3**(6): p. e2468.
11. Casillas-Ramirez, A., et al., *Past and future approaches to ischemia-reperfusion lesion associated with liver transplantation.* Life Sci, 2006. **79**(20): p. 1881-94.
12. Casillas-Ramirez, A., et al., *[Ischemia-reperfusion syndrome associated with liver transplantation: an update].* Gastroenterol Hepatol, 2006. **29**(5): p. 306-13.
13. Briceno, J., et al., *Prediction of graft dysfunction based on extended criteria donors in the model for end-stage liver disease score era.* Transplantation, 2010. **90**(5): p. 530-9.
14. Gastaca, M., *Extended criteria donors in liver transplantation: adapting donor quality and recipient.* Transplant Proc, 2009. **41**(3): p. 975-9.
15. Selzner, M., C.A. Camargo, and P.A. Clavien, *Ischemia impairs liver regeneration after major tissue loss in rodents: protective effects of interleukin-6.* Hepatology, 1999. **30**(2): p. 469-75.
16. Conti, A., et al., *Wide gene expression profiling of ischemia-reperfusion injury in human liver transplantation.* Liver Transpl, 2007. **13**(1): p. 99-113.
17. Avellini, C., et al., *Redox proteomics and immunohistology to study molecular events during ischemia-reperfusion in human liver.* Transplant Proc, 2007. **39**(6): p. 1755-60.
18. Abe, Y., et al., *Mouse model of liver ischemia and reperfusion injury: method for studying reactive oxygen and nitrogen metabolites in vivo.* Free Radic Biol Med, 2009. **46**(1): p. 1-7.

19. Ke, B., et al., *The CD154-CD40 T-cell co-stimulation pathway in liver ischemia and reperfusion inflammatory responses.* Transplantation, 2005. **79**(9): p. 1078-83.
20. Shen, X.D., et al., *Inflammatory responses in a new mouse model of prolonged hepatic cold ischemia followed by arterialized orthotopic liver transplantation.* Liver Transpl, 2005. **11**(10): p. 1273-81.
21. Ikemura, K., et al., *Decreased oral absorption of cyclosporine A after liver ischemia-reperfusion injury in rats: the contribution of CYP3A and P-glycoprotein to the first-pass metabolism in intestinal epithelial cells.* J Pharmacol Exp Ther, 2009. **328**(1): p. 249-55.
22. Li, S.Q. and L.J. Liang, *Protective mechanism of L-arginine against liver ischemic-reperfusion injury in rats.* Hepatobiliary Pancreat Dis Int, 2003. **2**(4): p. 549-52.
23. Malhi, H., G.J. Gores, and J.J. Lemasters, *Apoptosis and necrosis in the liver: a tale of two deaths?* Hepatology, 2006. **43**(2 Suppl 1): p. S31-44.
24. Emadali, A., et al., *Proteomic analysis of ischemia-reperfusion injury upon human liver transplantation reveals the protective role of IQGAP1.* Mol Cell Proteomics, 2006. **5**(7): p. 1300-13.
25. Buchman, T.G., et al., *Molecular biology of circulatory shock. Part II. Expression of four groups of hepatic genes is enhanced after resuscitation from cardiogenic shock.* Surgery, 1990. **108**(3): p. 559-66.
26. Lluis, J.M., et al., *Critical role of mitochondrial glutathione in the survival of hepatocytes during hypoxia.* J Biol Chem, 2005. **280**(5): p. 3224-32.
27. Lluis, J.M., et al., *Dual role of mitochondrial reactive oxygen species in hypoxia signaling: activation of nuclear factor-{kappa}B via c-SRC and oxidant-dependent cell death.* Cancer Res, 2007. **67**(15): p. 7368-77.
28. Metukuri, M.R., et al., *Expression and subcellular localization of BNIP3 in hypoxic hepatocytes and liver stress.* Am J Physiol Gastrointest Liver Physiol, 2009. **296**(3): p. G499-509.
29. Copple, B.L., et al., *Hypoxia-inducible factor-dependent production of profibrotic mediators by hypoxic hepatocytes.* Liver Int, 2009. **29**(7): p. 1010-21.
30. Lee, M.Y., et al., *Estradiol-17beta protects against hypoxia-induced hepatocyte injury through ER-mediated upregulation of Bcl-2 as well as ER-independent antioxidant effects.* Cell Res, 2008. **18**(4): p. 491-9.
31. Bogdanova, A., et al., *Hypoxic responses of Na+/K+ ATPase in trout hepatocytes.* J Exp Biol, 2005. **208**(Pt 10): p. 1793-801.
32. Zahrebelski, G., et al., *Progression of subcellular changes during chemical hypoxia to cultured rat hepatocytes: a laser scanning confocal microscopic study.* Hepatology, 1995. **21**(5): p. 1361-72.
33. Knobeloch, D., et al., *Human hepatocytes: isolation, culture, and quality procedures.* Methods Mol Biol, 2012. **806**: p. 99-120.
34. Kawahara, T., et al., *Factors affecting hepatocyte isolation, engraftment, and replication in an in vivo model.* Liver Transpl, 2010. **16**(8): p. 974-82.
35. Aninat, C., et al., *Expression of cytochromes P450, conjugating enzymes and nuclear receptors in human hepatoma HepaRG cells.* Drug Metab Dispos, 2006. **34**(1): p. 75-83.
36. Pan, C., et al., *Comparative proteomic phenotyping of cell lines and primary cells to assess preservation of cell type-specific functions.* Mol Cell Proteomics, 2009. **8**(3): p. 443-50.

37. Cerra, F.B., et al., *Hemorrhagic infarction: A reperfusion injury following prolonged myocardial ischemic anoxia.* Surgery, 1975. **78**(1): p. 95-104.
38. Toledo-Pereyra, L.H., R.L. Simmons, and J.S. Najarian, *Protection of the ischemic liver by donor pretreatment before transplantation.* Am J Surg, 1975. **129**(5): p. 513-7.
39. Eltzschig, H.K. and T. Eckle, *Ischemia and reperfusion--from mechanism to translation.* Nat Med, 2011. **17**(11): p. 1391-401.
40. Vardanian, A.J., R.W. Busuttil, and J.W. Kupiec-Weglinski, *Molecular mediators of liver ischemia and reperfusion injury: a brief review.* Mol Med, 2008. **14**(5-6): p. 337-45.
41. Zhai, Y., R.W. Busuttil, and J.W. Kupiec-Weglinski, *Liver ischemia and reperfusion injury: new insights into mechanisms of innate-adaptive immune-mediated tissue inflammation.* Am J Transplant, 2011. **11**(8): p. 1563-9.
42. Massip-Salcedo, M., et al., *The response of the hepatocyte to ischemia.* Liver Int, 2007. **27**(1): p. 6-16.
43. Jaeschke, H., *Reactive oxygen and mechanisms of inflammatory liver injury: Present concepts.* J Gastroenterol Hepatol, 2011. **26 Suppl 1**: p. 173-9.
44. Fondevila, C., R.W. Busuttil, and J.W. Kupiec-Weglinski, *Hepatic ischemia/reperfusion injury--a fresh look.* Exp Mol Pathol, 2003. **74**(2): p. 86-93.
45. Samarasinghe, D.A., M. Tapner, and G.C. Farrell, *Role of oxidative stress in hypoxia-reoxygenation injury to cultured rat hepatic sinusoidal endothelial cells.* Hepatology, 2000. **31**(1): p. 160-5.
46. Linfert, D., T. Chowdhry, and H. Rabb, *Lymphocytes and ischemia-reperfusion injury.* Transplant Rev (Orlando), 2009. **23**(1): p. 1-10.
47. Sato, Y., K. Tsukada, and K. Hatakeyama, *Role of shear stress and immune responses in liver regeneration after a partial hepatectomy.* Surg Today, 1999. **29**(1): p. 1-9.
48. Lalor, P.F., et al., *Vascular adhesion protein-1 mediates adhesion and transmigration of lymphocytes on human hepatic endothelial cells.* J Immunol, 2002. **169**(2): p. 983-92.
49. Pastor, C.M. and A. Hadengue, *Shear stress modulates the vascular tone in perfused livers isolated from normal rats.* Hepatology, 2000. **32**(4 Pt 1): p. 786-91.
50. Hisama, N., et al., *Kupffer cell production of cytokine-induced neutrophil chemoattractant following ischemia/reperfusion injury in rats.* Hepatology, 1996. **24**(5): p. 1193-8.
51. Malhi, H., M.E. Guicciardi, and G.J. Gores, *Hepatocyte death: a clear and present danger.* Physiol Rev, 2010. **90**(3): p. 1165-94.
52. Lemasters, J.J., *V. Necrapoptosis and the mitochondrial permeability transition: shared pathways to necrosis and apoptosis.* Am J Physiol, 1999. **276**(1 Pt 1): p. G1-6.
53. Lichtman, S.N. and J.J. Lemasters, *Role of cytokines and cytokine-producing cells in reperfusion injury to the liver.* Semin Liver Dis, 1999. **19**(2): p. 171-87.
54. Braet, F. and E. Wisse, *Structural and functional aspects of liver sinusoidal endothelial cell fenestrae: a review.* Comp Hepatol, 2002. **1**(1): p. 1.
55. Lutz, J., K. Thurmel, and U. Heemann, *Anti-inflammatory treatment strategies for ischemia/reperfusion injury in transplantation.* J Inflamm (Lond), 2010. **7**: p. 27.

56. Chen, Y. and R. Sun, *Toll-like receptors in acute liver injury and regeneration.* Int Immunopharmacol, 2011. **11**(10): p. 1433-41.
57. Murphy, S.P., P.M. Porrett, and L.A. Turka, *Innate immunity in transplant tolerance and rejection.* Immunol Rev, 2011. **241**(1): p. 39-48.
58. Broering, R., M. Lu, and J.F. Schlaak, *Role of Toll-like receptors in liver health and disease.* Clin Sci (Lond), 2011. **121**(10): p. 415-26.
59. Pradere, J.P., et al., *Toll-like receptor 4 and hepatic fibrogenesis.* Semin Liver Dis, 2010. **30**(3): p. 232-44.
60. Tsung, A., et al., *Hepatic ischemia/reperfusion injury involves functional TLR4 signaling in nonparenchymal cells.* J Immunol, 2005. **175**(11): p. 7661-8.
61. Wu, H.S., et al., *Toll-like receptor 4 involvement in hepatic ischemia/reperfusion injury in mice.* Hepatobiliary Pancreat Dis Int, 2004. **3**(2): p. 250-3.
62. Sumpter, T.L., et al., *Dendritic cells, the liver, and transplantation.* Hepatology, 2007. **46**(6): p. 2021-31.
63. Dhupar, R., et al., *Interferon regulatory factor 1 mediates acetylation and release of high mobility group box 1 from hepatocytes during murine liver ischemia-reperfusion injury.* Shock, 2011. **35**(3): p. 293-301.
64. Huang, H., et al., *Endogenous histones function as alarmins in sterile inflammatory liver injury through Toll-like receptor 9 in mice.* Hepatology, 2011. **54**(3): p. 999-1008.
65. Huang, Y., H. Rabb, and K.L. Womer, *Ischemia-reperfusion and immediate T cell responses.* Cell Immunol, 2007. **248**(1): p. 4-11.
66. Martin, M., et al., *Protective effects of early CD4(+) T cell reduction in hepatic ischemia/reperfusion injury.* J Gastrointest Surg, 2010. **14**(3): p. 511-9.
67. Dawson, T.L., et al., *Mitochondria as a source of reactive oxygen species during reductive stress in rat hepatocytes.* Am J Physiol, 1993. **264**(4 Pt 1): p. C961-7.
68. Murata, M., et al., *Role of intracellular calcium in superoxide-induced hepatocyte injury.* Hepatology, 1994. **19**(5): p. 1223-8.
69. Adkison, D., et al., *Role of free radicals in ischemia-reperfusion injury to the liver.* Acta Physiol Scand Suppl, 1986. **548**: p. 101-7.
70. Jaeschke, H., M.R. McGill, and A. Ramachandran, *Oxidant stress, mitochondria, and cell death mechanisms in drug-induced liver injury: lessons learned from acetaminophen hepatotoxicity.* Drug Metab Rev, 2012. **44**(1): p. 88-106.
71. Jaeschke, H. and J.R. Mitchell, *Mitochondria and xanthine oxidase both generate reactive oxygen species in isolated perfused rat liver after hypoxic injury.* Biochem Biophys Res Commun, 1989. **160**(1): p. 140-7.
72. Siriussawakul, A., A. Zaky, and J.D. Lang, *Role of nitric oxide in hepatic ischemia-reperfusion injury.* World J Gastroenterol, 2010. **16**(48): p. 6079-86.
73. Abu-Amara, M., et al., *Role of endothelial nitric oxide synthase in remote ischemic preconditioning of the mouse liver.* Liver Transpl, 2011. **17**(5): p. 610-9.
74. Yaylak, F., et al., *Liver tissue inducible nitric oxide synthase (iNOS) expression and lipid peroxidation in experimental hepatic ischemia reperfusion injury stimulated with lipopolysaccharide: the role of aminoguanidine.* J Surg Res, 2008. **148**(2): p. 214-23.
75. Tapuria, N., et al., *Modulation of microcirculatory changes in the late phase of hepatic ischaemia-reperfusion injury by remote ischaemic preconditioning.* HPB (Oxford), 2012. **14**(2): p. 87-97.

76. Afanas'ev, I.B., *Signaling functions of free radicals superoxide & nitric oxide under physiological & pathological conditions.* Mol Biotechnol, 2007. **37**(1): p. 2-4.
77. Wang, C.F., Z.Y. Wang, and J.Y. Li, *Dual protective role of HO-1 in transplanted liver grafts: a review of experimental and clinical studies.* World J Gastroenterol, 2011. **17**(26): p. 3101-8.
78. Perry, B.C., et al., *Tumor necrosis factor-alpha in liver ischemia/reperfusion injury.* J Invest Surg, 2011. **24**(4): p. 178-88.
79. Schwabe, R.F. and D.A. Brenner, *Mechanisms of Liver Injury. I. TNF-alpha-induced liver injury: role of IKK, JNK, and ROS pathways.* Am J Physiol Gastrointest Liver Physiol, 2006. **290**(4): p. G583-9.
80. Jia, C., *Advances in the regulation of liver regeneration.* Expert Rev Gastroenterol Hepatol, 2011. **5**(1): p. 105-21.
81. Teoh, N., et al., *Low-dose TNF-alpha protects against hepatic ischemia-reperfusion injury in mice: implications for preconditioning.* Hepatology, 2003. **37**(1): p. 118-28.
82. Amsterdam, A., K. Tajima, and R. Sasson, *Cell-specific regulation of apoptosis by glucocorticoids: implication to their anti-inflammatory action.* Biochem Pharmacol, 2002. **64**(5-6): p. 843-50.
83. Kuhnel, F., et al., *NFkappaB mediates apoptosis through transcriptional activation of Fas (CD95) in adenoviral hepatitis.* J Biol Chem, 2000. **275**(9): p. 6421-7.
84. Georgiev, P., et al., *Cholestasis protects the liver from ischaemic injury and post-ischaemic inflammation in the mouse.* Gut, 2007. **56**(1): p. 121-8.
85. Shibuya, H., et al., *Tumor necrosis factor-induced, superoxide-mediated neutrophil accumulation in cold ischemic/reperfused rat liver.* Hepatology, 1997. **26**(1): p. 113-20.
86. Ramaiah, S.K. and H. Jaeschke, *Role of neutrophils in the pathogenesis of acute inflammatory liver injury.* Toxicol Pathol, 2007. **35**(6): p. 757-66.
87. Adams, D.H., et al., *Mechanisms of immune-mediated liver injury.* Toxicol Sci, 2010. **115**(2): p. 307-21.
88. Jaeschke, H., et al., *Mechanisms of hepatotoxicity.* Toxicol Sci, 2002. **65**(2): p. 166-76.
89. Tacchini, L., L. Radice, and A. Bernelli-Zazzera, *Differential activation of some transcription factors during rat liver ischemia, reperfusion, and heat shock.* J Cell Physiol, 1999. **180**(2): p. 255-62.
90. Alchera, E., et al., *Adenosine-dependent activation of hypoxia-inducible factor-1 induces late preconditioning in liver cells.* Hepatology, 2008. **48**(1): p. 230-9.
91. Nath, B. and G. Szabo, *Hypoxia and hypoxia inducible factors: diverse roles in liver diseases.* Hepatology, 2012. **55**(2): p. 622-33.
92. Alchera, E., et al., *Molecular mechanisms of liver preconditioning.* World J Gastroenterol, 2010. **16**(48): p. 6058-67.
93. Amador, A., et al., *Ischemic pre-conditioning in deceased donor liver transplantation: a prospective randomized clinical trial.* Am J Transplant, 2007. **7**(9): p. 2180-9.
94. Guo, J.Y., et al., *Ischemic postconditioning attenuates liver warm ischemia-reperfusion injury through Akt-eNOS-NO-HIF pathway.* J Biomed Sci, 2011. **18**: p. 79.

95. Abe, Y., et al., *Liver epithelial cells proliferate under hypoxia and protect the liver from ischemic injury via expression of HIF-1 alpha target genes.* Surgery, 2012. **152**(5): p. 869-78.
96. Song, X., et al., *Combined preconditioning and postconditioning provides synergistic protection against liver ischemic reperfusion injury.* Int J Biol Sci, 2012. **8**(5): p. 707-18.
97. Beck-Schimmer, B., et al., *Protection of Pharmacological Postconditioning in Liver Surgery: Results of a Prospective Randomized Controlled Trial.* Ann Surg, 2012. **256**(5): p. 837-845.
98. Tirmenstein, M.A., et al., *Glutathione depletion and the production of reactive oxygen species in isolated hepatocyte suspensions.* Chem Biol Interact, 2000. **127**(3): p. 201-17.
99. Smith, M.K. and D.J. Mooney, *Hypoxia leads to necrotic hepatocyte death.* J Biomed Mater Res A, 2007. **80**(3): p. 520-9.
100. Yuan, L. and N. Kaplowitz, *Glutathione in liver diseases and hepatotoxicity.* Mol Aspects Med, 2009. **30**(1-2): p. 29-41.
101. Lemasters, J.J., et al., *The mitochondrial permeability transition in cell death: a common mechanism in necrosis, apoptosis and autophagy.* Biochim Biophys Acta, 1998. **1366**(1-2): p. 177-96.
102. Conde de la Rosa, L., et al., *Superoxide anions and hydrogen peroxide induce hepatocyte death by different mechanisms: involvement of JNK and ERK MAP kinases.* J Hepatol, 2006. **44**(5): p. 918-29.
103. Shabalina, I.G. and J. Nedergaard, *Mitochondrial ('mild') uncoupling and ROS production: physiologically relevant or not?* Biochem Soc Trans, 2011. **39**(5): p. 1305-9.
104. Pillai, V.C. and R. Mehvar, *Inhibition of NADPH-cytochrome P450 reductase by tannic acid in rat liver microsomes and primary hepatocytes: methodological artifacts and application to ischemia-reperfusion injury.* J Pharm Sci, 2011. **100**(8): p. 3495-505.
105. Brookes, P.S., et al., *Calcium, ATP, and ROS: a mitochondrial love-hate triangle.* Am J Physiol Cell Physiol, 2004. **287**(4): p. C817-33.
106. Kim, C., J.Y. Kim, and J.H. Kim, *Cytosolic phospholipase A(2), lipoxygenase metabolites, and reactive oxygen species.* BMB Rep, 2008. **41**(8): p. 555-9.
107. Dikalov, S., *Cross talk between mitochondria and NADPH oxidases.* Free Radic Biol Med, 2011. **51**(7): p. 1289-301.
108. Peglow, S., et al., *Allopurinol and xanthine oxidase inhibition in liver ischemia reperfusion.* J Hepatobiliary Pancreat Sci, 2011. **18**(2): p. 137-46.
109. Ishii, H., I. Kurose, and S. Kato, *Pathogenesis of alcoholic liver disease with particular emphasis on oxidative stress.* J Gastroenterol Hepatol, 1997. **12**(9-10): p. S272-82.
110. Jaeschke, H., *Mechanisms of Liver Injury. II. Mechanisms of neutrophil-induced liver cell injury during hepatic ischemia-reperfusion and other acute inflammatory conditions.* Am J Physiol Gastrointest Liver Physiol, 2006. **290**(6): p. G1083-8.
111. Bilzer, M., F. Roggel, and A.L. Gerbes, *Role of Kupffer cells in host defense and liver disease.* Liver Int, 2006. **26**(10): p. 1175-86.
112. Carreras, M.C. and J.J. Poderoso, *Mitochondrial nitric oxide in the signaling of cell integrated responses.* Am J Physiol Cell Physiol, 2007. **292**(5): p. C1569-80.

113. Morgan, M.J., Y.S. Kim, and Z.G. Liu, *TNFalpha and reactive oxygen species in necrotic cell death.* Cell Res, 2008. **18**(3): p. 343-9.
114. Croft, M., et al., *TNF superfamily in inflammatory disease: translating basic insights.* Trends Immunol, 2012. **33**(3): p. 144-52.
115. Hernandez-Alejandro, R., et al., *Reduction of Liver Ischemia Reperfusion Injury by Silencing of TNF-alpha Gene with shRNA.* J Surg Res, 2011.
116. Elgueta, R., et al., *Molecular mechanism and function of CD40/CD40L engagement in the immune system.* Immunol Rev, 2009. **229**(1): p. 152-72.
117. Shen, X., et al., *CD4 T cells promote tissue inflammation via CD40 signaling without de novo activation in a murine model of liver ischemia/reperfusion injury.* Hepatology, 2009. **50**(5): p. 1537-46.
118. Humphreys, E.H., et al., *Primary and malignant cholangiocytes undergo CD40 mediated Fas dependent apoptosis, but are insensitive to direct activation with exogenous Fas ligand.* PLoS One, 2010. **5**(11): p. e14037.
119. Afford, S.C., et al., *CD40 activation-induced, Fas-dependent apoptosis and NF-kappaB/AP-1 signaling in human intrahepatic biliary epithelial cells.* FASEB J, 2001. **15**(13): p. 2345-54.
120. Ahmed-Choudhury, J., et al., *CD40 mediated human cholangiocyte apoptosis requires JAK2 dependent activation of STAT3 in addition to activation of JNK1/2 and ERK1/2.* Cell Signal, 2006. **18**(4): p. 456-68.
121. Alabraba, E.B., et al., *Coculture of human liver macrophages and cholangiocytes leads to CD40-dependent apoptosis and cytokine secretion.* Hepatology, 2008. **47**(2): p. 552-62.
122. Afford, S.C., et al., *CD40 activation induces apoptosis in cultured human hepatocytes via induction of cell surface fas ligand expression and amplifies fas-mediated hepatocyte death during allograft rejection.* J Exp Med, 1999. **189**(2): p. 441-6.
123. Antoniades, C., et al., *The CD40/CD40 ligand system: linking inflammation with atherothrombosis.* J Am Coll Cardiol, 2009. **54**(8): p. 669-77.
124. Rizvi, M., et al., *CD40-CD40 ligand interactions in oxidative stress, inflammation and vascular disease.* Trends Mol Med, 2008. **14**(12): p. 530-8.
125. Xu, H., et al., *Platelet-derived or soluble CD154 induces vascularized allograft rejection independent of cell-bound CD154.* J Clin Invest, 2006. **116**(3): p. 769-74.
126. Akazawa, Y. and G.J. Gores, *Death receptor-mediated liver injury.* Semin Liver Dis, 2007. **27**(4): p. 327-38.
127. Li, X., et al., *Alleviation of ischemia-reperfusion injury in rat liver transplantation by induction of small interference RNA targeting Fas.* Langenbecks Arch Surg, 2007. **392**(3): p. 345-51.
128. Wang, Y., et al., *Temporal evolution of soluble Fas and Fas ligand in patients with orthotopic liver transplantation.* Cytokine, 2008. **41**(3): p. 240-3.
129. Li, B., et al., *Cell apoptosis and Fas gene expression in liver and renal tissues after ischemia-reperfusion injury in liver transplantation.* Transplant Proc, 2010. **42**(5): p. 1550-6.
130. Nakajima, H., et al., *Blockade of the Fas/Fas ligand interaction suppresses hepatocyte apoptosis in ischemia-reperfusion rat liver.* Apoptosis, 2008. **13**(8): p. 1013-21.

131. Liedtke, C. and C. Trautwein, *The role of TNF and Fas dependent signaling in animal models of inflammatory liver injury and liver cancer.* Eur J Cell Biol, 2011.
132. Shirley, S., A. Morizot, and O. Micheau, *Regulating TRAIL receptor-induced cell death at the membrane : a deadly discussion.* Recent Pat Anticancer Drug Discov, 2011. **6**(3): p. 311-23.
133. Cao, L., et al., *Enhancement of antitumor properties of TRAIL by targeted delivery to the tumor neovasculature.* Mol Cancer Ther, 2008. **7**(4): p. 851-61.
134. Yoon, J.H. and G.J. Gores, *Death receptor-mediated apoptosis and the liver.* J Hepatol, 2002. **37**(3): p. 400-10.
135. Fischer, R., T. Baumert, and H.E. Blum, *Hepatitis C virus infection and apoptosis.* World J Gastroenterol, 2007. **13**(36): p. 4865-72.
136. Afford, S.C. and D.H. Adams, *Following the TRAIL from hepatitis C virus and alcohol to fatty liver.* Gut, 2005. **54**(11): p. 1518-20.
137. Burkly, L.C., J.S. Michaelson, and T.S. Zheng, *TWEAK/Fn14 pathway: an immunological switch for shaping tissue responses.* Immunol Rev, 2011. **244**(1): p. 99-114.
138. Nakayama, M., et al., *Involvement of TWEAK in interferon gamma-stimulated monocyte cytotoxicity.* J Exp Med, 2000. **192**(9): p. 1373-80.
139. Donohue, P.J., et al., *TWEAK is an endothelial cell growth and chemotactic factor that also potentiates FGF-2 and VEGF-A mitogenic activity.* Arterioscler Thromb Vasc Biol, 2003. **23**(4): p. 594-600.
140. Hotta, K., et al., *Direct targeting of fibroblast growth factor-inducible 14 protein protects against renal ischemia reperfusion injury.* Kidney Int, 2011. **79**(2): p. 179-88.
141. Cabal-Hierro, L. and P.S. Lazo, *Signal transduction by tumor necrosis factor receptors.* Cell Signal, 2012.
142. Padanilam, B.J., A.J. Lewington, and M.R. Hammerman, *Expression of CD27 and ischemia/reperfusion-induced expression of its ligand Siva in rat kidneys.* Kidney Int, 1998. **54**(6): p. 1967-75.
143. Puppi, J., et al., *Improving the Techniques for Human Hepatocyte Transplantation: Report from a Consensus Meeting in London.* Cell Transplant, 2011.
144. Guo, L., et al., *Similarities and differences in the expression of drug-metabolizing enzymes between human hepatic cell lines and primary human hepatocytes.* Drug Metab Dispos, 2011. **39**(3): p. 528-38.
145. Aniagu, S.O., T.D. Williams, and J.K. Chipman, *Changes in gene expression and assessment of DNA methylation in primary human hepatocytes and HepG2 cells exposed to the environmental contaminants-Hexabromocyclododecane and 17-beta oestradiol.* Toxicology, 2009. **256**(3): p. 143-51.
146. Smith, C.M., et al., *Differential UGT1A1 induction by chrysin in primary human hepatocytes and HepG2 Cells.* J Pharmacol Exp Ther, 2005. **315**(3): p. 1256-64.
147. Hughes, R.D., et al., *Isolation of hepatocytes from livers from non-heart-beating donors for cell transplantation.* Liver Transpl, 2006. **12**(5): p. 713-7.
148. Sagias, F.G., et al., *N-acetylcysteine improves the viability of human hepatocytes isolated from severely steatotic donor liver tissue.* Cell Transplant, 2010. **19**(11): p. 1487-92.
149. Li, A.P., *Human hepatocytes: isolation, cryopreservation and applications in drug development.* Chem Biol Interact, 2007. **168**(1): p. 16-29.

150. Alexandrova, K., et al., *Large-scale isolation of human hepatocytes for therapeutic application.* Cell Transplant, 2005. **14**(10): p. 845-53.
151. Vondran, F.W., et al., *Isolation of primary human hepatocytes after partial hepatectomy: criteria for identification of the most promising liver specimen.* Artif Organs, 2008. **32**(3): p. 205-13.
152. Lecluyse, E.L. and E. Alexandre, *Isolation and culture of primary hepatocytes from resected human liver tissue.* Methods Mol Biol, 2010. **640**: p. 57-82.
153. Gonzalez, R., et al., *Cytoprotective properties of alpha-tocopherol are related to gene regulation in cultured D-galactosamine-treated human hepatocytes.* Free Radic Biol Med, 2007. **43**(10): p. 1439-52.
154. Dhawan, A., R.R. Mitry, and R.D. Hughes, *Hepatocyte transplantation for metabolic disorders, experience at King's College hospital and review of literature.* Acta Gastroenterol Belg, 2005. **68**(4): p. 457-60.
155. Berry, M.N. and D.S. Friend, *High-yield preparation of isolated rat liver parenchymal cells: a biochemical and fine structural study.* J Cell Biol, 1969. **43**(3): p. 506-20.
156. Jung, D., et al., *New Colorimetric reaction for end-point, continuous-flow, and kinetic measurement of urea.* Clin Chem, 1975. **21**(8): p. 1136-40.
157. Ahmed-Choudhury, J., et al., *Differential induction of nuclear factor-kappaB and activator protein-1 activity after CD40 ligation is associated with primary human hepatocyte apoptosis or intrahepatic endothelial cell proliferation.* Mol Biol Cell, 2003. **14**(4): p. 1334-45.
158. Rodrigues, C.M., et al., *Ursodeoxycholic acid may inhibit deoxycholic acid-induced apoptosis by modulating mitochondrial transmembrane potential and reactive oxygen species production.* Mol Med, 1998. **4**(3): p. 165-78.
159. Guicciardi, M.E. and G.J. Gores, *Is ursodeoxycholate an antiapoptotic drug?* Hepatology, 1998. **28**(6): p. 1721-3.
160. Schaffert, C.S., et al., *Alcohol metabolites and lipopolysaccharide: roles in the development and/or progression of alcoholic liver disease.* World J Gastroenterol, 2009. **15**(10): p. 1209-18.
161. Hewes, J.C., et al., *A prospective study of isolated human hepatocyte function following liver resection for colorectal liver metastases: the effects of prior exposure to chemotherapy.* J Hepatol, 2006. **45**(2): p. 263-70.
162. Laba, A., et al., *Characterization of human hepatocytes isolated from non-transplantable livers.* Arch Immunol Ther Exp (Warsz), 2005. **53**(5): p. 442-53.
163. Zhang, W., et al., *Role of reactive oxygen species in mediating hepatic ischemia-reperfusion injury and its therapeutic applications in liver transplantation.* Transplant Proc, 2007. **39**(5): p. 1332-7.
164. Gonzalez-Flecha, B., J.C. Cutrin, and A. Boveris, *Time course and mechanism of oxidative stress and tissue damage in rat liver subjected to in vivo ischemia-reperfusion.* J Clin Invest, 1993. **91**(2): p. 456-64.
165. Donato, M.T., et al., *CYP2A5/CYP2A6 expression in mouse and human hepatocytes treated with various in vivo inducers.* Drug Metab Dispos, 2000. **28**(11): p. 1321-6.
166. Jemnitz, K., et al., *Interspecies differences in acetaminophen sensitivity of human, rat, and mouse primary hepatocytes.* Toxicol In Vitro, 2008. **22**(4): p. 961-7.

167. Decker, K., *Biologically active products of stimulated liver macrophages (Kupffer cells).* Eur J Biochem, 1990. **192**(2): p. 245-61.
168. Jaeschke, H., *Reperfusion injury after warm ischemia or cold storage of the liver: role of apoptotic cell death.* Transplant Proc, 2002. **34**(7): p. 2656-8.
169. Taniai, H., et al., *Susceptibility of murine periportal hepatocytes to hypoxia-reoxygenation: role for NO and Kupffer cell-derived oxidants.* Hepatology, 2004. **39**(6): p. 1544-52.
170. Imamura, H., et al., *Role of Kupffer cells in cold ischemia/reperfusion injury of rat liver.* Gastroenterology, 1995. **109**(1): p. 189-97.
171. Caraceni, P., et al., *Source of oxygen free radicals produced by rat hepatocytes during postanoxic reoxygenation.* Biochim Biophys Acta, 1995. **1268**(3): p. 249-54.
172. Young, T.A., C.C. Cunningham, and S.M. Bailey, *Reactive oxygen species production by the mitochondrial respiratory chain in isolated rat hepatocytes and liver mitochondria: studies using myxothiazol.* Arch Biochem Biophys, 2002. **405**(1): p. 65-72.
173. Schulze-Bergkamen, H., et al., *The role of apoptosis versus oncotic necrosis in liver injury: facts or faith?* J Hepatol, 2006. **44**(5): p. 984-93.
174. Sasaki, H., et al., *Activation of apoptosis during the reperfusion phase after rat liver ischemia.* Transplant Proc, 1996. **28**(3): p. 1908-9.
175. Jaeschke, H. and J.J. Lemasters, *Apoptosis versus oncotic necrosis in hepatic ischemia/reperfusion injury.* Gastroenterology, 2003. **125**(4): p. 1246-57.
176. Loud, A.V., *A quantitative stereological description of the ultrastructure of normal rat liver parenchymal cells.* J Cell Biol, 1968. **37**(1): p. 27-46.
177. Schmucker, D.L., J.S. Mooney, and A.L. Jones, *Stereological analysis of hepatic fine structure in the Fischer 344 rat. Influence of sublobular location and animal age.* J Cell Biol, 1978. **78**(2): p. 319-37.
178. Willson, R.A., S.B. Wormsley, and U. Muller-Eberhard, *A comparison of hepatocyte size distribution in untreated and phenobarbital-treated rats as assessed by flow cytometry.* Dig Dis Sci, 1984. **29**(8): p. 753-7.
179. Braakman, I., et al., *Separation of periportal and perivenous rat hepatocytes by fluorescence-activated cell sorting: confirmation with colloidal gold as an exogenous marker.* Hepatology, 1991. **13**(1): p. 73-82.
180. Thalhammer, T., et al., *Separation of hepatocytes of different acinar zones by flow cytometry.* Cytometry, 1989. **10**(6): p. 772-8.
181. Gumucio, J.J., et al., *The isolation of functionally heterogeneous hepatocytes of the proximal and distal half of the liver acinus in the rat.* Hepatology, 1986. **6**(5): p. 932-44.
182. Wilton, J.C., et al., *Periportal- and perivenous-enriched hepatocyte couplets: differences in canalicular activity and in response to oxidative stress.* Biochem J, 1993. **292 (Pt 3)**: p. 773-9.
183. Bella, D.L., et al., *Cysteine metabolism in periportal and perivenous hepatocytes: perivenous cells have greater capacity for glutathione production and taurine synthesis but not for cysteine catabolism.* Amino Acids, 2002. **23**(4): p. 453-8.
184. Jungermann, K. and N. Katz, *Functional specialization of different hepatocyte populations.* Physiol Rev, 1989. **69**(3): p. 708-64.

185. Traber, P.G., J. Chianale, and J.J. Gumucio, *Physiologic significance and regulation of hepatocellular heterogeneity.* Gastroenterology, 1988. **95**(4): p. 1130-43.
186. Kato, Y., J. Tanaka, and K. Koyama, *Intralobular heterogeneity of oxidative stress and cell death in ischemia-reperfused rat liver.* J Surg Res, 2001. **95**(2): p. 99-106.
187. Rautou, P.E., et al., *Autophagy in liver diseases.* J Hepatol, 2010. **53**(6): p. 1123-34.
188. Lee, J., S. Giordano, and J. Zhang, *Autophagy, mitochondria and oxidative stress: cross-talk and redox signalling.* Biochem J, 2012. **441**(2): p. 523-40.
189. Czaja, M.J., *Functions of autophagy in hepatic and pancreatic physiology and disease.* Gastroenterology, 2011. **140**(7): p. 1895-908.
190. Gotoh, K., et al., *Participation of autophagy in the initiation of graft dysfunction after rat liver transplantation.* Autophagy, 2009. **5**(3): p. 351-60.
191. Chen, Y. and D.J. Klionsky, *The regulation of autophagy - unanswered questions.* J Cell Sci, 2011. **124**(Pt 2): p. 161-70.
192. Dreux, M. and F.V. Chisari, *Impact of the autophagy machinery on hepatitis C virus infection.* Viruses, 2011. **3**(8): p. 1342-57.
193. Tian, Y., et al., *Autophagy required for hepatitis B virus replication in transgenic mice.* J Virol, 2011. **85**(24): p. 13453-6.
194. Donohue, T.M., Jr., *Autophagy and ethanol-induced liver injury.* World J Gastroenterol, 2009. **15**(10): p. 1178-85.
195. Bursch, W., et al., *Active cell death induced by the anti-estrogens tamoxifen and ICI 164 384 in human mammary carcinoma cells (MCF-7) in culture: the role of autophagy.* Carcinogenesis, 1996. **17**(8): p. 1595-607.
196. Ohsumi, Y. and N. Mizushima, *Two ubiquitin-like conjugation systems essential for autophagy.* Semin Cell Dev Biol, 2004. **15**(2): p. 231-6.
197. Ichimura, Y., et al., *A ubiquitin-like system mediates protein lipidation.* Nature, 2000. **408**(6811): p. 488-92.
198. Scherz-Shouval, R., et al., *The COOH terminus of GATE-16, an intra-Golgi transport modulator, is cleaved by the human cysteine protease HsApg4A.* J Biol Chem, 2003. **278**(16): p. 14053-8.
199. Kabeya, Y., et al., *LC3, GABARAP and GATE16 localize to autophagosomal membrane depending on form-II formation.* J Cell Sci, 2004. **117**(Pt 13): p. 2805-12.
200. Yorimitsu, T. and D.J. Klionsky, *Autophagy: molecular machinery for self-eating.* Cell Death Differ, 2005. **12 Suppl 2**: p. 1542-52.
201. Schroedl, C., et al., *Hypoxic but not anoxic stabilization of HIF-1alpha requires mitochondrial reactive oxygen species.* Am J Physiol Lung Cell Mol Physiol, 2002. **283**(5): p. L922-31.
202. Biederbick, A., H.F. Kern, and H.P. Elsasser, *Monodansylcadaverine (MDC) is a specific in vivo marker for autophagic vacuoles.* Eur J Cell Biol, 1995. **66**(1): p. 3-14.
203. Zhang, J.Q., et al., *Antitumor effect of matrine in human hepatoma G2 cells by inducing apoptosis and autophagy.* World J Gastroenterol, 2010. **16**(34): p. 4281-90.
204. Mizushima, N., *Methods for monitoring autophagy.* Int J Biochem Cell Biol, 2004. **36**(12): p. 2491-502.

205. Salvioli, S., et al., *JC-1, but not DiOC6(3) or rhodamine 123, is a reliable fluorescent probe to assess delta psi changes in intact cells: implications for studies on mitochondrial functionality during apoptosis.* FEBS Lett, 1997. **411**(1): p. 77-82.
206. Gravance, C.G., et al., *Assessment of equine sperm mitochondrial function using JC-1.* Theriogenology, 2000. **53**(9): p. 1691-703.
207. Munafo, D.B. and M.I. Colombo, *A novel assay to study autophagy: regulation of autophagosome vacuole size by amino acid deprivation.* J Cell Sci, 2001. **114**(Pt 20): p. 3619-29.
208. Haga, S., et al., *Preventing hypoxia/reoxygenation damage to hepatocytes by p66(shc) ablation: up-regulation of anti-oxidant and anti-apoptotic proteins.* J Hepatol, 2008. **48**(3): p. 422-32.
209. Crenesse, D., et al., *JNK(1)/SAPK(1) involvement in hypoxia-reoxygenation-induced apoptosis in rat hepatocytes.* Transplant Proc, 2001. **33**(1-2): p. 260-1.
210. Cotgreave, I.A., *N-acetylcysteine: pharmacological considerations and experimental and clinical applications.* Adv Pharmacol, 1997. **38**: p. 205-27.
211. Youle, R.J. and D.P. Narendra, *Mechanisms of mitophagy.* Nat Rev Mol Cell Biol, 2011. **12**(1): p. 9-14.
212. Scherz-Shouval, R. and Z. Elazar, *Regulation of autophagy by ROS: physiology and pathology.* Trends Biochem Sci, 2011. **36**(1): p. 30-8.
213. Mijaljica, D., M. Prescott, and R.J. Devenish, *Mitophagy and mitoptosis in disease processes.* Methods Mol Biol, 2010. **648**: p. 93-106.
214. Conde de la Rosa, L., H. Moshage, and N. Nieto, *[Hepatocyte oxidant stress and alcoholic liver disease].* Rev Esp Enferm Dig, 2008. **100**(3): p. 156-63.
215. Block, K.I., et al., *Impact of antioxidant supplementation on chemotherapeutic efficacy: a systematic review of the evidence from randomized controlled trials.* Cancer Treat Rev, 2007. **33**(5): p. 407-18.
216. Rosser, B.G. and G.J. Gores, *Liver cell necrosis: cellular mechanisms and clinical implications.* Gastroenterology, 1995. **108**(1): p. 252-75.
217. Golstein, P. and G. Kroemer, *Cell death by necrosis: towards a molecular definition.* Trends Biochem Sci, 2007. **32**(1): p. 37-43.
218. Wang, Y., et al., *Arsenic induces mitochondria-dependent apoptosis by reactive oxygen species generation rather than glutathione depletion in Chang human hepatocytes.* Arch Toxicol, 2009. **83**(10): p. 899-908.
219. Motoyama, S., et al., *Hydrogen peroxide derived from hepatocytes induces sinusoidal endothelial cell apoptosis in perfused hypoxic rat liver.* Gastroenterology, 1998. **114**(1): p. 153-63.
220. Bilzer, M., et al., *Prevention of Kupffer cell-induced oxidant injury in rat liver by atrial natriuretic peptide.* Am J Physiol, 1999. **276**(5 Pt 1): p. G1137-44.
221. Yuzawa, H., et al., *Inhibitory effects of safe and novel SOD derivatives, galactosylated-SOD, on hepatic warm ischemia/reperfusion injury in pigs.* Hepatogastroenterology, 2005. **52**(63): p. 839-43.
222. Sener, G., et al., *Protective effect of MESNA (2-mercaptoethane sulfonate) against hepatic ischemia/reperfusion injury in rats.* Surg Today, 2005. **35**(7): p. 575-80.
223. He, S.Q., et al., *Delivery of antioxidative enzyme genes protects against ischemia/reperfusion-induced liver injury in mice.* Liver Transpl, 2006. **12**(12): p. 1869-79.

224. Menger, M.D. and B. Vollmar, *Pathomechanisms of ischemia-reperfusion injury as the basis for novel preventive strategies: is it time for the introduction of pleiotropic compounds?* Transplant Proc, 2007. **39**(2): p. 485-8.
225. Baumgardner, J.N., et al., *N-acetylcysteine attenuates progression of liver pathology in a rat model of nonalcoholic steatohepatitis.* J Nutr, 2008. **138**(10): p. 1872-9.
226. Grattagliano, I., G. Vendemiale, and B.H. Lauterburg, *Reperfusion injury of the liver: role of mitochondria and protection by glutathione ester.* J Surg Res, 1999. **86**(1): p. 2-8.
227. Mochida, S., et al., *Oxidative stress in hepatocytes and stimulatory state of Kupffer cells after reperfusion differ between warm and cold ischemia in rats.* Liver, 1994. **14**(5): p. 234-40.
228. Andrade Jr, D.R., D.R. Andrade, and S.A. Santos, *Study of rat hepatocytes in primary culture submitted to hypoxia and reoxygenation: action of the cytoprotectors prostaglandin E1, superoxide dismutase, allopurinol and verapamil.* Arq Gastroenterol, 2009. **46**(4): p. 333-40.
229. Baraona, E., et al., *Zonal redox changes as a cause of selective perivenular hepatotoxicity of alcohol.* Pharmacol Biochem Behav, 1983. **18 Suppl 1**: p. 449-54.
230. Kera, Y., K.E. Penttila, and K.O. Lindros, *Glutathione replenishment capacity is lower in isolated perivenous than in periportal hepatocytes.* Biochem J, 1988. **254**(2): p. 411-7.
231. Levine, B. and G. Kroemer, *Autophagy in aging, disease and death: the true identity of a cell death impostor.* Cell Death Differ, 2009. **16**(1): p. 1-2.
232. Yin, X.M., W.X. Ding, and W. Gao, *Autophagy in the liver.* Hepatology, 2008. **47**(5): p. 1773-85.
233. Huett, A., G. Goel, and R.J. Xavier, *A systems biology viewpoint on autophagy in health and disease.* Curr Opin Gastroenterol, 2010. **26**(4): p. 302-9.
234. Lu, Z., et al., *Participation of autophagy in the degeneration process of rat hepatocytes after transplantation following prolonged cold preservation.* Arch Histol Cytol, 2005. **68**(1): p. 71-80.
235. Loos, B., et al., *At the core of survival: autophagy delays the onset of both apoptotic and necrotic cell death in a model of ischemic cell injury.* Exp Cell Res, 2011. **317**(10): p. 1437-53.
236. Kohrmann, M., et al., *Fast, convenient, and effective method to transiently transfect primary hippocampal neurons.* J Neurosci Res, 1999. **58**(6): p. 831-5.
237. Gardmo, C., et al., *Transfection of adult primary rat hepatocytes in culture.* Biochem Pharmacol, 2005. **69**(12): p. 1805-13.
238. Park, J.S., et al., *Comparative nucleic acid transfection efficacy in primary hepatocytes for gene silencing and functional studies.* BMC Res Notes, 2011. **4**: p. 8.
239. Domart, M.C., et al., *Concurrent induction of necrosis, apoptosis, and autophagy in ischemic preconditioned human livers formerly treated by chemotherapy.* J Hepatol, 2009. **51**(5): p. 881-9.
240. Cui, Q., et al., *Augmentation of oridonin-induced apoptosis observed with reduced autophagy.* J Pharmacol Sci, 2006. **101**(3): p. 230-9.

241. Kohli, R., et al., *Mitochondrial reactive oxygen species signal hepatocyte steatosis by regulating the phosphatidylinositol 3-kinase cell survival pathway.* J Biol Chem, 2007. **282**(29): p. 21327-36.
242. Wang, J.H., et al., *Autophagy suppresses age-dependent ischemia and reperfusion injury in livers of mice.* Gastroenterology, 2011. **141**(6): p. 2188-2199 e6.
243. Tanida, I., *Autophagy basics.* Microbiol Immunol, 2011. **55**(1): p. 1-11.
244. Kim, I. and J.J. Lemasters, *Mitochondrial degradation by autophagy (mitophagy) in GFP-LC3 transgenic hepatocytes during nutrient deprivation.* Am J Physiol Cell Physiol, 2011. **300**(2): p. C308-17.
245. Kim, J.S., et al., *Role of the mitochondrial permeability transition in apoptotic and necrotic death after ischemia/reperfusion injury to hepatocytes.* Curr Mol Med, 2003. **3**(6): p. 527-35.
246. Wang, Y., et al., *Macroautophagy and chaperone-mediated autophagy are required for hepatocyte resistance to oxidant stress.* Hepatology, 2010. **52**(1): p. 266-77.
247. Kim, J.S., et al., *Impaired autophagy: A mechanism of mitochondrial dysfunction in anoxic rat hepatocytes.* Hepatology, 2008. **47**(5): p. 1725-36.
248. Pardo, M. and O. Tirosh, *Protective signalling effect of manganese superoxide dismutase in hypoxia-reoxygenation of hepatocytes.* Free Radic Res, 2009. **43**(12): p. 1225-39.
249. Tong, J., X. Yan, and L. Yu, *The late stage of autophagy: cellular events and molecular regulation.* Protein Cell, 2010. **1**(10): p. 907-15.
250. Zucchini-Pascal, N., G. de Sousa, and R. Rahmani, *Lindane and cell death: at the crossroads between apoptosis, necrosis and autophagy.* Toxicology, 2009. **256**(1-2): p. 32-41.
251. Esposti, D.D., et al., *Autophagy is induced by ischemic preconditioning in human livers formerly treated by chemotherapy to limit necrosis.* Autophagy, 2010. **6**(1): p. 172-4.
252. Eliopoulos, A.G. and L.S. Young, *The role of the CD40 pathway in the pathogenesis and treatment of cancer.* Curr Opin Pharmacol, 2004. **4**(4): p. 360-7.
253. Anand, S.X., et al., *Membrane-associated CD40L and sCD40L in atherothrombotic disease.* Thromb Haemost, 2003. **90**(3): p. 377-84.
254. Chan, F.K., et al., *A domain in TNF receptors that mediates ligand-independent receptor assembly and signaling.* Science, 2000. **288**(5475): p. 2351-4.
255. Chen, Y., et al., *Internalization of CD40 regulates its signal transduction in vascular endothelial cells.* Biochem Biophys Res Commun, 2006. **345**(1): p. 106-17.
256. Eliopoulos, A.G., et al., *CD40 induces apoptosis in carcinoma cells through activation of cytotoxic ligands of the tumor necrosis factor superfamily.* Mol Cell Biol, 2000. **20**(15): p. 5503-15.
257. Eliopoulos, A.G., et al., *TRAF1 is a critical regulator of JNK signaling by the TRAF-binding domain of the Epstein-Barr virus-encoded latent infection membrane protein 1 but not CD40.* J Virol, 2003. **77**(2): p. 1316-28.
258. Prasad, M.L., et al., *Mutational screening of the CD40 ligand (CD40L) gene in patients with X linked hyper-IgM syndrome (XHIM) and determination of carrier status in female relatives.* J Clin Pathol, 2005. **58**(1): p. 90-2.

259. Armitage, R.J., et al., *Molecular and biological characterization of a murine ligand for CD40.* Nature, 1992. **357**(6373): p. 80-2.
260. Armitage, R.J., et al., *Identification of a source of biologically active CD40 ligand.* Eur J Immunol, 1992. **22**(8): p. 2071-6.
261. Gauchat, J.F., et al., *Induction of human IgE synthesis in B cells by mast cells and basophils.* Nature, 1993. **365**(6444): p. 340-3.
262. van Kooten, C., *Immune regulation by CD40-CD40-l interactions - 2; Y2K update.* Front Biosci, 2000. **5**: p. D880-693.
263. Watanabe, M., et al., *Distribution of inflammatory cells in adventitia changed with advancing atherosclerosis of human coronary artery.* J Atheroscler Thromb, 2007. **14**(6): p. 325-31.
264. Cipollone, F., et al., *Enhanced soluble CD40 ligand contributes to endothelial cell dysfunction in vitro and monocyte activation in patients with diabetes mellitus: effect of improved metabolic control.* Diabetologia, 2005. **48**(6): p. 1216-24.
265. Callard, R.E., et al., *CD40 ligand and its role in X-linked hyper-IgM syndrome.* Immunol Today, 1993. **14**(11): p. 559-64.
266. Bradham, C.A., et al., *Mechanisms of hepatic toxicity. I. TNF-induced liver injury.* Am J Physiol, 1998. **275**(3 Pt 1): p. G387-92.
267. Sugimoto, K., et al., *Expression of functional CD40 in human hepatocellular carcinoma.* Hepatology, 1999. **30**(4): p. 920-6.
268. Tang, Y., et al., *Up-regulation of the expression of costimulatory molecule CD40 in hepatocytes by hepatitis B virus X antigen.* Biochem Biophys Res Commun, 2009. **384**(1): p. 12-7.
269. Kondo, T., et al., *Essential roles of the Fas ligand in the development of hepatitis.* Nat Med, 1997. **3**(4): p. 409-13.
270. Galle, P.R., et al., *Involvement of the CD95 (APO-1/Fas) receptor and ligand in liver damage.* J Exp Med, 1995. **182**(5): p. 1223-30.
271. Harada, K., et al., *Enhanced apoptosis relates to bile duct loss in primary biliary cirrhosis.* Hepatology, 1997. **26**(6): p. 1399-405.
272. Engel, D., et al., *The immunobiology of CD154-CD40-TRAF interactions in atherosclerosis.* Semin Immunol, 2009. **21**(5): p. 308-12.
273. Eliopoulos, A.G., *Cell signaling. "Make and brake" in signaling.* Science, 2008. **321**(5889): p. 648-9.
274. Ha, Y.J. and J.R. Lee, *Role of TNF receptor-associated factor 3 in the CD40 signaling by production of reactive oxygen species through association with p40phox, a cytosolic subunit of nicotinamide adenine dinucleotide phosphate oxidase.* J Immunol, 2004. **172**(1): p. 231-9.
275. Williams, K.T., et al., *C4b binding protein binds to CD154 preventing CD40 mediated cholangiocyte apoptosis: a novel link between complement and epithelial cell survival.* PLoS One, 2007. **2**(1): p. e159.
276. Hollenbaugh, D., et al., *Expression of functional CD40 by vascular endothelial cells.* J Exp Med, 1995. **182**(1): p. 33-40.
277. Friedman, S.L., *Molecular regulation of hepatic fibrosis, an integrated cellular response to tissue injury.* J Biol Chem, 2000. **275**(4): p. 2247-50.
278. Marra, F., *Hepatic stellate cells and the regulation of liver inflammation.* J Hepatol, 1999. **31**(6): p. 1120-30.

279. Schwabe, R.F., et al., *CD40 activates NF-kappa B and c-Jun N-terminal kinase and enhances chemokine secretion on activated human hepatic stellate cells.* J Immunol, 2001. **166**(11): p. 6812-9.
280. Hess, S., et al., *CD40 function in nonhematopoietic cells. Nuclear factor kappa B mobilization and induction of IL-6 production.* J Immunol, 1995. **155**(10): p. 4588-95.
281. Cao, H.J., et al., *Activation of human orbital fibroblasts through CD40 engagement results in a dramatic induction of hyaluronan synthesis and prostaglandin endoperoxide H synthase-2 expression. Insights into potential pathogenic mechanisms of thyroid-associated ophthalmopathy.* J Biol Chem, 1998. **273**(45): p. 29615-25.
282. Delmas, Y., et al., *[Platelet-associated CD154: a new interface in haemostasis and in the inflammatory reaction].* Med Sci (Paris), 2005. **21**(10): p. 825-31.
283. Khandoga, A., et al., *Platelet-endothelial cell interactions during hepatic ischemia-reperfusion in vivo: a systematic analysis.* Microvasc Res, 2003. **65**(2): p. 71-7.
284. Lisman, T. and R.J. Porte, *The role of platelets in liver inflammation and regeneration.* Semin Thromb Hemost, 2010. **36**(2): p. 170-4.
285. Murakami, K., et al., *Human endothelial cells augment early CD40 ligand expression in activated CD4+ T cells through LFA-3-mediated stabilization of mRNA.* J Immunol, 1999. **163**(5): p. 2667-73.
286. Zhou, F., et al., *CD154-CD40 interactions drive hepatocyte apoptosis in murine fulminant hepatitis.* Hepatology, 2005. **42**(2): p. 372-80.
287. Laxmanan, S., et al., *CD40: a mediator of pro- and anti-inflammatory signals in renal tubular epithelial cells.* J Am Soc Nephrol, 2005. **16**(9): p. 2714-23.
288. Matsuzawa, A., et al., *ROS-dependent activation of the TRAF6-ASK1-p38 pathway is selectively required for TLR4-mediated innate immunity.* Nat Immunol, 2005. **6**(6): p. 587-92.
289. Uehara, T., et al., *c-Jun N-terminal kinase mediates hepatic injury after rat liver transplantation.* Transplantation, 2004. **78**(3): p. 324-32.
290. Kobayashi, M., et al., *P38 mitogen-activated protein kinase inhibition attenuates ischemia-reperfusion injury of the rat liver.* Surgery, 2002. **131**(3): p. 344-9.
291. King, L.A., et al., *Role of p38 and JNK in liver ischemia and reperfusion.* J Hepatobiliary Pancreat Surg, 2009. **16**(6): p. 763-70.
292. Lalor, P. and G.B. Nash, *Adhesion of flowing leucocytes to immobilized platelets.* Br J Haematol, 1995. **89**(4): p. 725-32.
293. Suzuki, M., K. Aoshiba, and A. Nagai, *Oxidative stress increases Fas ligand expression in endothelial cells.* J Inflamm (Lond), 2006. **3**: p. 11.
294. Xu, H., et al., *Studies investigating pretransplant donor-specific blood transfusion, rapamycin, and the CD154-specific antibody IDEC-131 in a nonhuman primate model of skin allotransplantation.* J Immunol, 2003. **170**(5): p. 2776-82.
295. Ha, Y.J., H.J. Seul, and J.R. Lee, *Ligation of CD40 receptor in human B lymphocytes triggers the 5-lipoxygenase pathway to produce reactive oxygen species and activate p38 MAPK.* Exp Mol Med, 2011. **43**(2): p. 101-10.
296. Xia, M., et al., *Phosphoinositide 3-kinase mediates CD40 ligand-induced oxidative stress and endothelial dysfunction via Rac1 and NADPH oxidase 2.* J Thromb Haemost, 2010. **8**(2): p. 397-406.

297. Ueno, T., et al., *Influence of genetic polymorphisms in oxidative stress related genes and smoking on plasma MDA-LDL, soluble CD40 ligand, E-selectin and soluble ICAM1 levels in patients with coronary artery disease.* Med Sci Monit, 2009. **15**(7): p. CR341-8.
298. Mebratu, Y. and Y. Tesfaigzi, *How ERK1/2 activation controls cell proliferation and cell death: Is subcellular localization the answer?* Cell Cycle, 2009. **8**(8): p. 1168-75.
299. Lei, K. and R.J. Davis, *JNK phosphorylation of Bim-related members of the Bcl2 family induces Bax-dependent apoptosis.* Proc Natl Acad Sci U S A, 2003. **100**(5): p. 2432-7.
300. Chang, L., et al., *The E3 ubiquitin ligase itch couples JNK activation to TNFalpha-induced cell death by inducing c-FLIP(L) turnover.* Cell, 2006. **124**(3): p. 601-13.
301. Bu, S.Z., et al., *p38 Mitogen-activated protein kinases is required for counteraction of 2-methoxyestradiol to estradiol-stimulated cell proliferation and induction of apoptosis in ovarian carcinoma cells via phosphorylation Bcl-2.* Apoptosis, 2006. **11**(3): p. 413-25.
302. Cursio, R., et al., *Fas ligand expression following normothermic liver ischemia-reperfusion.* J Surg Res, 2005. **125**(1): p. 30-6.
303. Ding, W.X., et al., *Bid-dependent generation of oxygen radicals promotes death receptor activation-induced apoptosis in murine hepatocytes.* Hepatology, 2004. **40**(2): p. 403-13.
304. Garcia-Ruiz, C. and J.C. Fernandez-Checa, *Redox regulation of hepatocyte apoptosis.* J Gastroenterol Hepatol, 2007. **22 Suppl 1**: p. S38-42.
305. Andre, P., et al., *CD40L stabilizes arterial thrombi by a beta3 integrin--dependent mechanism.* Nat Med, 2002. **8**(3): p. 247-52.
306. Sullivan, B.P., et al., *Protective and damaging effects of platelets in acute cholestatic liver injury revealed by depletion and inhibition strategies.* Toxicol Sci, 2010. **115**(1): p. 286-94.
307. Ohtaki, Y., et al., *Hepatic platelet accumulation in Fas-mediated hepatitis in mice.* Int Immunopharmacol, 2009. **9**(9): p. 1071-8.
308. Hong, S.W., et al., *The protective effect of resveratrol on dimethylnitrosamine-induced liver fibrosis in rats.* Arch Pharm Res, 2010. **33**(4): p. 601-9.
309. Reese, P.P., et al., *Donor age and cold ischemia interact to produce inferior 90-day liver allograft survival.* Transplantation, 2008. **85**(12): p. 1737-44.
310. Zwacka, R.M., et al., *CD4(+) T-lymphocytes mediate ischemia/reperfusion-induced inflammatory responses in mouse liver.* J Clin Invest, 1997. **100**(2): p. 279-89.
311. Pillai, A.A. and J. Levitsky, *Overview of immunosuppression in liver transplantation.* World J Gastroenterol, 2009. **15**(34): p. 4225-33.
312. Minguela, A., et al., *CD28/CTLA-4 and CD80/CD86 costimulatory molecules are mainly involved in acceptance or rejection of human liver transplant.* Hum Immunol, 2000. **61**(7): p. 658-69.
313. Boros, P., et al., *Organ transplantation in rodents: novel applications of long-established methods.* Transpl Immunol, 2007. **18**(1): p. 44-52.
314. Khandoga, A., et al., *CD4+ T cells contribute to postischemic liver injury in mice by interacting with sinusoidal endothelium and platelets.* Hepatology, 2006. **43**(2): p. 306-15.

315. Olive, P.L., et al., *Carbonic anhydrase 9 as an endogenous marker for hypoxic cells in cervical cancer.* Cancer Res, 2001. **61**(24): p. 8924-9.
316. Varia, M.A., et al., *Pimonidazole: a novel hypoxia marker for complementary study of tumor hypoxia and cell proliferation in cervical carcinoma.* Gynecol Oncol, 1998. **71**(2): p. 270-7.
317. Lee, Y.M., et al., *Determination of hypoxic region by hypoxia marker in developing mouse embryos in vivo: a possible signal for vessel development.* Dev Dyn, 2001. **220**(2): p. 175-86.
318. Schemmer, P., et al., *Reperfusion injury in livers due to gentle in situ organ manipulation during harvest involves hypoxia and free radicals.* J Pharmacol Exp Ther, 1999. **290**(1): p. 235-40.
319. Terada, N., et al., *Immunohistochemical detection of hypoxia in mouse liver tissues treated with pimonidazole using "in vivo cryotechnique".* Histochem Cell Biol, 2007. **128**(3): p. 253-61.
320. Hanschen, M., et al., *Reciprocal activation between CD4+ T cells and Kupffer cells during hepatic ischemia-reperfusion.* Transplantation, 2008. **86**(5): p. 710-8.
321. Buhler, L., et al., *Anti-CD154 monoclonal antibody and thromboembolism.* Transplantation, 2001. **71**(3): p. 491.
322. Badell, I.R., et al., *Nondepleting anti-CD40-based therapy prolongs allograft survival in nonhuman primates.* Am J Transplant, 2012. **12**(1): p. 126-35.
323. Page, A., et al., *CD40 blockade combines with CTLA4Ig and sirolimus to produce mixed chimerism in an MHC-defined rhesus macaque transplant model.* Am J Transplant, 2012. **12**(1): p. 115-25.
324. Mani, H. and D.E. Kleiner, *Liver biopsy findings in chronic hepatitis B.* Hepatology, 2009. **49**(5 Suppl): p. S61-71.
325. Malhi, H. and G.J. Gores, *Cellular and molecular mechanisms of liver injury.* Gastroenterology, 2008. **134**(6): p. 1641-54.
326. Erion, M.D., et al., *Liver-targeted drug delivery using HepDirect prodrugs.* J Pharmacol Exp Ther, 2005. **312**(2): p. 554-60.
327. de Mochel, N.S., et al., *Hepatocyte NAD(P)H oxidases as an endogenous source of reactive oxygen species during hepatitis C virus infection.* Hepatology, 2010. **52**(1): p. 47-59.
328. Sakuma, S., et al., *Xanthine oxidase-derived reactive oxygen species mediate 4-oxo-2-nonenal-induced hepatocyte cell death.* Toxicol Appl Pharmacol, 2010. **249**(2): p. 127-31.
329. Siraki, A.G., et al., *Endogenous and endobiotic induced reactive oxygen species formation by isolated hepatocytes.* Free Radic Biol Med, 2002. **32**(1): p. 2-10.
330. Lemasters, J.J., et al., *Mitochondrial calcium and the permeability transition in cell death.* Biochim Biophys Acta, 2009. **1787**(11): p. 1395-401.
331. Shen, H.M. and S. Pervaiz, *TNF receptor superfamily-induced cell death: redox-dependent execution.* FASEB J, 2006. **20**(10): p. 1589-98.
332. Trachootham, D., et al., *Redox regulation of cell survival.* Antioxid Redox Signal, 2008. **10**(8): p. 1343-74.
333. Paquet, P. and G.E. Pierard, *Toxic epidermal necrolysis: revisiting the tentative link between early apoptosis and late necrosis (review).* Int J Mol Med, 2007. **19**(1): p. 3-10.

334. Zhang, Y., et al., *Redox control of the survival of healthy and diseased cells.* Antioxid Redox Signal, 2011. **15**(11): p. 2867-908.